Studies on Thioether Macrocylic Complexes

By

Martin J. Sullivan

Thesis presented for the Degree of
Dr. of Philosophy
University of Edinburgh
1993

To my Mother and Father

Forsan et haec olim meminisse iuvabit.

(The Day may dawn when this plight

shall be sweet to remember)

Virgil, Aeneid, i. 203

(Trans. by Jackson)

Declaration

Except where specific reference has been made to other sources, the work presented in this thesis is the original work of the author. It has not been submitted, in whole or in part, for any other degree. Certain of the results have already been published.

Acknowledgements

I should like to extend my thanks to my supervisor Dr M. Schröder for his help, support and encouragement over the course of this work. I also wish to thank Dr A. J. Blake and Dr R. O. Gould for their help and advice in all matters of X- ray crystallography.

I wish to thank Dr S. G. Henderson for his instruction on the use of the Joel ^{31}P N.M.R. instrument and to Dr D. Reed, Mr J. Miller, and Miss H. Grant for running various N.M.R spectra, and for training on the Brücker WP80 N.M.R. spectrometer. In addition I would like to thank Mrs E. McDougall and Mr A. Taylor for performing the elemental analysis and mass spectral measurements respectively.

I am indebted to the SERC for financial support, Johnson-Matthey for the generous loan of platinum group metal complexes, and the University of Edinburgh for the use of their facilities. I would like to express my gratitude to Mrs A. Aiton for typing this thesis.

I would like to thank Gill, Andy, Steve, and all the members of the Schröder group for their help and encouragement during the course of this work. In particular, I would like to thank Dr Y. V. Roberts and Dr M. Halcrow for their advice, help and fruitful discussions. Finally I would like to thank my brother Michael and his wife Gill for their generous support and kindness, both spiritual and alimentary.

ABSTRACT

An introduction to macrocyclic chemistry, with particular emphasis on [9]aneS$_3$ (1,4,7- trithiacyclononane) and thioether macrocyclic transition metal complexes of groups VIII and IX is presented.

The reaction of [RuCl$_2$(PPh$_3$)([9]aneS$_3$)] with TlPF$_6$ in CH$_2$Cl$_2$ at 298K results in the formation of a mixture of complexes, [Ru(PPh$_3$)([9]aneS$_3$)(μ-Cl)]$_2$(PF$_6$)$_2$ and [Ru(PPh$_3$)([9]aneS$_3$)(μ-Cl)$_2$Tl]$_2$(PF$_6$)$_2$, which have been both characterised by X-ray crystallography. The synthesis of pure [Ru(PPh$_3$)([9]aneS$_3$)(μ-Cl)]$_2$(PF$_6$)$_2$ and [Ru(PPh$_3$)([9]aneS$_3$)(μ-Cl)$_2$Tl]$_2$(PF$_6$)$_2$ is described. Both complexes react with acetonitrile to form [Ru(NCCH$_3$)Cl(PPh$_3$)([9]aneS$_3$)](PF$_6$).

The reaction of [RuCl$_2$(PPh$_3$)([9]aneS$_3$)] with TlPF$_6$ in CH$_3$NO$_2$ leads to the isolation of the complexes [Ru(NCCH$_2$CH$_3$)Cl(PPh$_3$)([9]aneS$_3$)](PF$_6$) and [RuCl(NC$_3$H$_3$O)(PPh$_3$)([9]aneS$_3$)](PF$_6$). The X-Ray structure of the latter complex is described. The complexes form by reacting with two impurities (ethyl cyanide and isoxazole) present in CH$_3$NO$_2$.

The addition of TlPF$_6$ to [RuCl$_2$(PPh$_3$)([9]aneS$_3$)] in CH$_3$NO$_2$ and THT forms the complex [RuCl(PPh$_3$)(THT)([9]aneS$_3$)](PF$_6$). The single crystal X-ray structure of this complex reveals the presence of a 1 : 1 mixture of the THT complex, [RuCl(PPh$_3$)(THT)([9]aneS$_3$)](PF$_6$) and a THT-S-oxide complex, [RuCl(PPh$_3$)(THT-S-oxide)([9]aneS$_3$)](PF$_6$). The THT-S-oxide complex forms during crystallisation.

The synthesis of [RuCl$_2$([n]aneS$_4$)] (n = 12, 14, 16) is described. The complexes, [RuCl$_2$([n]aneS$_4$)] (n = 12, 14) adopt *cis*–configurations, whereas it is proposed that [RuCl$_2$([16]aneS$_4$)] adopts a *trans*–configuration. The synthesis of [RhCl(PR$_3$)([n]aneS$_4$)](PF$_6$)$_2$ (n = 12, PR$_3$ = PPh$_3$, PCy$_3$, PMe$_2$Ph; n = 14, PR$_3$ = PMe$_2$Ph) is achieved by reacting [RhCl$_2$([n]aneS$_4$)](PF$_6$) with TlPF$_6$ and excess PR$_3$ in refluxing acetone under N$_2$. The single crystal X-ray structure of [RhCl(PPh$_3$)([12]aneS$_4$)](PF$_6$)$_2$ is reported.

The chemical oxidation of [9]aneS$_3$ is investigated. The complete oxidation of [9]aneS$_3$ is achieved by reacting [9]aneS$_3$ with H$_2$O$_2$ in glacial acetic acid at 60°C, yielding the trisulfone O$_6$[9]aneS$_3$, which has been characterised by X-ray crystallography. The attempted synthesis of the trisulfone, O$_3$[9]aneS$_3$ is discussed.

Chapter 1

A brief introduction to some general aspects of macrocyclic chemistry is presented.

Chapter 2

An introduction to general thioether macrocyclic chemistry , with particular emphasis on [9]aneS_3 and thioether transition metal complexes of groups VIII and IX is given. The broad aims of this study are introduced and discussed.

Chapter 3

A brief introduction to catalysis by known Ru(II) complexes is given.

Reaction of [$RuCl_2(PPh_3)$([9]aneS_3)] with $TlPF_6$ in CH_2Cl_2 at 298K results in the formation of a mixture of [$Ru(PPh_3)$([9]aneS_3)(μ-Cl)]$_2(PF_6)_2$ and [$Ru(PPh_3)$([9]aneS_3)(μ-Cl)$_2$Tl]$_2(PF_6)_2$. The single crystal X-ray structure of [$Ru(PPh_3)$([9]aneS_3)(μ-Cl)]$_2(PF_6)_2$ shows the two Ru(II) ions to be bridged by two Cl-ligands [Ru–Cl = 2.4654(10) and 2.4945(10) Å] . The PPh_3 groups are mutually *anti* . The single crystal X-ray structure of [$Ru(PPh_3)$([9]aneS_3)(μ-Cl)$_2$Tl]$_2(PF_6)_2$ shows the two Ru ions spanned by a Tl_2Cl_4 'ladder'.

The synthesis of pure [$Ru(PPh_3)$([9]aneS_3)(μ-Cl)]$_2(PF_6)_2$ and [$Ru(PPh_3)$([9]aneS_3)(μ-Cl)$_2$Tl]$_2(PF_6)_2$ are described. Both complexes react with acetonitrile to form [$Ru(NCCH_3)Cl(PPh_3)$([9]aneS_3)](PF_6), indicating that the bridge can be easily cleaved, and [$Ru(PPh_3)$([9]aneS_3)(μ-Cl)$_2$Tl]$_2(PF_6)_2$ loses TlCl in acetone to form [$Ru(PPh_3)$([9]aneS_3)(μ-Cl)]$_2(PF_6)_2$.

Chapter 4

An introduction to CH_3NO_2 and its complexes is given.

A discussion of the product which is formed by the reaction of $[RuCl_2(PPh_3)([9]aneS_3)]$ with $TlPF_6$ in CH_3NO_2 is given. Single crystal X-ray crystallography identifies the presence of a C-bound furyl complex, $[RuCl(C_4H_3O)(PPh_3)([9]aneS_3)]$ and ir, ^1H N.M.R., ^{31}P N.M.R. and ^{13}C N.M.R. spectroscopy suggests that another complex is also present which is assigned as $[Ru(Z(CH_2CH_3)_n)Cl(PPh_3)([9]aneS_3)](PF_6)_m$, where Z,n and m are unknown.

A discussion of possible mechanisms for the formation of these two complexes is presented. The presence of impurities in CH_3NO_2 leads to the identification of one of the products as $[Ru(NCCH_2CH_3)Cl(PPh_3)([9]aneS_3)](PF_6)$, since propionitrile is an impurity in CH_3NO_2. On re-examining the spectroscopic evidence the identity of a previously unknown impurity in CH_3NO_2 is discussed and identified as isoxazole. The X-ray data, previously assigned as a "C-bound furyl" complex, are re-interpreted and are consistent with the the complex, $[RuCl(NC_3H_3O)(PPh_3)([9]aneS_3)](PF_6)$. The identification of $[RuCl(NC_3H_3O)(PPh_3)([9]aneS_3)](PF_6)$ and $[RuCl(NCCH_2CH_3)(PPh_3)([9]aneS_3)]PF_6$ are confirmed by reacting $[RuCl_2(PPh_3)([9]aneS_3)]$ with $TlPF_6$ in isoxazole or propionitrile respectively.

Chapter 5

An introduction to pyrrole, pyrrolidine, tetrahydrothiophene (THT) and thiophene complexes of transition metals is given.

The reaction of $[RuCl_2(PPh_3)([9]aneS_3)]$ with $TlPF_6$ in the presence of pyrrole, pyrrolidine or thiophene in CH_2Cl_2 or CH_3NO_2 results in the formation of $[Ru(PPh_3)([9]aneS_3)(\mu\text{-}Cl)]_2(PF_6)_2$ and $[Ru(PPh_3)([9]aneS_3)(\mu\text{-}Cl)_2Tl]_2(PF_6)_2$. However, the addition of $TlPF_6$ to $[RuCl_2(PPh_3)([9]aneS_3)]$ in CH_3NO_2 and THT forms the complex $[RuCl(PPh_3)(THT)([9]aneS_3)](PF_6)$. The single crystal X-ray structure of this complex reveals the presence of a 1 : 1 mixture of the THT complex, $[RuCl(PPh_3)(THT)([9]aneS_3)](PF_6)$ and a THT-S-oxide complex, $[RuCl(PPh_3)(THT\text{-}S\text{-}oxide)([9]aneS_3)](PF_6)$. The THT-S-oxide complex forms during crystallisation.

Chapter 6

An introduction to Ru and Rh tetrathioether macrocyclic complexes is presented.

The synthesis of $[RuCl_2([n]aneS_4)]$ (n = 12, 14, 16) is described. The complexes, $[RuCl_2([n]aneS_4)]$ (n = 12, 14) adopt a *cis*–configurations, whereas it is proposed that $[RuCl_2([16]aneS_4)]$ adopts a *trans*–configuration. The reaction of $[MCl_2([n]aneS_4)](PF_6)_z$ (M = Ru, Z = 0, n = 12, 14, 16; M = Rh, Z = 1, n= 12, 14, 16) with $TlPF_6$ in CH_3NO_2 in the presence of tetrahydrofuran leads to the formation of $[RuCl(NCCH_2CH_3)([n]aneS_4)](PF_6)_{z+1}$.

The synthesis of $[RhCl(PR_3)([n]aneS_4)](PF_6)_2$ (n = 12, PR_3 = PPh_3, PCy_3, PMe_2Ph; n = 14, PR_3 = PMe_2Ph) is achieved by reacting $[RhCl_2([n]aneS_4)](PF_6)$ with $TlPF_6$ and excess PR_3 in refluxing acetone under N_2. No reaction of $[MCl(PR_3)([n]aneS_4)](PF_6)_r$ (r = 1, M = Ru, PR_3 = PPh_3, n = 12, 14, 16; r = 2, M = Rh, n = 12, PR_3 = PPh_3, PCy_3, PMe_2Ph; n = 14, PR_3 = PMe_2Ph) is observed with $TlPF_6$ in CH_3NO_2 in the presence of THF confirming that the second Cl^- is more difficult to remove than the first one.

Chapter 7

The chemical and physical properties of sulfoxides and sulfone are discussed, with particular emphasis on preparative methods.

The chemical oxidation of [9]aneS$_3$ is investigated. The complete oxidation of [9]aneS$_3$ is achieved by reacting [9]aneS$_3$ with H_2O_2 in glacial acetic acid at 60°C, yielding the trisulfone O_6[9]aneS$_3$. This compound has been characterised by ir and N.M.R. spectroscopy, elemental analysis and X-ray diffraction.

The attempted synthesis of the trisulfoxide, O_3[9]aneS$_3$ is described. The usual product on gentle oxidation of [9]aneS$_3$ was a compound or compounds containing both the sulfoxide and sulfone functional groups. Possible reasons for the difficulties in synthesising O_3[9]aneS$_3$ are discussed.

Appendix

An introduction to deprotonation of thioether macrocycles is given. The deprotonation of $[Rh([9]aneS_3)_2]^{3+}$ results in the formation of $[Rh([9]aneS_3)([9]aneS_3\text{-}H)]^{2+}$ and another minor product. The minor product is proposed as being the complex, $[Rh([9]aneS_3)(SCHCH_2)(SCH_2CH_2SCHCH_2)]^{+}$. The electrochemistry of $[Rh([9]aneS_3)([9]aneS_3\text{-}H)]^{2+}$ shows a two electron reduction at E = -1.04 V Vs Fc / Fc^+ and a reversible reduction at $E_{1/2}$ = 1.54 V Vs Fc / Fc^+ in 0.1 M $TBAPF_6$ in CH_3CN. The conversion of $[Rh([9]aneS_3)([9]aneS_3\text{-}H)]^{2+}$ to $[Rh([9]aneS_3)_2]^{3+}$ is discussed.

Table of Contents

		Page
Chapter 1	An Introduction to Macrocyclic Chemistry	1
1.1	General	1
1.2	The Thermodynamic Macrocyclic Effect	1
1.3	The Kinetic Macrocyclic Effect	7
1.4	The Stabilisation of Unusual Oxidation States	8
1.5	Biological Systems	10
1.6	Catalysis	19
Chapter 2	The Chemistry of Thioether Macrocycles	27
2.1	The Synthesis of Thioether Macrocycles	27
2.2	The Structure of [9]aneS_3	33
2.3	Thioether Macrocyclic Complexes	34
2.3.1	Group VIII Thioether Macrocyclic Complexes	37
2.3.2	Group IX Thioether Macrocyclic Complexes	41
2.4	Aims of Research	44
Chapter 3	Synthesis of Dimeric Complexes of Ru(II) with [9]aneS_3	47
3.1	Introduction	47
3.2	Results and Discussion	52
3.2.1	The Thalliation of [$RuCl_2(PPh_3)$([9]aneS_3)]	52
3.2.1.1	The Crystal Structure of [$Ru(PPh_3)$([9]aneS_3)(μ-Cl)]$_2$(PF_6)$_2$	53
3.2.1.2	The Cystal Structure of [$Ru(PPh_3)$([9]aneS_3)(μ-Cl)$_2$Tl]$_2$(PF_6)$_2$	57
3.2.2	The Synthesis and Reactivity of [$Ru(PPh_3)$([9]aneS_3)(μ-Cl)]$_2$(PF_6)$_2$	62

3.2.3	The Synthesis and Reactivity of $[Ru(PPh_3)([9]aneS_3)(\mu\text{-}Cl)_2Tl]_2(PF_6)_2$	65
3.3	Conclusion	68
3.4	Experimental	69
Chapter 4	The Thalliation of $[RuCl_2(PPh_3)([9]aneS_3)]$ in CH_3NO_2	75
4.1	Introduction	75
4.2	The Reaction of $[RuCl_2(PPh_3)([9]aneS_3)]$ with $TlPF_6$ in CH_3NO_2	78
4.2.1	Results and Discussion	78
4.2.2	The Crystal Structure of $[RuCl(C_4H_3O)(PPh_3)([9]aneS_3)]$	82
4.2.3	N.M.R. spectroscopic study of $[RuCl(C_4H_3O)(PPh_3)([9]aneS_3)]$	88
4.2.4	F.A.B. mass spectroscopic study of $[RuCl(C_4H_3O)(PPh_3)([9]aneS_3)]$	95
4.2.5	Summary	98
4.3	Factors Influencing the formation of the Furyl and ethyl complexes	100
4.3.1	Possible Intermediates	100
4.3.2	The Possible Disproportionation of THF to a diethyl ether Complex and the C-Bound furyl Complex	102
4.3.3	The Role of Tl in the Reaction of $[RuCl_2(PPh_3)([9]aneS_3)]$ with $TlPF_6$ in CH_3NO_2 in the presence of THF	103
4.3.4	C–H and C–C Bond Activation of Cyclic Ethers	104
4.3.5	The Nature of the Solvent	108
4.3.6	Summary	114
4.4	The Key Role of Nitromethane	115
4.5	Summary and Conclusion	131
4.6	Experimental	132

Chapter 5	Synthesis of Half Sandwich Ru(II) Complexes with [9]aneS$_3$ and Sulfur and Nitrogen Analogues of Furan and THF	143
5.1	Introduction	143
5.2	Results and Discussion	146
5.2.1	The Reaction of [RuCl$_2$(PPh$_3$)([9]aneS$_3$)] with TlPF$_6$ and Thiophene and THT	146
5.2.2	The Crystal Structure of [RuCl(PPh$_3$)(THT)([9]aneS$_3$)](PF$_6$)	147
5.2.3	The Reaction of [RuCl$_2$(PPh$_3$)([9]aneS$_3$)] with TlPF$_6$ and Pyrrole and Pyrrolidine	155
5.3	Summary	158
5.4	Experimental	158
Chapter 6	Rhodium and Ruthenium Complexes of [n]aneS$_4$	164
6.1	Introduction	164
6.2	Ruthenium Complexes of [n]aneS$_4$ (n = 12, 14, 16)	169
6.2.1	The synthesis and reactivity of [RuCl$_2$([n]aneS$_4$)] (n = 12, 14, 16)	169
6.2.2	The reactivity of [RuCl(PPh$_3$)([n]aneS$_4$)](PF$_6$) complexes	171
6.3	Rhodium Complexes of [n]aneS$_4$ (n = 12, 14, 16)	175
6.3.1	The reactivity of [RhCl$_2$([n]aneS$_4$)](PF$_6$) (n = 12, 14, 16)	175
6.3.2	The Synthesis of [RhCl(PR$_3$)([n]aneS$_4$)](PF$_6$)$_2$ (n = 12, 14, 16; PR$_3$ = PMe$_2$Ph, PPh$_3$, PCy$_3$) complexes	175
6.3.3	The crystal structure of [RhCl(PPh$_3$)([n]aneS$_4$)](PF$_6$)$_2$	181
6.3.4	The reactivity of [RhCl(PR$_3$)([n]aneS$_4$)](PF$_6$)$_2$ Complexes (n = 12, 14)	184
6.4	Summary	186
6.5	Experimental	187

Chapter 7	The Oxidation of [9]aneS$_3$	198
7.1	Introduction	198
7.2	The Synthesis of O$_6$[9]aneS$_3$	206
7.3	The Attempted Synthesis of O$_3$[9]aneS$_3$	211
7.4	Summary	221
7.5	Experimental	221
Appendix	The Deprotonation of Thioether Macrocycles	229
	References	236
	Abbreviations	xxiii
	Lecture Courses and Meetings Attended	xxv
	Publications	xxvi

List of Figures

		Page
Figure 1.1	Ligands and their Abbreviations	2
Figure 1.2	The Kinetic Rate of Formation and Dissociation of $[Cu(Me_6[14]aneN_4)]^{2+}$ and $[Cu(2\text{-}3\text{-}2\ tet)]^{2+}$	3
Figure 1.3	A Representation of the Free Ligands and their Complexes	5
Figure 1.4	A Representation of $[Ni([14]aneS_4)]^{2+}$ and $[Ni([14]aneN_4)]^{2+}$ and their Open-Chain Analogues	6
Figure 1.5	An Explanation of the Miltiple Juxtapositional Fixedness	7
Figure 1.6	A Representation of Enterobectin	12
Figure 1.7	Models of Enterobectin	12
Figure 1.8	A View of the Model for the Core of Ferritin	13
Figure 1.9	A Representation of Chlorophyll a and b	14
Figure 1.10	A Representation of Haemoglobin	15
Figure 1.11	A View of a Picket Fence Model of Haemoglobin	15
Figure 1.12	A Representation of a Cytochrome	16
Figure 1.13	Representations of Cytochrome C and Cytochrome P_{450}	16
Figure 1.14	Some Examples of the Reactions Catalysed by Coenyme B_{12}	18
Figure 1.15	A View of the Metal Centre of Vitamin B_{12}	18
Figure 1.16	A Representation of Coenzyme B_{12}	19
Figure 1.17	A Representation of the [Co(Pc)] Complex	21
Figure 1.18	A View of the Ru Co-facial Porphyrin Comples	22
Figure 1.19	The Imidazole Derivative for the Ru Co-facial	22
Figure 1.20	A Representation of the Ru/Ni Complex	24
Figure 2.1	Thioether Macrocycles Synthesised using the Cs_2CO_3/ DMF Methodology	30
Figure 2.2	Thioether Macrocycles Synthesised using the $\{Mo(CO)_3\}$ Methodology	30

Figure 2.3	A Representation of $[Co_2\{\mu\text{-}C_2(CH_2SCH_2CH_2)S\}(CO)_6]$	31
Figure 2.4	Thioether Macrocycles Incorporating a Thiophene Unit	32
Figure 2.5	Mixed Donor Macrocycles Incorporating a Thioether	32
Figure 2.6	A View of the Single Crystal X-Ray Structure of [9]aneS_3	33
Figure 2.7	Some Possible Conformations of [9]aneS_3	34
Figure 2.8	A View of the Single Crystal X-Ray Structure of $[Pd([9]aneS_3)_2]^{2+}$	35
Figure 2.9	A View of the Single Crystal X-Ray Structure of $[Pt([9]aneS_3)_2]^{2+}$	36
Figure 2.10	A View of the Single Crystal X-Ray Structure of $[Pd([9]aneS_3)_2]^{3+}$	36
Figure 2.11	A View of the Single Crystal X-Ray Structure of $[Fe([9]aneS_3)_2]^{3+}$	38
Figure 2.12	A View of the Single Crystal X-Ray Structure of $[Fe([16]aneS_4)]I_2$	38
Figure 2.13	A View of the Single Crystal X-Ray Structure of $[RuCl(NCMe)(CO)([9]aneS_3)]^+$	39
Figure 2.14	A View of the Single Crystal X-Ray Structure of $[Os_4(CO)_{13}([12]aneS_3)]$	41
Figure 2.15	A View of the Single Crystal X-Ray Structure of $[Rh([9]aneS_3)_2]^{3+}$	43
Figure 2.16	A View of the Single Crystal X-Ray Structure of $[Rh_2(COD)_2([20]aneS_6)]^{2+}$	43
Figure 2.17	A View of the Single Crystal X-Ray Structure of $[Au([9]aneS_3)_2]^+$	46
Figure 2.18	A View of the Single Crystal X-Ray Structure of $[Au([9]aneS_3)_2]^{2+}$	46
Figure 2.19	A View of the Single Crystal X-Ray Structure of $[Au([9]aneS_3)_2]^{3+}$	46

Figure 3.1	A View of the Single Crystal X-Ray Structure of $[RuCl_2(PPh_3)([9]aneS_3)]^+$	48
Figure 3.2	A View of the Single Crystal X-Ray Structure of $[RuCl(NCMe)(PPh_3)([9]aneS_3)](PF_6)$	50
Figure 3.3	A View of the Single Crystal X-Ray Structure of $[Ru(PPh_3)([9]aneS_3)(\mu\text{-}Cl)]_2(PF_6)_2$	55
Figure 3.4	A View of the Single Crystal X-Ray Structure of $[(PPh_3)Ru(DPF)(\mu\text{-}Cl)_2Cl]_2$	56
Figure 3.5	A View of the Single Crystal X-Ray Structure of $[Ru(PPh_3)([9]aneS_3)(\mu\text{-}Cl)_2Tl]_2(PF_6)_2$	59
Figure 3.6	An Alternative View of the Single Crystal X-Ray Structure of $[Ru(PPh_3)([9]aneS_3)(\mu\text{-}Cl)_2Tl]_2(PF_6)_2$	60
Figure 3.7	A Representatiion of the Complex $[Pt_3(CO)_3(PCy_3)_3Tl][Rh(C_8H_{12})Cl_2)]$	61
Figure 3.8	A Representation of the Complex $[\{C_6H_3(CH_3)_3\}_6Tl_4][GaBr_4]$	61
Figure 3.9	The Reaction of $TlPF_6$ with $[RuCl_2(PPh_3)([9]aneS_3)]$	62
Figure 3.10	The ^1H N.M.R. Spectrum (d^6-acetone) of $[Ru(PPh_3)([9]aneS_3)(\mu\text{-}Cl)]_2(PF_6)_2$	64
Figure 3.11	The ^1H N.M.R. Spectrum (d^6-acetone) of $[Ru(PPh_3)([9]aneS_3)(\mu\text{-}Cl)_2Tl]_2(PF_6)_2$	67
Figure 4.1	Resonance forms of CH_3NO_2 and $CH_2NO_2^-$	76
Figure 4.2	Nitromethane Tautomers	76
Figure 4.3	A Representation of $[Pd(Ph\text{-}N{=}N\text{-}Ph)(CH_3NO_2)_2]^+$	77
Figure 4.4	A Representation of $[(CH_2NO_2)Ru(H)(PPh_3)_3]$	77
Figure 4.5	A View of the Single Crystal X-Ray Structure of trans-bis(Dimethylglyoximato)-(nitromethyl)(pyridine)cobalt (III)	77
Figure 4.6	The Synthesis of $[Au_2\{(CH_2)_2PPh_2)\}_2(O_2CPh)2(CHNO_2)]$	78
Figure 4.7	^1H N.M.R. Spectrum of the product isolated in Section 4.2.1	79
Figure 4.8	^{13}C N.M.R. Spectrum of the product isolated in Section 4.2.1	80

Figure 4.9	A Representation of the Ortho-Metallated Complex, $[RuCl(C_6H_4PPh_2)([9]aneS_3)]$.	81
Figure 4.10	A View of the Single Crystal X-Ray Structure of $[RuCl(C_6H_4PPh_2)(NH\{SiMe_2CH_2PPh_2\}_2)]$	82
Figure 4.11	A Representation of the Furyl Complex, $[RuCl(C_4H_3O)(PPh_3)([9]aneS_3)]$.	82
Figure 4.12	A View of the Single Crystal X-Ray Structure of $[RuCl(C_4H_3O)(PPh_3)([9]aneS_3)].HPF_6$.	85
Figure 4.13	Representations of some Carbene Complexes of THF	87
Figure 4.14	A Representation of $[Mn(CO)_4(CHCH_2CH_2OC–)–Pt(PMe_3)_2]$	87
Figure 4.15	A Representation of $[CpMo(CO)_2(PPh_3)(C_4H_3O)]$	88
Figure 4.16	A Representation of $[Cp^*Ru(C_4H_4O)]Cl$	88
Figure 4.17	The ^{31}P N.M.R. Spectrum of the product isolated in Section 4.2.1	90
Figure 4.18	The ^1H N.M.R. Spectrum (d^6-acetone, 360MHz) of the product isolated in Section 4.2.1	91
Figure 4.19	The ^1H N.M.R. Spectrum (d^6-acetone, 360MHz, Irradiated at $\delta = 0.97$ p.p.m.) of the product isolated in Section 4.2.1	92
Figure 4.20	A Representation of the Ethyl Complex, $[Ru(Z(CH_2CH_3)_n)Cl(PPh_3)([9]aneS_3)](PF_6)_m$	93
Figure 4.21	The F.A.B. Mass Spectrum of the product isolated in Section 4.2.1	97
Figure 4.22	The Synthesis of the Furyl and Ethyl Complexes	99
Figure 4.23	Possible Intermediates in the Conversion of Et_2O to a Furyl Ligand	101
Figure 4.24	Representations of Dihydrofurans	101
Figure 4.25	The Disproportionation Reaction of THF	103
Figure 4.26	The Photochemical Cyclisation of Unsaturated Ethers Catalysed by $Cu(CF_3SO_2)$	105

Figure 4.27	The ^1H N.M.R. Spectrum of the product of $[RuCl_2(PPh_3)([9]aneS_3)]$ with $TlPF_6$ in THF	109
Figure 4.28	The F.A.B. Mass Spectrum of the product of $[RuCl_2(PPh_3)([9]aneS_3)]$ with $TlPF_6$ in THF	110
Figure 4.29	A Possible Structure of the 2,3– or 2,5– DHF Polymer	111
Figure 4.30	The ^1H N.M.R. Spectrum of $[RuCl(NCCH_2CH_3)(PPh_3)([9]aneS_3)]PF_6$	117
Figure 4.31	The ^{13}C N.M.R. Spectrum of $[RuCl(NCCH_2CH_3)(PPh_3)([9]aneS_3)]PF_6$	118
Figure 4.32	The ^1H N.M.R. Spectrum of Prolabo CH_3NO_2	122
Figure 4.33	The G.C. / Mass Spectrum of Prolabo CH_3NO_2	125
Figure 4.34	The ^1H N.M.R. Spectrum of $[RuCl(NC_3H_3O)(PPh_3)([9]aneS_3)]PF_6$	126
Figure 4.35	The ^{13}C N.M.R.spectrum of $[RuCl(NC_3H_3O)(PPh_3)([9]aneS_3)]PF_6$	127
Figure 4.36	A View of the X-Ray Structure of $[RuCl(NC_3H_3O)(PPh_3)([9]aneS_3)]PF_6$	130
Figure 5.1	Five embered Heterocycles	143
Figure 5.2	A Representation of $[Os(NH_3)_5(2,3\text{–}\eta^2\text{–pyrrole})]^{2+}$	144
Figure 5.3	Possible Modes of Co-ordination of Thiophene	144
Figure 5.4	A Representation of $[\{(C_4H_3S)CH_2Cp\}Ru(PPh_3)_2]$	144
Figure 5.5	A View of the Single Crystal X-Ray Structure of $[RuCl(C_4H_8S)(PPh_3)([9]aneS_3)](PF_6)$	149
Figure 5.6	The Proposed Active Species in the Catalytic Oxidation of Thioethers to Sulfoxides by $[RuCl_2(DMSO)_4]$	152
Figure 5.7	A Representation of $[CpFe(CO)(C_4H_3S)]$	153
Figure 5.8	A Representation of $[Cp_2Mo_2(CO)_4(C_4H_4S)]$	153
Figure 5.9	A Representation of $[Pt(PEt_3)_2(SC_4H_7)]$	153
Figure 5.10	A Representation of $[Os(CO)_9(H)(PPh_3)(SC_4H_3)]$	153

Figure 5.11	A Representation of [RuCl(THT)(1,5–DTCO)(1,5–DTCO-O)] (BPh_4)	155
Figure 5.12	A Representation of a Possible Ru Vinyl Thioether Complex	158
Figure 6.1	A View of the Single Crystal X-Ray Structure of [$RuCl_2$([14]aneS_4)]	165
Figure 6.2	A View of the Single Crystal X-Ray Structure of [Ru(CO)(PPh_3)([12]aneS_4)]$^{2+}$	165
Figure 6.3	A View of the Single Crystal X-Ray Structure of [$RhCl_2$([14]aneS_4)](PF_6)	167
Figure 6.4	A View of the Single Crystal X-Ray Structure of [$RhCl_2$([16]aneS_4)](PF_6)	167
Figure 6.5	A View of the Single Crystal X-Ray Structure of [Rh_2([14]aneS_4)$_2$](PF_6)	168
Figure 6.6	A View of the Single Crystal X-Ray Structure of [Rh_2(Cp^*)$_2Cl_2$([14]aneS_4)$_2$](PF_6)	168
Figure 6.7	The ^{1}H N.M.R. Spectrum (d^6-acetone) of the yellow product isolated from the reaction of $TlPF_6$ to [$RuCl_2$([14]aneS_4)]	172
Figure 6.8	A View of the Single Crystal X-Ray Structure of [RuCl(PPh_3)([14]aneS_4)](PF_6)	173
Figure 6.9	A View of the Single Crystal X-Ray Structure of [RuCl(PPh_3)([16]aneS_4)](PF_6)	173
Figure 6.10	A View of the Single Crystal X-Ray Structure of [Ru(NCMe)(PPh_3)([12]aneS_4)](PF_6)$_2$	174
Figure 6.11	A View of the Single Crystal X-Ray Structure of [Ru(NCMe)$_2$([16]aneS_4)](PF_6)$_2$	174
Figure 6.12	The ^{1}H N.M.R. Spectrum (CD_3CN) of [RhCl(PPh_3)([12]aneS_4)](PF_6)$_2$	177
Figure 6.13	The ^{13}C N.M.R. Spectrum (CD_3CN) of [RhCl(PPh_3)([12]aneS_4)](PF_6)$_2$	178

Figure 6.14	The ^{31}P N.M.R. Spectrum (CD_3CN) of $[RhCl(PPh_3)([12]aneS_4)](PF_6)_2$	179
Figure 6.15	A View of the Single Crystal X-Ray Structure of $[RhCl(PPh_3)([12]aneS_4)](PF_6)_2$	183
Figure 6.16	A View of the Single Crystal X-Ray Structure of $[RhCl(PEt_2Ph)([12]aneS_4)](PF_6)_2$	184
Figure 7.1	The Ligands Discussed in Chapter 7	198
Figure 7.2	Cis and Trans Isomerisation in Cyclic Sulfoxides	199
Figure 7.3	The General Synthesis of Sulfoxides and Sulfones	200
Figure 7.4	A Representation of the Sulfonium Salt, $[C_6H_{11}S_3]^+$	204
Figure 7.5	A Representation of the Dithioether Dication	204
Figure 7.6	A View of the Single Crystal X-Ray Structure of $[Fe(O[9]aneS_3)([9]aneS_3)]^{2+}$	206
Figure 7.7	A View of the Single Crystal X-Ray Structure of $O_6[9]aneS_3$	210
Figure 7.8	An Alternative View of the Single Crystal X-Ray Structure of $O_6[9]aneS_3$	210
Figure 7.9	Possible Compounds Synthesised when Oxidising $[9]aneS_3$	212
Figure A.1	A View of the Single Crystal X-Ray Structure of $[Rh([9]aneS_3)([9]aneS_3\text{-}H)]^{2+}$	229
Figure A.2	The ^1H N.M.R. Spectrum of $[Rh([9]aneS_3)([9]aneS_3\text{-}H)]^{2+}$	232
Figure A.3	The Possible Structures Formed when Double Deprotonating $[Rh([9]aneS_3)_2]^{3+}$	233

List Of Schemes

		page
Scheme 1.1	The Metathetical Reaction for the Definition of the Thermodynamic Macrocyclic Effect	4
Scheme 1.2	Oxidation of Organic Substates by O_2	15
Scheme 1.3	The Proposed Catalytic Mechanism for the Oxidation of Organic Substrates by Cytochrome P_{450}	17
Scheme 1.4	The Proposed Mechanism for the Reduction of O_2 by a Co-facial Porphyrin Complex	20
Scheme 1.5	The Proposed Mechanism for the Catalytic Conversion of H_2 and CO to H_2CO by $[Rh(OEP)]_2$	24
Scheme 1.6	The Proposed Mechanism for the Catalytic Conversion of CO_2 to CO by $[Ni([14]aneN_4)]^{2+}$	25
Scheme 1.7	The Proposed Mechanism for the Catalytic Epoxidation of an Alkene by PhIO in the presence of Metalloproteins	26
Scheme 1.8	Chiral Epoxidations of Alkenes Catalysed by Chiral Metalloproteins	26
Scheme 2.1	The Synthesis of $[9]aneS_3$	28
Scheme 2.2	The Synthesis of $[9]aneS_3$ using the $\{Mo(CO_3)\}$ fragment as a Catalyst	29
Scheme 2.3	The Synthesis of a Thioether Cage Ligand	31
Scheme 2.4	The Synthesis of $(Benzo)_2$–$[18]aneS_6$ and Benzo–$[9]aneS_3$	40
Scheme 3.1	The Interconversion of $[Ru(PPh_3)([9]aneS_3)(\mu\text{-}Cl)]_2(PF_6)_2$ and $[Ru(PPh_3)([9]aneS_3)(\mu\text{-}Cl)_2Tl]_2(PF_6)_2$ and $[Ru(NCMe)Cl(PPh_3)([9]aneS_3)](PF_6)$	68
Scheme 4.1	The Formation of $[Co^{(III)}(OEP)(C_4H_7O)]$	86
Scheme 4.2	The Synthesis of $LiCu(C_4H_8O)_2$	88
Scheme 4.3	The Reaction of $[RuCl_2(PPh_3)([9]aneS_3)]$ with $TlPF_6$ in CH_3NO_2 in the Presence of a Proposed Furyl Source	100

Scheme 4.4	The Conversion of Methylhexene to Benzene and Toluene	104
Scheme 4.5	The Proposed Mechanism for the Synthesis of $[CpMo(CO)_2(PPh_3)(C_4H_3O)]$	106
Scheme 4.6	The Synthesis of THF	119
Scheme 5.1	The Conversion of Thiophene to Furan by $[Cp^*Rh(C_4Me_4S)]^{2+}$	145
Scheme 5.2	The Reaction of $[RuCl_2(PPh_3)([9]aneS_3)]$ with $TlPF_6$ and THT	148
Scheme 7.1	Oxidation to Polysulfoxides	201
Scheme 7.2	The Unselective Oxidation of Thioethers	201
Scheme 7.3	The Selective Oxidation of Thioethers	202
Scheme 7.4	The Electrochemical Oxidation of Thioethers	202
Scheme 7.5	The Photochemical Oxidation of Thioethers	203
Scheme 7.6	The Oxidation of Thioethers by ROOH	211
Scheme 7.7	The Proposed Mechanism for the Oxidation of Thioethers by Peracids	214
Scheme 7.8	The Oxidation of Thioethers by Periodate	214
Scheme 7.9	The Oxidation of Thioethers by PhIO	215
Scheme 7.10	The Proposed Mechanism for the Oxidation of Thioethers by $PhI(OAc)_2$	215
Scheme 7.11	The Oxidation of Co-ordinated $[9]aneS_3$	217
Scheme 7.12	The Formation of an Oxy-Bridged Species	219
Scheme 7.13	The Oxidation of an Oxy-Bridged Species	219
Scheme 7.14	Sulfoxide / Thioether Oxygen Exchange	220
Scheme 7.15	The Interconversion of a Disulfoxide to a Sulfone	220
Scheme A.1	The Deprotonation of Co-ordinated $[9]aneS_3$	230
Scheme A.2	The Double Deprotonation of Co-ordinated $[9]aneS_3$	230
Scheme A.3	The Formation of a Vinyl-Thioether Moiety from $[Ru(L_4)(PPh_3)_2]$	231

List Of Tables

		Page
Table 1.1	Biologically Important Transition Metals	11
Table 3.1	The Synthesis of Half Sandwich Ru [9]aneS$_3$ Complexes	49
Table 3.2	The Synthesis of Ru [9]aneS$_3$ Half Sandwich Complexes	50
Table 3.3	^{31}P N.M.R. Spectral Data of Complexes of the Type [Ru(PR$_3$)([9]aneS$_3$)(X)(Y)]$^{n+}$	51
Table 3.4	Selected Bond Lengths (Å), Angles (°) and Torsion Angles (°) with Standard Deviations for [Ru(PPh$_3$)([9]aneS$_3$)(μ-Cl)]$_2$(PF$_6$)$_2$	54
Table 3.5	Selected Bond Lengths (Å), Angles (°) and Torsion Angles (°) with Standard Deviations for [Ru(PPh$_3$)([9]aneS$_3$)(μ-Cl)$_2$Tl]$_2$(PF$_6$)$_2$	58
Table 4.1	Selected Bond Lengths (Å), Angles (°) and Torsion Angles (°) with Standard Deviations for [RuCl(C$_4$H$_3$O)(PPh$_3$)([9]aneS$_3$)].HPF$_6$	84
Table 4.2	X-Ray Crystallographic Data for a Series of Ru(II) [9]aneS$_3$ Complexes	83
Table 4.3	Comparison of ^{1}H N.M.R. and ^{31}P N.M.R. Spectra	94
Table 4.4	The N.M.R. Spectral Data for [Ru(Z(CH$_2$CH$_3$)$_n$)Cl(PPh$_3$)([9]aneS$_3$)](PF$_6$)$_m$	94
Table 4.5	The N.M.R. Spectral Data for [RuCl(C$_4$H$_3$O)(PPh$_3$)([9]aneS$_3$)]	95
Table 4.6	The Boiling and Freezing Points of CH$_3$NO$_2$, EtCN and Isoxazole	124
Table 4.7	Selected Bond Lengths (Å), Angles (°) and Torsion Angles (°) with Standard Deviations for [RuCl(NC$_3$H$_3$O)(PPh$_3$)([9]aneS$_3$)]PF$_6$	129
Table 4.8	Experimental Conditions for the Reaction of [RuCl$_2$(PPh$_3$)([9]aneS$_3$)] with TlPF$_6$	138

Table 5.1	Selected Bond Lengths (Å), Angles (°) and Torsion Angles (°) with Standard Deviations for $[RuCl(C_4H_8S)(PPh_3)([9]aneS_3)](PF_6)$	150
Table 5.2	Anisotropic Thermal Parameters in $Å^2$ for $[RuCl(C_4H_8S)(PPh_3)([9]aneS_3)](PF_6)$	151
Table 5.3	Experimental Conditions	163
Table 6.1	Selected Spectral Properties of $[Rh(PR_3)Cl([12]aneS_4)](PF_6)_2$	180
Table 6.2	Selected Bond Lengths (Å), Angles (°) and Torsion Angles (°) with Standard Deviations for $[Rh(PPh_3)Cl([12]aneS_4)](PF_6)_2$	182
Table 6.3	A Comparison of Bond Lengths(Å) of Rh [n]$aneS_4$ Complexes	185
Table 6.4	Experimental Conditions for the Reaction of [12]$aneS_4$ and $[RhCl_3(PMe_2Ph)_3]$	195
Table 6.5	Experimental Conditions for the Reaction of [12]$aneS_4$ and $[RhCl_3(PEt_2Ph)_3]$	196
Table 6.6	Experimental Conditions for the Attempted Synthesis of $[RhCl(PR_3)([14]aneS_4)](PF_6)_2$ from $[RhCl_2([14]aneS_3)]PF_6$	196
Table 6.7	Experimental Conditions for the Attempted Synthesis of $[RhCl(PR_3)[16]aneS_4](PF_6)_2$ from $[RhCl_2([14]aneS_3)]PF_6$	197
Table 7.1	^1H N.M.R. and ^{13}C N.M.R. Spectral Data of t-butylthian-1-oxide	199
Table 7.2	The Internal Geometry of Free and Co-ordinated DMSO	204
Table 7.3	Selected Bond Lengths (Å), Angles (°) and Torsion Angles (°) with Standard Deviations for O_6[9]$aneS_3$	209
Table 7.4	The ir Spectra of the Oxidised Products	211
Table 7.5	Experimental Conditions for the oxidation of [9]$aneS_3$ with H_2O_2 and t-BuOOH	222
Table 7.6	Experimental Conditions for the Oxidation of [9]$aneS_3$ by Periodate	225

Table 7.7 Experimental Conditions for the Oxidation of [9]aneS_3 by $NaBrO_2$ 226

Table 7.8 Experimental Conditions for the Oxidation of [9]aneS_3 by PhIO or $PhI(OAc)_2$ 226

Table 7.9 Experimental Conditions for the Oxidation of [9]aneS_3 Catalysed by [Fe(TPP)Cl] 226

Table 7.10 Experimental Conditions for the Oxidation of [9]aneS_3 metal Complexes 227

Chapter One

AN INTRODUCTION TO MACROCYCLIC COMPLEXES

1.1 General

A considerable body of literature exists in the area of macrocyclic co-ordination chemistry, but it is only within the last thirty years that synthetic strategies for new macrocycles have been developed[1-6]. The first synthesis of a new macrocyclic ligand was effected in 1960 by Curtis and co-workers[7], and more recently, the development of high yield and reliable template synthetic methods for new macrocycles[8] has led to considerable interest in this field of chemistry.

A macrocyclic compound is generally defined as a cyclic compound with nine or more members (including heteroatoms) with at least three donor atoms[1, 2]. In general, macrocyclic complexes are characterised by their increased kinetic inertness and thermodynamic stability compared with their open-chain analogues and this phenomenon is referred to as the Macrocyclic Effect, which will be discussed in Section 1.2. Sections 1.3–1.6 will present a brief introduction to some aspects of general macrocyclic chemistry. Chapter 2 will discuss thioether macrocycles and their transition metal complexes. The ligands and abbreviations used throughout this work are shown in
Figure 1.1

1.2 The Thermodynamic Macrocyclic Effect

The term 'Macrocyclic Effect' was first used by Cabbiness and Margerum[9] to describe the enhanced stability and kinetic inertness of $[Cu(Me_6[14]aneN_4)]^{2+}$ compared to $[Cu(2\text{–}3\text{–}2\ tet)]^{2+}$. These ligands and complexes are shown in Figure 1.2.[9]

Figure 1.1 Ligands and their Abbreviations.

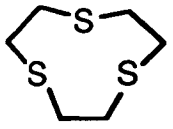

[9]aneS$_3$

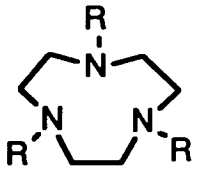

R=H, [9]aneN$_3$
R=CH$_3$, Me$_3$[9]aneN$_3$

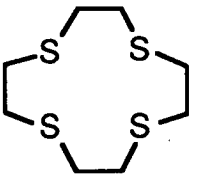

[12]aneS$_4$

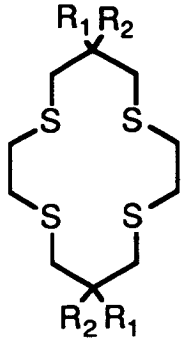

R$_1$=R$_2$=H, [14]aneS$_4$
R$_1$=H,R$_2$=CH$_3$, Me$_2$[14]aneS$_4$
R$_1$=R$_2$=CH$_3$, Me$_4$[14]aneS$_4$

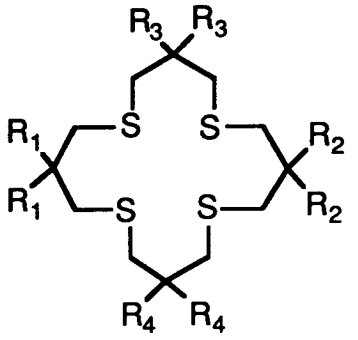

R$_1$=R$_2$=R$_3$=R$_4$=H, [16]aneS$_4$
R$_1$=CH$_3$,R$_1$=R$_2$=R$_3$=H, Me$_2$ [16]aneS$_4$
R$_1$=R$_2$=CH$_3$,R$_3$=R$_4$=H, Me$_4$[16]aneS$_4$
R$_1$=R$_2$=R$_3$=R$_4$=CH$_3$, Me$_8$[16]aneS$_4$

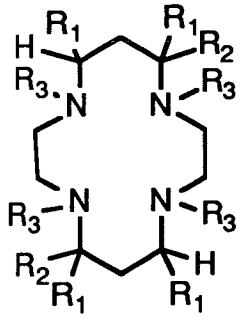

R$_1$=R$_2$=R$_3$=H, [14]aneN$_4$
R$_1$=CH$_3$,R$_2$=R$_3$=H, Me$_4$[14]aneN$_4$
R$_1$=R$_2$=CH$_3$,R$_3$=H, Me$_6$[14]aneN$_4$
R$_1$=R$_2$=R$_3$=CH$_3$, Me$_{10}$[14]aneN$_4$

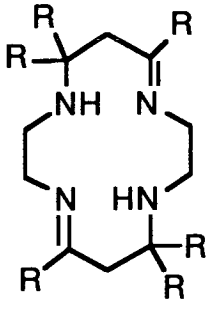

R=H, [14]dieneN$_4$
R=CH$_3$, [14]dieneN$_4$

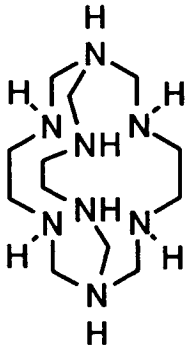

Sep

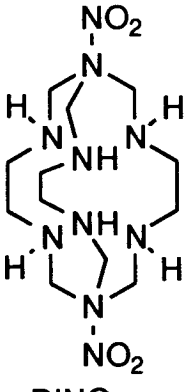

DiNOsar

Figure 1.1 cont

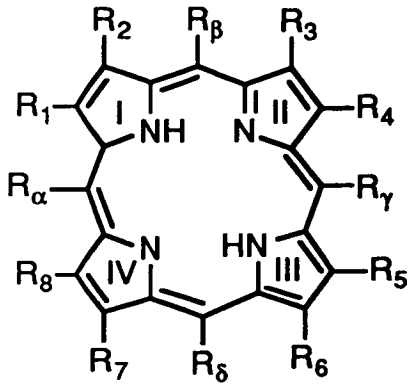

Porphyrin
R_1-R_8 = H, $R_{\alpha\beta\gamma\delta}$ =Ph ; TPP
R_1-R_8 = H, $R_{\alpha\beta\gamma\delta}$ = Mesityl ; TMP
R_1-R_8 = H, $R_{\alpha\beta\gamma\delta}$ = $PhSO_3^-$; TPPS
R_1-R_8=Et, $R_{\alpha\beta\gamma\delta}$ = H ; OEP

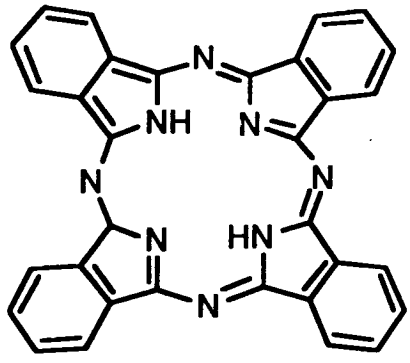

Phthalocyanine

In general the abbreviations used throughout this work are based on the rules proposed in Ref. 2. In summary, the size of the macrocycle is expressed in Arabic numerals enclosed in square brackets, a term denoting the saturation (e.g. ene, ane, diene) follows, and the number and nature of the ligating atoms is stated finally. Porphyrins and Phthalocyanines are abbreviated in the standard way.

Figure 1.2 The Kinetic Rate of Formation and Dissociation of $[Cu(Me_6[14]aneN_4)]^{2+}$ and $[Cu(2\text{-}3\text{-}2\ tet)]^{2+}$.

$$Cu^{2+} + L \rightleftharpoons [Cu(L)]^{2+}$$

Kf = Kinetic rate constant for the formation of $[Cu(L)]^{2+}$
Kd = Kinetic rate constant for the dissociation of $[Cu(L)]^{2+}$

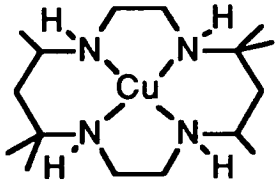

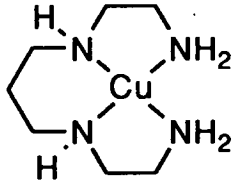

$Kf(M^{-1}sec^{-1})$	5.8×10^{-2}	8.9×10^{4}
$Kd(sec^{-1})$	3.6×10^{-7}	4.1
$Ks = Kf/Kd\ (M^{-1})$	1.61×10^{5}	2.17×10^{4}

The thermodynamic macrocyclic effect is defined as the Gibbs free energy ($\Delta G_f = \Delta H_f - T\Delta S_f$) for the metathetical reaction shown in Scheme 1.1. The thermodynamic origins of the Effect are still under discussion and the exact size of the enthalpic and entropic terms, as well as the magnitude of the Effect itself, depends greatly on the nature of the ligands, as well as the solvent and metal ions involved[1-3, 10-12].

Scheme 1.1 The Metathetical Reaction for the Definition of the Thermodynamic Macrocyclic Effect

$$[M(L_{open})]^{n+} + L_{mac} \rightleftharpoons [M(L_{mac})]^{n+} + L_{open}$$

L_{mac} = macrocyclic ligand L_{open} = open chain ligand

A major contribution to the **enthalpic** term of the Macrocyclic Effect is the conformational changes the ligands have to make in order to complex a metal ion. L_{open} has to change from a linear minimum energy conformation to a cyclic one in order to complex a metal ion, whereas L_{mac} is said to be 'pre-organised' for co-ordination[13, 14].

The exact size of the energy required to change conformation in the macrocyclic ligand will depend on the extent of reorganisation required for the ligand to complex to a metal ion. For example, in [14]aneS_4 the free ligand adopts a conformation in the solid state in which all the sulfur atoms lie in the *exo*-conformation, that is with the sulfur donor lone pairs directed away from the macrocyclic cavity[15]. Clearly, for the ligand to co-ordinate to a metal ion, a reorganisation of the ligand is required. However in [9]aneS_3, all three sulfurs are *endodentate* [16], so in principle very little change is required for complexation to occur. [9]aneS_3 may therefore be regarded as 'pre-organised' for complexation to a metal ion[14]. This concept is illustrated diagrammatically in Figure 1.3.

Figure 1.3 Representations of the Free Ligands and their Complexes

[14]aneS4 - requires a high degree of conformational change

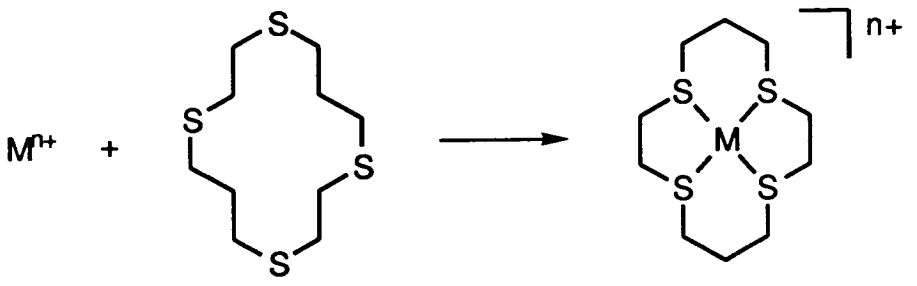

[9]aneS3 - pre-organised for complexation

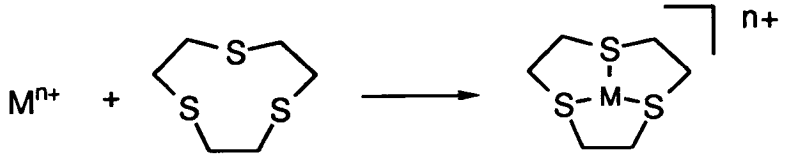

Another contribution to the enthalpic term arises from the difference in solvation energies of L_{mac} and L_{open}. This depends critically on the ring size of the macrocycle, the solvent medium, and the metal ion to be complexed. Margerum and co-workers measured ΔH_f for $[Ni([14]aneS_4)]^{2+}$ [17], $[Ni(TTT)]^{2+}$ [17], $[Ni([14]aneN_4)]^{2+}$ [18], $[Ni(2\text{-}3\text{-}2tet)]^{2+}$ [18] (Figure 1.4). The difference in energy between the tetrathioether ligands was substantially lower than the difference between the tetraaza ligands. This was attributed to the difference in solvation energies between N and S. In thioether ligands there is very little difference in the solvation energies of L_{mac} and L_{open}, the enthalpic contribution to the Macrocyclic Effect is almost entirely due to the conformational changes described above. In tetraaza ligands, due to hydrogen bonding, there is a large difference in the solvation energies of the ligands and hence a larger enthalpic contribution to the Macrocyclic Effect.[18]

Figure 1.4 A Representation of $[Ni([14]aneS_4)]^{2+}$ and $[Ni([14]aneN_4)]^{2+}$ and their Open-Chain Analogues.

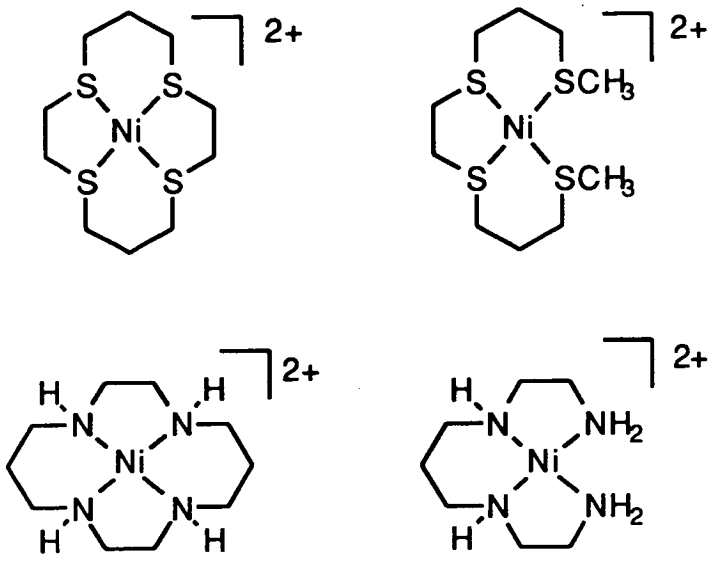

The enthalpic component is also largely affected by the size of the metal ion, and the macrocyclic cavity hole size. A mis-match between the size of the metal and the ligand will result in weaker M–L bands and/or an increase in macrocyclic ring strain, which in turn will reduce the enthalpic term[14, 19, 20]. Thus, in $[Cu([13]aneN_4)]^{2+}$ a relative mis-match between the cavity and the metal ion radius forces the complex to adopt a strained stereo chemistry [20], which should result in a lower enthalpic contribution to the Macrocyclic Effect.

The **entropic** contribution to the Macrocyclic Effect is related to the number of degrees of freedom available in the system. On complexation, the degrees of freedom of the macrocyclic ligand and the open-chain ligand will be reduced. However, since the free open-chain ligand has more degrees of freedom than the free macrocyclic ligand, there is an overall **increase** in the entropy on release of the free open-chain ligand[13, 14].

1.3 The Kinetic Macrocyclic Effect

The kinetic inertness of macrocyclic complexes is well-established and arises from the kinetic Macrocyclic Effect, which was analysed in a study of formation and dissociation rate constants of $[Cu(Me_6[14]aneN_4)]^{2+}$ and its open-chain analogue. The results and the reactions are shown in Figure 1.2[21].

The reason for the differences between the rate constants was explained by Busch *et al* [22], and termed the 'Multiple Juxtapositional Fixedness'. During the formation and, more noticeably, the dissociation of macrocyclic complexes, considerable strain is placed on the rigid framework of the macrocyclic complexes, leading to difficulties in both forming and dissociating the ligand from the metal ion. In the case of the open-chain ligands, complexation and decomplexation reactions 'enfold' or 'unzip' in a relatively easy manner, as illustrated for both cases in Figure 1.5.

Figure 1.5 A Representation of the Multiple Juxtapositional Fixedness

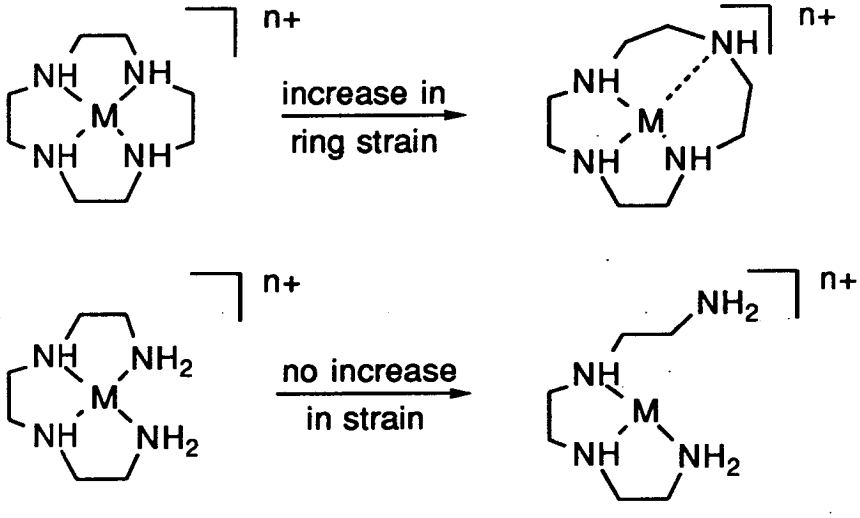

1.4 The Stabilisation of Unusual Oxidation States

The enhanced kinetic inertness and thermodynamic stability has contributed to the ability of macrocyclic complexes to stabilise metals in unusual oxidation states[1, 3-6, 23-25]. The uncommon Ni(I) and Ni(III) oxidation states[27, 35] have been stabilised by aza macrocycles. The complexes $[Ni^{(III)}L_n]^{3+}$ (n = 1, L = Me_x[12–16]aneN_4, x = 0, 1 , 4 , 6 , 10 [26-43], Me_6[14]dieneN_4[1, 2]; n = 2, L = [9]aneN_3[46-48]) and $[Ni^{(I)}L_n]^{+}$(n = 1, L = Me_x[12–16]aneN_4, x = 0, 1, 4, 6, 10[37-39,49], Me_6[14]dieneN_4[44]) are formed from their Ni(II) analogues by electrochemical[37-40, 43-47, 49], chemical[36, 48] or by pulse radiolytical[49] methods. Ni(I) and/or Ni(III) have been suggested as catalytic intermediates in the interconversion of H_2 and H^+ in Nickel *Hydrogenases*[50]. The structure of these enzymes is unclear, but it is proposed that there is one nickel per molecule, as well as an [4Fe–4S] iron cluster[50]. Although which Ni oxidation state is involved *in vivo* has not been confirmed, the complexes $[Ni(L)_n]^{m+}$ described above have proven that both Ni(I) and Ni(III) species can be generated with these ligands[50-52]. Monovalent Cu(III) species are also proposed in a number of biological systems (e.g. galactose oxidase)[28] and in order to gain a greater understanding of these enzymes, the formation of Cu(III) macrocyclic model systems has been studied[53]. Some aspects of macrocyclic chemistry relevant to bioinorganic chemistry will be discussed in Section 1.5.

The extremely rare oxidation state, Hg(III), has been characterised by electrochemical oxidation, at low temperature, of $[Hg([14]aneN_4)]^{2+}$, the resulting complex $[Hg([14]aneN_4)]^{3+}$ having a half life of 5 seconds at 77K [54].

Likewise, the rare d^7 second and third row metal ions[29, 55, 56] have been stabilised using macrocyclic complexes. They are usually formed by one electron reduction by electrochemical or pulse radiolytical methods. Rh(II) complexes are usually dimeric[55] and there are a number of dimeric Rh(II) porphyrin complexes in the literature[56]. If, however, the porphyrin is substituted at the α, β, γ and δ positions, as in TPP or TMP, it is possible to synthesise a monomeric

$[Rh^{(II)}(Por)]$. These complexes can be prepared by reducing the $[Rh^{(III)}(Por)\ X]$ complexes (X = Cl, CH_3, dimethylamine) [57-59] or directly by reacting $[Rh(CO)_2Cl_2]_2$ with H_2TPP in acetic acid[60]. $[Rh^{(II)}(Por)]$ reacts with RCH_3 (R = aryl)[61] and alkenes[62] to form $[Rh(CH_2R)(Por)]$ (Por = OEP, TPP) and $[(Por)RhCH_2(R)Rh(Por)]$ (Por = OEP). $[Rh^{(II)}(Pc)]$ (Pc = Phthalocyanine) complexes have also been synthesised[63]. The Rh(II) complexes also act as catalysts in many systems and the use of macrocyclic complexes as catalysts will be discussed in Section 1.6. $[Rh^{(II)}L]^{2+}$ complexes can also be synthesised by using hexaaza cage compounds such as diNOsar and sep[64]. These cage ligands can also be used to stabilise the d^7 Pt(III) metal ion, these $[Pt^{(III)}L]^{3+}$ complexes are formed by reduction of $[Pt^{(IV)}L]^{4+}$ [1, 3, 65], while $[Pd([9]aneN_3)_2]^{3+}$can be generated by electrochemical oxidation of the Pd(II) precursor complex, $[Pd^{(II)}([9]aneN_3)_2]^{2+}$[66]. The Pd(III) complex is surprisingly stable in H_2O, and can be synthesised directly from $PdCl_2$[1, 2]. Thioether macrocycles, in particular $[9]aneS_3$, have been very successful in stabilising d^7 metal centres and other rare metal oxidation states[26]. These complexes will be discussed in Chapter 2.

The two-electron oxidation of Fe(III) porphyrins, chlorins (hydrogenated porphyrins) and phthalocyanines is of great importance in understanding the mechanism of a number of haem containing enzymes, for example in Cytochrome P_{450} [1, 3]. The one-electron oxidation of Fe(II) porphyrins can result in a Fe(IV) oxo species, $[(O)Fe^{(IV)}(Por)]$. The further oxidation of this complex can result in the formation of π-cation radical $[(O)Fe^{(IV)}(Por\cdot)]^+$ [67-73]. These complexes are highly unstable; however, a stable complex (at 8°C) has been synthesised with a porphyrin substituted with 12 Phenyl rings (1→8 = phenyl, $\alpha = \beta = \gamma = \delta$ = (2, 6 dichloro)phenyl)[72]. A π-radical cation of [Fe(OEP)Cl] has been characterised by X-ray crystallography and reveals it to be dimeric in the solid state[73]. Porphyrin π-cation radicals have been synthesised as a metal free species[74] and also for a number of other metals (for example Co(III), Mg(II),

Li(I), Zn(II) and Fe(III)[75]). These complexes could be utilised in a number of areas of chemistry, such as molecular devices[54], modelling biological systems (Section 1.5) and catalysis (Section 1.6).

1.5 Biological Systems

Several transition metals are known to be involved with biological processes. The main uses of these metals are in catalysis, storage and sequestering and transportation. The role of the metal and examples of enzymes in which they are present are shown in Table 1.1[76, 77].

Metalloproteins are proteins that incorporate one or more metal atoms as a normal part of their structures, in some cases it is possible to remove these metals without collapse of the overall structure[78]. These naturally occurring molecules are frequently extremely large, and so understanding the function of the metal, and in some cases identifying the metal itself, is a major challenge. In order to increase our understanding of a particular biological system, models incorporating the structural information known are synthesised. These model complexes are often interesting in themselves, as they can exhibit unusual stereochemistry or may be catalysts in their own right, usually being less selective and more versatile than the original systems[1, 4]. The metalloporphyrin models for Cytochrome P_{450} will be discussed in the next Section 1.6.

The sequestering of minerals such as Fe and V is essential for small microbes, since they have very little storage capacity and must therefore constantly acquire nutrients. Siderophores are used to sequester Fe from the environment[79, 80], and an example of one of these siderophores, enterobectin is shown in Figure 1.6. The complex $[Fe(ent)]^{3-}$ has not been studied by X-ray

crystallography, but the structure of Fe model complexes[81-83] and $[V(ent)]^{2-}$ [84] have been studied and some of the structures are shown in Figure 1.7.

Table 1.1 BIOLOGICALLY IMPORTANT TRANSITION METALS

METAL	FOUND	FUNCTION	ROLE/ENZYMES
Vanadium	All lower plants All animals	Not fully known Deficiency retards growth	Vanadium containing Nitrogenase ($N2+6H^+ +6e^- \rightarrow 2NH_3+3H_2O$)
Chromium	All higher animals	RNA synthesis	No enzymes known
Molybdenum	All organisms	Electron transfer	Mo-containing Nitrogenases
		Enzyme catalysts	Nitrate reductases ($NO_3^- +8e^- +9H^+ \rightarrow 2NH_3+3H_2O$ CO Dehydrogenases ($CO+H_2O \rightarrow CO+2H^+ +2e^-$)
Tungsten	Some bacteria	Unknown	Unknown/promotes growth of some bacteria
Iron	Almost all organisms	Enzyme catalysts	e.g. Haemoglobin, Myoglobin, Catalases ($2H_2O_2 \rightleftharpoons 2H_2O+O_2$)
Cobalt	All animals Not higher plants Most bacteria	Enzyme catalysts	Coenzyme B_{12} Isomerases C-C band formation (and cleavage)
Nickel	Most organisms	Enzyme catalysts	Co Dehydrogenase ($CO+H_2O \rightleftharpoons CO_2+2H^+ +2e^-$) Some Hydrogenases ($H_2 \rightleftharpoons 2H^+ +2e^-$)
Copper	All aerobic organisms	Enzyme catalysts	e.g. Galactose Oxidase (Oxidation) Plastocyanin Azurin
Zinc	All(?) organisms	DNA production	e.g. Carbonic anhydrase ($CO+H_2O \rightleftharpoons H_2CO_3 \rightleftharpoons H^+ +HCO_3^-$)
		Enzyme catalysts	Carboxypeptidase

Figure 1.6 A Representation of Enterobectin

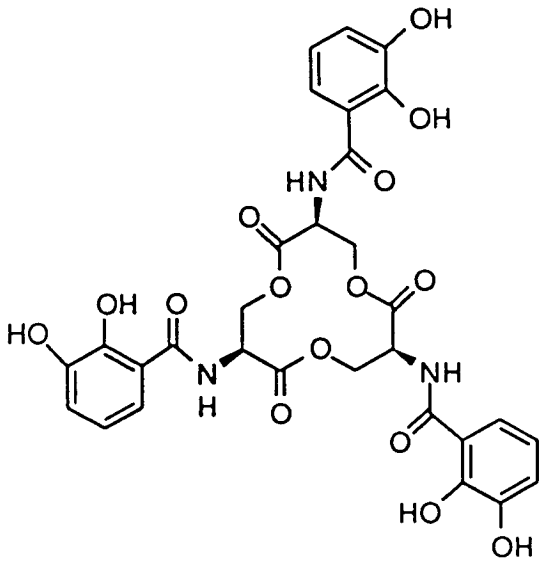

Figure 1.7 Models of Enterobectin

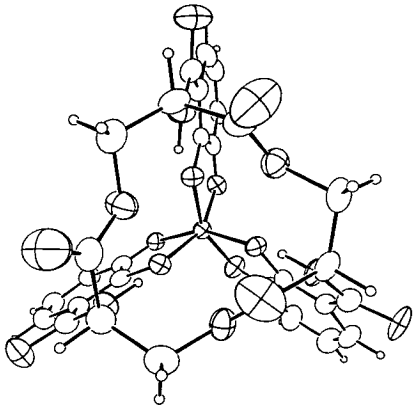

$[V(ENT)]^{2-}$

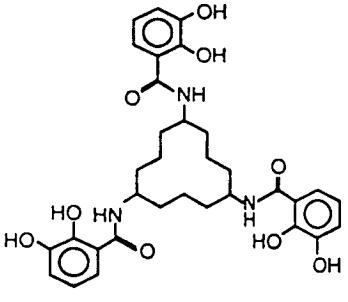

Carbocyclic Derivative

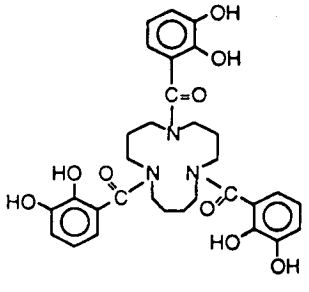

Cycam

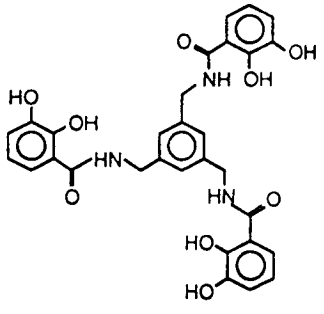

Mecam

Several different methods exist for transportation and storage of Fe. The naturally occurring metalloproteins are transferrins and ferritins. Transferrins have a molecular weight of about 80,000 and consist of a single polypeptide chain, which binds two Fe(III) ions. Transferrin is not well understood but when the Fe(III) is reduced to Fe(II) the iron is released from the enzyme[85]. Although no precise structure of any Ferritin is known, the compounds are reasonably well characterised. A crystal structure of an apoferritin (the protein with no Fe in it) consists of 24 equivalent subunits, which are arranged in a hollow spherical shell and the inner cavity is around 70Å in diameter[86]. The crystal structure of the core cannot be studied, since it does not have a definite orientation with respect to the outer shell. The core is filled with an Fe(III) oxyhydroxophosphate complex. An EXAFS spectrum suggests that each of the Fe(III)'s are surrounded by 6 or 7 oxygens at an average distance of 1.92 Å with 7±1 Fe(III) neighbours at an average distance of 3.95Å[86]. This core has been modelled structurally and the model also mimics the chemical and spectral properties of the metalloprotein Ferritin, and this is shown in Figure 1.8[87].

Figure 1.8 A View of the Model of the Core of Ferritin

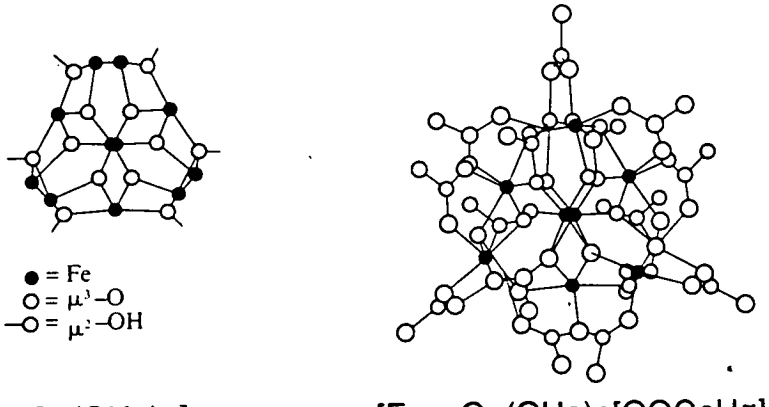

$[Fe_{11}O_6(OH_2)_6]$ core

$[Fe_{11}O_6(OH_2)_6[OOC_6H_5]_{15}$

A large number of metalloproteins are known to contain the tetrapyrrole unit[1, 6-8, 29, 88]. Chlorophyll a and b initiate the photoredox process, photosynthesis, in green plants and bacteria, both are illustrated schematically in Figure 1.9. Two additional ligands co-ordinate along the axis perpendicular to the plane of the porphyrin in the naturally occurring enzymes, one of which is thought to be a H_2O molecule[88].

Figure 1.9 A Representation of Chlorophyll a & b

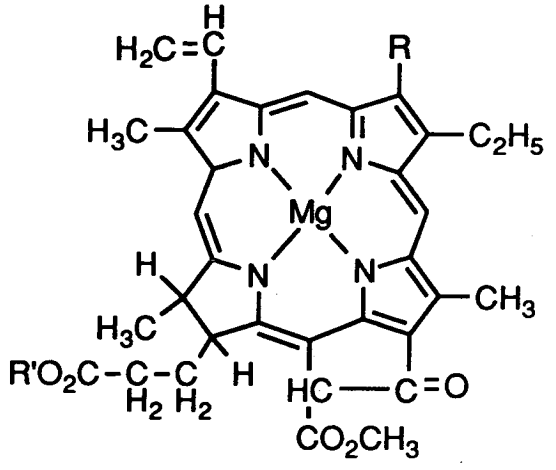

Chlorophyll a : R' = $C_{20}H_{39}$; R = CH_3
Chlorophyll b : R' = $C_{20}H_{39}$; R = CHO

The tetrapyrrole unit is also present in the haem of haemoglobin and myoglobin which reversibly bind and transport O_2. The haem ($Fe^{(II)}$protoporphyrin) can be separated from its protein but is rapidly oxidised to Fe(III)[88]. A representation of the molecule is shown in Figure 1.10[29]. A number of models for haemoglobin have been synthesised[29, 89-96]. Collman *et al* have prepared and characterised an oxygenated 'picket' fence haem which unambiguously shows O_2 in the molecule as bent (see Figure 1.11)[95, 96].

Figure 1.10 A Representation of Haemoglobin

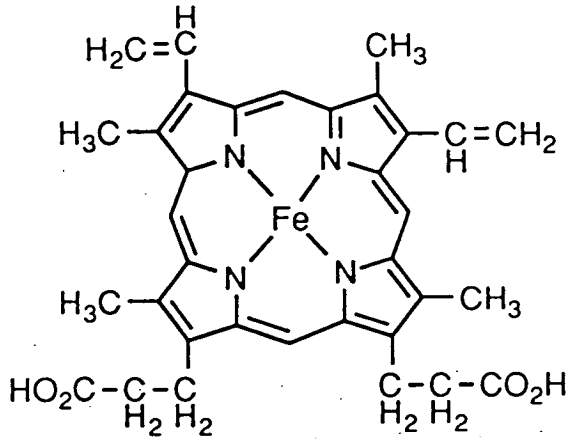

Figure 1.11 A View of a Picket Fence Model of Haemoglobin

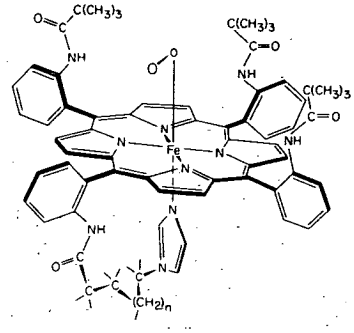

Another important enzyme that incorporates the Fe(II)protoporphyrin unit within a protein complex are the Cytochromes. The differences between the Cytochromes and the haemoglobins are the slight variations of the functional groups attached to the porphyrin and the protein itself[88, 97, 98]. A general representation of a Cytochrome is shown in Figure 1.12.

Scheme 1.2 Oxidation of an Organic Substrate by O_2.

$$RH + O_2 \longrightarrow ROH + H_2O + A$$

A - biological reducing agent (NAD or FAD)

Cytochrome C is used to transport electrons in biological systems, and Cytochrome P_{450} is used to oxidise organic molecules by molecular O_2 (Scheme 1.2) . The main differences between these Cytochromes are the fifth ligand, the way the protein holds the haem and the proteins themselves. The fifth ligand in Cytochrome C is an imidazole; in Cytochrome P_{450} it is the thiolate of cysteine. Both are sandwiched between proteins and held in a pincer action. However, in Cytochrome P_{450} these proteins cover only pyrrole ring B, whilst in Cytochrome C they completely cover the haem except for the outer rings of c and d (Figure 1.13)[76, 97].

Figure 1.12 A Representation of a Cytochrome

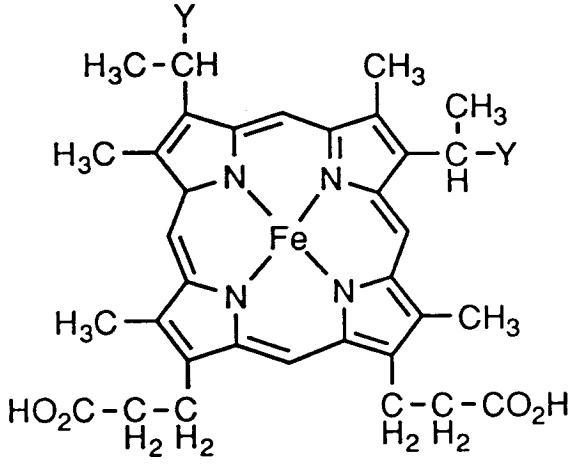

Figure 1.13 Representations of Cytochrome c and Cytochrome P_{450}

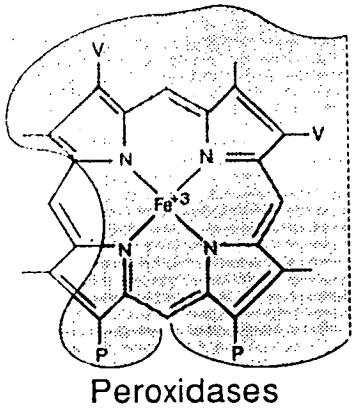

Peroxidases

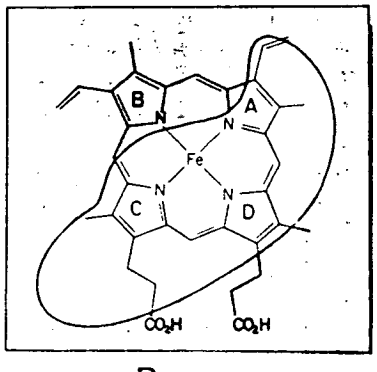

P450

Shaded areas are the region of the haem that are not accessible to organic substrates

The catalytic cycle for the oxidation of organic substrates by Cytochrome P_{450} is shown in Scheme 1.3 and illustrates how the oxidation state of the Fe changes during the course of the cycle[1, 76, 99]. π-cation radical complexes are thought to be the active oxy intermediates which transfer the oxygen atom to the substrate. These were discussed in Section 1.4. This system has been modelled using [Fe(TMP)Cl] or [Fe(TPP)Cl] with various oxidising agents and have been used to oxidise a wide range of organic compounds, including alkenes to epoxides. This will be discussed in the following Section 1.6.

Scheme 1.3 The Proposed Catalytic Mechanism for the Oxidation of Organic Substrates by Cytochrome P_{450}.

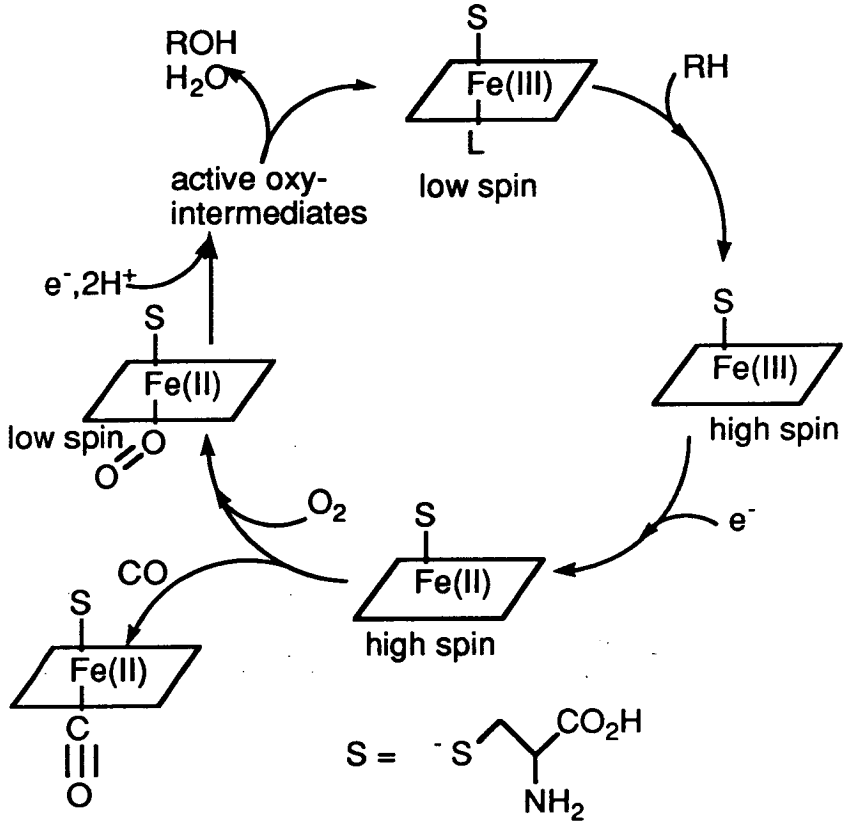

Coenzyme B_{12}, in the presence of other enzymes, catalyse a number of important reactions involving C-C band cleavage and formation (for examples see Figure 1.14), and is one of the few well-defined cobalt containing biochemicals[100]. It contains a corrin tetrapolypyrrole ligand. Its cyanide derivative (Vitamin B_{12}) was the first to be structurally characterised by X-ray

crystallography, and is shown in Figure 1.15. In the naturally occurring coenzyme B_{12}, an alkyl unit is present instead of the cyanide (Figure 1.16)[1, 6-8, 100-102].

Figure 1.14 Some Examples of the Reactions Catalysed by Coenzyme B_{12}

Methylmalonyl-CoA Mutase

L-Leucine-2,3-Amino mutase

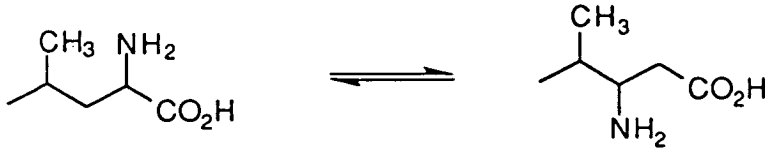

Diol Dehydrogenase

Figure 1.15 A View of the Metal Centre of Vitamin B_{12}

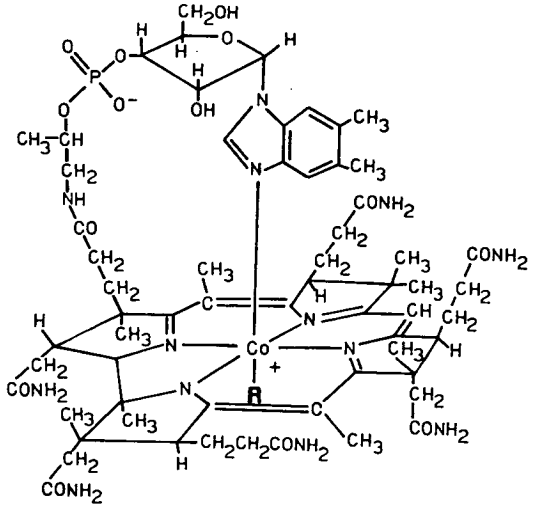

Figure 1.16 A Representation of Coenzyme B12

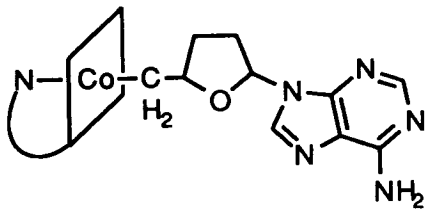

1.6 Catalysis

The ability of naturally occurring macrocycles to catalytically reduce O_2, N_2 and other small molecules suggests that synthetic macrocycles should also be of use in catalysis. The ability of macrocycles to protect and control the stereochemical and electronic properties of a metal ion accounts for this usage in activating small molecules.

The electrocatalytic reduction of O_2 is of great interest since this could provide a basis for a fuel cell. O_2 can be reduced by either two or four electrons to produce H_2O_2 or H_2O respectively[103-105]. The study of this reaction has centred on porphyrins[106-115] and phthalocyanines[116-118] usually with Co or Fe metal ions, although O_2 complexes with Ni, Cu and Co aza macrocycles have also been synthesised[119-122]. In metalloporphyrins and phthalocyanines, Co^{2+} usually converts O_2 to H_2O_2 and Fe^{2+} usually converts O_2 to the more desirable product H_2O, but only in alkaline media. However, if the electronic structure of a phthalocyanine is perturbed, it is possible to change the reactivity[116-118] : Thus, the complex [Co(Pc)] (Figure 1.17) can reduce O_2 to H_2O over the pH range 1 to 14. Interestingly, the Fe(II) analogue can only reduce O_2 to H_2O between pH 7 and 14[117, 118]. A stacked complex $[Co^{(III)}(CN)(Pc)]_n$[116], as well as a Cobalt cofacial porphyrin can catalyse the four electron reduction of O_2 to H_2O. The proposed mechanism for this reduction by the Cobalt cofacial porphyrin complex is shown in Scheme 1.4[110]. In a similar cofacial porphyrin complex, the dioxygen bridged species has been isolated[111]. The four electron reduction of O_2 has also been catalysed by an Ir porphyrin, [Ir(OEP)H][115] and has also been

photocatalysed by using $[Co(Me_6[14]aneN_4)]^{3+}$ as an electron relay and $[Ru(bipy)_3]^{3+}$ as a sensitiser[123].

Scheme 1.4 The Proposed Mechanism for the Reduction of O_2 by Cofacial Porphyrin Complexes

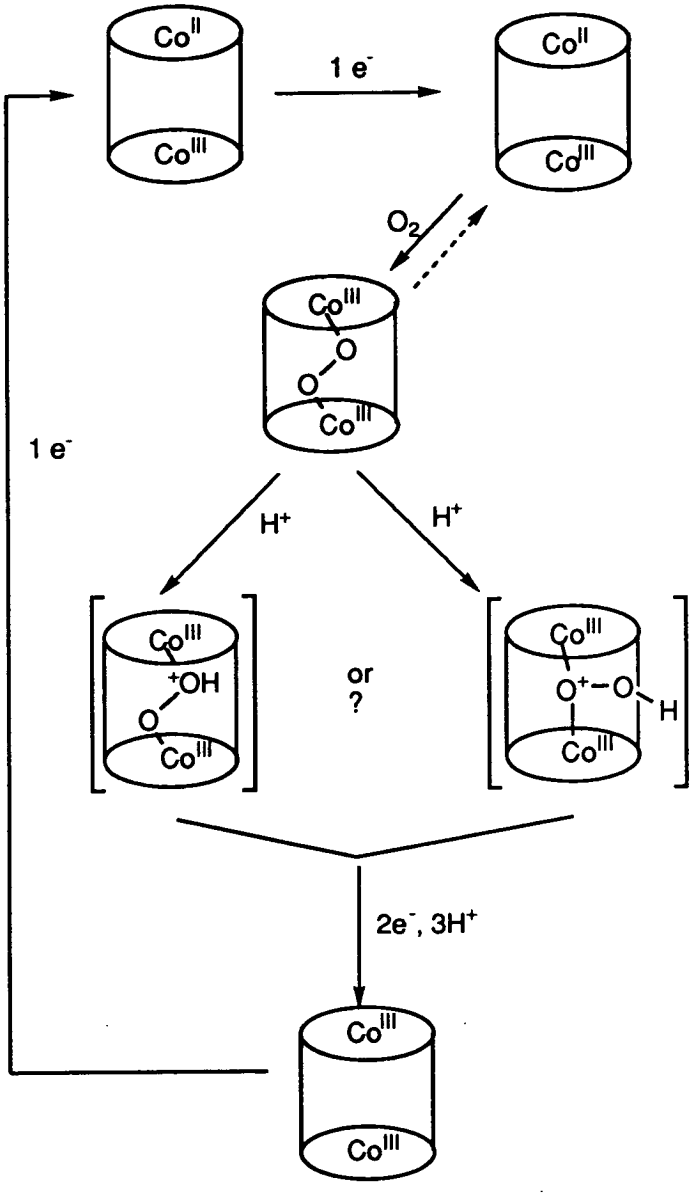

Figure 1.17 A Representation of the [Co(Pc)] Complex.

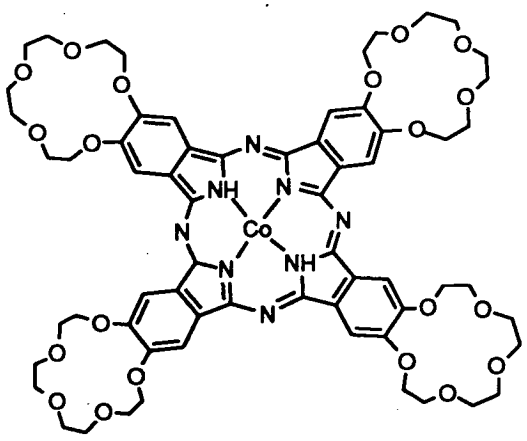

One of the favoured fuel cells is the H_2/O_2 system, in which H_2 is oxidised as O_2 is reduced[105]. Work on activating H_2 by macrocyclic complexes has recently been examined by Collman *et al* in a series of Ru and Os porphyrins[124-126]. A novel H_2 complex with a Ru cofacial porphyrin has been isolated, and the H_2 is thought to lie along the axis perpendicular to the Ru—Ru axis. This species is shown in Figure 1.18. This compound is not capable of catalytic oxidation. The mononuclear porphyrin complex [M(OEP)L(H_2)](M = Os, Ru; L = THF or Im*) (See Figure 1.19) have also been synthesised but only [Ru(OEP)(H_2)(THF)] seems capable of catalysing the oxidation of H_2 to H_2O. It has been shown that [Ru(OEP)(H_2)(THF)] is thermodynamically capable of catalytic oxidation[126], and when the starting material [Ru(OEP)$(THF)_2$] is deposited on the electrode surface under H_2, catalytic oxidation occurs. However, it is not thought that the [Ru(OEP)H_2(THF)] complex catalyses the reaction, but that the dimer, $[Ru(OEP)]_2$ is responsible for the oxidation. The intermediate in this reaction is thought to have a similar structure to the cofacial Ru porphyrin species shown in Figure 1.18.

Figure 1.18 A View of the Ru Cofacial Porphyrin Complex

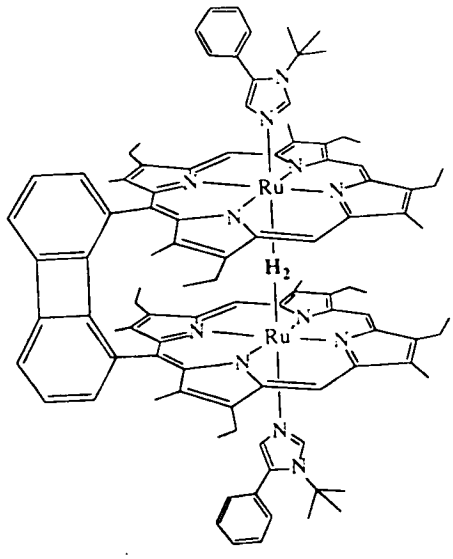

Figure 1.19 The Imidazole Derivative for the Ru Porphyrin Complexes

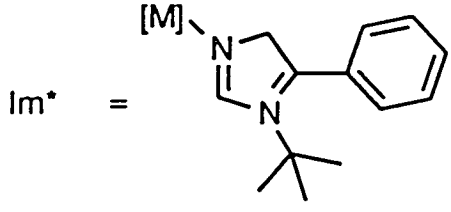

The activation of N_2 is another major aim in catalysis and is related to the biological process. The application of macrocyclic complexes to the catalytic conversion of N_2 to reduced compounds such as hydrazine and ammonia is of great interest commercially. A number of Ru and Os porphyrin complexes exist with one or two N_2 molecules co-ordinated to the metal[127-130]. A thioether Mo complex $[Mo(Me_8[16]aneS_4)(N_2)_2]$ has been isolated and structurally characterised[131]. These complexes do not catalytically reduce N_2. The H_2 in the Ru cofacial porphyrin complex, shown in Figure 1.18, can easily be exchanged for N_2[132, 133]. The structure is similar to the H_2 complex, with a linear N_2 ligand. However, its exact orientation is not known[91, 92]. The N_2 in the complex can also be displaced by hydrazine or ammonia. The conversion of ammonia to N_2 (the reverse of the biological process) can be achieved by addition of base to $[Ru_2(Por)(NH_3)_2]$, if the addition is stoicheiometrically

controlled the hydrazine, diazine and ammine complexes, as well as the N_2 one can all be isolated[133]. The protonation of the N_2 complex does not occur with trifluoroacetic acid, and so no catalytic reduction of N_2 has been possible[132, 133]. Macrocyclic complexes have reduced NO_2^- [134] and NO_3^- [135] electrocatalytically using $[Fe(TPPS)]^{3-}$ and $[Co([14]aneN_4)]^{3+}$ respectively. $[Ni([14 \text{ or } 15]aneN_4)]^{2+}$ has also electrocatalytically converted N_2O to N_2 [136].

The catalytic reduction of CO to CO_2 has been achieved using macrocyclic complexes. $[Rh(OEP)]_2$ catalyses the conversion of H_2/CO mixtures into H_2CO and CH_3OH. The mechanism for this is shown in Scheme 1.5 [137-141]. The electrocatalytic reduction of CO_2 by macrocyclic complexes yield a number of products, such as oxalic acid[142-153], glycolic acid[143], formic acid[144], methanol[144] and CO[145-153]. Most interesting is the catalytic reduction to CO. [Co(Pc)] on carbon electrodes can convert CO_2 to CO, but a significant amount of water electrolysis also occurs to give $H_{2(g)}$ as well[145]. The reduction by $[M([14]aneN_4)]^{2+}$ (M=Co,Ni) and other tetraazamacrocycles has been studied[148-153]. The most efficient and selective (for CO production, even in pure water) is $[Ni([14]aneN_4)]^{2+}$. This system is very durable, since it can be cycled over 1000 times with no appreciable deterioration. The mechanism is shown in Scheme 1.6[148, 149], and has recently been supported by theoretical calculations[154]. A derivative of the macrocycle $[14]aneN_4$ incorporating a 1, 10 phen group has recently been synthesised. When this new ligand is complexed with Ni(II) and a {Ru(1, 10 phen)$_2$} fragment added, the resulting complex, shown in Figure 1.20, can photocatalytically reduce CO_2 to CO[155].

Figure 1.20 A Representation of the Ru/Ni Complex

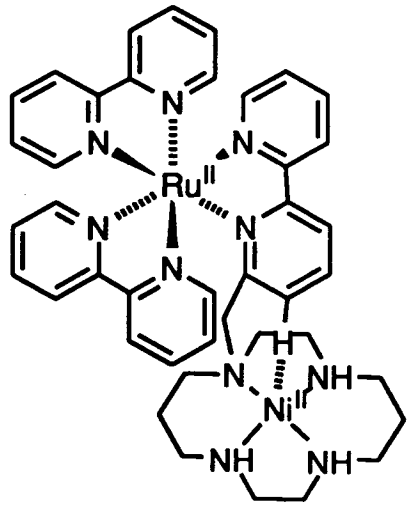

Scheme 1.5 Proposed Mechanism of the Catalytic Conversion of H_2 and CO to H_2CO By $[Rh(OEP)]_2$

Formation of dimer from [Rh(OEP)H]

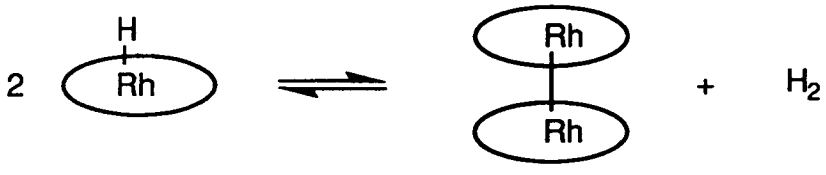

Initiation/Termination:

$$[Rh(OEP)]_2 \rightleftharpoons 2\ {}^{\bullet}Rh(OEP)$$

Propagation:

$$^{\bullet}Rh(OEP) + CO \rightleftharpoons {}^{\bullet}(CO)Rh(OEP)$$

$$^{\bullet}(CO)Rh(OEP) + HRh(OEP) \rightleftharpoons (CHO)Rh(OEP) + {}^{\bullet}Rh(OEP)$$

$$(CHO)Rh(OEP) + H_2 \rightleftharpoons HRh(OEP) + H_2CO$$

Scheme 1.6 Proposed Mechanism for the Catalytic Conversion of CO_2 to CO by $[Ni([14]aneN_4)]^{2+}$

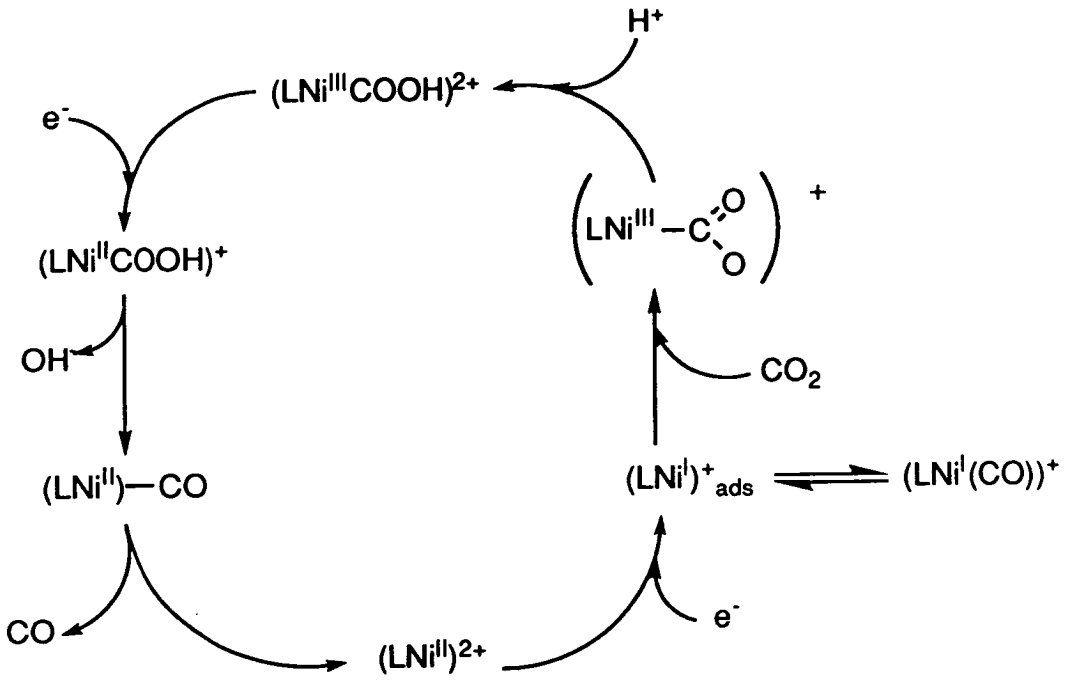

The catalytic oxidation of organic molecules has been another field of macrocyclic chemistry that has been extensively studied[141, 156]. Metalloproteins are excellent and versatile catalysts for a number of oxidations. Alkenes can be readily converted to epoxides using PhIO, H_2O_2, NaOCl, RO_2H and other oxidising agents, by both metalloproteins[1, 6-8] and aza macrocycles[156]. The mechanism for the epoxidation of an alkene by PhIO catalysed by [Fe(TPP)Cl] and the resulting products are shown in Scheme 1.7[157, 158]. By using chiral porphyrins, chiral epoxides may be produced with enantiomeric excesses of up to 84%[156, 159-164].

The hydroxylation of alkanes can be accomplished by using PhIO, NaOCl, O_2, H_2O_2 and other oxidising agents with metalloproteins as catalysts. In certain cases, heteroaromatic N-oxides can be used as the oxygen source, instead of a conventional oxidising agent[156, 173]. Further, if chiral porphyrins are used, chiral products may result[156, 166-168], and an example of this is shown in Scheme 1.8. These metalloporphyrins will catalyse most organic oxidations, and

the conversion of thioethers to sulfoxides has been performed[169]. This will be discussed in Chapter 7.

Scheme 1.7 The Proposed Mechanism for the Catalytic Epoxidation of an Alkene by PhIO by Metalloproteins.

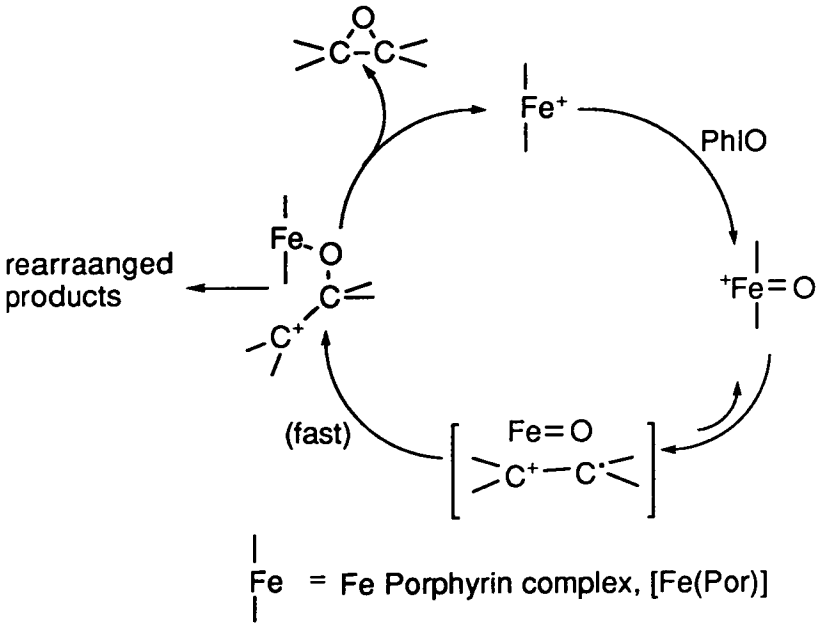

Scheme 1.8 Chiral Epoxidation of Alkenes Catalysed by Chiral Metalloproteins.

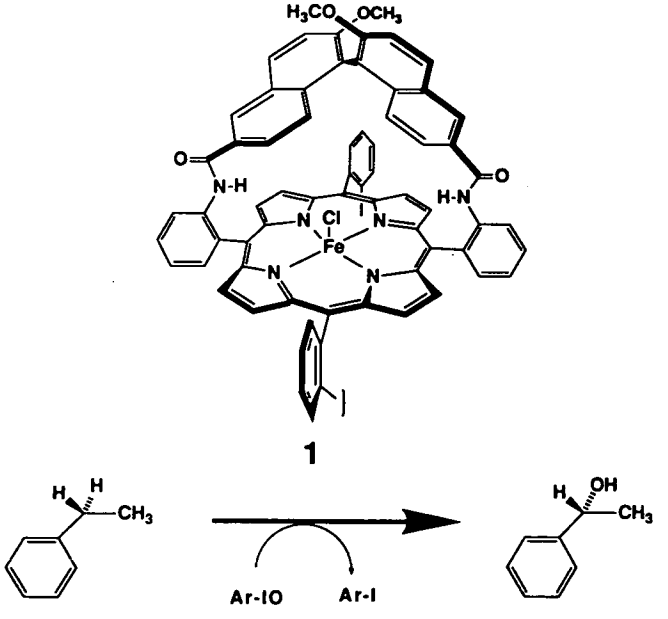

Chapter Two

THE CHEMISTRY OF THIOETHER MACROCYCLES

2.1 The Synthesis of Thioether Macrocycles

During the last ten years thioether macrocyclic chemistry has undergone rapid development, undoubtedly due to the exploitation of new reliable and high yielding synthetic routes to these ligands. The first preparation of cyclic polyethers was achieved some twenty-five years ago by Pederson using alkali metal ions for the preparation of macrocycles containing between three and twenty oxygen atoms with a ring size varying from nine to sixty[170]. The formation of thioether macrocycles using alkali metals is much less effective, owing to weaker sulfur-metal inter-attractions[181]. The synthetic methods generally used involve high dilution and long reaction times[26].

[9]aneS_3 was first reported in 1886 by Mansfield and was thought to have been made by reacting ethylene bromide with Na_2S in ethanol[171]. In 1920 Ray claimed that [9]aneS_3 could be formed by addition of KSH to ethylene bromide[172]. However, these claims were disproved in a series of experiments conducted in the mid-1920s by Bennet *et al* [173]. In 1934, the first two thioether macrocycles, [16]aneS_4 and [18]aneS_6, were synthesised in less than 2% yield by reacting dithiolates with dihalides in ethanol[174], but the first study of the co-ordination chemistry of a purely thioether macrocyclic ligand was carried out in 1969 by Busch *et al* using Ni(II) and [14]aneS_4 [175]. The co-ordination chemistry of thioether macrocycles will be discussed in Section 2.3.

[9]aneS_3 was first synthesised in a yield of less than 0.04% by Ochrymoycz *et al* in 1977, by reacting the disodium salt of 3-thiapentane-1,4-dithiolate with 1,2-dichloroethane[176]. Subsequently, the benzyltrimethylammonium salt of the dithiolate was used in high dilution to increase the yield to 4.4%. This method also produced the [2+2] addition product [18]aneS_6 in a 32% yield (Scheme 2.1) [177].

Scheme 2.1 Synthesis of [9]aneS3

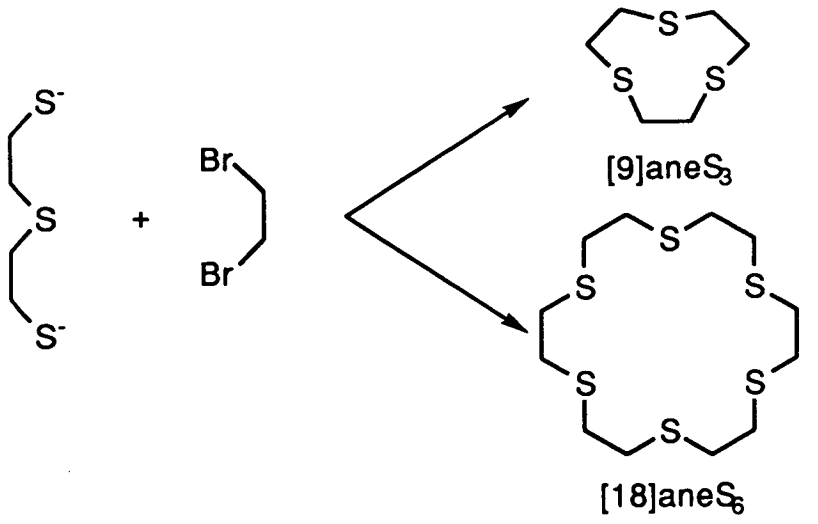

In 1984, a high yield (>60%) synthetic route to [9]aneS3 was achieved by Sellman *et al* by utilising a {Mo(CO)3} moiety as a template for the reaction. This is shown in Scheme 2.2[178]. $[NMe_4]_2[S(CH_2)_2S(CH_2)_2S]$ reacts with $[Mo(CO)_3(CH_3CN)_3]$ to form $[Mo(CO)_3(S(CH_2)_2S(CH_2)_2S)]^{2-}$ which then reacts with ethylene bromide to produce the [9]aneS3 complex, $[Mo(CO)_3([9]aneS_3)]$. The [9]aneS3 ligand can then be substituted with the dithiolate by stirring in DMSO at 298K for forty eight hours, thereby making the reaction catalytic in terms of {Mo(CO)3}[178]. A large-scale general synthesis of thioether macrocycles has been achieved by Buter and Kellogg using Cs_2CO_3/DMF with high dilution[179]. When this same method is applied to [9]aneS3, a yield of 50% was reported[26]. Employing the same technique, [12]aneS4 and [14]aneS4 can be synthesised in 88% and 76% yields respectively[178-181]. The ligands [9]aneS3, [12]aneS4, [14]aneS4 and [16]aneS4, which are used in this thesis, are all now commercially available.

Scheme 2.2 Synthesis of [9]aneS$_3$ using a {Mo(CO)$_3$} Fragment as a Catalyst.

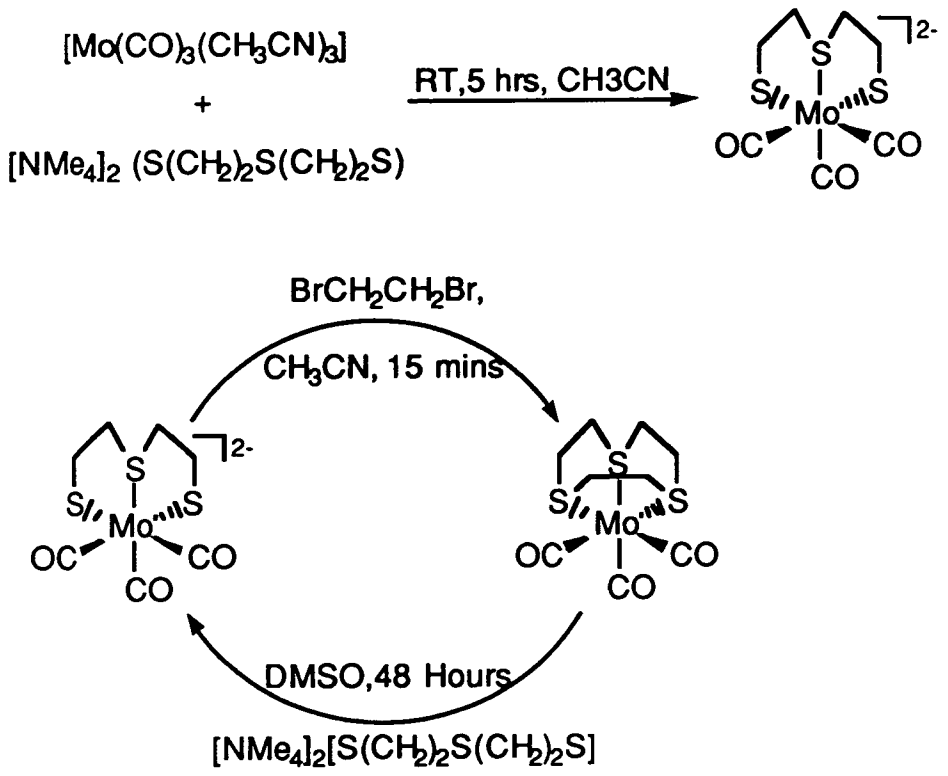

Several derivatives of these thioether macrocycles have been synthesised using the Cs_2CO_3/DMF methodology. For example, the rigidity of the ring has been increased by incorporating benzene ring[182], and the ring size has been increasing it from [9] to [10][183] (Figure 2.1). The incorporation of a ketone[184-186], an alkene[184-186], alkyl[187] or alkoxy[187] functional group into the macrocyclic ring has also been achieved by using this methodology (Figure 2.1). The Cs_2CO_3/DMF synthetic method has also been used to prepare a novel S_6 thioether cage (Scheme 2.3)[188].

The main alternative preparative methodology utilizes the {Mo(CO)$_3$} fragment as a template. Thus, the macrocycles, benzo[12]aneS$_3$ and benzo[14]aneS$_3$[189-191], a novel [13]aneS$_4$ derivative[192] and a series of C-functionalised [9]aneS$_3$ derivatives[193] have all been prepared. These ligands are illustrated in Figure 2.2.

Figure 2.1 Thioether Macrocycles Synthesised Using The Cs_2CO_3/DMF Methodology

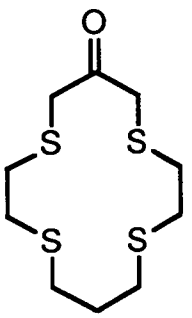

$(CH_2)_n$

n = 0,1

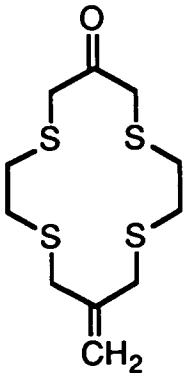

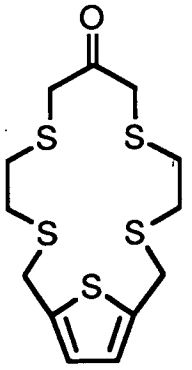

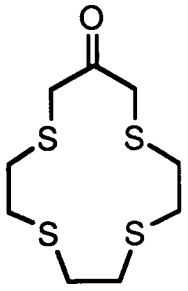

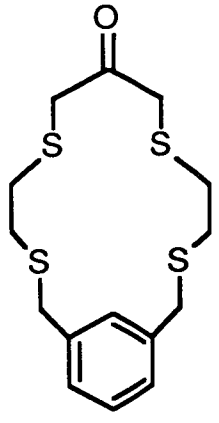

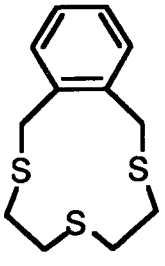

TT[9]OB

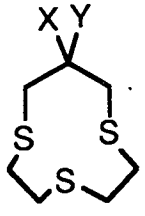

X=Y=H ; [10]aneS_3
X=OH,Y=H ; Hydroxy[10]aneS_3
X,Y= O ; Keto[10]aneS_3

Figure 2.2 Thioether Macrocycles Synthesised Using The {$Mo(CO)_3$} Methodology

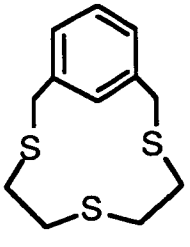

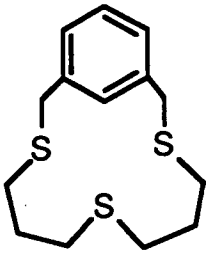

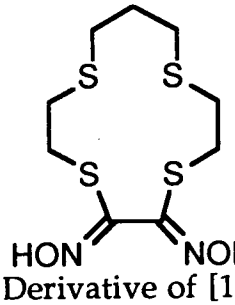

NOH Derivative of [13]aneS_4

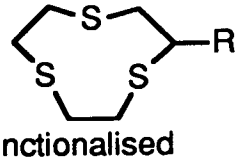

C-functionalised
[9]aneS_3

R = CH_3, CH_2OH,OH,
OR (R = alkyl), CH_2OCH_3,
C_6H_4-4-Br, CH_2OCH_2Ph

Scheme 2.3 The Synthesis of a Thioether Cage Ligand

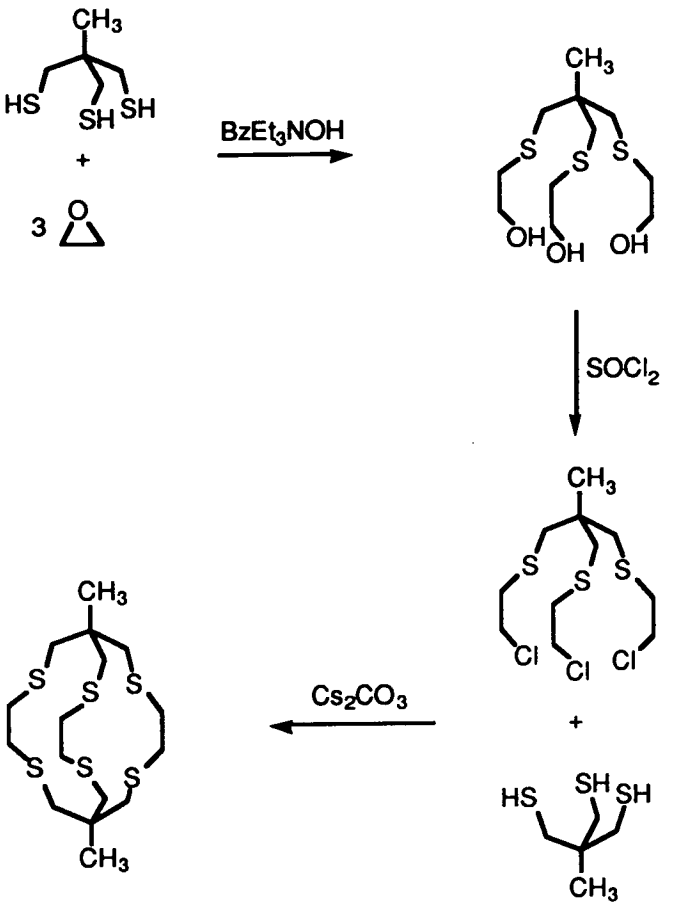

An interesting [11]aneS$_3$ macrocycle has been made by reacting [Co_2(μ-(HOCH$_2$C≡CCH$_2$OH)(CO)$_6$] with bis(2-mercaptoethyl)sulfide in the presence of HBF_4 to form the complex [Co_2{μ-C_2(CH$_2$SCH$_2$CH$_2$)$_2$S}(CO)$_6$]. In this complex the Co is co-ordinated to the macrocyclic ligand through two carbon donors, as opposed to the expected sulfur ligation (Figure 2.3)[194].

Figure 2.3 A Representation of [Co_2{μ-C_2(CH$_2$SCH$_2$CH$_2$)$_2$S}(CO)$_6$]

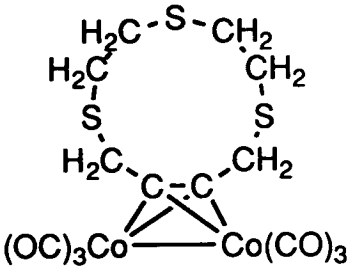

A series of thioether macrocycles incorporating a thiophene unit (Figure 2.4) has been synthesised by reacting a dithiolate with 2,5–bis(chloromethyl) thiophene in high dilution in refluxing ethanol [195, 196]. These thiophene-containing macrocycles have been complexed to a number of transition metal ions [e.g. W(0)[197], Mo(0)[197], Pd(II)[198] and Cu(II)[198]].

Figure 2.4 Thioether Macrocycles Incorporating a Thiophene Unit.

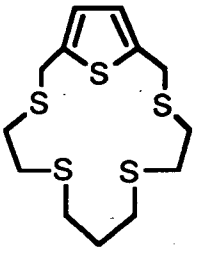

[16]aneS$_5$

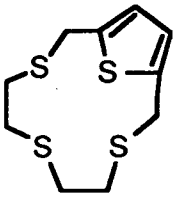

[12]aneS$_4$

A number of mixed donor macrocycles have been characterised which incorporate a thioether donor, of particular interest being macrocycles which incorporate both hard and soft donors, for example, mixed N and S donor macrocycles (e.g. [18]aneN$_2$S$_4$ and its derivatives[199-205]) or O and S donors (e.g. [15]aneS$_2$O$_3$ and its derivatives[24, 206-209]). All the macrocycles in the series [9]aneN$_x$S$_y$ (x + y = 3)[24, 210-212] and [14]aneS$_x$N$_y$ (x + y = 4)[213, 214] have been prepared along with some derivatives (e.g. [10]aneN$_2$S[215], [9]aneN$_2$S with two pendant CO$_2$Me groups[217], or with the N-donor incorporated into a pyridine unit[217]) (Figure 2.5).

Figure 2.5 Mixed Donor Macrocycles Incorporating a Thioether.

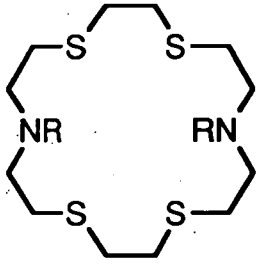

R=H ; [18]aneN$_2$S$_4$
R=CH$_3$; [18]aneN$_2$S$_4$

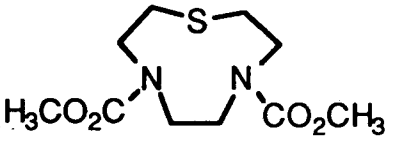

[9]aneN$_2$S with two pendant arms

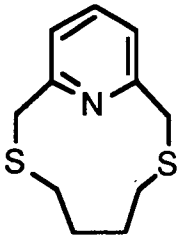

[12]aneN$_2$S

2.2 The Structure of [9]aneS$_3$

The single crystal X-ray structure of [9]aneS$_3$ shows that it adopts a [333] *endo* conformation of C_3 symmetry with the S-atoms directed towards the centre of the macrocyclic ring[16] (Figure 2.6). The conformational analysis in the gas phase, using photoelectron spectroscopy suggests that this conformation is retained[218]. However, a gas phase electron diffraction study showed that this conformation was, at best, only present as a minor component in a mixture of predominantly other conformers. It seemed that the C_1 conformer was present, since it gave the best fit with experimental data, although the C_2 conformer may also be present in a mixture of C_1 and C_2 conformers (Figure 2.7) [219]. In solution it seems that [9]aneS$_3$ adopts a wide range of structures, each one with a considerable population[220]. The change in conformation, when this compound is oxidised, will be discussed in chapter 7.

Figure 2.6 A View of the Single Crystal X-Ray Structure of [9]aneS$_3$

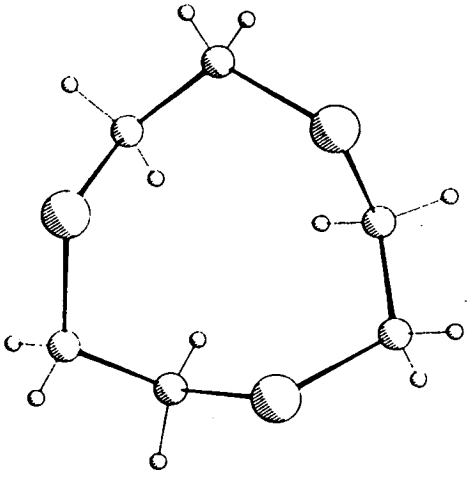

Figure 2.7 Some Possible Conformations of [9]aneS$_3$

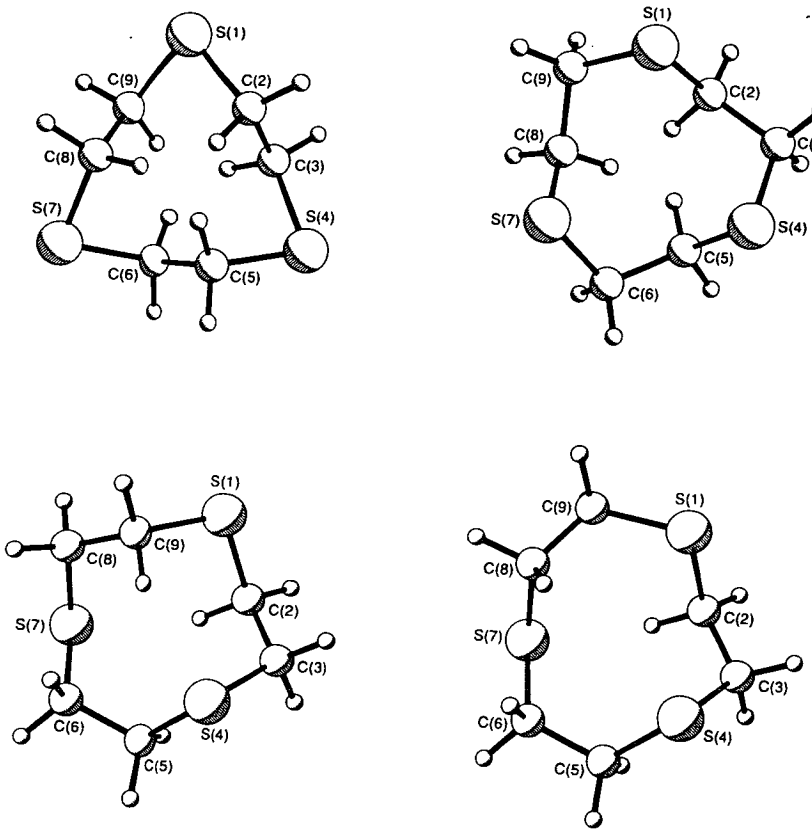

2.3 Thioether Macrocyclic Complexes

A number of reviews dealing with the chemistry and complexes of thioether macrocycles have appeared[26, 33, 181, 221-224]. In recent years, [9]aneS$_3$ complexes have received particular attention since they can stabilise some unusual oxidation states of metals, e.g. $[Au^{(II)}([9]aneS_3)_2]^{2+}$ [225, 226], $[Pd^{(III)}([9]aneS_3)_2]^{3+}$ [26, 222, 227] and $[Pt^{(III)}([9]aneS_3)_2]^{3+}$ [26, 222, 228]. The Au, Pt and Pd complexes $[M([9]aneS_3)_2]^{2+}$ (M = Au, Pt, Pd) can be prepared by reacting $[MCl_4]^{2-}$ with [9]aneS$_3$, and can be oxidised either electrochemically or chemically to afford the $[M([9]aneS_3)_2]^{3+}$ complexes[227-229]. The single crystal structure of $[Pd([9]aneS_3)_2]^{2+}$ (Figure 2.8) shows each [9]aneS$_3$ to be bound in a bidentate manner to give a $[PdS_4]^{2+}$ square planar complex. The two remaining thioether donors are situated at apical sites and are involved in long-range

interactions [Pd-S_{equ} = 2.332(3), 2.311(3)Å, Pd-S_{ap} = 2.952(4)Å][268]. The single crystal X-ray structure of the Pt(II) complex $[Pt([9]aneS_3)_2]^{2+}$ shows the Pt ion to also be in a square planar environment [Pt-S_{equ} = 2.246(8), 2.293(8), 2.305(8) and 2.261(7)Å]. However, only one of the remaining thioether donors interacts with the Pt(II) ion [Pt-S_{ap} = 2.884(7)Å] , the remaining sulfur is a distance of 4.04Å away. (Figure 2.9)[228]. The structure of these complexes can be explained as a compromise between the stereochemical preference of the d^8 metal ion to be square planar, and the ligand to be facially co-ordinated[26, 222]. The crystal structure of the Pd(III) complex $[Pd([9]aneS_3)_2]^{3+}$ is shown in Figure 2.10. The d^7 Pd(III) ion is found in a tetragonally distorted octahedral stereochemistry [Pd-S = 2.5448(15), 2.3558(14) and 2.3692(15)Å] . On changing the Pd ion from d^8 to d^7, the Pd-S_{ap} distance changes from 2.952(4) to 2.5448(15)Å, which is consistent with the increased charge at the metal centre and the stereochemical preference of the metal ions[26, 266]. Recently other trithioether macrocycles, (TT[9]OB and [10]aneS_3) have been co-ordinated to the Pd(II) metal ion[230-232].

The complexes of thioether macrocycles with transition metals from groups VIII and IX will be discussed in the following subsections 2.3.1 and 2.3.2.

Figure 2.8 A View of the Single Crystal X-Ray Structure of $[Pd([9]aneS_3)_2]^{2+}$

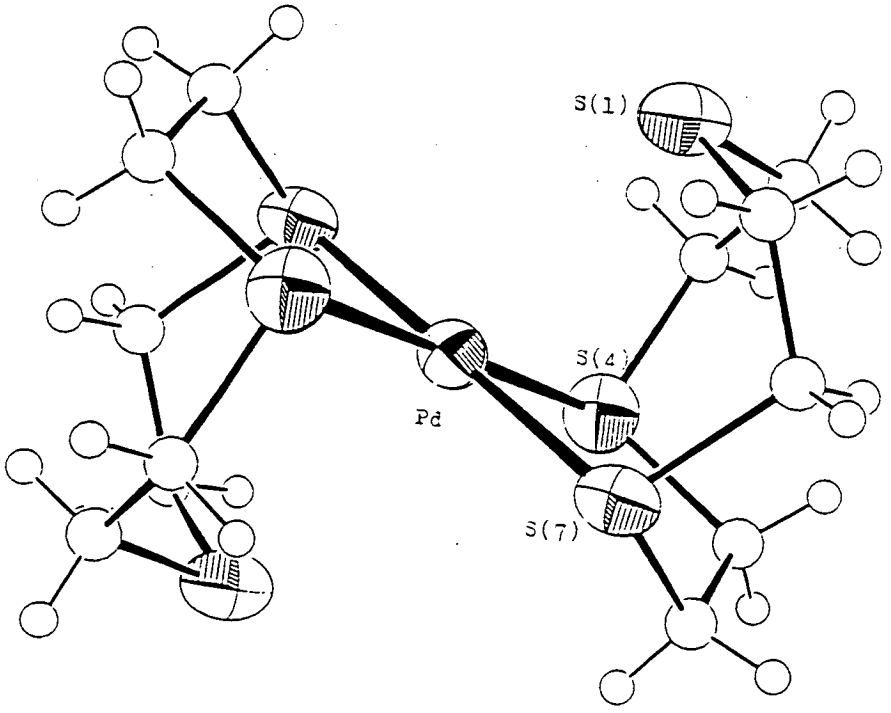

Figure 2.9 A View of the Single Crystal X-Ray Structure of $[Pt([9]aneS_3)_2]^{2+}$

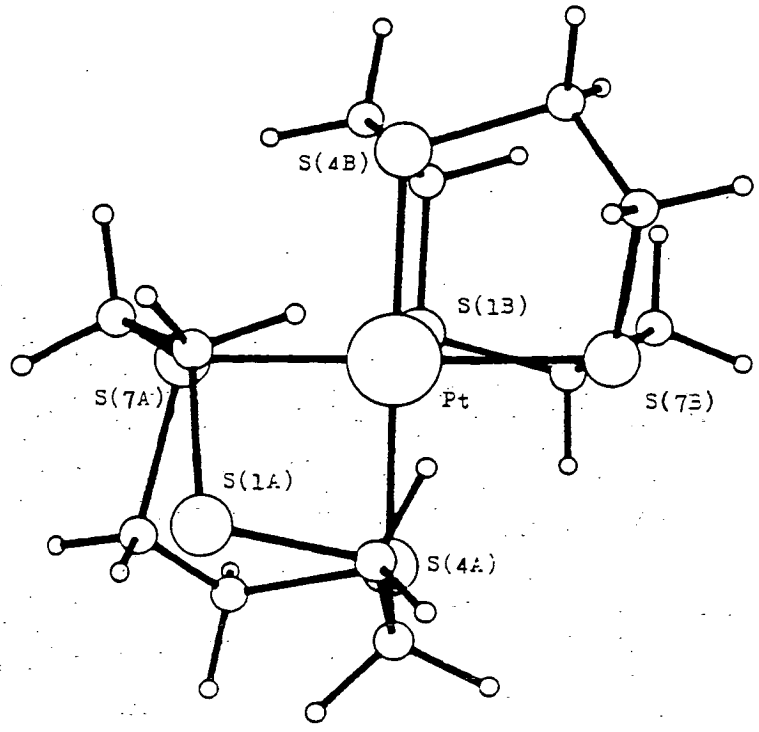

Figure 2.10 A View of the Single Crystal X-Ray Structure of $[Pd([9]aneS_3)_2]^{3+}$

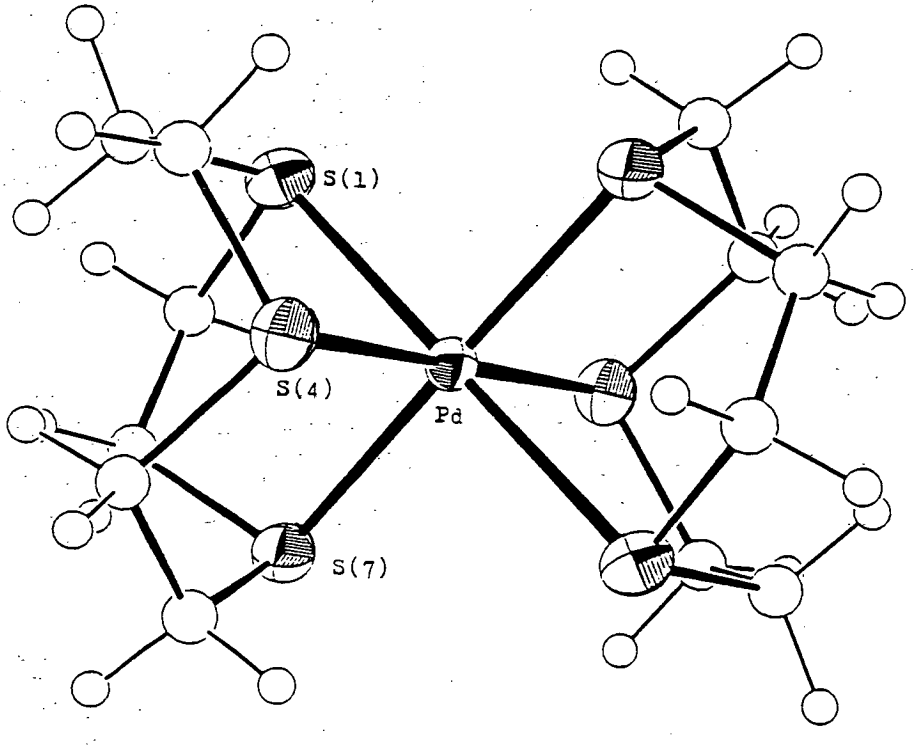

2.3.1 Group VIII thioether macrocyclic complexes

Reaction of $[Fe(OH_2)_6](ClO_4)_2$ or $FeCl_2.4H_2O$ with [9]aneS$_3$ in MeOH affords the low spin homoleptic complex, $[Fe([9]aneS_3)_2]^{2+}$ whose single crystal X-ray structure shows [9]aneS$_3$ to be facially bound to an octahedral Fe(II) metal centre [Fe-S = 2.251(1), 2.241(1), 2.259(1)Å] [233]. $[Fe([9]aneS_3)_2]^{2+}$ undergoes a reversible one-electron oxidation at $E_{1/2}$ = 0.98V Vs Fc^+/Fc, which has been assigned as a $Fe^{(II)}/Fe^{(III)}$ couple. $[Fe([9]aneS_3)_2]^{2+}$can also be chemically oxidised with PbO_2 in 1M H_2SO_4 to yield the highly unstable complex, $[Fe^{(III)}([9]aneS_3)_2]^{3+}$ [234]. The electronic and Mössbauer spectroscopy of this Fe(III) complex reveals the d^5 metal ion to be low spin[234, 235] and the single crystal X-ray structure of $[Fe^{(III)}([9]aneS_3)_2]^{3+}$ (Figure 2.11) shows the Fe to be octahedrally co-ordinated to the six sulfurs of the [9]aneS$_3$ macrocycles [Fe–S = 2.280(3), 2.2846(3), 2.276(3) Å] . On oxidation from Fe(II) to Fe(III) the Fe–S bond lengths increase, giving direct evidence for the π-acceptor properties of thioether macrocyclic ligands[234]. The Fe(III) complex is stabilised in acidic solutions[234], since the use of acidic media inhibits the deprotonation and ring-opening reactions which can occur with [9]aneS$_3$ (See Appendix).

Tetrathioether macrocycle complexes with Fe(II) have been reported. The crystal structure of $[Fe([16]aneS_4)]I_2$ shows the Fe ion to be co-ordinated to four sulfur donors [Fe-S = 2.475(1) and 2.485(1) Å] (Figure 2.12). There is some doubt over the Fe-I bonds in this structure [Fe-I = 2.8896(2) Å] [236]. The Mössbauer spectra of the complexes, $[Fe([16]aneS_4)]X_2$ (X = I, Br) indicates that it is an unusual high spin Fe(II) square planar complex [237], this contrasts with the complex, $[Fe(NCCH_3)_2([14]aneS_4)]^{2+}$, whose Mössbauer spectra is consistent with a low spin complex[237].

Hexathioether macrocyclic Fe complexes have been previously characterised[238, 239]. Reaction of (benzo)$_2$–[18]aneS$_6$ with $Fe(C_2O_4).2H_2O$ in acidified nitroethane affords the violet complex $[Fe\{(benzo)_2–[18]aneS_6\}]^{2+}$ [238].

This complex can also be synthesised by reacting [Fe(CO)(S–Ph–S)$_2$S)] with S($C_2H_4Br)_2$ as shown in Scheme 2.4[238].

Figure 2.11 A View of the Single Crystal X-Ray Structure of [Fe([9]aneS$_3$)$_2$]$^{3+}$

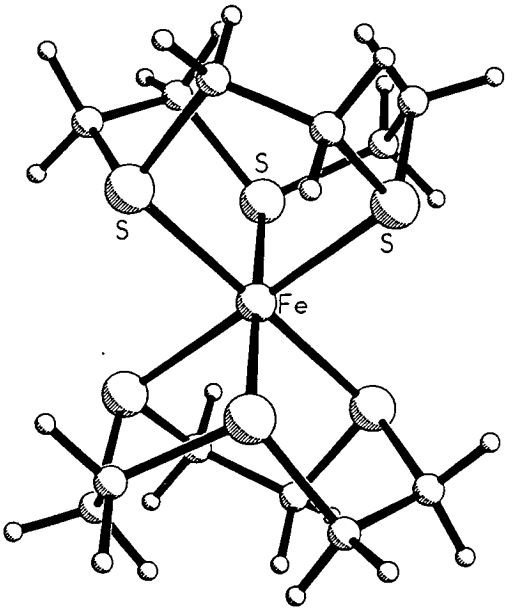

Figure 2.12 A View of the Single Crystal X-Ray Structure of [Fe([16]aneS$_4$)]I$_2$

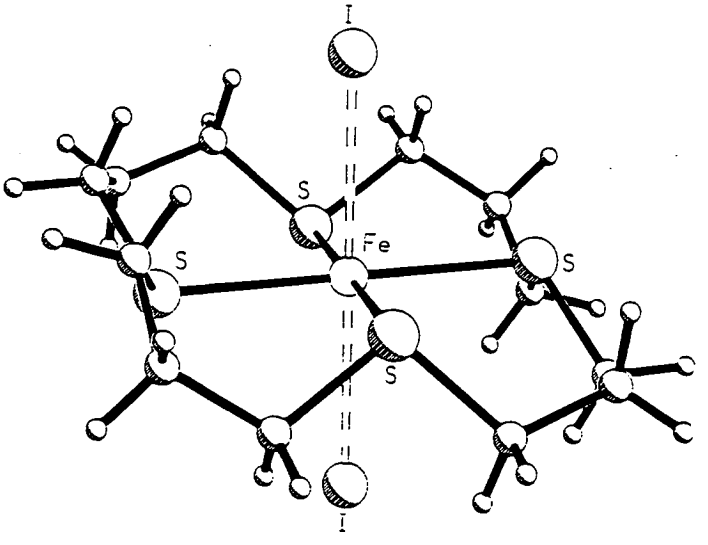

A series of homoleptic hexathioether complexes of Ru(II) have been prepared by reacting [n]aneS_3 (n = 9, 12) or [m]aneS_6 (m=18, 20) with $[Ru(DMSO)_6]^{2+}$ [26, 222, 239]. The complexes, $[Ru([n]aneS_3)_2]^{2+}$, can also be made by reacting [n]aneS_3 with $[Ru_2Cl_4(arene)_2]$ (arene=C_6H_6, C_6Me_6, 4-$MeC_6H_4{}^iPr$). However, when [18]aneS_6 is reacted with $[Ru_2Cl_4(arene)_2]$ the mixed sandwich complex $[Ru_2Cl_2(arene)_2([18]aneS_6)]^{2+}$ is formed[26, 240]. A variety of Ru sandwich complexes of trithioether macrocycles have also been characterised. The single crystal X-ray structure of $[Ru(NCCH_3)Cl(CO)([9]aneS_3)]^+$ shows the octahedral Ru(II) ion to be co-ordinated to a [9]aneS_3 [Ru–S = 2.3139(11), 2.3115(13) and 2.3923(13)Å] , an acetonitrile [Ru–N = 2.072(9)Å] , a carbonyl [Ru–C = 1.884(4)Å] and Cl^- donor [Ru–Cl = 2.4150(14)Å] (Figure 2.13)[26, 240-242]. The preparation of the sandwich complex, $[RuBr_2(CO)(Benzo–[9]aneS_3)]$ has been achieved by using template methods (Scheme 2.4)[243].

The synthesis and reactivity of $[RuCl_2(PPh_3)([9]aneS_3)]$ will be discussed in Chapter 3 and Ru tetrathioether macrocyclic complexes will be discussed in Chapter 6.

Figure 2.13 A View of the Single Crystal X-Ray Structure of $[Ru([9]aneS_3)(NCMe)(CO)Cl]^+$

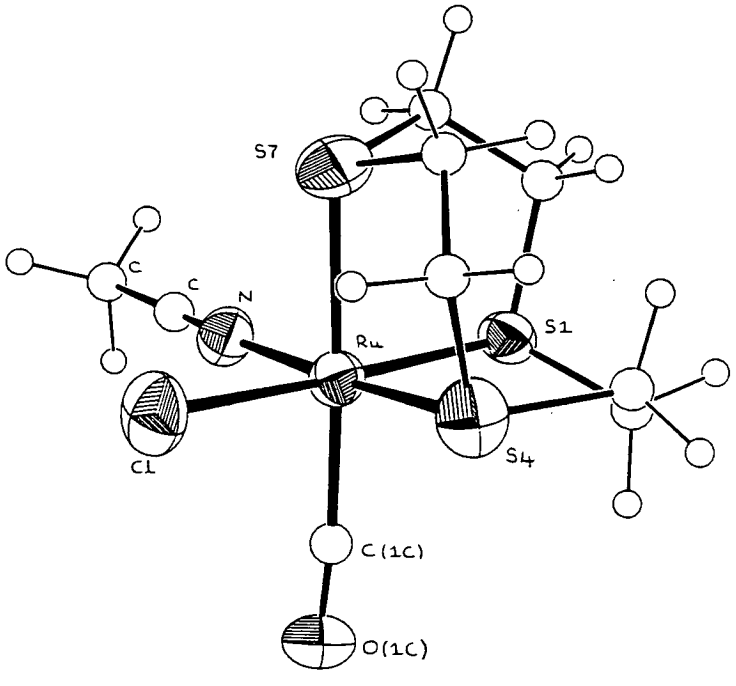

Scheme 2.4 The Synthesis of (Benzo)2–[18]aneS6 and Benzo–[9]aneS3

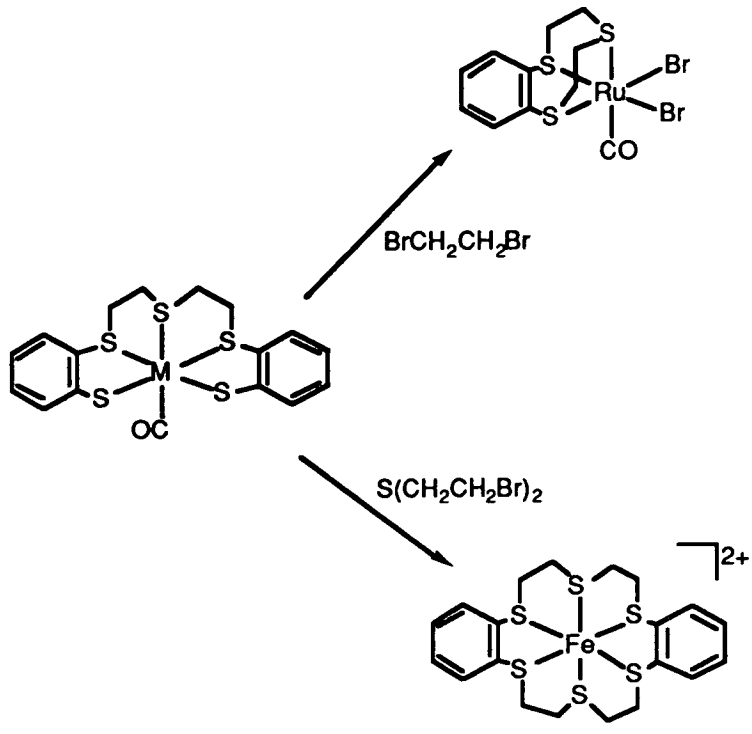

The addition of [9]aneS3 or [18]aneS6 to $[OsCl_2(4\text{-}Me\text{-}C_6H_4{}^iPr)]_2$ in refluxing ethanol affords the complexes $[Os(4\text{-}MeC_6H_4{}^iPr)(L)]^{2+}$ and $[Os(L)_2]^{2+}$ (L = [9]aneS3)[275] or $[Os_2Cl_2(4\text{-}Me\text{-}C_6H_4{}^iPr)_2(L)]^{2+}$ (L = [18]aneS6)[240]. The bis-[9]aneS3 complex, $[Os([9]aneS_3)_2]^{2+}$ can also be synthesised by reacting $[NH_4]_2[OsCl_6]$ with [9]aneS3 in refluxing $H_2O/DMF/CH_3OH$ for 48 hours[244]. The addition of [9]aneS3 to $[Os(H)_2(CO)_2(PPh_3)_2]$ affords the complex $[Os(H)(CO)(PPh_3)([9]aneS_3)]^+$ which has been characterised by X-ray diffraction[244] and the green complex $[OsCl_4([14]aneS_4)]$ has been prepared by reacting Na_2OsCl_6 with [14]aneS4 in refluxing 2-ethoxyethanol[245].

The reaction of Os and Ru carbonyl clusters with [12]aneS3 has also been investigated. $[Os_3(CO)_{12}]$ reacts with [12]aneS3 to form $[Os_3(CO)_{11}([12]aneS_3)]$ and $[Os_4(CO)_{13}([12]aneS_3)]$. The latter complex has been analysed by X-ray diffraction and shows one of the sulfurs of the macrocycle co-ordinated to the 'wing-tips' of

the Os_4 butterfly (Figure 2.14). $[Ru(CO)_{12}]$ reacts with [12]aneS_3 to form a number of products including $[Ru_4(CO)_{11}([12]aneS_3)]$, $[Ru_5(CO)_{13}([12]aneS_3)]$ and $[Ru_6(CO)_{16}([12]aneS_3)]$[246].

Figure 2.14 A View of the Single Crystal X-Ray Structure of $[Os_4(CO)_{13}([12]aneS_3)]$

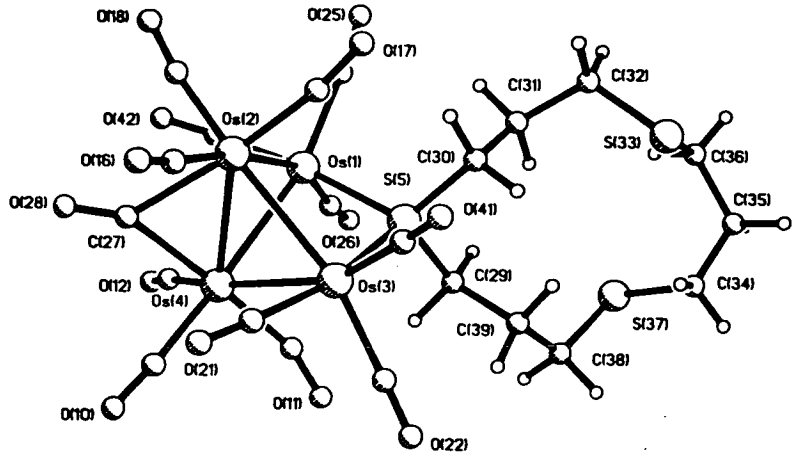

2.3.2. Group IX thioether macrocyclic complexes

$[Co([9]aneS_3)_2]^{2+}$ was synthesised ten years ago and was one of the first transition metal complexes of [9]aneS_3[247]. It is a violet, low spin Co(II) complex and the X-ray crystal structure shows the Co ion to be in a tetragonally compressed octahedral stereochemistry surrounded by six thioethers[247, 248]. The low spin complexes $[Co\{(benzo)_n\text{–}[18]aneS_6\}]^{2+}$ (n = 0, 2) can also be synthesised[236, 249]. However, the complex $[Co([18]aneS_6)]^{2+}$ has a tetragonally elongated octahedral stereochemistry [249] unlike its [9]aneS_3 analogue. The complexes $[Co(L)_n]^{2+}$ (n = 1, L = [18]aneS_6, $(bzo)_2$[18]aneS_6); n = 2, L = [9]aneS_3, [10]aneS_3, [12]aneS_3)[26, 247, 248, 250, 251] are known and can be electrochemically oxidised (n = 1, L = [18]aneS_6, n = 2, L = [9]aneS_3, [10]aneS_3)[248, 249, 251] or chemically oxidised (n=2, L=[9 or 10]aneS_3)[250, 251] to form $[Co(L)_n]^{3+}$. The

electron self-exchange rate for the $Co^{II/III}$ couple in the complex $[Co([9]aneS_3)_2]^{n+}$ has been determined using N.M.R. line broadening techniques to give an estimated rate constant of $1.6 \times 10^5\ M^{-1}s^{-1}$ at 25°C (I = 0.2 M)[252]. The effects of pressure on the transfer rate[253] and the effect of increasing the ring size from [9] to [10] have also been investigated[251]. The mixed sandwich complex $[Co([9]aneN_3)([9]aneS_3)]^{3+}$ has been synthesised and its electron exchange rate (II/III) is $4.2 \times 10^4\ M^{-1}s^{-1}$ at 25° C (I = 0.2 M).

A series of cis-[14]aneS$_4$ and (benzo)–[15]aneS$_4$ complexes of $[Co(X_2)L]^+$ (X = Cl, Br, NCS, NO_2, $^1/_2C_2O_4$, $MeS(CH_2)_2SMe$)[254, 255] have been prepared and characterised by i.r. and u.v. spectroscopy[254]. The ^{59}Co N.M.R. spectra of some of these complexes (X = Cl, Br, $MeS(CH_2)_2SMe$) has also been recorded[26]. A Co(II) complex, $[Co(L)_2]^{2+}$ (L = a NOH derivative of [13]aneS$_4$ {see Figure 2.2}) has been synthesised but is co-ordinated to the two macrocycles through the aza-pendant arms. This complex should be able to co-ordinate another two metals and allow investigation into the interaction of these metals[192].

The homoleptic hexathioether Rh(III) complexes, $[Rh^{(III)}([n]aneS_3)_2]^{3+}$ (n=9, 10, 12) can be prepared by reacting $[Rh(OH_2)_6]^{3+}$ or Rh(III) triflate with [n]aneS$_3$[26, 256, 257]. The crystal structure of $[Rh([9]aneS_3)_2]^{3+}$ (Figure 2.15) reveals the Rh(III) ion to have a symmetric octahedral geometry [Rh–S = 2.3316(14), 2.3335(12), 2.3334(12)Å] [256, 257]. These complexes can be electrochemically reduced by one electron to form a rare example of a d^7 Rh(II) complex. This complex has been characterised by E.S.R. and spectroelectrochemistry. It can be further reduced to form a $[Rh^{(I)}([n]aneS_3)_2]^+$ complex whose exact structure is unknown[256-258]. The Rh(I) and Ir(I) complexes $[M([9]aneS_3)(COD)]^+$ can be formed by reacting $[MCl(COD)]_2$ (M = Ir, Rh, COD = Cyclooctadiene) with [9]aneS$_3$ in CH_3OH (M = Rh) or CH_2Cl_2 (M = Ir). Using a similar method, the complexes $[M([9]aneS_3)(COE)_2]^+$ (M = Rh, Ir, COE = Cyclooctene),

$[M([9]aneS_3)(C_2H_4)_2]^+$ (M = Rh, Ir), $[M([9]aneS_3)(tcne)(CH_3CN)]^+$ (M = Rh), $[M([9]aneS_3)(C_2H_4)(PR_3)]^+$ (M = Rh, R = Ph, Cy), and $[M([9]aneS_3)(CO)(PPh_3)]^+$ (M = Rh) can also be synthesised[259]. The complexes $[Rh([9]aneS_3)(COD)]^+$ and $[Rh([9]aneS_3)(C_2H_4)_2]^+$ have been structurally characterised as 5 co-ordinate with the $[9]aneS_3$ bound facially to Rh(I). The reaction of $[RhCl(COD)]_2$ with $[20]aneS_6$ affords the dimeric complex $[Rh_2(COD)_2([20]aneS_6)]^{2+}$ the crystal structure of which shows the thioether macrocycle bridging the two Rh centres (Figure 2.16)[260]. A similar thioether bridge exists in the complex $[M(Cp^*)Cl_2([18]aneS_6)]^{2+}$ (M = Rh, Ir)[19]. Rh complexes with tetrathioether ligands will be discussed in Chapter 6.

Figure 2.15 A View of the Single Crystal X-Ray Structure of $[Rh([9]aneS_3)_2]^{3+}$

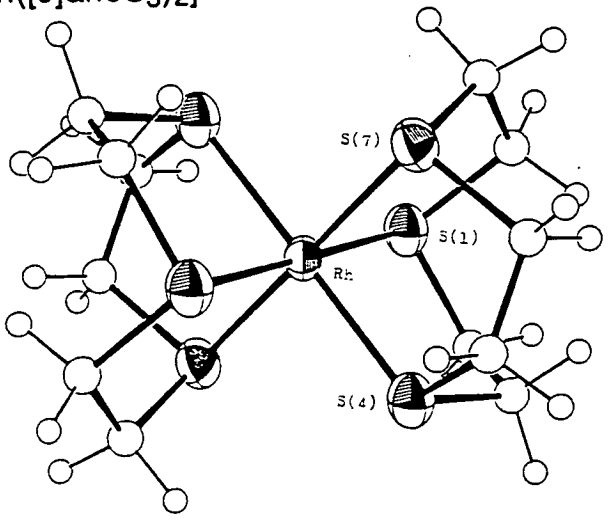

Figure 2.16 A View of the Single Crystal X-Ray Structure of $[Rh_2(COD)_2([20aneS_6)]^{2+}$

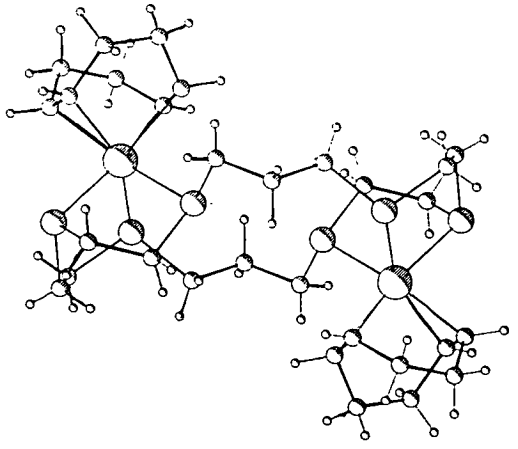

The addition of [9]aneS$_3$ to IrCl$_3$ affords the complexes [IrCl$_3$([9]aneS$_3$)][26, 222] which can be reacted further to produce [Ir([9]aneS$_3$)$_2$]$^{3+}$[26, 222]. The homoleptic hexathioether octahedral stereochemistry of [Ir([9]aneS$_3$)$_2$]$^{3+}$ has been confirmed by X-ray diffraction[261]. A higher yield route to this complex is to react [IrCl(COE)$_2$]$_2$ (COE = cyclooctene) with [9]aneS$_3$ in ethanol, followed by treatment with HNO$_3$[261]. In this case, an intermediate Ir-H species, [Ir(H)([9]aneS$_3$)$_2$]$^{2+}$ can be isolated whose crystal structure shows one [9]aneS$_3$ to be co-ordinated through all three sulfurs in a facial manner, and the other as a bidentate ligand, the sixth ligand being the hydride. IrCl$_3$ reacts with [14]aneS$_4$ to afford the [IrCl$_2$([14]aneS$_4$)][262].

2.4 Aims of Research

Macrocyclic polythioethers enjoy several distinctive features. Unlike monodentate and chelate thioethers they bind effectively to a wide range of metal ions[19]. Crown thioethers can use their filled 3p orbital to act as a π-donors[235], or their empty 3d or S-C σ^*-orbital to act as a π-acceptor[241]. They are also notable for their ability to change their conformation to suit the preferred stereochemistry of the metal ions. This is illustrated by the complexes [Au([9]aneS$_3$)$_2$]$^{n+}$ (n=1, 2, 3). All these complexes have been structurally characterised. The single crystal X-ray structure of [Au([9]aneS$_3$)$_2$]$^+$ (Figure 2.17) shows the Au(I) metal ion to be in a distorted tetrahedral stereochemistry, with one [9]aneS$_3$ being bound as a monodentate ligand [Au(I)–S = 2.3026Å] and the other asymmetrically bound [Au(I)–S = 2.350(7), 2.733(8), and 2.858(8)Å] . This structure is a compromise between the d^{10} metal ion's preference for a linear geometry and [9]aneS$_3$ imposing its preference to bind facially[226]. On oxidation to [Au$^{(II)}$([9]aneS$_3$)$_2$]$^{2+}$ the stereochemistry changes to a tetragonally elongated octahedron with both [9]aneS$_3$ macrocycles being bound in a tridentate manner (Figure 2.18) [Au(II)–S$_{equ}$ = 2.452(5), 2.462(5) Au$\cdots$S$_{ap}$=2.839(5)Å] [225]. Further

oxidation of the Au complexes to $[Au^{(III)}([9]aneS_3)_2]^{3+}$ affords a complex which also adopts a tetragonally elongated octahedral stereochemistry: $Au–S_{equ}$ = 2.348(4) and 2.354(4)Å, $Au\cdots S_{ap}$ = 2.926(4)Å[265] (Figure 2.19). A similar change in stereochemistry is seen with $[Cu^{(I)}([9]aneS_3)_2]^{+}$ [263] and $[Cu^{(II)}([9]aneS_3)_2]^{2+}$[247]. Thus [9]aneS$_3$ has the ability to bind in a tridentate (e.g. $[Rh([9]aneS_3)_2]^{3+}$ (Figure 2.15)), a bidentate (e.g. $[Pt([9]aneS_3)_2]^{2+}$ (Figure 2.9)) or monodentate (e.g. $[Au([9]aneS_3)_2]^{+}$ (Figure 2.17)) manner. This flexibility allows [9]aneS$_3$ to co-ordinate to a wide variety of metal ions.

The main aim of the work described in this thesis was to the synthesise, characterise and investigate the reactivity of half-sandwich Ru(II) complexes of the trithioether macrocycle, [9]aneS$_3$. In such half-sandwich complexes [9]aneS$_3$ would act as a six electron donor using three co-ordination sites around the Ru(II) metal ion, and therefore would be analogous to Cp, arene, triphos and trispyrazolylborate ligands. Ru(II) half-sandwich complexes can form catalytically active complexes, a number of which will be discussed in Chapter 4. The synthesis and characterisation of a chloro-bridged dimer and a Ru/Tl cluster are discussed in Chapter 3. The thalliation reactions of $[RuCl_2(PPh_3)([9]aneS_3)]$ in nitromethane are the subject of Chapters 4 and 5. Chapter 6 extends this work to tetrathioether macrocycles with both Ru(II) and Rh(III). Chapter 7 describes the attempted synthesis of the trisulfoxide ligand, O$_3$[9]aneS$_3$, and the synthesis and characterisation of the trisulfone O$_6$[9]aneS$_3$. Finally, the appendix discusses the deprotonation reactions of thioether ligands, and, in particular, the complex $[Rh([9]aneS_3)_2]^{3+}$.

Figure 2.17 A View of the Single Crystal X-Ray Structure of $[Au([9]aneS_3)_2]^+$

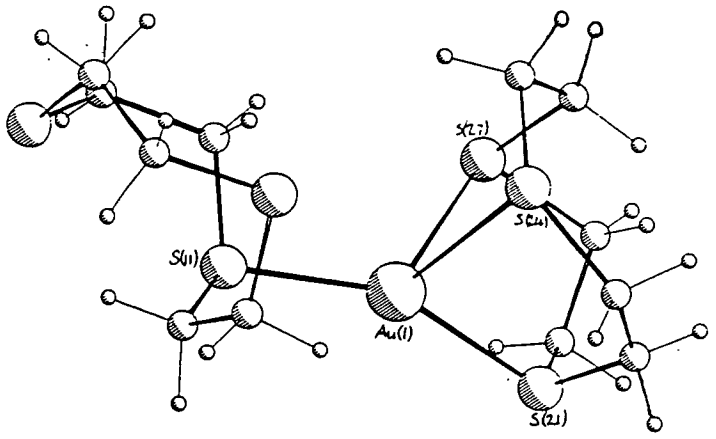

Figure 2.18 A View of the Single Crystal X-Ray Structure of $[Au([9]aneS_3)_2]^{2+}$

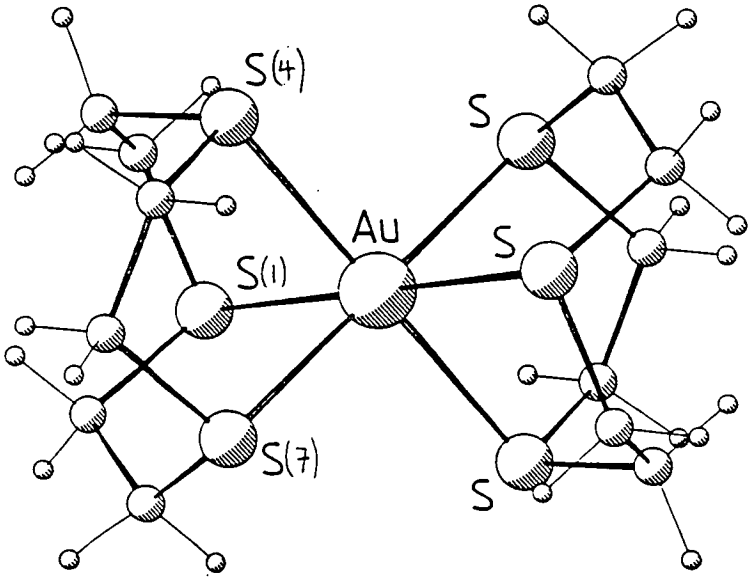

Figure 2.19 A View of the Single Crystal X-Ray Structure of $[Au([9]aneS_3)_2]^{3+}$

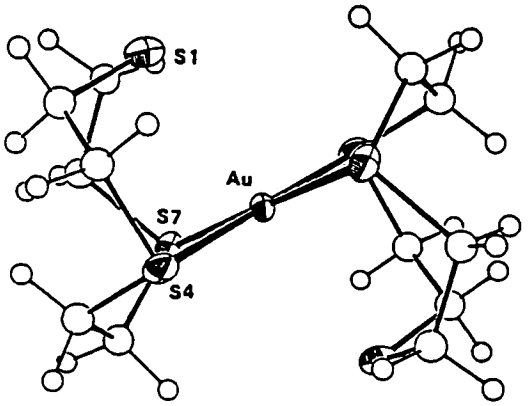

Chapter Three

SYNTHESIS OF DIMERIC COMPLEXES OF Ru(II) WITH [9]aneS$_3$

3.1 Introduction

A considerable volume of literature has been published on the chemistry of Ruthenium[34, 264, 265]. The common Ru oxidation state, Ru(II), has been extensively studied. One of the reasons for this interest is the ability of Ru complexes to act as catalysts. For example, the complex [$RuCl_2(PPh_3)_3$] acts as a catalyst for a number of reactions, including isomerisation of alkenes, dienes, aldehydes, ketones and carboxylic acids[264-267], hydroformulation of alkenes[266, 267] and the oxidation of alkenes and alcohols in the presence of O_2 or hydroperoxides[34, 264, 265].

The complex, [$RuCl_2(PPh_3)_3$] is also a useful starting material for the synthesis of a large number of complexes[26, 241, 266, 267]. Work in the Edinburgh group has shown that addition of [9]aneS$_3$ to [$RuCl_2(PPh_3)_3$] in refluxing EtOH yields a yellow compound [$RuCl_2(PPh_3)$([9]aneS$_3$)] (Table 3.1)[26, 241] . [$RuCl_2(PPh_3)$([9]aneS$_3$)] reacts with $TlPF_6$, in the presence of a donor ligand (L) to yield a range of complexes, [$RuCl(L)(PPh_3)$([9]aneS$_3$)]$^+$ (L = Py,PMe_2Ph, PhCN, $P(OMe)_2Ph$) (Table 3.2)[241]. Using the same synthetic strategy, the complexes [$RuX_2(EPPh_3)$([9]aneS$_3$)] (X = Cl,E = P, As; X = Br, E = P) (Table 3.1) and [$RuX(EPPh_3)$([9]aneS$_3$)](PF_6) (X = Cl, E = P, As; L = Py, PMe_2Ph ; X = Br, E = P, L = Py, PMe_2Ph) (Table 3.2)[241] may be synthesised from [$RuX_2(EPPh_3)_3$].

The single crystal X-ray structure of [$RuCl_2(PPh_3)$([9]aneS$_3$)] has recently been reported, and confirms the octahedral Ru(II) ion to be facially bound to a [9]aneS$_3$ macrocycle [Ru–S = 2.270(2), 2.269(2) and 2.356(2)Å], two Cl^- donors [Ru–Cl = 2.456(2) and 2.449(2)Å] and a phosphine ligand [Ru–P = 2.345(2)Å] (Figure 3.1)[268].

The ^{31}P N.M.R. spectra of half sandwich Ru [9]aneS$_3$ complexes can help to identify the products, and is also a very good indicator of the purity of the

samples. The ^{31}P N.M.R. spectral data of half sandwich Ru [9]aneS_3 complexes is listed in Table 3.3 [241, 242].

The reaction of [RuCl(R)(CE)(PPh_3)$_2$] {E = O, R = C_6H_4Me, CH=CHPh, CPh=CHPh; E = S, R = (MeO_2C)C=CH(CO_2Me)} with [9]aneS_3 yields the half-sandwich Ru complexes [Ru(CE)(R)(PPh_3)([9]aneS_3)]Cl[269]. However the addition of [9]aneS_3 to [RuCl(CR=CPhH)(CS)(PPh_3)$_2$] affords the thiocinnamoyl complex [Ru(PPH_3)(η^2-SCCPh=CHR')([9]aneS_3)]$^+$ (R = H, Ph), via vinyl-thiocarbonyl ligand coupling[269].

Figure 3.1 A View of the Single Crystal X-Ray Structure of [$RuCl_2$(PPh_3)([9]aneS_3)]

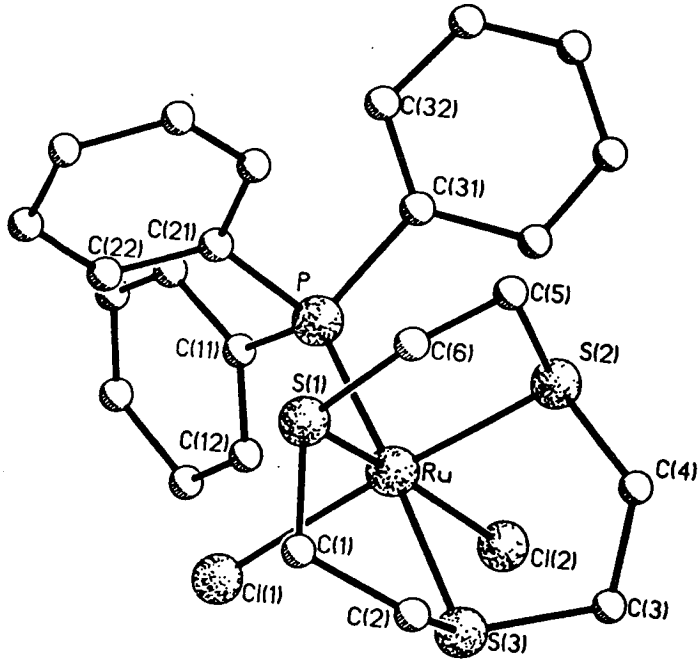

Table 3.1 The Synthesis of Half Sandwich Ru [9]aneS$_3$ Complexes

$[RuCl_3(PR_2Ph)_3]$ + $[9]aneS_3$	NH_4PF_6, CH_2Cl_2 / Reflux	$[RuCl(PR_2Ph)_2([9]aneS_3)]PF_6$ R=Me, Et
$[RuX_2(PEt_2Ph)_3]$ + $[9]aneS_3$	NH_4PF_6, EtOH / Reflux	$[RuX(PEt_2Ph)([9]aneS_3)]PF_6$ X=Cl, Br
$[RuX_2(PPh_3)_3]$ + $[9]aneS_3$	EtOH / Reflux	$[RuX_2(PPh_3)([9]aneS_3)]$ X=Cl, Br
$[RuCl_3(AsPh_3)_2(MeOH)]$ + $[9]aneS_3$	EtOH / Reflux	$[RuCl_2(AsPh_3)([9]aneS_3)]$
$[RuCl_2(CO)(PPh_3)_2(DMF)]$ + $[9]aneS_3$	NH_4PF_6, EtOH / Reflux	$[RuCl(CO)PPh_3([9]aneS_3)]PF_6$
$[RuCl_2(CO)(PEt_2Ph)_2(DMF)]$ + $[9]aneS_3$	NH_4PF_6, EtOH / Reflux	$[RuCl(CO)(PEt_2Ph)([9]aneS_3)]PF_6$ + $[RuCl(CO)(DMF)(PEt_2Ph)([9]aneS_3)]PF_6$
$[RuCl_2(CS)(PPh_3)_3]$ + $[9]aneS_3$	NH_4PF_6, EtOH / Reflux	$[RuCl_2(PPh_3)([9]aneS_3)]PF_6$ + $[RuCl(CS)(PPh_3)([9]aneS_3)]PF_6$
$[Ru(H)_2(CO)(PPh_3)_3]$ + $[9]aneS_3$	acetone, NH_4PF_6 / N_2 / Reflux	$[Ru(H)(CO)(PPh_3)([9]aneS_3)]PF_6$
$[RuCl(H)(CS)(PPh_3)_3]$ + $[9]aneS_3$	$LiClO_4, CH_2Cl_2$ / Reflux	$[Ru(H)(CS)(PPh_3)([9]aneS_3)]ClO_4$

Table 3.2 The Synthesis of Ru [9]aneS$_3$ Half Sandwich Complexes

$[RuCl_2(PPh_3)([9]aneS_3)]$ + $TlPF_6$ $\xrightarrow{CH_2Cl_2,\ L}$ $[RuCl(L)(PPh_3)([9]aneS_3)]PF_6$ L=Py, PMe_2Ph, PhCN, $P(OMe)_2Ph$

$[RuBr_2(PPh_3)([9]aneS_3)]$ + $TlPF_6$ $\xrightarrow{CH_2Cl_2,\ L}$ $[RuBr(L)(PPh_3)([9]aneS_3)]PF_6$ L=Py, PMe_2Ph

$[RuCl_2(AsPh_3)([9]aneS_3)]$ + $TlPF_6$ $\xrightarrow{CH_2Cl_2,\ L}$ $[RuCl(L)(AsPh_3)([9]aneS_3)]PF_6$ L=Py, PMe_2Ph

Figure 3.2 A View of the Single Crystal X-Ray Structure of $[RuCl(NCCH_3)(PPh_3)([9]aneS_3)](PF_6)$

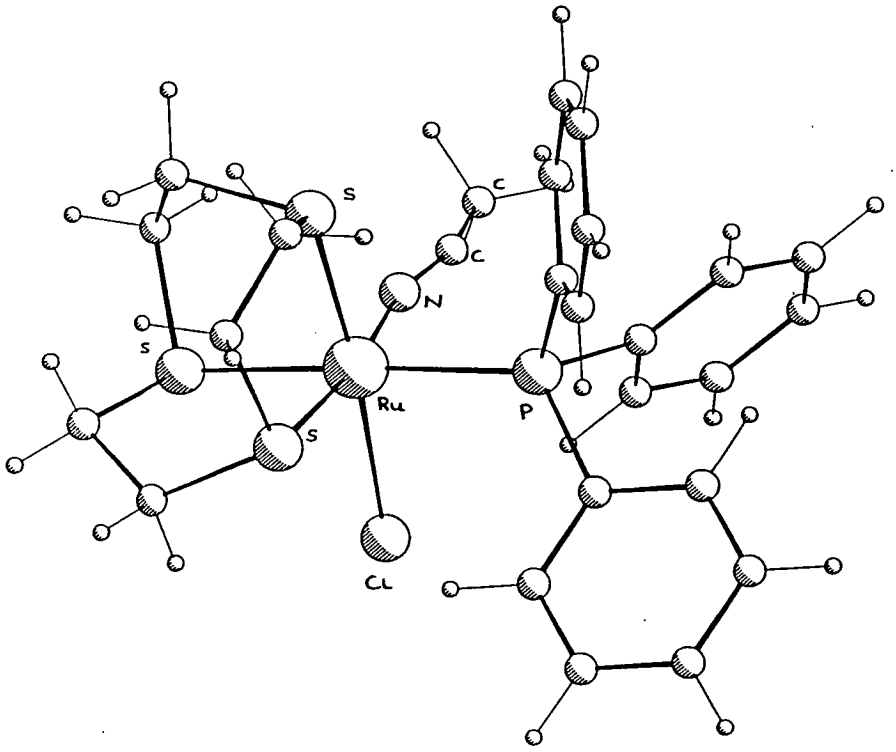

Table 3.3 ^{31}P N.M.R. Spectral Data of Complexes of the type $[Ru(PR_3)(X)(Y)([9]aneS_3)]^{n+}$

Complex	N.M.R Solvent	^{31}P N.M.R. δ in p.p.m.
$[RuCl(PMe_2Ph)_2([9]aneS_3)]^+$	$CDCl_3$	4.84
$[RuCl(PMe_2Ph)(AsPh_3)([9]aneS_3)]^+$	d^6-acetone	2.69
$[RuCl(PMe_2Ph)(PPh_3)([9]aneS_3)]^+$	$CDCl_3$	1.99(d, PMe_2Ph) 28.50(d, PPh_3) J^2_{pp} = 36 Hz
$[RuBr(PMe_2Ph)(PPh_3)([9]aneS_3)]^+$	$CDCl_3$	-0.74(d.PMe_2Ph) 27.76(d,(PPh_3) J^2_{pp} = 35Hz
$[RuCl_2(PPh_3)([9]aneS_3)]$	CD_3NO_2	22.96
$[RuCl_2(PPh_3)([9]aneS_3)]$	$CDCl_3$	35.0
$[RuBr_2(PPh_3)([9]aneS_3)]$	CD_3NO_2	22.08
$[RuCl(Py)(PPh_3)([9]aneS_3)]^+$	d^6-acetone	34.41
$[RuBr(Py)(PPh_3)([9]aneS_3)]^+$	d^6-acetone	33.92
$[RuCl(NCPh)(PPh_3)([9]aneS_3)]^+$	d^6-acetone	32.72
$[RuCl(CO)(PPh_3)([9]aneS_3)]^+$	d^6-acetone	30.83
$[RuCl(CS)(PPh_3)([9]aneS_3)]^+$	d^6-acetone	32.08
$[RuH(CO)(PPh_3)([9]aneS_3)]^+$	d^6-acetone	48.19
$[RuCl(P(OMe)_3)(PPh_3)([9]aneS_3)]^+$	d^6-acetone	113.0($P(OMe)_2Ph$) 32.0(PPh_3) J^2_{pp} = 44 Hz
$[RuCl(PEt_2Ph)_2([9]aneS_3)]^+$	d^6-acetone	21.30
$[RuBr(PEt_2Ph)_2([9]aneS_3)]^+$	CD_3NO_2	23.14
$[RuCl(PEt_2Ph)(CO)([9]aneS_3)]^+$	CD_3NO_2	31.52

One of the aims of the work described in Chapters 3, 4 and 5 was to investigate the reaction of $TlPF_6$ with $[RuCl_2(PPh_3)([9]aneS_3)]$. In the co-ordinating solvent CH_3CN, the reaction of $TlPF_6$ with $[RuCl_2(PPh_3)([9]aneS_3)]$ yields the complex $[RuCl(NCCH_3)(PPh_3)([9]aneS_3)]PF_6$, whose ^{31}P N.M.R. spectrum (CD_3CN) shows resonances at δ = 35.44 (PPh_3), - 145 (septet, J = 710Hz, PF_6^-). The single crystal X-ray structure of this complex confirms the octahedral stereochemistry of the Ru(II) ion which co-ordinates to a facially bound $[9]aneS_3$ [Ru–S = 2.348(16), 2.248(14), and 2.332(15)Å] , a Cl^- [Ru–Cl = 2.439(11)Å] , a phosphine [Ru–P = 2.360(14)Å] and an acetonitrile ligand [Ru–N = 2.01(9)Å] (Figure 3.2)[241]. This complex, $[RuCl(NCCH_3)(PPh_3)([9]aneS_3)]PF_6$ has been dissolved in refluxing CH_3CN with an excess of $TlPF_6$, but no further substitution took place[241]. Nor was any reaction observed when $[RuCl(NCCH_3)(PPh_3)([9]aneS_3)]PF_6$ and $TlPF_6$ were refluxed in CH_2Cl_2 in the presence of donor ligands[241]. The reaction of $[RuCl_2(PPh_3)([9]aneS_3)]$ with $TlPF_6$ in non-co-ordinating solvents is investigated in this chapter, since the possible product $[RuCl(Solv)(PPh_3)([9]aneS_3)]PF_6$ should be reactive to further substitution, and therefore a useful precursor for half-sandwich Ru complexes.

3.2 Results and Discussion

3.2.1 The Thalliation of $[RuCl_2(PPh_3)([9]aneS_3)]$

The reaction of $[RuCl_2(PPh_3)([9]aneS_3)]$ with $TlPF_6$ in CH_2Cl_2 at 298K leads to the formation of a dark yellow solution and a small amount of white precipitate of TlCl. Removing the TlCl and reducing the solution to dryness reveals a yellow/orange product. The ir spectrum of this product shows bands indicating the presence of $[9]aneS_3$, PPh_3 and PF_6^-

[υ (cm^{-1}) = 1483(ms), 1435(s), 1410(ms), 1090(s), 835(vs), 555(s), 528(s), 513(ms), 499(m)] . However, this product slowly decomposes in acetone, CH_3NO_2 or CH_3CN to afford more white precipitate of TlCl. Due to this decomposition, the ^1H N.M.R. spectrum (d^6-acetone) is broad with resonances at δ = 2.5–3.2 (m, [9]aneS_3) and 7.3–8.0(m, PPh_3) p.p.m.

The reaction of [$RuCl_2(PPh_3)$([9]aneS_3)] with $TlPF_6$ in CD_3NO_2 and d^8-THF at 298K affords a white precipitate and a yellow solution after stirring for fifteen hours. Filtering the mixture and reducing the volume results in a clear dark solution, which slowly evaporates to yield orange and yellow crystals. Both samples are suitable for X-ray analysis.

3.2.1.1 The Crystal Structure of [$Ru(PPh_3)$([9]aneS_3)(μ-Cl)]$_2(PF_6)_2$

The single crystal X-ray structure of the <u>orange</u> complex shows that it is the bis-chloro-bridged Ru(II/II) dimer, [$Ru(PPh_3)$([9]aneS_3)(μ-Cl)]$_2(PF_6)_2$. Each Ru ion is octahedrally co-ordinated to one P-donor (Ru-P = 2.3741(10)Å), two bridging Cl^- donors [Ru-Cl = 2.4654(10), 2.4945(10)Å] and a facially bound [9]aneS_3 [Ru-S = 2.2880(10), 2.3456(10), and 2.2817(10)Å] (Figure 3.3 and Scheme 3.1). The distance between the Ru atoms is 3.7769(6)Å and between the Cl atoms is 3.2151(18)Å. The $RuCl_2Ru$ bridging unit is planar [$\angle$Ru-Cl-Ru = 99.19(3)° and $\angle$Cl-Ru-Cl = 80.81(3)°]. The two halves of the cation are related by inversion through ($^1/_2$, 0, $^1/_2$). Selected bond lengths and angles are given in Table 3.4 and a view of the X-ray crystal structure of the cation is shown in Figure 3.3.

Table 3.4 Bond Lengths (Å), Angles (°) and Torsion Angles (°) with standard deviations for $[Ru(PPh_3)([9]aneS_3)(\mu\text{-}Cl)]_2^{2+}$

Ru	—	Cl	2.4654	(10)	C(3)	—	S(4)	1.822 (4)
Ru	—	S(1)	2.2880	(10)	S(4)	—	C(5)	1.828 (4)
Ru	—	S(4)	2.3456	(10)	C(5)	—	C(6)	1.519 (6)
Ru	—	S(7)	2.2817	(10)	C(6)	—	S(7)	1.835 (4)
Ru	—	P	2.3741	(10)	S(7)	—	C(8)	1.855 (4)
Ru	—	Cl(')	2.4945	(10)	C(8)	—	C(9)	1.517 (5)
S(1)	—	C(2)	1.843	(4)	P	—	C(11P)	1.8476 (23)
S(1)	—	C(9)	1.833	(4)	P	—	C(21P)	1.8513 (24)
C(2)	—	C(3)	1.526	(5)	P	—	C(31P)	1.8385 (22)

Cl	—	Ru	—	S(1)	97.52 (3)	Ru	—	Cl	—	Ru(') 99.19 (3)
Cl	—	Ru	—	S(4)	83.54 (3)	Ru	—	S(1)	—	C(2) 107.32 (13)
Cl	—	Ru	—	S(7)	169.97 (3)	C(2)	—	S(1)	—	C(9) 99.48 (17)
Cl	—	Ru	—	P	92.80 (3)	S(1)	—	C(2)	—	C(3) 112.0 (3)
Cl	—	Ru	—	Cl(')	80.81 (3)	C(2)	—	C(3)	—	S(4) 112.5 (3)
S(1)	—	Ru	—	S(4)	87.29 (3)	C(3)	—	S(4)	—	C(5) 102.39 (18)
S(1)	—	Ru	—	S(7)	88.13 (3)	S(4)	—	C(5)	—	C(6) 110.2 (3)
S(1)	—	Ru	—	P	90.59 (3)	C(5)	—	C(6)	—	S(7) 112.5 (3)
S(1)	—	Ru	—	Cl(')	170.70 (3)	C(6)	—	S(7)	—	C(8) 99.50 (18)
S(4)	—	Ru	—	S(7)	88.48 (3)	S(7)	—	C(8)	—	C(9) 113.2 (3)
S(4)	—	Ru	—	P	175.50 (3)	S(1)	—	C(9)	—	C(8) 113.6 (3)
S(4)	—	Ru	—	Cl(')	83.43 (3)	C(11P)	—	P	—	C(21P) 103.41 (10)
S(7)	—	Ru	—	P	95.43 (3)	C(11P)	—	P	—	C(31P) 107.33 (10)
S(7)	—	Ru	—	Cl(')	92.27 (3)	C(21P)	—	P	—	C(31P) 95.68 (10)
P	—	Ru	—	Cl(')	98.61 (3)					

C(9)	—	S(1)	—	C(2)	—	C(3)	-	134.2	(3)	S(4)	— C(5) — C(6) — S(7) 52.5 (3)
C(2)	—	S(1)	—	C(9)	—	C(8)		77.3	(3)	C(5)	— C(6) — S(7) — C(8) 64.5 (3)
S(1)	—	C(2)	—	C(3)	—	S(4)		45.7	(3)	C(6)	— S(7) — C(8) — C(9) -129.5 (3)
C(2)	—	C(3)	—	S(4)	—	C(5)		64.2	(3)	S(7)	— C(8) — C(9) — S(1) 37.8 (4)
C(3)	—	S(4)	—	C(5)	—	C(6)		-138.9	(3)		

Figure 3.3 A View of the Single Crystal X-Ray Structure of $[Ru(PPh_3)([9]aneS_3)(\mu\text{-}Cl)]_2(PF_6)_2$

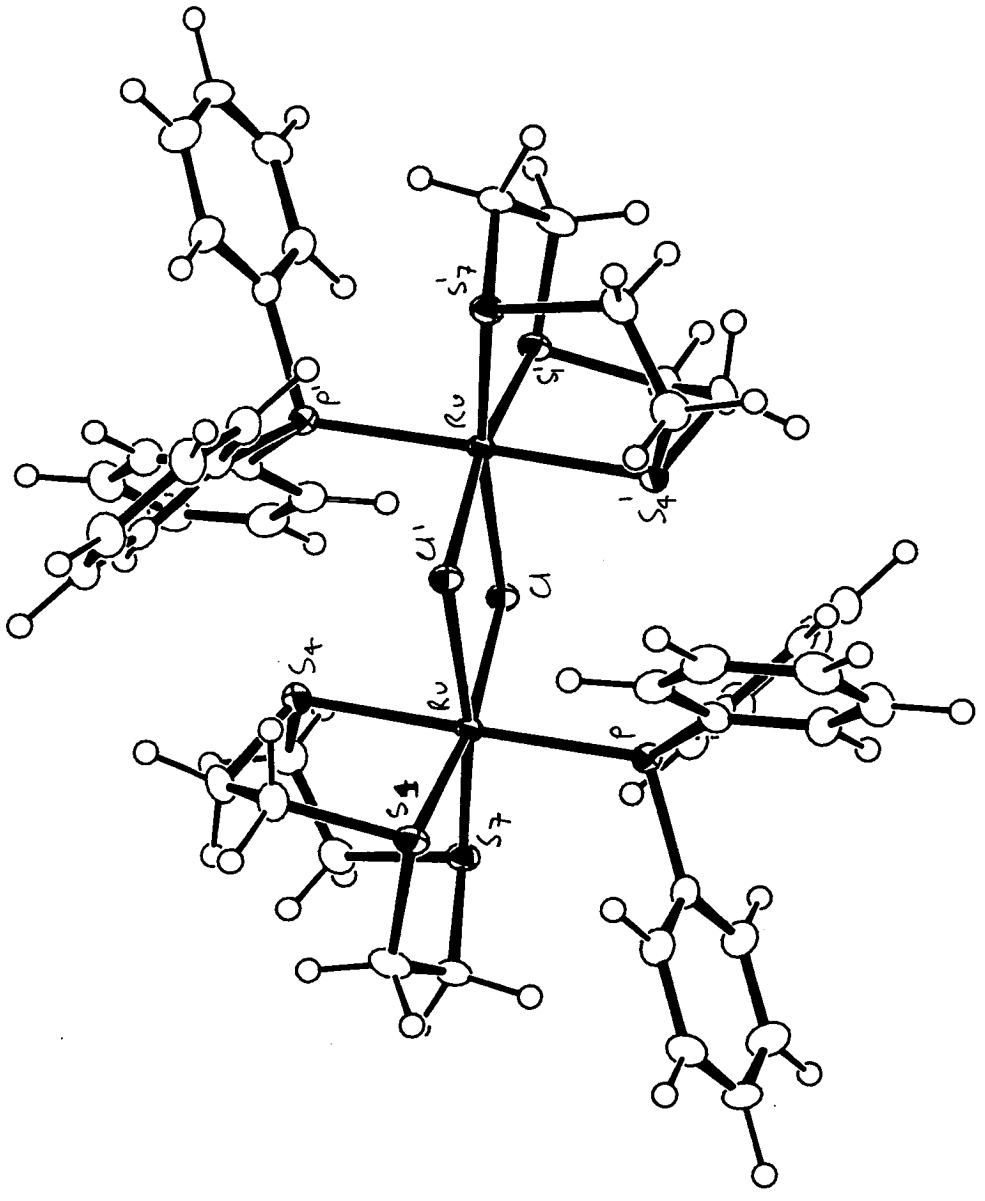

A number of other chloro-bridged Ru dimers are reported in the literature[34, 264-267]. The single crystal X-ray structure of the complex $[\{(PR_3)(CO)_2Ru(\mu\text{-}Cl)\}_2]$ [PR_3 = P(t-Bu)$_2$(p-tolyl)] shows a Ru···Ru bond distance of 2.632(2)Å suggesting that there is a bond between the two Ru(I) metal ions. The crystal structure also shows the $\{RuCl_2Ru\}$ fragment to be non planer[270]. Triply chloro-bridged dimers of the type $[(X)(Y)(Z)(Ru(\mu\text{-}Cl)_3Ru(X')(Y')(Z')]$ have also been synthesised, and the crystal structure of $[(PPh_3)_2(SC)Ru(\mu\text{-}Cl)_3RuCl(PPh_3)_2]$ solved. In this case the Ru···Ru distance is 3.35(2)Å[271]. A large number of bis-chloro bridged Ru(II)/Ru(II) dimers have also been characterised[34, 265]. The crystal structure of the novel dimer $[(PPh_3)Ru(DPF)(\mu\text{-}Cl)Cl]_2$ (DPF = 3,3',4,4',-tetramethyl-1,1'-diphosphaferrocene) has been reported (Figure 3.4)[272]. The $\{RuCl_2Ru\}$ moiety is planar, and the Ru···Ru is 3.683(2)Å[272], which is similar to the Ru···Ru distance of 3.7768(6)Å in the orange complex $[Ru(PPh_3)[9]aneS_3(\mu\text{-}Cl)]_2(PF_6)_2$.

Figure 3.4 A Representation of $[(PPh_3)Ru(DPF)(\mu\text{-}Cl)_2Cl]_2$

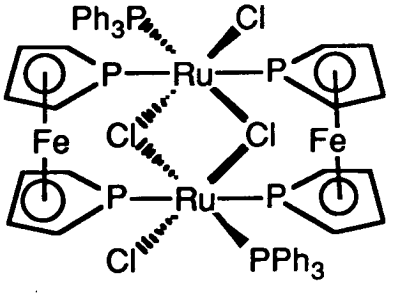

3.2.1.2 The Crystal Structure of $[Ru(PPh_3)([9]aneS_3)(\mu\text{-}Cl)_2Tl]_2(PF_6)_2$

The single crystal X-ray structure of the **yellow** product confirms it to be the Ru(II)/Ru(II) dimer, $[Ru(PPh_3)([9]aneS_3)(\mu\text{-}Cl)_2Tl]_2(PF_6)_2$. Each Ru(II) ion is octahedrally co-ordinated to a facially bound [9]$aneS_3$ [Ru-S = 2.2804(13), 2.3501(13) and 2.2821(13)Å] , two bridging Cl^- donors [Ru-Cl = 2.4416(12) and 2.4526(12)Å] and a phosphine donor [Ru-P = 2.3539(12)Å] . The Ru(II) ions in $[Ru(PPh_3)([9]aneS_3)(\mu\text{-}Cl)_2Tl]_2(PF_6)_2$ have a similar stereochemistry to those in $[Ru(PPh_3)([9]aneS_3)(\mu\text{-}Cl)]_2(PF_6)_2$. However, in the yellow complex $[Ru(PPh_3)([9]aneS_3)(\mu\text{-}Cl)_2Tl]_2(PF_6)_2$, the bridging group is a novel Tl_2Cl_4 'ladder' species (Figures 3.5 and 3.6). The Tl(I) ion in this bridging group shows an unusual, distorted trigonal planar geometry [$\angle Cl(1)TlCl(2) = 69.36(3)°$, $\angle Cl(1)TlCl(1') = 72.66$ and $\angle Cl(2)TlCl(1') = 107.38(3)°$] . The two halves of the cation are related by an inversion centre at (0,1,1). Selected bond lengths and angles are shown in Table 3.5 and views of the X-ray structure are shown in Figures 3.5 and 3.6.

A number of Tl-heterometallic complexes containing transition metals are described in the literature[273-285], although most of them contain direct M-Tl interactions[273-279]. Only a few structures contain a Tl to metal bridging unit, M-X-Tl[280-285], and only two of these species contain a bridging halide. Mingos *et al* prepared the complex $[Pt_3(CO)_3(PCy_3)_3Tl][Rh(C_8H_{12}Cl_2)]$ (Cy = cyclohexyl), which incorporates both Pt–Tl bonds as well as a Rh···Cl···Tl moiety (Figure 3.7)[284]. Schmidbauer *et al* have reacted $[GaBr_4]^-$ with $[Tl(C_6H_3Me_3)_2]^{1-}$ and $[Tl(C_6H_3Me_3)]^{1-}$ to afford $[\{C_6H_3(CH_3)_3\}_6Tl_4][GaBr_4]_4$. The single crystal X-ray structure of this complex reveals a series of Ga···Br···Tl interactions (Figure 3.8)[285].

Table 3.5 Bond Lengths (Å), Angles (°) and Torsion Angles (°) with standard deviations $[Ru(PPh_3)([9]aneS_3)(\mu\text{-}Cl)_2Tl]_2^{2+}$

Tl(1)	—	Ru(1)	4.0596 (4)	S(1)	—	C(9)	1.835 (5)
Tl(1)	—	Cl(1)	3.0734 (11)	C(2)	—	C(3)	1.488 (8)
Tl(1)	—	Cl(2)	3.0026 (12)	C(3)	—	S(4)	1.821 (6)
Tl(1)	—	S(4)	3.6481 (13)	S(4)	—	C(5)	1.803 (6)
Ru(1)	—	Cl(1)	2.4416 (12)	C(5)	—	C(6)	1.493 (8)
Ru(1)	—	Cl(2)	2.4526 (12)	C(6)	—	S(7)	1.837 (5)
Ru(1)	—	S(1)	2.2804 (13)	S(7)	—	C(8)	1.802 (5)
Ru(1)	—	S(4)	2.3501 (13)	C(8)	—	C(9)	1.509 (8)
Ru(1)	—	S(7)	2.2821 (13)	P(1)	—	C(1A)	1.8453 (25)
Ru(1)	—	P(1)	2.3539 (12)	P(1)	—	C(1B)	1.8416 (25)
S(1)	—	C(2)	1.819 (5)	P(1)	—	C(1C)	1.8508 (24)

Cl(1)	—	Tl(1)	—	Cl(2)	69.35(3)	C(2)	—	Cl	—	C(9)	101.41 (25)
Cl(1)	—	Ru(1)	—	Cl(2)	89.89(4)	S(1)	—	C(2)	—	C(3)	115.6 (4)
Cl(1)	—	Ru(1)	—	S(1)	87.40(4)	C(2)	—	C(3)	—	S(4)	112.0 (4)
Cl(1)	—	Ru(1)	—	S(4)	86.47(4)	Ru(1)	—	S(4)	—	C(3)	105.71 (18)
Cl(1)	—	Ru(1)	—	S(7)	173.30(4)	Ru(1)	—	S(4)	—	C(5)	102.49 (19)
Cl(1)	—	Ru(1)	—	P(1)	91.88(4)	C(3)	—	S(4)	—	C(5)	101.8 (3)
Cl(2)	—	Ru(1)	—	S(1)	170.57(4)	S(4)	—	C(5)	—	C(6)	114.0 (4)
Cl(2)	—	Ru(1)	—	S(4)	83.08(4)	C(5)	—	C(6)	—	S(7)	113.2 (4)
Cl(2)	—	Ru(1)	—	S(7)	93.10(4)	Ru(1)	—	S(7)	—	C(6)	106.09 (18)
Cl(2)	—	Ru(1)	—	P(1)	94.67(4)	Ru(1)	—	S(7)	—	C(8)	103.48 (18)
S(1)	—	Ru(1)	—	S(4)	87.74(5)	C(6)	—	S(7)	—	C(8)	101.14 (25)
S(1)	—	Ru(1)	—	S(7)	88.70(5)	S(7)	—	C(8)	—	C(9)	115.3 (4)
S(1)	—	Ru(1)	—	P(1)	94.44(4)	S(1)	—	C(9)	—	C(8)	112.1 (4)
S(4)	—	Ru(1)	—	S(7)	87.94(4)	Ru(1)	—	C(8)	—	C(1A)	118.76 (9)
S(4)	—	Ru(1)	—	P(1)	177.21(4)	Ru(1)	—	P(1)	—	C(1B)	111.20 (9)
S(7)	—	Ru(1)	—	P(1)	93.85(4)	Ru(1)	—	P(1)	—	C(1C)	118.48 (8)
Tl(1)	—	Cl(1)	—	Ru(1)	94.10(18)	C(1A)	—	P(1)	—	C(1B)	104.73 (11)
Tl(1)	—	Cl(2)	—	Ru(1)	95.65(18)	C(1A)	—	P(1)	—	C(1C)	98.32 (11)
Ru(1)	—	S(1)	—	C(2)	103.62(18)	C(1B)	—	P(1)	—	C(1C)	1103.24 (11)
Ru(1)	—	S(1)	—	C(9)	106.57(18)						

C(9)	—	S(1)	—	C(2)	—	C(3)	-70.2 (4)	S(4)	—	C(5)	—	C(6)	—	S(7)	-45.2 (5)
C(2)	—	S(1)	—	C(9)	—	C(8)	129.8 (4)	C(5)	—	C(6)	—	S(7)	—	C(8)	133.2 (4)
S(1)	—	C(2)	—	C(3)	—	S(4)	-44.1 (5)	C(6)	—	S(7)	—	C(8)	—	C(9)	-70.7 (4)
C(2)	—	C(3)	—	S(4)	—	C(5)	132.0 (4)	S(7)	—	C(8)	—	C(9)	—	S(1)	-41.0 (5)
C(3)	—	S(4)	—	C(5)	—	C(6)	-68.4 (4)								

Figure 3.5 A View of the Single Crystal X-Ray Strucure of $[Ru(PPh_3)([9]aneS_3)(\mu\text{-}Cl)_2Tl]_2(PF_6)_2$

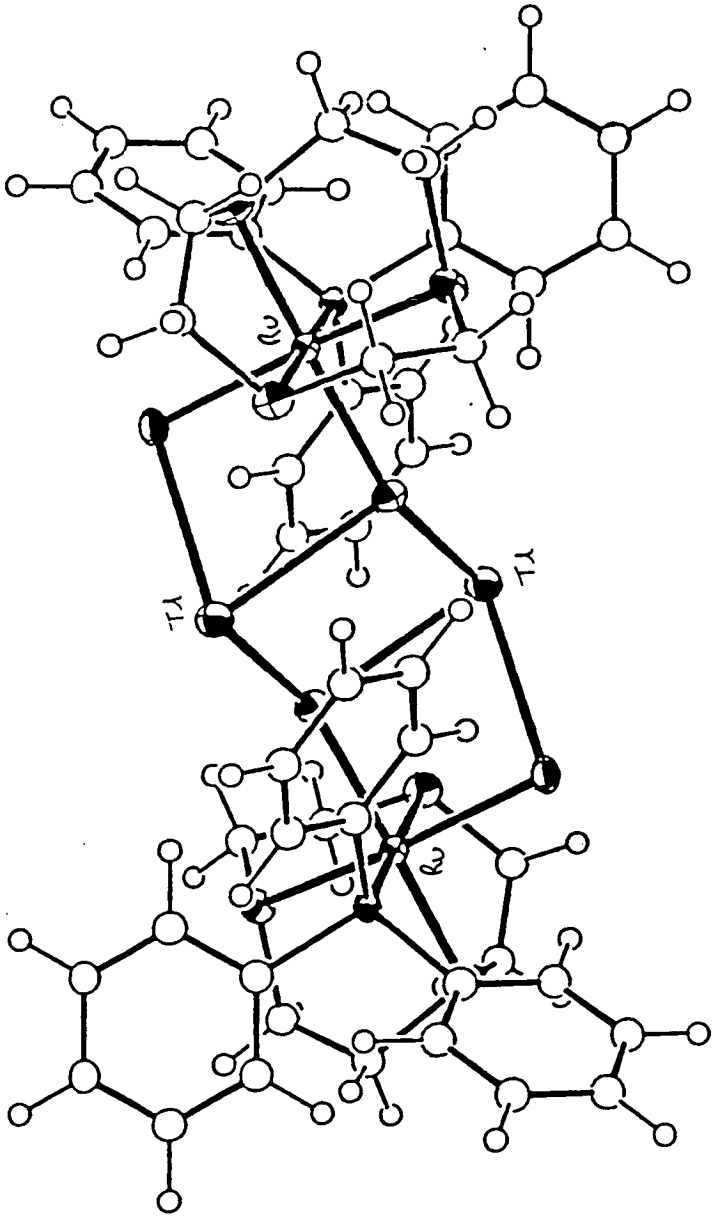

Figure 3.6 An Alternative View of the Single Crystal X-Ray Strucure of $[Ru(PPh_3)([9]aneS_3)(\mu\text{-}Cl)_2Tl]_2(PF_6)_2$

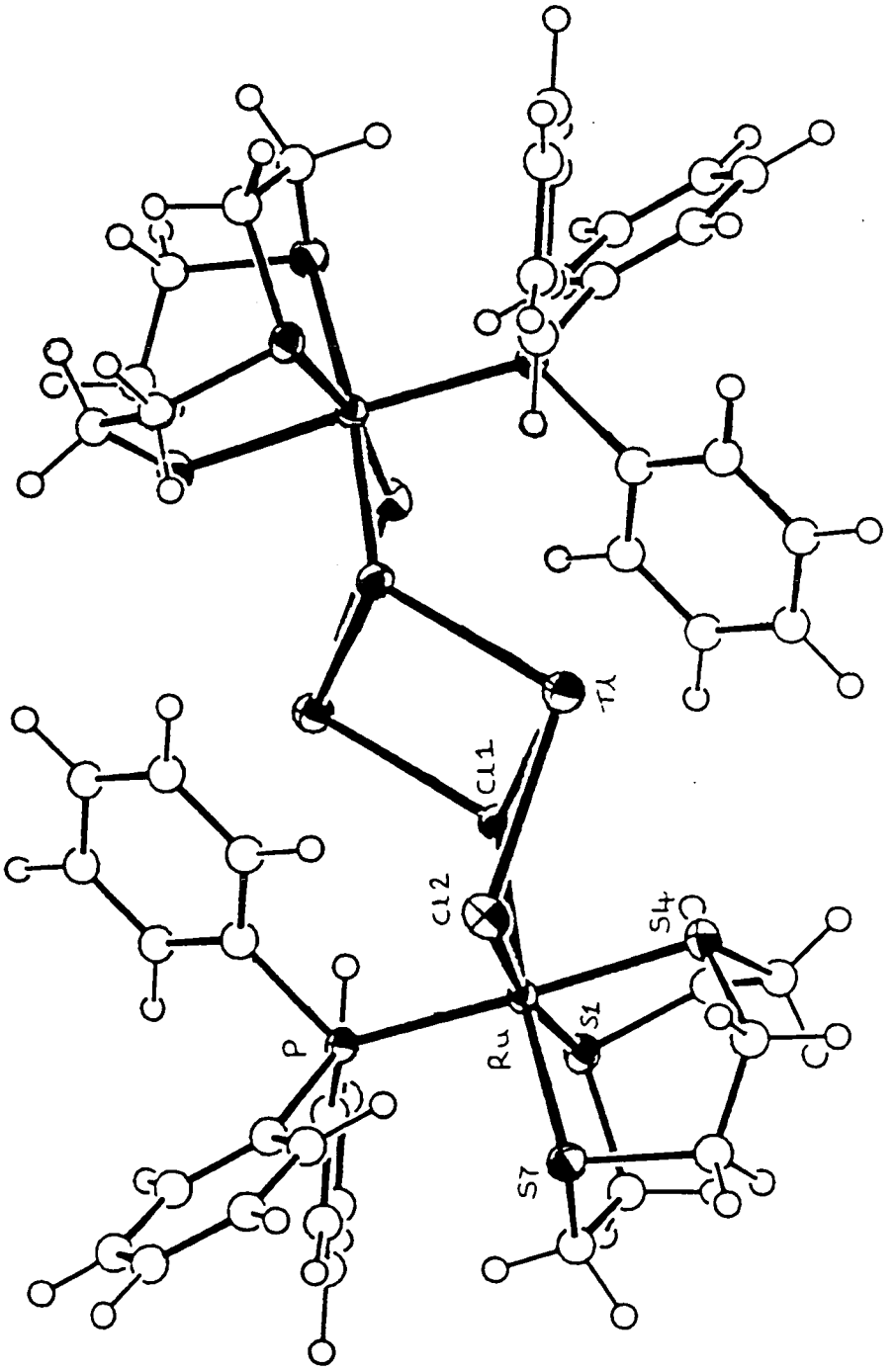

Figure 3.7 A Representation of the Complex $[Pt_3(CO)_3(PCy_3)_3Tl][Rh(C_8H_{12})Cl_2]$.

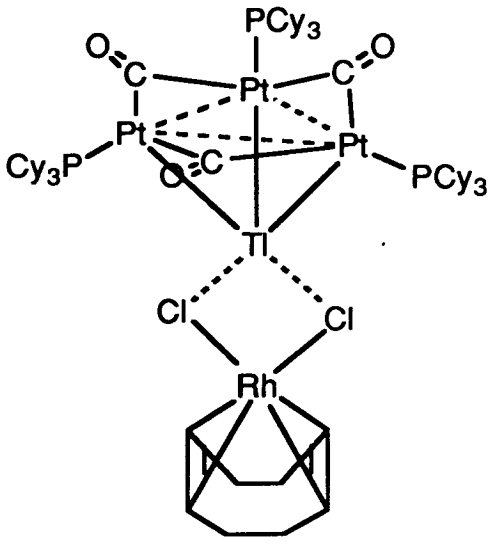

Figure 3.8 A Representation of the Complex $[\{C_6H_3(CH_3)_3\}_6Tl_4][GaBr_4]$

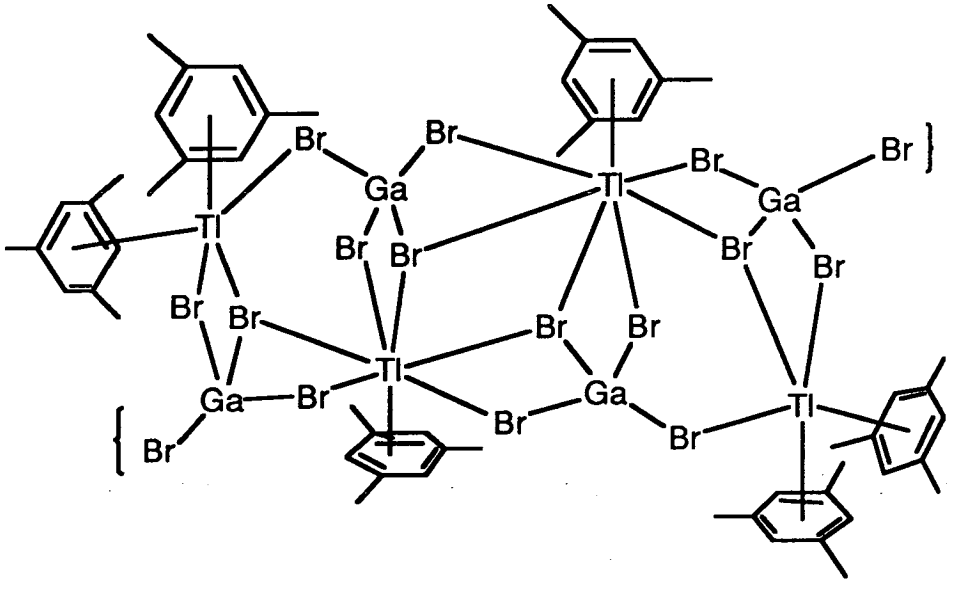

The formation of the complex, $[Ru(PPh_3)([9]aneS_3)(\mu\text{-}Cl)_2Tl]_2^{2+}$ suggests that the first step in the thalliation reaction involves the interaction of Tl^+ with the Ru-Cl bond to form a Ru-Cl:→Tl species. Subsequent elimination of TlCl in the presence of a co-ordinating ligand, L, affords the complex $[RuCl(L)PPh_3([9]aneS_3)]^+$ (Figure 3.9).

Figure 3.9 The Reaction of $TlPF_6$ with $[RuCl_2(PPh_3)([9]aneS_3)]$

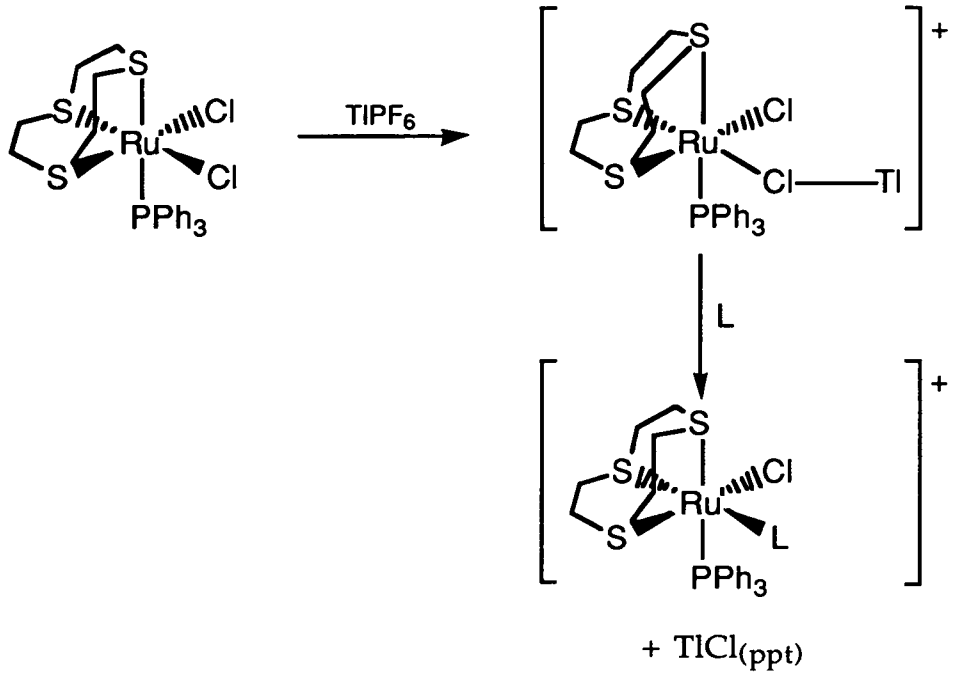

Thus, addition of $TlPF_6$ to $[RuCl_2(PPh_3)([9]aneS_3)]$ in CH_2Cl_2 at 298K yields a mixture of two dimeric Ru complexes, which have been identified as $[Ru(PPh_3)([9]aneS_3)(\mu\text{-}Cl)]_2(PF_6)_2$ and $[Ru(PPh_3)([9]aneS_3)(\mu\text{-}Cl)_2Tl_2](PF_6)_2$ by X-ray diffraction. However, pure samples of these complexes are not formed when the reaction takes place at 298K. In order to investigate their reactivity and chemistry, pure samples of both complexes have to be prepared.

3.2.2 The Synthesis and Reactivity of $[Ru(PPh_3)([9]aneS_3)(\mu\text{-}Cl)]_2(PF_6)_2$

The addition of $TlPF_6$ to $[RuCl_2(PPh_3)([9]aneS_3)]$ in CD_3NO_2 or acetone results in a mixture of the two dimeric Ru complexes, $[Ru(PPh_3)([9]aneS_3)(\mu\text{-}Cl)]_2(PF_6)_2$ and $[Ru(PPh_3)([9]aneS_3)(\mu\text{-}Cl)_2Tl]_2(PF_6)_2$ discussed in Section 3.2.1 above. However, the reaction between $[RuCl_2(PPh_3)([9]aneS_3)]$ and $TlPF_6$ in refluxing acetone or CH_2Cl_2 affords a copious quantity of white precipitate (TlCl). Filtration of the mixture results in a golden yellow solution which yields an orange solid on removal of solvent.

Dissolving this product in acetone and allowing it to stand for one day results in a further small amount of white precipitate and a clear golden yellow solution. Addition of hexane to this solution forms an orange precipitate which is collected and dried. The ir spectrum of the isolated product indicates the presence of [9]aneS$_3$, PPh$_3$ and PF_6^- [υ cm^{-1} = 1480(ms), 1432(s), 1410(ms), 1089(ms), 835(vs), 552(s), 526(s), 513(ms), 499(ms)] . The ^{1}H N.M.R. spectrum (d^6-acetone) of this orange complex shows resonances at δ = 2.2–3.5 (m, broad, [9]aneS$_3$) and 7.35–8.0 p.p.m.(m, PPh$_3$) (Figure 3.10), while the ^{31}P N.M.R. (d^6-acetone) spectrum reveals resonances at δ = -145(septet, J = 710Hz, PF_6^-) and 33.4 p.p.m.(s, PPh$_3$). The F.A.B. mass spectrum shows peaks with the correct isotopic distribution at m/e = 716, 614 and 579, which are assigned to $\{Ru_2Cl_2(PPh_3)([9]aneS_3)\}^+$, $\{RuCl_2(PPh_3)([9]aneS_3)\}^+$ and $\{RuCl(PPh_3)([9]aneS_3)\}^+$ respectively. The product can therefore be assigned as the dimer $[Ru(PPh_3)([9]aneS_3)(\mu\text{-}Cl)]_2(PF_6)_2$, whose crystal structure is shown in Figure 3.3.

When $[Ru(PPh_3)([9]aneS_3)(\mu\text{-}Cl)]_2(PF_6)_2$ was dissolved in CH_3CN a yellow solution formed. Removing the solvent and recrystallising the residue results in a lemon yellow solid, which can be recrystallised from acetone and hexane. The ir and ^{1}H N.M.R. spectra of this product are the same as $[RuCl(NCCH_3)(PPh_3)([9]aneS_3)]PF_6$, which was first synthesised in Edinburgh by Hyde[286]. This result indicates that the chloro-bridged dimer is easily cleaved, and in co-ordinating solvents the species in solution is $[Ru(solv)Cl(PPh_3)([9]aneS_3)]PF_6$ (solv = solvent).

Figure 3.10 The ^{1}H N.M.R. Spectrum (d^{6}-acetone) of $[Ru(PPh_3)([9]aneS_3)(\mu\text{-}Cl)]_2(PF_6)_2$

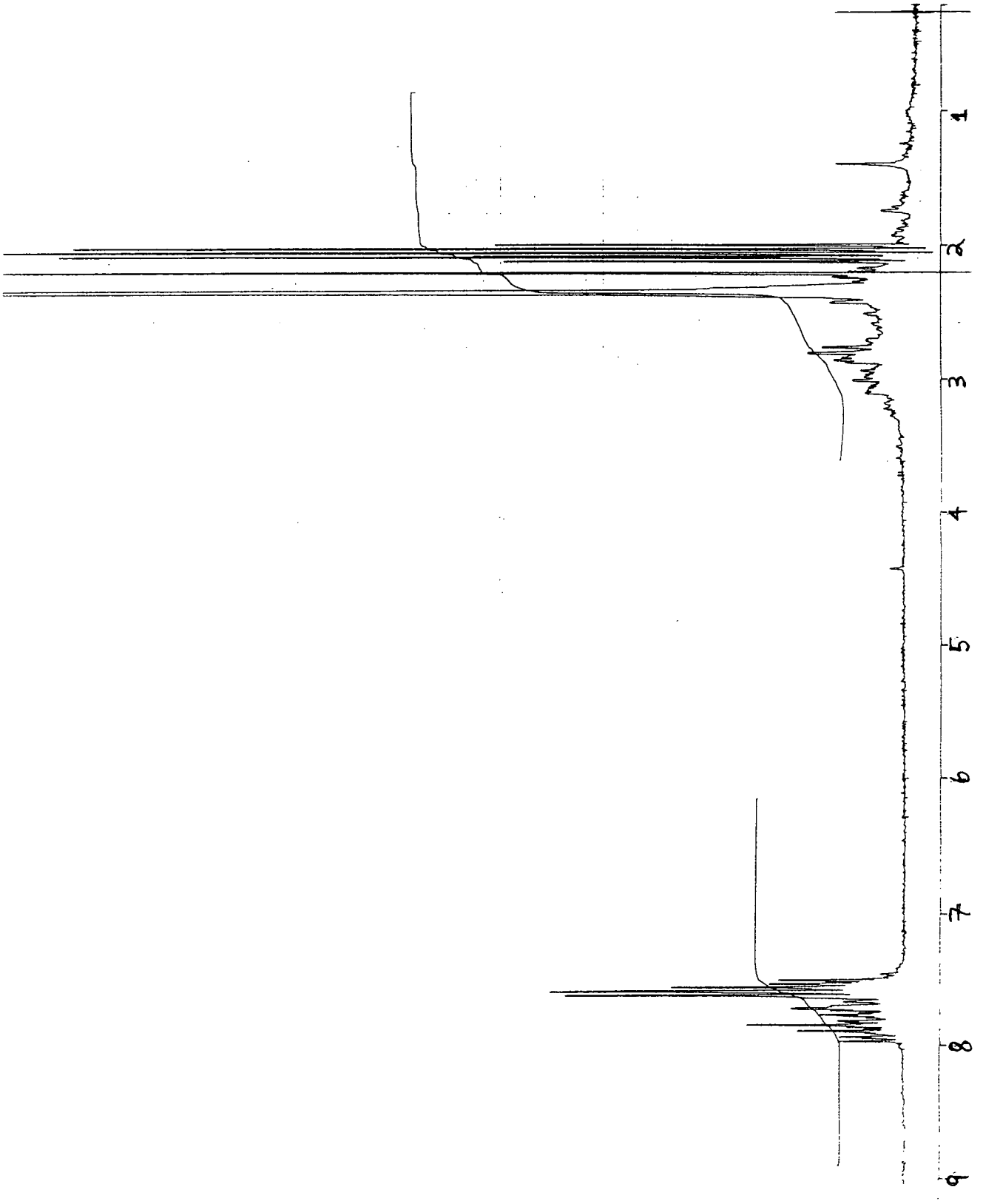

3.2.3 The Synthesis and Reactivity of $[RuCl(PPh_3)([9]aneS_3)(\mu\text{-}Cl)_2Tl]_2(PF_6)_2$

A number of problems occurred in the synthesis of pure $[Ru(PPh_3)([9]aneS_3)(\mu\text{-}Cl)]_2Tl](PF_6)_2$. The complex rapidly decomposes in solution, forming a white precipitate of TlCl. This decomposition is slower at reduced temperatures. The synthesis of the RuTl dimeric complex also needs to be carried out under an inert atmosphere. In acetone, regardless of whether a low temperature and an inert atmosphere are used, the reaction of $[RuCl_2(PPh_3)([9]aneS_3)]$ and $TlPF_6$ results in a white precipitate of TlCl. Filtering this mixture through celite and reducing the solution to dryness reveals a solid, whose ir, ^1H N.M.R. and F.A.B. mass spectra are identical to the mixture of products, $[Ru(PPh_3)([9]aneS_3)(\mu\text{-}Cl)]_2(PF_6)_2$ and $[Ru(PPh_3)([9]aneS_3)(\mu\text{-}Cl)_2Tl]_2(PF_6)_2$ discussed in Section 3.2.1.

The reaction of $TlPF_6$ with $[RuCl_2(PPh_3)([9]aneS_3)]$ in CH_2Cl_2 at 0° C under N_2 yields a clear solution. Rapidly reducing this solution to dryness yields a yellow solid. The ir spectrum of this product confirms the presence of $[9]aneS_3$, PPh_3 and PF_6^- with bands observed at υ cm^{-1} = 1482(ms), 1434(s), 1409(ms), 1090(s), 840(vs), 558(s), 527(ms), 513(m), 449(m). The F.A.B. mass spectrum of the product shows peaks with the correct isotopic distribution at m/e = 819, 614 and 579, which can be assigned as $\{RuCl_2Tl(PPh_3)([9]aneS_3)\}^+$, $\{RuCl_2(PPh_3)([9]aneS_3)\}^+$ and $\{RuCl(PPh_3)([9]aneS_3)\}^+$ respectively. The ^1H N.M.R. spectrum (d^6-acetone,230K) confirms the presence of $[9]aneS_3$ and PPh_3 with resonances at δ = 2.5–3.5 (broad, m, $[9]aneS_3$) and 7.3-8.0p.p.m.(m, PPh_3) (Figure 3.11). The product is therefore assigned as the Ru/Tl dimer, $[RuCl(PPh_3)([9]aneS_3)(\mu\text{-}Cl)_2Tl]_2(PF_6)_2$ whose X- ray crystal structure is shown in Figures 3.5 and 3.6. The ^{31}P N.M.R. spectrum(d^6-acetone) shows resonances at δ= -145(septet, J = 710 Hz, PF_6^-), 33.5 and 32.7 p.p.m. Both the ^{31}P and the ^1H N.M.R. spectra are both broadened due to the precipitation of the white precipitate of TlCl which forms during the accumulation of the spectra. The

^{31}P N.M.R. spectrum exhibits two signals in the PPh_3 region at δ = 32.8 and 33.5 p.p.m.. The signal at δ = 33.5 p.p.m. is probably due to the Ru dimer, $[Ru(PPh_3)([9]aneS_3)(\mu\text{-}Cl)]_2(PF_6)_2$. However, it is not clear whether this dimer is present in the original product as a minor impurity, or whether it is formed in solution during the accumulation of the spectrum. The resonance at δ = 32.8 p.p.m. in the ^{31}P N.M.R. spectrum is assigned to the PPh_3 group in the complex, $[Ru(PPh_3)([9]aneS_3)(\mu\text{-}Cl)_2Tl]_2(PF_6)_2$.

The yellow complex, $[Ru(PPh_3)([9]aneS_3)(\mu\text{-}Cl)Tl_2]_2(PF_6)_2$ dissolves in acetone at 298K and after 24 hours, a copious precipitation of TlCl forms. Removing the TlCl, reducing the solution in volume and adding hexane yields an orange precipitate, which is collected and dried. The ir, ^1H N.M.R. and ^{31}P N.M.R spectra of this orange complex are identical to the Ru dimer, $[Ru(PPh_3)([9]aneS_3)(\mu\text{-}Cl)]_2(PF_6)_2$, discussed in Section 3.2.2.

Dissolving the yellow complex, $[Ru(PPh_3)([9]aneS_3)(\mu\text{-}Cl)_2Tl]_2(PF_6)_2$ in CH_3CN results in a large quantity of TlCl being precipitated and when this mixture is filtered a bright yellow solution is isolated. Reducing this solution in volume and recrystallising it from acetone and hexane results in a lemon yellow solid of which ir, ^1H N.M.R. and ^{31}P N.M.R spectra are the same as the complex, $[RuCl(NCCH_3)(PPh_3)([9]aneS_3)]PF_6$.

Figure 3.11 The ^{1}H N.M.R. Spectrum (d^{6}-acetone) of $[Ru(PPh_3)([9]aneS_3)(\mu\text{-}Cl)_2Tl]_2(PF_6)_2$

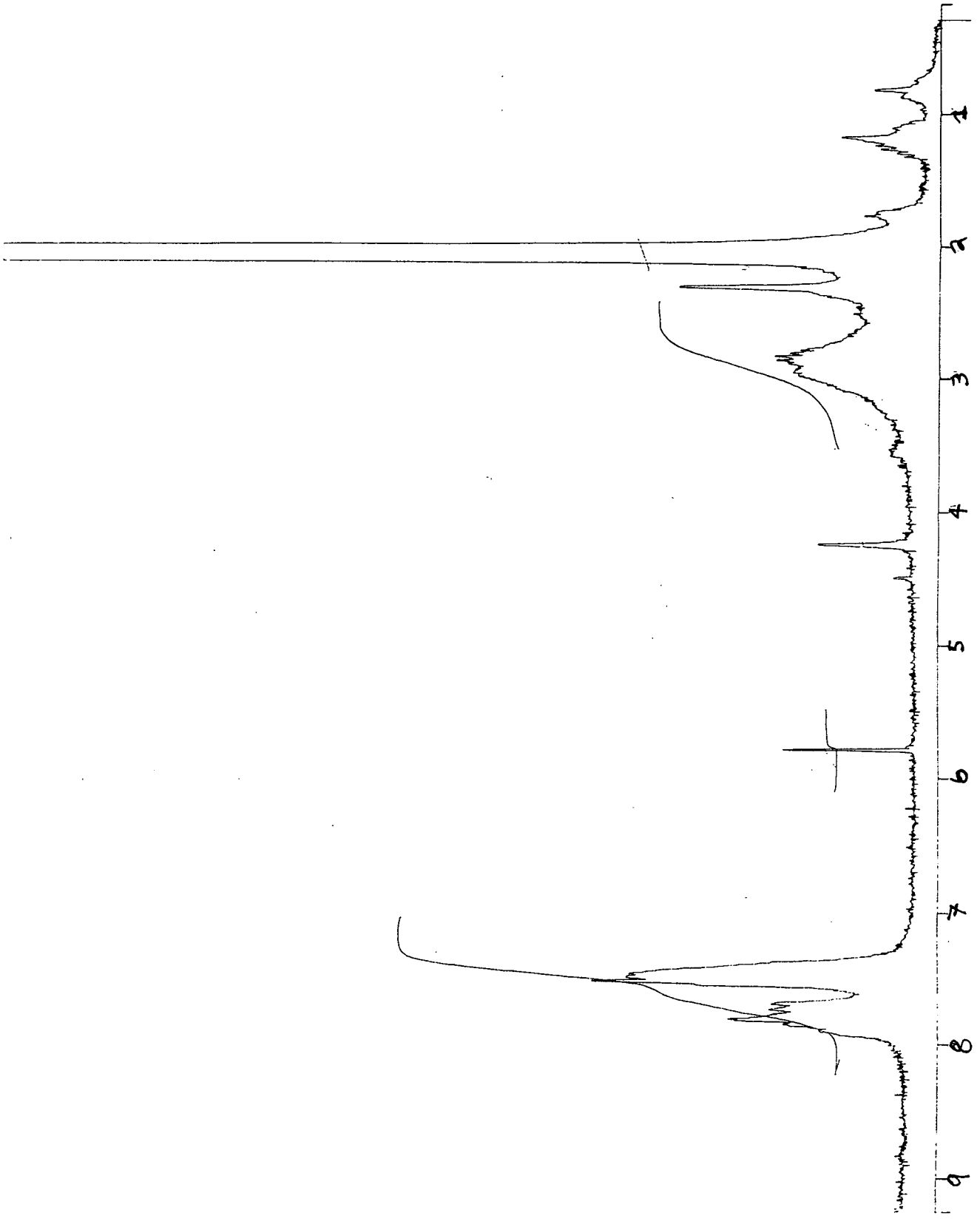

3.3 Conclusion

The complexes $[Ru(PPh_3)([9]aneS_3)(\mu\text{-}Cl)]_2(PF_6)_2$ and $[Ru(PPh_3)([9]aneS_3)(\mu\text{-}Cl)_2Tl]_2(PF_6)_2$ have been synthesised and characterised by ir, ^1H N.M.R. and ^{31}P N.M.R. and F.A.B. mass spectroscopy and their structures have been confirmed by X-ray analysis. The bridges in both dimeric complexes are easily cleaved in co-ordinating solvents, thus when the complexes are dissolved in CH_3CN they form $[RuCl(PPh_3)(NCCH_3)([9]aneS_3)]PF_6$. $[Ru(PPh_3)([9]aneS_3)(\mu\text{-}Cl)_2Tl]_2(PF_6)_2$ dissolves in acetone to afford a white precipitate of TlCl and the Ru dimer, $[Ru(PPh_3)([9]aneS_3)(\mu\text{-}Cl)]_2(PF_6)_2$. A summary of the synthesis and reactivity of $[Ru(PPh_3)([9]aneS_3)(\mu\text{-}Cl)]_2PF_6$ and $[Ru(PPh_3)([9]aneS_3)(\mu\text{-}Cl)_2Tl]_2(PF_6)_2$ is shown in Scheme 3.1.

Scheme 3.1 The Interconversion of $[Ru(PPh_3)([9]aneS_3)(\mu\text{-}Cl)]_2(PF_6)_2$, $[Ru(PPh_3)([9]aneS_3)(\mu\text{-}Cl)_2Tl]_2(PF_6)_2$ and $[RuCl(PPh_3)(NCCH_3)([9]aneS_3)]PF_6$.

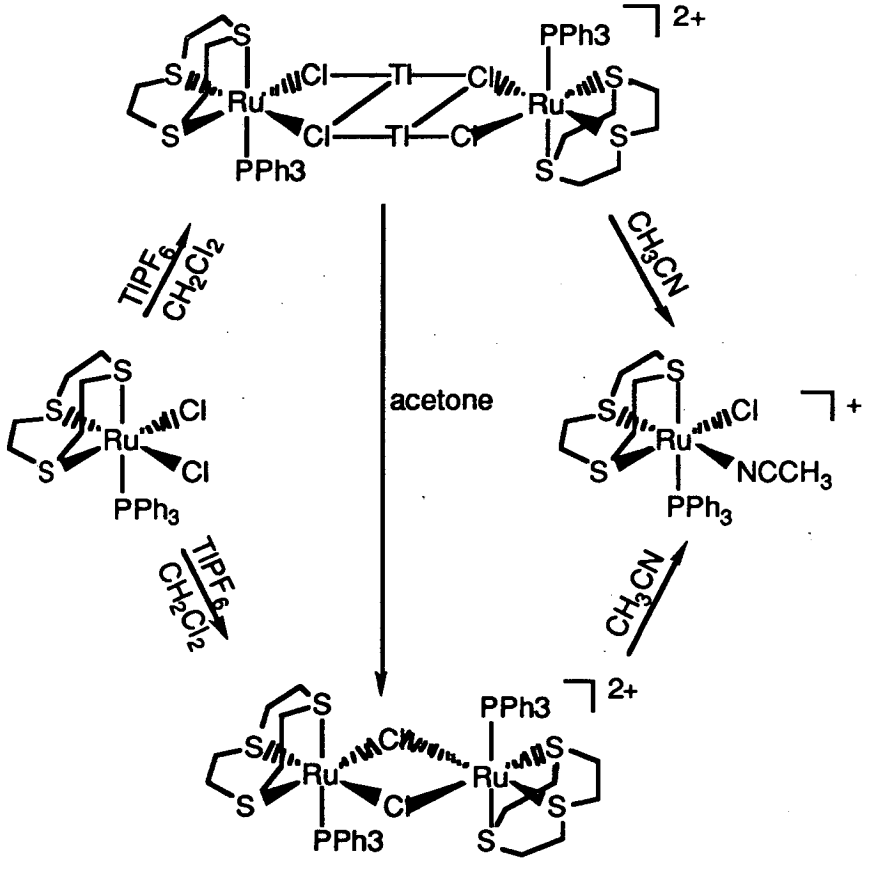

3.4 Experimental Physical Measurements

Infrared spectra (4000–250cm^{-1}) were recorded on a Perkin-Elmer 598 or FT1600 series spectrometer, using the KBr Disc method. ^{1}H N.M.R. spectra were recorded on a Brüker WP80 instrument operating at 80.13 MHz. ^{13}C(Dept) and proton decoupled ^{13}C N.M.R. spectra were recorded at 50.31 MHz using the Brüker WP200 spectrometer. The proton decoupled ^{31}P N.M.R. spectra were recorded on the Joel FX90Q spectrometer operating at 36.4 MHz. F.A.B. mass spectra, unless otherwise stated, were obtained in a 3-NOBA matrix on a Kratos MS50TC spectrometer.

Reagents

$RuCl_3.nH_2O$ was provided as a generous loan from Johnson-Matthey P.L.C. [9]aneS_3 was purchased from Aldrich. Dichloromethane was purified by standing it over KOH and dried by distillation over P_2O_5. Acetonitrile was dried by distillation over P_2O_5. All other solvents were Analar grade and used without further purification. $[RuCl_2(PPh_3)_3]$ was prepared by literature methods[287], and $[RuCl_2(PPh_3)([9]aneS_3)]$ was prepared by the method used by Christie[241]. Unless otherwise stated, an inert atmosphere was not used.

3.4.1. The Reaction of $[RuCl_2(PPh_3)([9]aneS_3)]$ with $TlPF_6$ in CH_2Cl_2 or Acetone

$[RuCl_2(PPh_3)([9]aneS_3)]$ (55 mg, 0.080 mM) was added to CH_2Cl_2 (10 cm^3) and $TlPF_6$ (35 mg, 0.1 mM) was added and the system stirred for six hours during which time a white precipitate formed. The white solid was removed by filtration through celite, and the resulting dark yellow solution reduced in volume to near dryness and recrystallised from acetone/hexane. The resulting light orange solid was dried under vacuum for three days. (Yield = 43 mg).
Ir spectrum υ(cm^{-1}) : 3050(w), 2980-2920(w, broad), 1711(m), 1665(m, H_2O), 1618(w), 1585(w), 1572(w), 1485(ms), 1435(s), 1410(ms), 1362(w), 1293(mw),

1217(w), 1193(w), 1146(w), 1090(s), 1025(w), 994(w), 835(vs), 750(ms), 695(s), 555(s), 528(s), 513(ms), 499(ms), 420(w).

^1H N.M.R.spectrum (d^6-acetone, 298K) δ = 1.28(s), 2.5–3.2 (s, broad), 7.3–8.0(m) p.p.m.

^{31}P N.M.R.spectrum (d^6-acetone, 298K) δ = -145 (septet, J = 710Hz, PF_6^- (weak signal)) p.p.m.

F.A.B. Mass Spectrum found m/e = 819, 716, 614, 579, 551, 516;

calculated for $\{^{205}Tl^{35}Cl_2{}^{102}Ru(PPh_3)([9]aneS_3)\}^+$: 819, $\{^{102}Ru_2{}^{35}Cl_2(PPh_3)([9]aneS_3)\}^+$: 716, $\{^{102}Ru^{35}Cl_2(PPh_3)([9]aneS_3)\}^+$: 614, $\{^{102}Ru^{35}ClPPh_3([9]aneS_3)\}^+$: 579, $\{^{102}Ru^{35}ClPPh_3(S(CH_2)_2S(CH_2)S\}^+$: 551, $\{^{102}Ru(PPh_3)(S(CH_2)_2S(CH_2)S)\}^+$: 516.

3.4.2 $[RuCl_2(PPh_3)([9]aneS_3)]$ with $TlPF_6$ in CD_3NO_2

$[RuCl_2(PPh_3)([9]aneS_3)]$ (40 mg, 0.65 mM) and $TlPF_6$ (23 mg, 0.65 mM) were stirred in CD_3NO_2 and d^8-THF (4:1 v/v, 5 cm^3) for fifteen hours. The resulting white precipitate was removed by filtration through celite, and the filtrate reduced to a small volume (1–2 cm^3). The solution was then left to slowly evaporate in air. Orange and yellow crystals formed within two days.

Orange crystals — $[Ru(PPh_3)([9]aneS_3)(\mu\text{-}Cl)]_2(PF_6)_2$

Yellow crystals — $[Ru(PPh_3)([9]aneS_3)(\mu\text{-}Cl)_2Tl](PF_6)_2$

3.4.2.1 Crystal structure determination of $[Ru(PPh_3)([9]aneS_3)(\mu\text{-}Cl)]_2(PF_6)_2$

Crystal data:– $C_{48}H_{54}Cl_2P_2Ru_2S_6.2PF_6.2CD_3NO_2$. MWt = 1570.18, monoclinic, $P2_{1/n}$, a = 14.5986(24), b = 13.1911(23), c = 15.6282(17)Å, β = 103.425(9)°, V = 2927.3Å^3 [from 2θ values of 31 reflections measured at $\pm\omega$ (24°≤2θ≤26°), T = 150±0.1K, λ = 0.71073Å], D_e = 1.781 gcm^{-3}, Z = 2, F(0,0,0) = 1586. Orange tablet, 0.085x0.23x0.23 mm, μ(Mo-K_α) = 9.44 cm^{-1}.

Data collection and processing:– Stöe Stadi-4 diffractometer, graphite monochromated Mo-K_α radiation, ω-2θ scans, 3631 unique data measured (2θ max = 45°, h = -15→15, k = 0→14, l = 0→16) giving 3222 data with $F \geq 4\sigma(F)$. No significant crystal decay or movement was observed. Absorption correction (NPM) was applied, min = 0.3813, max = 0.4247.

Structure solution and refinement:– The Ru position was located by Patterson synthesis[288]. Non-H atoms were located and refined by iterative least squares refinement and Fourier transformation. All non-H atoms were refined anisotropically (for F fragments only if occupancy >50% of one atom). The PF_6^- group was spinning about one F-P-F axis. The disorder was treated by split occupancy refinement. H-atoms were included at fixed calculated positions. Phenyl rings were constrained as idealised, planar hexagons and CD_3 groups were fixed but allowed to rotate about their C–N bond. At convergence $\omega^{-1} = \sigma^2(F) + 0.000565(F)^2$, R,Rw = 0.0293, 0.0434, S = 1.312 for 354 parameters. For the final ΔF synthesis, max and min residues were 0.47 and -0.69eÅ^{-3}. Views of the cation were generated by XP[289], and tables utilised CALC[290]. Primed atoms are related to their unprimed equivalents by inversion through ($^1/_2$, 0, $^1/_2$). Scattering factors were inlaid, or taken from Ref 291.

3.4.2.2 Crystal structure determination of $[Ru(PPh_3)([9]aneS_3)(\mu\text{-}Cl_2)Tl]_2(PF_6)_2$

Crystal data:– $Ru_2Tl_2C_{48}H_{54}Cl_4P_4F_{12}S_6.4CD_3NO_2$. MWt = 2184.155, triclinic, P_1, a = 10.2202(23), b = 10.7668(18), c = 16.4498(24)Å, α = 96.206(15)°, β = 100.971(16)°, γ = 90.862(14)°, V = 1765.4Å^3 [from 2θ values of 42 reflections measured at $\pm\omega$ ($31° \leq 2\theta \leq 32°$), T = 150±0.1K, λ =0.71073Å], D_e = 2.053 gcm^{-3}, Z = 1, F(0,0,0) = 1052, yellow columnar crystal, 9.078x1.55x0.43 mm, μ(Mo-K_α) = 9.44 cm^{-1}.

Data collection and processing:– Stöe Stadi-4 diffractometer, graphite monochromated Mo-K_α radiation, ω-2θ scans, 4520 unique data measured

(2θ max = 45°, h = -11→10, k = -11→11, l = 0→17) giving 4193 data with $F \geq 4\sigma(F)$. No significant crystal decay or movement was observed. No absorption correction was applied.

Structure solution and refinement:– The Ru position was located by Patterson synthesis[288]. Non-H atoms were located and refined by iterative least squares refinement and Fourier transformations. All non-H atoms were refined anisotropically (for O and F fragments only if occupancy >50% of one atom). The PF_6^- group was spinning about one F-P-F axis. The disorder was treated by split occupancy refinement. H-atoms were included at fixed calculated positions. Phenyl rings were constrained as idealised, planar hexagons and CD_3 groups were fixed but allowed to rotate about their C–N bond. At convergence $\omega^{-1} = \sigma^2(F) + 0.000138(F)^2$, R,Rw = 0.0251, 0.0321, S = 1.053 for 439 parameters. For the final ΔF synthesis, max and min residues were 0.72 and -0.71eÅ^3. Views of the cations were generated by XP[289], and tables utilised CALC[290]. Scattering factors were inlaid, or taken from Ref 291.

3.4.3 The Synthesis of $[Ru(PPh_3)([9]aneS_3)(\mu\text{-}Cl)_2]_2(PF_6)_2$

(a) The reaction was carried out as in 3.4.1; however the solution was refluxed for twelve hours. (Yield 43 mg, 66%).

(b) The reaction was carried out as in 3.4.1; however, acetone (10 cm^3) at reflux was stirred for twelve hours. (Yield 45 mg, 69%).

In both cases, the physical and chemical characteristics of the resulting orange solid were identical.

Ir spectrum υ(cm^{-1}) : 3054(ms), 2980(ms), 2920(m), 1629(mw), 1480(ms), 1432(s), 1410(ms), 1192(mw), 1090(s), 1025(w), 999(mw), 835(vs), 748(s), 699(s), 552(s), 526(s), 513(ms), 499(ms).

^{1}H N.M.R.spectrum (d^6-acetone, 298K) δ = 1.1(t), 1.28(s), 2.2–3.5(m), 7.2–8.0(m) p.p.m.

^{31}P N.M.R.spectrum (d^6-acetone, 298K) δ = -145(septet, J=710Hz, PF_6^-), + 33.4 p.p.m.

F.A.B. Mass Spectrum found m/e = 716, 614, 579, 551;

calculated for $\{^{102}Ru_2{}^{35}Cl_2(PPh_3)([9]aneS_3)\}^+$: 716, $\{^{102}Ru^{35}Cl_2(PPh_3)([9]aneS_3)\}^+$: 614, $\{^{102}Ru^{35}Cl(PPh_3)([9]aneS_3)\}^+$: 579, $\{^{102}Ru^{35}Cl(PPh_3)(S(CH_2)_2S(CH_2)S\}^+$: 551.

3.4.4 The Synthesis of $[Ru(PPh_3)([9]aneS_3)(\mu\text{-}Cl)_2Tl)]_2(PF_6)_2$

The reaction was carried out in a similar manner as the one described in 3.4.1, except that the solution was degassed and stirred at 0° C for six hours under N_2. The resulting yellow solution was reduced quickly to dryness. (Yield 25 mg, 32%)

Ir spectrum $\upsilon(cm^{-1})$: 3054(ms), 2963(m), 2920(w), 1669(mw), 1482(ms), 1434(s), 1409(ms), 1261(ms), 1091(s), 840(vs), 746(m), 697(s), 558(s), 527(s), 513(m), 499(m), 460(w), 426(w).

^1H N.M.R. spectrum (d^6-acetone, -43° C, sealed tube, N_2) δ = 0.8(broad), 2.5–3.2 (broad), 4.24(s), 5.7(s), 7.2–8.0(m)p.p.m.

^{31}P N.M.R. spectrum (d^6-acetone, -40° C, sealed tube N_2) δ = 33.5, 32.8, -145 (3 of 7, J = 710Hz, PF_6^-)p.p.m.

F.A.B. Mass Spectrum found m/e = 819, 614, 579, 551, 516;

calculated for $\{^{102}Ru_2{}^{35}Cl_2(PPh_3)([9]aneS_3)^{205}Tl\}^+$: 819, $\{^{102}Ru^{35}Cl_2(PPh_3)([9]aneS_3)\}^+$: 614, $\{^{102}Ru^{35}Cl(PPh_3)([9]aneS_3)\}^+$: 579, $\{^{102}Ru^{35}Cl(PPh_3)(S(CH_2)_2S(CH_2)S\}^+$: 551, $\{^{102}R(PPh_3)(S(CH_2)_2S(CH_2)S\}^+$: 516.

3.4.5 The Synthesis of $[RuCl(NCCH_3)(PPh_3)([9]aneS_3)]PF_6$ from $[Ru(PPh_3)([9]aneS_3)(\mu\text{-}Cl)]_2(PF_6)_2$

$[Ru(PPh_3)([9]aneS_3)(\mu\text{-}Cl)]_2(PF_6)_2$ (48 mg, 0.033 mM) was added to CH_3CN (10 cm^3) and stirred for fifteen hours. The solution was then evaporated to near dryness and acetone and hexane added. A yellow precipitate formed which was filtered and dried. (Yield 46 mg, 91%)

Ir spectrum $\upsilon(cm^{-1})$: 3048(m), 2986(ms), 2920(m), 2040(m.CN) , 1620(m), 1586(w), 1482(ms), 1435(s), 1410(ms), 1295(m), 1266(m), 1188(mw), 1090(s), 999(ms), 910(ms), 835(m), 699(s), 580(ms), 558(s), 528(ms), 517(ms), 501(ms).

^1H N.M.R.spectrum (CD_3CN, 298K) δ = 2.5–3.5 (m, [9]aneS_3), 7.2–8.0 (m, PPh_3) p.p.m.

^{31}P N.M.R.spectrum (CD_3CN, 298K) δ = -145 (septet, J = 710Hz, PF_6^-), +35.4 p.p.m.

F.A.B. Mass Spectrum found m/e = 620, 579, 551;

calculated for $\{^{102}Ru^{35}Cl(NCCH_3)(PPh_3)([9]aneS_3)\}^+$: 620,

$\{^{102}Ru^{35}Cl(PPh_3)([9]aneS_3)\}^+$: 579, $\{^{102}Ru^{35}Cl(PPh_3)(S(CH_2)_2S(CH_2)S\}^+$: 551.

3.4.6 The Synthesis of $[RuCl(NCCH_3)(PPh_3)[9]aneS_3]$ from $[Ru(PPh_3)([9]aneS_3)(\mu\text{-}Cl)_2Tl]_2(PF_6)_2$

$[Ru(PPh_3)([9]aneS_3)(\mu\text{-}Cl)]_2(PF_6)_2$ (38 mg, 0.022 mM) was dissolved in CH_3CN(10 cm^3) and stirred for six hours, during which time a white precipitate formed which was removed by filtration through celite. The resulting yellow solution was evaporated to near dryness, and acetone/hexane added and the yellow precipitate collected and dried. (Yield = 25 mg, 74%)

The ir, ^1H N.M.R., ^{31}P N.M.R. and F.A.B. mass spectra were similar to 3.4.5

3.4.7 The Conversion of $[Ru(PPh_3)([9]aneS_3)(\mu\text{–}Cl)_2Tl]_2(PF_6)_2$ to $[RuCl(PPh_3)([9]aneS_3)]_2(PF_6)_2$

[Ru(PPh3)([9]aneS3)(Cl2Tl]2(PF6)2 (29 mg, 0.017 mM) was dissolved in acetone(10 cm-3) and stirred for six hours, during which time a white precipitate of TlCl formed. The TlCl was removed by filtration through celite, and the dark yellow solution was evaporated to near dryness, and hexane added. The resulting orange solid had infrared, ^1H N.M.R., ^{31}P N.M.R. and F.A.B. mass spectra similar to the dimer 3.4.3.

Chapter Four

THE THALLIATION OF $[RuCl_2(PPh_3)([9]aneS_3)]$ IN CH_3NO_2

4.1 Introduction

The reaction of $[RuCl_2(PPh_3)([9]aneS_3)]$ with $TlPF_6$ in co-ordinating and non-co-ordinating solvents was discussed in Chapter 3. In non-co-ordinating solvents, such as CH_2Cl_2, the dimeric Ru species, $[Ru(PPh_3)([9]aneS_3)(\mu\text{-}Cl)]_2(PF_6)_2$ and the Ru/Tl ladder complex, $[Ru(PPh_3)([9]aneS_3)(\mu\text{-}Cl)_2Tl]_2(PF_6)_2$ is isolated, whereas in co-ordinating solvents, such as CH_3CN, the complex, $[RuCl(solv)(PPh_3)([9]aneS_3)](PF_6)$ (solv = solvent) is formed. $[RuCl(NCCH_3)(PPh_3)([9]aneS_3)](PF_6)$ is relatively inert to further substitution, the acetonitrile ligand being relatively strongly bound to the Ru(II) centre. In order to facilitate substitution in complexes of the type, $[RuCl(solv)(PPh_3)([9]aneS_3)]PF_6$ a solvent with less co-ordinating ability than CH_3CN but more than CH_2Cl_2 has to be used. CH_3NO_2 is such a solvent. This chapter gives a **chronological** account of the study of the reaction of $[RuCl_2(PPh_3)([9]aneS_3)]$ with $TlPF_6$ in CH_3NO_2.

CH_3NO_2 is a weak proton acceptor with a pk_a value $\approx$ -12 for its conjugate acid in aqueous sulfuric acid[292]. In contrast, it is a relatively strong proton donor with a pk_a = 10.2 in aqueous solution[292]. The reason for this considerable acidity lies in the resonance forms which are available to both CH_3NO_2 and its conjugate base (Figure 4.1)[292]. CH_3NO_2 can also tautomerise to form the structures shown in Figure 4.2. In aqueous solution, the nitronic acid form is only present in very low concentration[292].

Figure 4.1 Resonance forms of CH_3NO_2 and $CH_2NO_2^-$

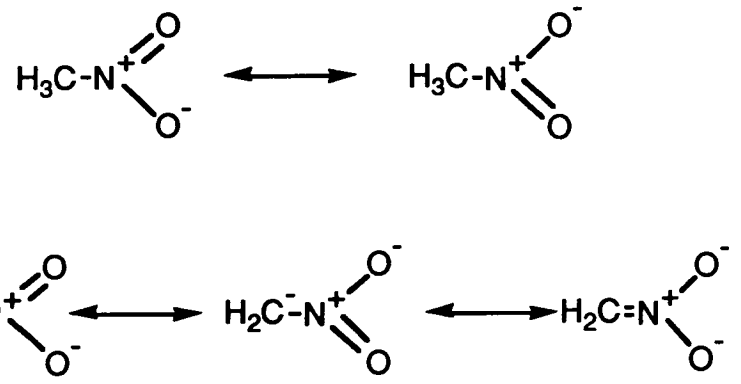

Figure 4.2 Nitromethane Tautomers

Several O-bound CH_3NO_2 complexes of transition metals have been reported[293-298]. The usual synthetic method for preparing these CH_3NO_2 complexes is to react a halogen-containing starting material with a dehalogenating agent e.g. $AgPF_6$. Thus, the complexes, $[M(CH_3NO_2)_6]^{2+}$ (M = Mg, Ca, Sr, Mn, Fe, Co, Ni, Zn)[294] and $[Mo(NO)_2(CH_3NO_2)_4](PF_6)_2$[295] have all been characterised, as has the Pd(II) complex shown in Figure 4.3[296]. The reaction of $[(PEt_2Ph)_3Ru(\mu\text{-}Cl)_3RuCl(PEt_2Ph)_3]$ in CH_2Cl_2 with an equimolar amount of $TlBF_4$ and CH_3NO_2 results in the complex $[(PEt_2Ph)_3Ru(\mu\text{-}Cl)_3Ru(CH_3NO_2)(PEt_2Ph)_2]BF_4$[297]. An alternative synthetic strategy to CH_3NO_2 complexes is by electrochemically oxidising or reducing complexes in CH_3NO_2. Thus, the electrochemical oxidation of [Ru(TPP)(CO)] in CH_3NO_2 results in the formation of $[Ru(TPP)(CO)(CH_3NO_2)]$ [298]. The bond dissociation energy of $[Cu(CH_3NO_2)_2]^+$ relative to $[Cu(CH_3CH_2Cl)_2]^+$ has been measured as 7.9 kcal mol^{-1} [293].

Transition metal complexes with $CH_2NO_2^-$ have also been studied previously [299-303]. $CH_2NO_2^-$ may co-ordinate through its O-atoms (Figure 4.4)[299] or through the C-atom[300-303]. A number of C-bound $CH_2NO_2^-$ complex have been structurally characterised by X-ray crystallography[302], and the complex

trans-bis(dimethylglyoximato)(nitromethyl)(pyridine) cobalt (III) is shown in Figure 4.5. A $CH_2NO_2^-$ derivative of coenzyme B_{12} (see Chapter 1) has also been characterised[302]. The double deprotonation of CH_3NO_2 by a dinuclear Au(I) complex results in the formation of the novel $CHNO_2^{2-}$ bridging unit, which has been characterised by X-ray crystallography (Figure 4.6)[303].

Figure 4.3 A Representation of $[Pd(Ph\text{-}N{=}N\text{-}Ph)(CH_3NO_2)_2]^+$

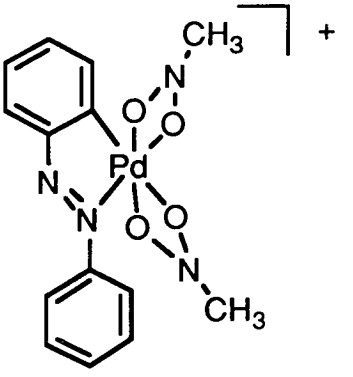

Figure 4.4 A Representation of $[(CH_2NO_2)Ru(H)(PPh_3)_3]$

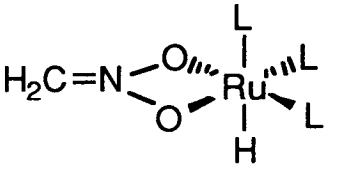

L=PPh_3

Figure 4.5 A View of the Single Crystal X-Ray Structure of trans-bis(Dimethylglyoximato)-(nitromethyl)(pyridine)cobalt(III)

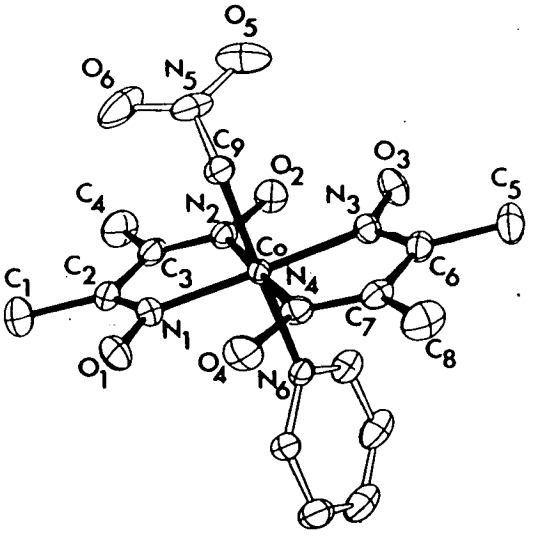

Figure 4.6 The Synthesis of $[Au_2\{(CH_2)_2PPh_2\}_2(O_2CPh)_2(CHNO_2)]$

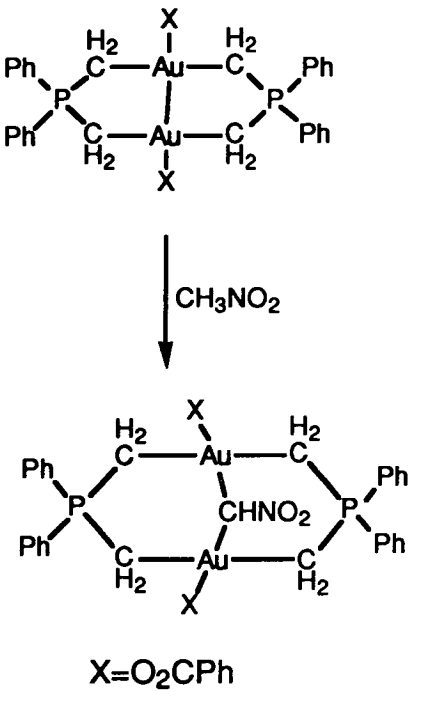

X=O_2CPh

4.2 The Reaction of $[RuCl_2(PPh_3)([9]aneS_3)]$ with $TlPF_6$ in CH_3NO_2

4.2.1 Results and Discussion

The addition of $TlPF_6$ to $[RuCl_2(PPh_3)([9]aneS_3)]$ in CH_3NO_2 at 298K for sixteen hours in air affords a white precipitate of TlCl and a yellow solution. Filtration of the mixture through celite yields a clear solution, which is then reduced in volume. Addition of Et_2O results in a yellow precipitate which is collected, dried and recrystallised from acetone/Et_2O. The ir spectrum of the product shows that PPh_3, $[9]aneS_3$ and PF_6^- are all present [υ (cm^{-1}) = 1482, 1434, 1409, 835, 555, 528, 517 and 499] . The ^1H N.M.R. (CD_3NO_2) spectrum shows resonances at δ = 0.96 (t, J = 7.5Hz), 1.5–3.5 (m, $[9]aneS_3$), 6.5 (t, J = 2Hz), 7.35–7.85 (m, PPh_3), 8.26 (d, J = 2Hz) and 8.95 (d, J = 2Hz) (Figure 4.7). The ^{13}C N.M.R. spectrum exhibits resonances in the region δ = 29–36 p.p.m. assigned to the co–ordinated $[9]aneS_3$ as well as resonances in the phenyl region δ = 126–133 p.p.m. (PPh_3), and unusual resonances at δ = 7.8, 11.4, 106.2, 152.4, 160.1 and 206.9 (Figure 4.8).

Figure 4.7 The ^{1}H N.M.R. Spectrum of the Product iosolated from Section 4.2.1

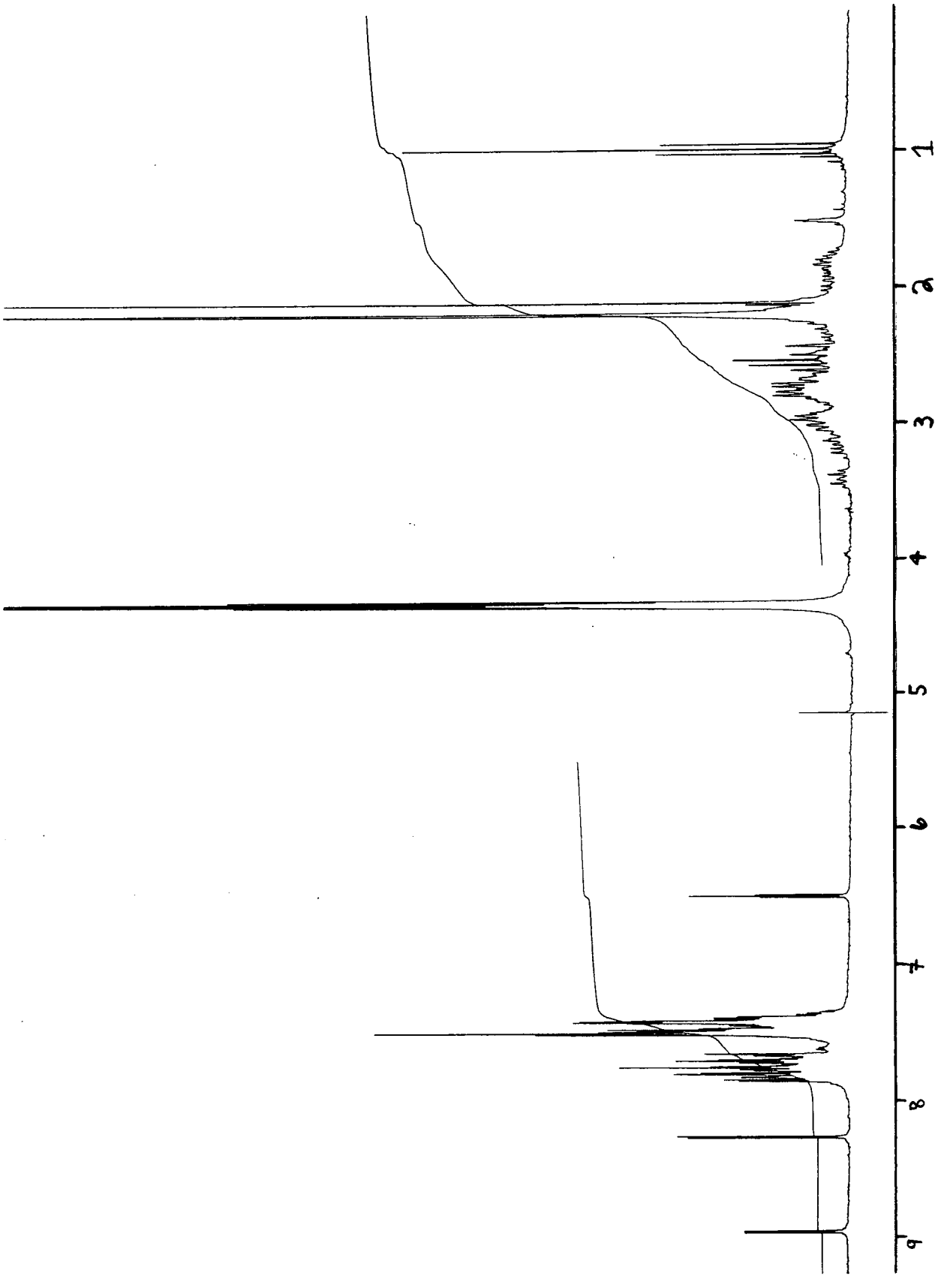

Figure 4.8 The ^{13}C N.M.R. Spectrum of the Product iosolated from Section 4.2.1

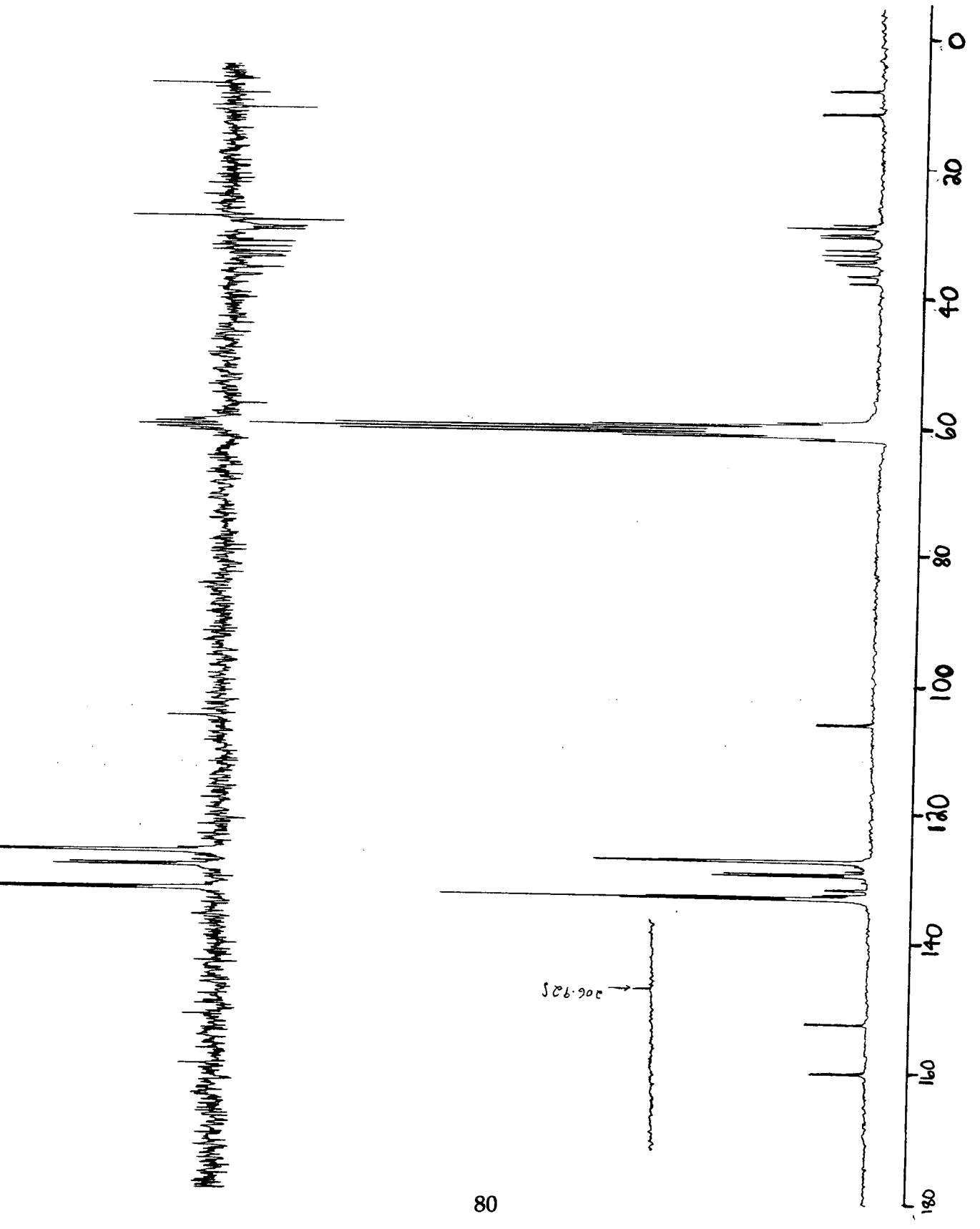

The unusual high field resonances in the ^{1}H N.M.R. and ^{13}C N.M.R. spectra were originally assigned to orthometallation of one of the phenyl rings of PPh_3 (Figure 4.9). A number of examples of orthometallated Ru complexes have been reported[304-306]. The crystal structure of $[RuCl(C_6H_4PPh_2)(NH\{SiMe_2CH_2PPh_2\}_2)]$ has been solved and clearly shows the ortho carbon of one of the phenyl groups of PPh_3 co-ordinated to the Ru(II) metal ion (Figure 4.10)[304, 305]. However, orthometallation in our system would result in four novel proton and five unusual carbon resonances. This is inconsistent with the observed N.M.R. spectra which shows only three novel proton resonances (δ = 6.5, 8.25 and 8.94 p.p.m.) and four unusual carbon resonances (δ = 106.2, 152.4, 160.1 and 206.1 p.p.m.). It is possible that the 'missing' resonances of the orthometallated complex may overlap with the phenyl rings of the PPh_3 group. However, no ^{31}P coupling is observed in the high field resonances at δ = 106.2, 152.4, 160.1 and 206.1 p.p.m., thus ruling out an orthometallated Ru species. The high frequency of the chemical shifts in the ^{1}H and ^{13}C N.M.R. spectra of the unknown ligand, together with the small coupling constant (J = 2Hz) associated with the ^{1}H N.M.R. resonances at δ = 6.5, 8.26 and 8.95 p.p.m. suggests that the unknown ligand is a four carbon membered aromatic species, possibly a furyl moiety (see Figure 4.11).

Figure 4.9 A Representation of the Ortho-Metallated Complex, $[RuCl(C_6H_4PPh_2)([9]aneS_3)]$

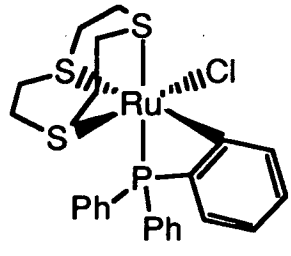

Figure 4.10 A View of the Single Crystal X-Ray Structure of $[RuCl(C_6H_4PPh_2)\ (NH\{SiMe_2CH_2PPh_2\}_2)]$

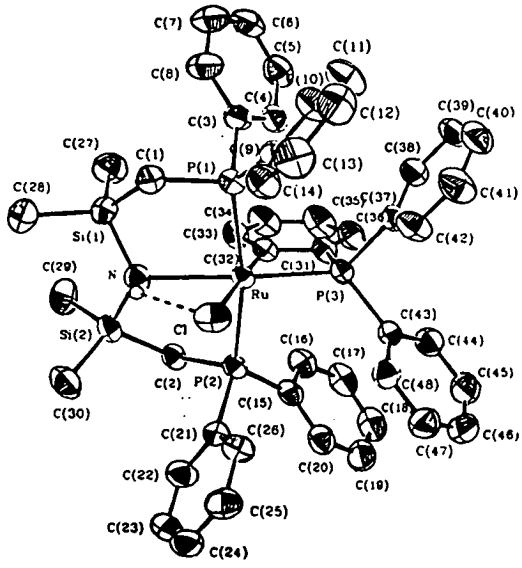

Figure 4.11 A Representation of the Furyl Complex, $[RuCl(C_4H_3O)(PPh_3)([9]aneS_3)]$

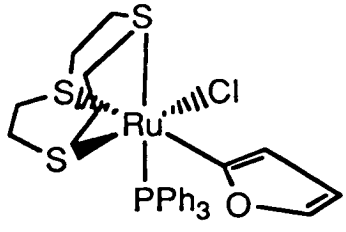

4.2.2 The crystal structure of $[Ru(C_4H_3O)Cl(PPh_3)([9]aneS_3)]HPF_6$

Crystals which were suitable for X-ray analysis can be grown by vapour diffusion of Et_2O into CH_3NO_2. The crystal structure confirms the distorted octahedral stereochemistry of the Ru(II) ion. The Ru(II) co-ordinates to a Cl^- [Ru–Cl = 2.4507 (21) Å], a PPh_3 [Ru–P = 2.3477(20)Å], and a facially bound [9]aneS$_3$ [Ru–S = 2.3006(23), 2.2942(21) and 2.3562(21)Å]. A C-bound furyl group is bound to the metal ion in the remaining sixth site [Ru–C = 2.085(6)]. A view of the cation is shown in Figure 4.12 and selected bond lengths and angles are shown in Table 4.1. Although the protons on the furyl ring are placed in calculated positions, the internal bond lengths [O(1)–C(2) = 1.408(9), C(2)–C(3) = 1.227(11),

C(3)–C(4) = 1.408(13), C(4)–C(5) = 1.323(14) and C(5)–O(1) = 1.368(14)Å] and the torsion angles [max = 1.2(10)°] indicate that the ring is a planar aromatic furyl as opposed to a saturated THF ligand. Since the C-bound furyl is formally a uninegative donor, the complex should be neutral for Ru(II); however, the crystal structure shows the complex to be monocationic, with an additional positive charge residing somewhere in the complex. The bond lengths of the complex are consistent with those associated with a Ru(II) complex (see Table 4.2) and the complex is also diamagnetic, since no observable line-broadening in the N.M.R. spectra is observed. Therefore, it must be assumed that there is a proton associated with one of the ligands. The location of the proton in the single crystal X-ray structure can not be determined, but it may be associated with the O-atom of the furyl group, although no O–H resonance is observed in the ^1H N.M.R. spectrum, nor are any OH stretches seen in the ir spectrum.

Table 4.2 X-Ray Crystallographic Data for a Series of Ru(II) [9]aneS_3 Complexes

Bond Lengths	Complexes		
	$[RuCl_2(PPh_3)([9]aneS_3)]$ (Å)	$[Ru(PPh_3)([9]aneS_3)(\mu\text{-}Cl)]_2(PF_6)_2$ (Å)	$[Ru(PPh_3)([9]aneS_3)(\mu\text{-}Cl)_2Tl]_2(PF_6)_2$ (Å)
Ru–P	2.345 (2)	2.3741 (10)	2.3539 (12)
Ru–Cl(1)	2.456 (2)	2.4945 (10)	2.4526 (12)
Ru–Cl(2)	2.449 (2)	2.4654 (10)	2.4416 (12)
$Ru–S_{(p)}$	2.356 (2)	2.3456 (10)	2.3501 (13)
$Ru–S_{(Cl)}$	2.270 (2)	2.2880 (10)	2.2821 (13)
$Ru–S_{(Cl)}$	2.269 (2)	2.2817 (10)	2.2804 (13)

Notes

$Ru–S_{(p)}$ is the sulfur trans to the PPh_3 group
$Ru–S_{(Cl)}$ is the sulfur trans to the Cl group

Table 4.1 Selected Bond Lengths (Å) and Angles (°) and Torsion Angles (°) with standard deviations for $[RuCl(C_4H_3O)(PPh_3)[9]aneS_3)].HPF_6$

Ru–Cl	2.4507(21)	C(6)–S(7)	1.837(8)
Ru–S(1)	2.3006 (23)	S(7)–C(8)	1.828 (9)
Ru–S(4)	2.2942 (21)	C(8)–S(9)	1.501 (13)
Ru–S(7)	2.3562 (21)	O(1F)–C(2F)	1.408 (9)
Ru–P(1)	2.3477 (20)	O(1F)–C(5F)	1.368 (12)
Ru–C(2F)	2.085 (6)	C(2F)–C(3F)	1.277 (11)
S(1)–C(2)	1.816 (10)	C(3F)–C(4F)	1.408 (13)
S(1)–C(9)	1.847 (10)	C(4F)–C(5F)	1.323 (14)
C(2)–C(3)	1.505 (13)	P(1)–C(11)	1.830 (5)
C(3)–S(4)	1.826 (9)	P(1)–C(21)	1.826 (5)
S(4)–C(5)	1.826 (8)	P(1)–C(31)	1.835 (5)
C(5)–C(6)	1.502 (12)		

Cl–Ru–S(1)	95.05 (7)	C(2F)–S(1)–C(9)	101.1 (4)
Cl–Ru–S(4)	171.56 (7)	S(1)–C(2)–C(3)	115.0 (6)
Cl–Ru–S(7)	83.60 (7)	C(2)–C(3)–S(4)	113.5 (6)
Cl–Ru–P(1)	94.35 (7)	C(3)–S(4)–C(5)	100.0 (4)
Cl–Ru–C(2F)	89.32 (18)	S(4)–C(6)–S(7)	114.1(6)
S(1)–Ru–S(4)	88.35 (8)	C(5)–C(6)–S(7)	111.1 (6)
S(1)–Ru–S(7)	87.68 (8)	C(6)–S(7)–C(8)	102.4 (4)
S(1)–Ru–P(1)	94.59 (7)	S(7)–C(8)–C(9)	113.4 (6)
S(1)–Ru–C(2F)	173.85 (18)	S(1)–C(9)–C(8)	112.5 (6)
S(4)–Ru–S(7)	87.99 (7)	C(2F)–O(1F)–C(5F)	107.5 (6)
S(4)–Ru–P(1)	94.02 (7)	O(1F)–C(2F)-C(3F)	104.9 (6)
S(4)–Ru–C(2F)	89.42 (18)	C(2F)–C(3F)–C(4F)	113.8 (8)
S(7)–Ru–P(1)	177.00(7)	C(3F)–C(4F)–C(5F)	103.7 (9)
S(7)–Ru–C(2F)	86.51 (18)	O(1F)–C(5F)–C(4F)	110.1 (9)
P(1)–Ru–C(2F)	91.28 (18)		

C(9)–S(1)–C(2)–C(3)	74.1 (7)	C(6)–S(7)–C(8)–C(9)	64.2 (7)
C(2)–S(1)–C(9)–C(8)	-133.1 (7)	S(7)–C(8)–C(9)–S(1)	46.7 (8)
S(1)–C(2)–C(3)–S(4)	39.4 (9)	C(5F)–O(1F)–C(2F)–C(3F)	-1.1 (9)
C(2)–C(3)–S(4)–C(5)	-129.3 (7)	C(2F)–O(1F)–C(5F)–C(4F)	0.7 (10)
C(3)–S(4)–C(5)–C(6)	66.9 (7)	O(1F)–C(2F)–C(3F)–C(4F)	1.2 (10)
S(4)–C(5)–C(6)–S(7)	49.1 (7)	C(2F)–C(3F)–C(4F)–C(5F)	-0.8 (11)
C(5)–C(6)–S(7)–C(8)	-135.7 (7)	C(3F)–C(4F)–C(5F)-O(1F)	0.1 (11)

Figure 4.12 A View of the Single Crystal X-Ray Structure of $[RuCl(C_4H_3O)(PPh_3)([9]aneS_3)].HPF_6$

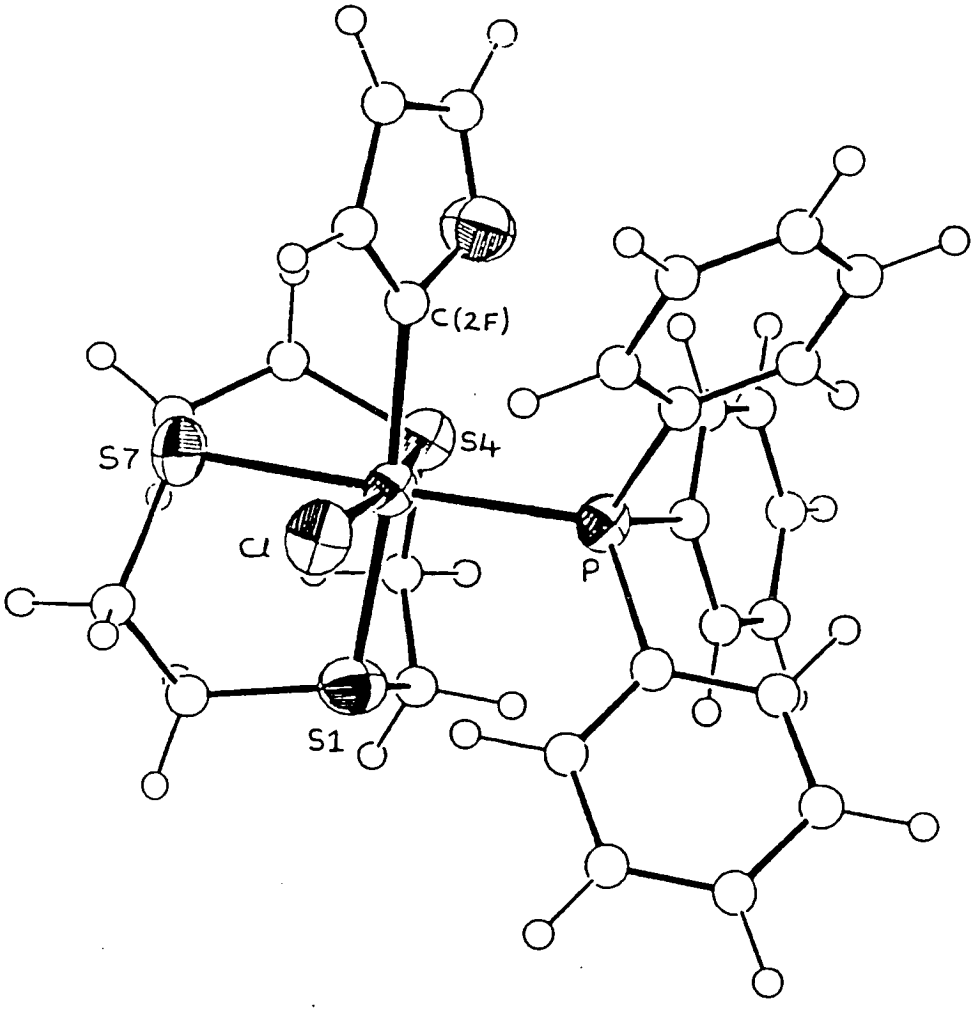

The metallation of cyclic ethers has been previously reported: [$Co^{(II)}$(OEP)] reacts with THF in the presence of excess $NaBH_4$ to afford a C-bound THF species, [$Co^{(III)}$(OEP)(C_4H_7O)]. The mechanism is thought to be a radical process and is shown in Scheme 4.1[307]. The double deprotonation of an α–methylene group in cyclic ethers and esters has recently been reported, and results in the formation of carbene complexes (Figure 4.13)[308-311]. A number of 2,3 dihydrofurans have been co-ordinated to transition metals[312, 313]; for example the MnPt dimer [$(CO)_4Mn(CHCH_2CH_2CH_2OC)Pt(PMe_3)_2$] in which the 2,3–DHF bridges the two metal centres (Figure 4.14) has been prepared [312]. [$M(N_2)(dppe)_2$](M = Mo, W) reacts with THF in the presence of alkylbromides to form [$M(Br)(N{\equiv}N–N–CH–O–CH_2CH_2–CH_2)(dppe)_2$] which, on addition of acid, forms [$M(Br)(N–N{=}N–CHCH_2CH_2CH_2OH(dppe)_2]^+$. This reaction is thought to proceed by a radical process[311].

Scheme 4.1 The Formation of [$Co^{(III)}$(OEP)(C_4H_7O)]

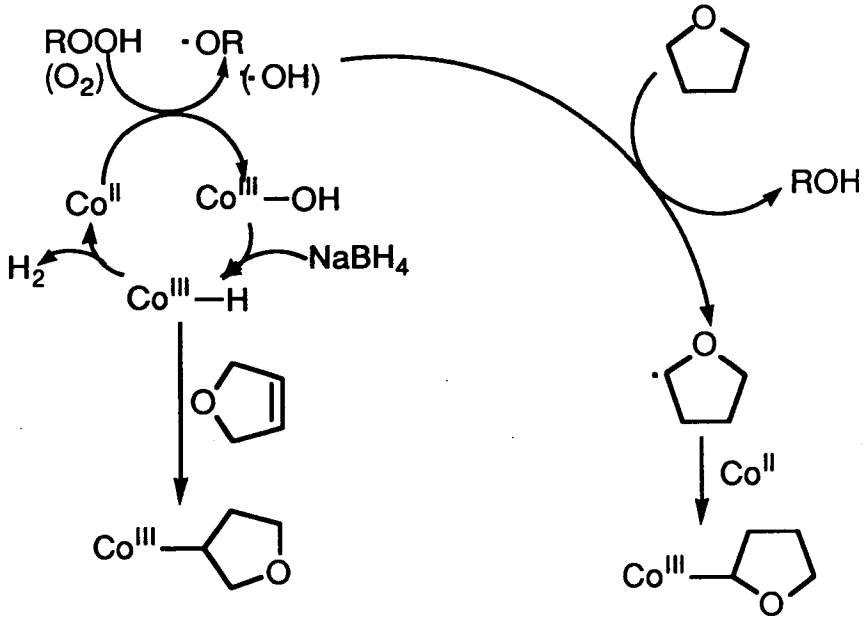

Figure 4.13 Representations of some Carbene Complexes of THF

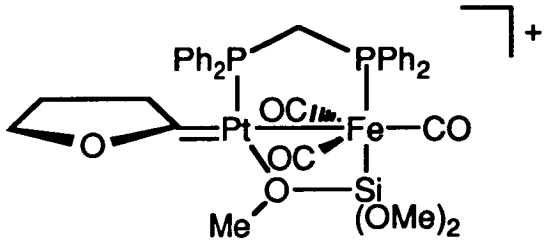

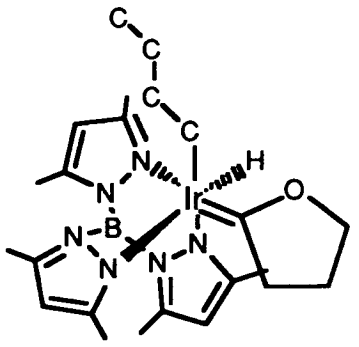

$[Fe(CO)_3(Si(OMe)_3(Ph_2PCH_2PPh_2)(C_4H_6O)]$ $TpIr(H)(C_4H_9)(C_4H_6O)]$

Figure 4.14 A Representation of $[Mn(CO)_4(CHCH_2CH_2OC\text{-})\text{-}Pt(PMe_3)_2]$

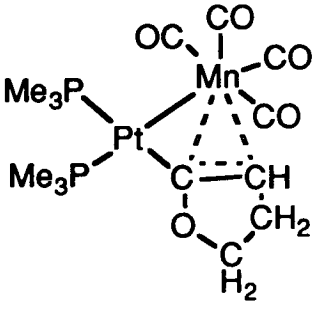

Metal C–bound furyl groups have been widely utilised in organic synthesis[314]. The most widely used reagent is furyl lithium, which is prepared by reacting a halofuran with Li^{t}Bu. Numerous substitution reactions can then be performed on this complex[315]. Interestingly, if CuI is added to $Li(C_4H_3O)$, then the complex $[LiCu(C_4H_3O)_2]$ can be isolated (Scheme 4.2)[316]. Other Cu C–bound furyl complexes have also been used in organic synthesis, and are usually formed by reacting the halofuran with Li^{n}Bu/CuBr[317]. The formation of $[CpMo(CO)_2(PPh_3)(C_4H_3O)]$ (Figure 4.15) will be discussed in Section 4.3[318]. The first π–bound furyl complex, $[Cp^*Ru(C_4H_4O)]X$ has been prepared by reacting $[Cp^*RuCl]_n$ with furan, and is shown in Figure 4.16[319].

Figure 4.15 A Representation of $[CpMo(CO)_2(PPh_3)(C_4H_3O)]$

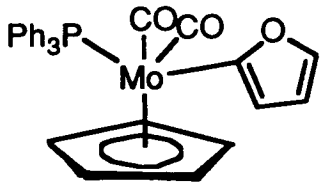

Figure 4.16 A Representation of $[Cp^*Ru(C_4H_4O)](Cl)$

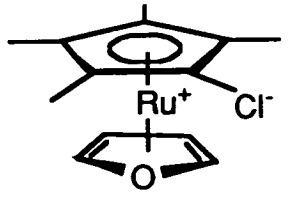

Scheme 4.2 The Synthesis Of $LiCu(C_4H_8O)_2$

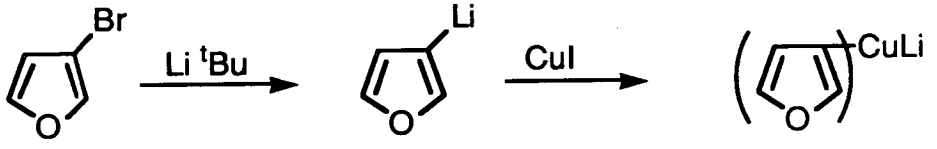

A thorough inspection of the spectroscopic properties of our C–bound furyl complex, $[RuCl(C_4H_3O)(PPh_3)([9]aneS_3)]HPF_6$ was undertaken in order to confirm its formation and to identify any by-products which may also be present.

4.2.3 N.M.R. spectroscopic study of $[RuCl(C_4H_3O)(PPh_3)([9]aneS_3)]$

The ^1H N.M.R. and ^{13}C N.M.R. spectra in CD_3NO_2 of the yellow product isolated when $[RuCl_2(PPh_3)([9]aneS_3)]$ is reacted with $TlPF_6$ in CH_3NO_2 in the presence of Et_2O (see Section 4.2.1) are shown in Figures 4.7 and 4.8. The ^{31}P N.M.R. (CD_3NO_2) spectrum of this product shows two resonances in the PPh_3 region at δ = 34.7, and 35.7 p.p.m. (Figure 4.17), in addition to the PF_6^- resonance at δ = -145 (septet, J = 710Hz) p.p.m. This indicates the presence of <u>two</u> PPh_3 containing complexes. One of these can be assigned as the complex $[RuCl(C_4H_3O)(PPh_3)([9]aneS_3)]$, but the other resonance must be due to a different product. Initially it was thought that the second product might be due to a complex containing a co-ordinated CH_3NO_2 formed either by displacement of the

C–bound furyl from the complex, $[RuCl(C_4H_3O)(PPh_3)([9]aneS_3)]$ or as an intermediate in the reaction of $[RuCl_2(PPh_3)([9]aneS_3)]$ with $TlPF_6$ in CH_3NO_2. The ^{31}P N.M.R. spectrum of the product isolated in section 4.2.1 does not show any change when left in the N.M.R. solvent for three weeks. This suggests that the complex $[RuCl(solv)(PPh_3)([9]aneS_3)]^+$ (solv = solvent [d^6-acetone or CD_3NO_2]) is not formed by the simple substitution of a C-bound furyl with the N.M.R. solvent. In any case, it seemed improbable that the N.M.R. solvent (CD_3NO_2 or d^6-acetone) would be able to displace the uninegative furyl ligand in the complex. However, the complex $[RuCl(solv)(PPh_3)[9]aneS_3]^+$ could be formed prior to being dissolved in the N.M.R. solvent.

A triplet at $\delta = 0.96$ (t, J = 7.5Hz) is observed in the ^1H N.M.R. spectrum (Figure 4.18) of the yellow product described in Section 4.2.1 . When this resonance ($\delta = 0.96$) is irradiated, the resonance at $\delta = 2.61$ (q, J = 7.5Hz) p.p.m. turns from a quartet to a singlet (Figure 4.19), thus indicating that this quartet is coupled to the triplet at $\delta = 0.96$ p.p.m. This implies the presence of an ethyl group in the mixture of complexes.

A further splitting of the resonance at $\delta = 2.61$ p.p.m. is observable (J = 0.6Hz), which may be due to the long-range coupling to the co-ordinated ^{31}P in the PPh_3 group. This ethyl group is not due to free Et_2O since the ^1H N.M.R. spectrum of Et_2O in CD_3NO_2 shows resonances at $\delta = 1.17$ (t, J = 7Hz) and 3.4(q, J = 7Hz). The resonances for both free Et_2O and the complex containing an ethyl group can be seen in Figure 4.18.

The ^{13}C (DEPT) N.M.R. spectrum (CD_3NO_2) of the product isolated when $[RuCl_2(PPh_3)([9]aneS_3)]$ is reacted with $TlPF_6$ in CH_3NO_2 shows resonances at $\delta = 7.8$ (CH or CH_3) and 11.4 (CH_2) p.p.m. which can also be assigned to the presence of an ethyl group. The ethyl complex is assigned as $[RuCl(Z(CH_2CH_3)_n)(PPh_3)([9]aneS_3)](PF_6)_m$ (Figure 4.20), where Z, n and m are unknown

Figure 4.17 The ^{31}P N.M.R. Spectrum of the Product iosolated from Section 4.2.1

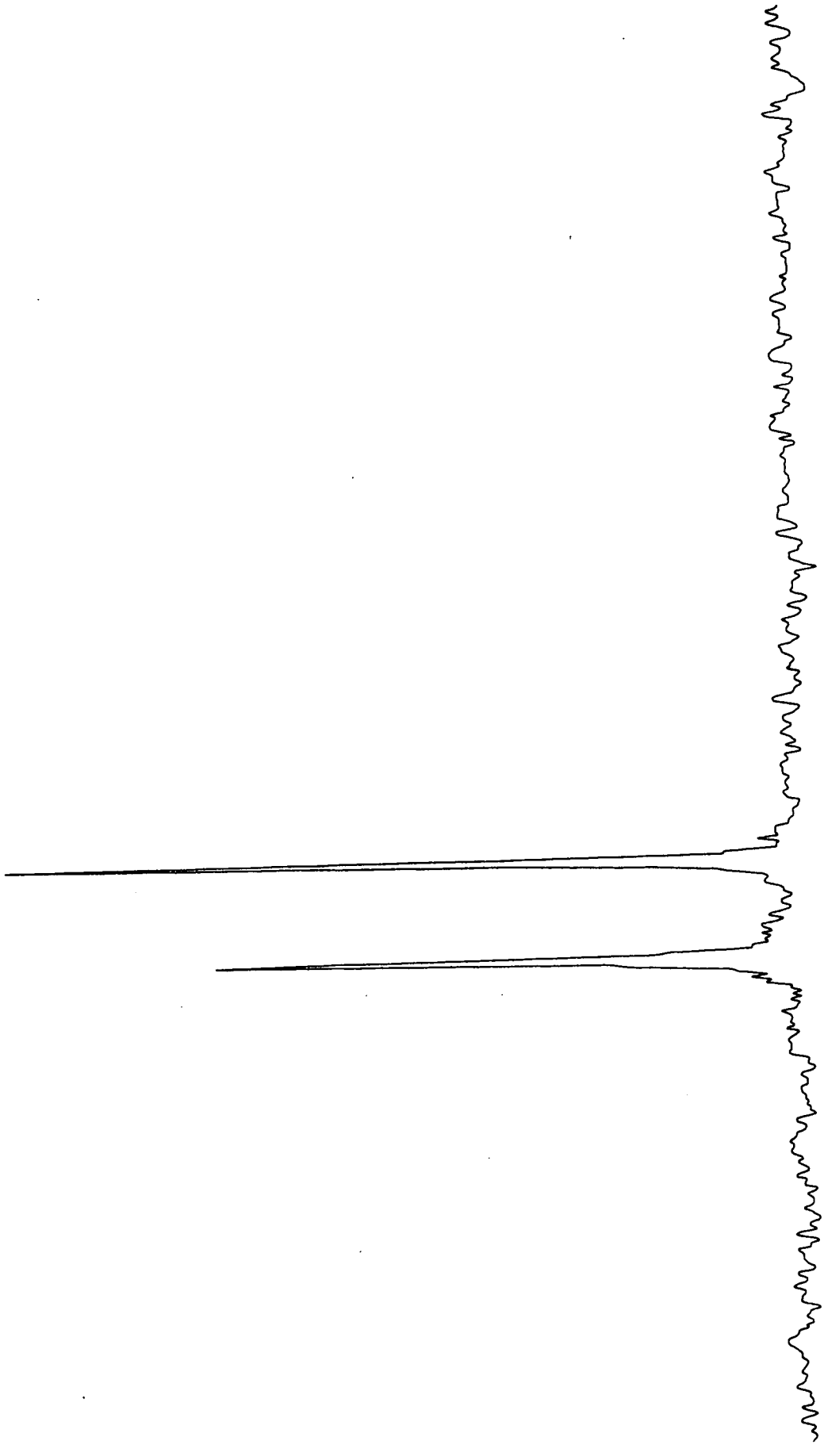

Figure 4.18 The ^{1}H N.M.R. (d^{6}-acetone,360MHz) Spectrum the Product iosolated from Section 4.2.1

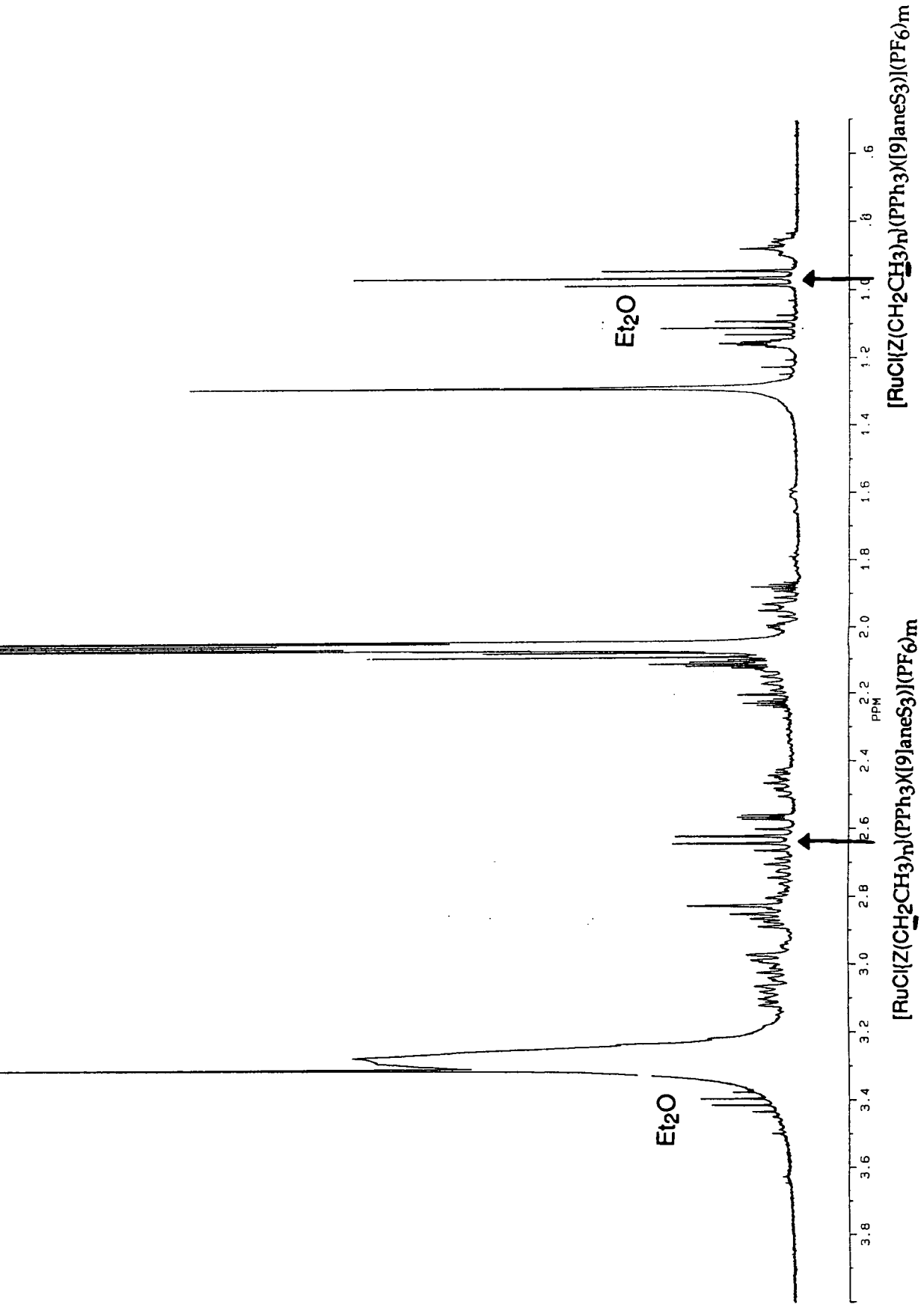

Figure 4.19 The ^{1}H N.M.R. (d^{6}-acetone,360MHz, Irradiated at δ=0.97 p.p.m.) Spectrum of the Product iosolated from Section 4.2.1

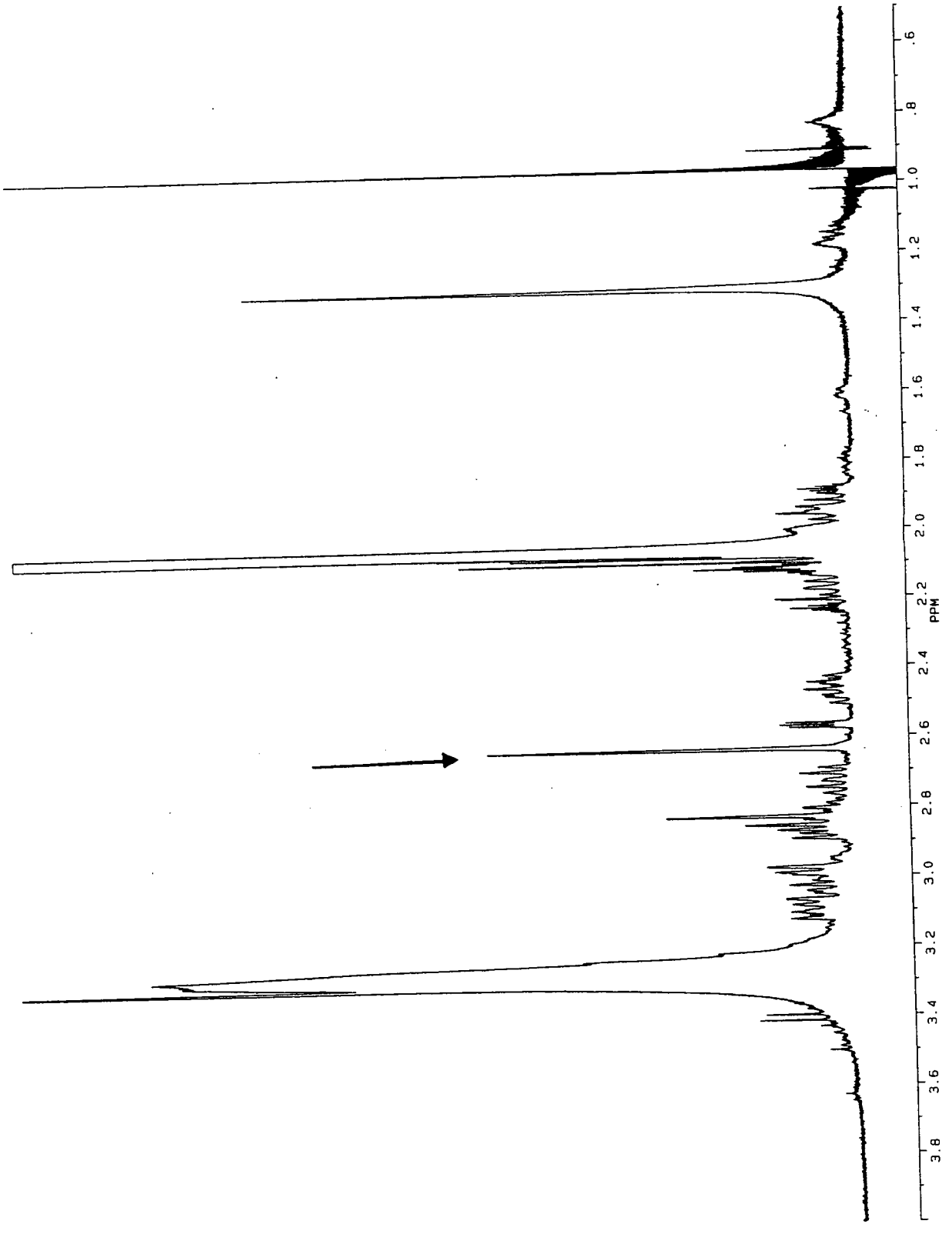

Figure 4.20 A Representation of the Ethyl Complex, $[Ru(Z(CH_2CH_3)_n)Cl(PPh_3)([9]aneS_3)](PF_6)_m$

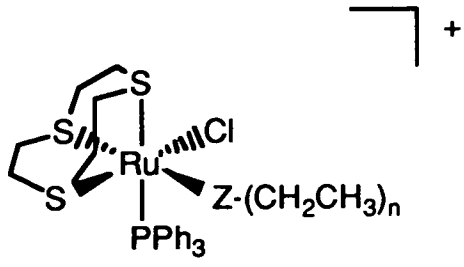

Therefore, the reaction of $[RuCl_2(PPh_3)([9]aneS_3)]$ with $TlPF_6$ in CH_3NO_2 may afford a mixture of products containing a C–bound furyl complex, $[RuCl(C_4H_3O)(PPh_3)([9]aneS_3)]$ and an ethyl complex, $[RuCl(Z(CH_2CH_3)_n)(PPh_3)([9]aneS_3)](PF_6)_m$. The % composition of these complexes can be calculated by comparing the ^1H N.M.R. integrals of the C–bound furyl complex (δ = 6.5, 8.5, 9.1), the ethyl complex (δ = 0.97 (t)) with the integrals of the phenyl region. The results for a series of experiments in which various factors are varied (see Section 4.3) are shown in Table 4.3. Furthermore, it appears that the ^{31}P N.M.R. (d^6-acetone) resonance at δ = 33.4 p.p.m. is related to the ^1H N.M.R. (d^6-acetone) resonance at δ = 0.97 (t, $(CH_3CH_2)n$) p.p.m. and the ^{31}P N.M.R. (d^6-acetone) resonance at δ = 32.2 p.p.m. is related to the ^1H N.M.R. (d^6-acetone) furyl resonances at δ = 6.5 (t), 8.5 (d) and 9.1 (d) p.p.m. The N.M.R. spectal data for both these products, $[RuCl(Z(CH_2CH_3)_n)(PPh_3)([9]aneS_3)](PF_6)_m$ and $[RuCl(C_4H_3O)(PPh_3)([9]aneS_3)]$ are summarised in Tables 4.4 and 4.5.

Table 4.3 Comparison of ^{1}H and ^{31}P N.M.R. spectra

Ratio of the ^{1}H N.M.R. integrals of the furyl and ethyl resonances[(i)]	Ratio of the ^{31}P N.M.R. intensities of the resonances at δ=32.2 and 33.4	% composition of the complexes[(ii)]	
		C-Furyl	Ethyl[(iii)]
1 : 4.6	1 : 5.1	15	70
1 : 2.6	1 : 3.2	25	65
1 : 2.2	1 : 1.9	30	65
1 : 1	1 : 1	50	50
1.3 : 1	1.2 : 1	60	40
2.2 : 1	2.1 : 1	65	30

Notes

(i) Different conditions lead to different composition (see section 4.3)

(ii) Estimated ± 5% error on composition

(iii) Ethyl % composition based on n = 1 in the ethyl complex, $[Ru(Z(CH_2CH_3)_n)Cl(PPh_3)([9]aneS_3)](PF_6)_m$

Table 4.4 The N.M.R. Spectral Data for $[Ru(Z(CH_2CH_3)_n)Cl(PPh_3)([9]aneS_3)](PF_6)_m$

		CD_3NO_2	d^6-acetone	Assignment
^{1}H N.M.R. Spectrum p.p.m.	δ=	0.96(t, δ=7.5 Hz)	0.97(t, δ=7.5 Hz)	$C\underline{H}_2CH_3$
		—	2.61(q, δ=7.5 Hz)	$C\underline{H}_3CH_2$
		1.5–3.5 (m)	1.8–3.4 (m)	$[9]aneS_3$
		7.35–7.85 (m)	7.4–7.85 (m)	PPh_3
^{13}C N.M.R. Spectrum p.p.m.	δ=	7.8	8.3	$\underline{C}H_2CH_3$
		11.4	11.8	$CH_2\underline{C}H_3$
		29–38	27–40	$[9]aneS_3$
		126–133	127–135	PPh_3
^{31}P N.M.R. p.p.m.	δ=	35.7	33.4	$\underline{P}Ph_3$
		-145 (Septet J = 710 Hz)	-145 (Septet J = 710 Hz)	$\underline{P}F_6^-$

Table 4.5 The N.M.R. Spectral Data for $[RuCl(C_4H_3O)(PPh_3)([9]aneS_3)]$

	CD_3NO_2	d^6-acetone	Assignment
^1H N.M.R. Spectrum p.p.m.	1.5–3.5 (m)	1.8–3.4 (m)	$[9]aneS_3$
	6.46 (t, J=2Hz)	6.56 (t, J=2Hz)	C-Furyl
	7.35–7.85 (m)	7.4–7.85 (m)	PPh_3
	8.26 (d, J=2Hz)	8.52 (d, J=2Hz)	C-Furyl
	8.95 (d, J=2Hz)	9.01 (d, J=2Hz)	C-Furyl
^{13}C N.M.R. Spectrum p.p.m.	29–36	27–40	$[9]aneS_3$
	106.2	108.1	C-Furyl
	126–133	127–135	PPh_3
	152.4	153.5	C-Furyl
	160.1	162.1	C-Furyl
	206.9	—	C-Furyl
^{31}P N.M.R. p.p.m.	34.7	32.2	PPh_3
	-145 (Septet, J = 710 Hz)	-145 (Septet, J = 710 Hz)	PF_6^-

4.2.4 F.A.B. mass spectroscopic study of $[RuCl(C_4H_3O)(PPh_3)([9]aneS_3)]$ and $[Ru(Z(CH_2CH_3)_nCl(PPh_3)([9]aneS_3)](PF_6)_m$

The mass spectrum of the mixture of complexes $[RuCl(C_4H_3O)(PPh_3)([9]aneS_3)]$ and $[Ru(Z(CH_2CH_3)_n)Cl(PPh_3)([9]aneS_3)](PF_6)_m$ in 3-NOBA shows peaks at m/e = 779, 648, 634, 579, 551 and 516, of which 579 and 551 peaks are the largest (Figure 4.21). The peaks at 648 and 579 can be assigned to $\{^{102}Ru(C_4H_3O)^{35}Cl(PPh_3)([9]aneS_3)]+2H\}^+$ and $\{^{102}Ru^{35}Cl(PPh_3)([9]aneS_3)\}^+$. The peaks at 779 and 634 could not be easily assigned. The difference between these two peaks is 145, and corresponds to a PF_6^- counter ion, implying that these two peaks are related. The difference between 634 and 579 is 55. This may correspond to a complex of the type $[RuCl(X)PPh_3[9]aneS_3]^{m+}$ where X has a mass of 55. No solvent used in preparation of the products has this weight, the nearest being

acetone which has a mass of 58. The only other possibility is $\{^{102}Ru(OH_2)THF(PPh_3)([9]aneS_3)+H\}^+$ and its PF_6^- salt, $\{^{102}Ru(OH_2)THF(PPh_3)([9]aneS_3)+HPF_6\}^+$, which might indicate that the second Cl^- may be removed during the reaction. The peaks at 551 and 516 can be assigned to $\{^{102}Ru^{35}Cl(PPh_3)(S(CH_2)_2S(CH_2)_2S)\}^+$ and $\{^{102}Ru(PPh_3)(S(CH_2)_2S(CH_2)_2S)\}^+$. To verify whether the dithiolate complex, $[RuCl(PPh_3)(S(CH_2)_2S(CH_2)_2S)(L)]$ forms in the reaction, or whether it forms as a breakdown product during the F.A.B. mass spectroscopic experiment, a selected mass F.A.B. spectrum is recorded.

A double focus mass spectrometer has three main regions. The first region is the first magnetic field, the second is the field free zone and the third is the second magnetic field. In a selected mass F.A.B. spectrum, a peak is selected after the first magnetic field. This peak breaks down in the field free region of the mass spectrometer and is analysed in the second magnetic field. A selected mass F.A.B. spectrum of the product isolated in Section 4.2.1, of the peak at 579 shows only a breakdown product at m/e = 553. This peak at m/e = 553 is not observed in the standard F.A.B. mass spectrum. This may be due to the overlap of this peak with the isotopic distribution associated with the large peak at 551. However, in the selected mass F.A.B. mass spectrum no peak at m/e = 551 is observed, thus indicating that the peak at m/e = 579 is not responsible for the production of 551 peak in the field free region of the mass spectrometer. Thus, the species $[RuCl(PPh_3)(S(CH_2)_2S(CH_2)_2S)]$ is not formed in the spectrometer, but it still could be formed during the fast atom bombardment in the 3-NOBA matrix. Therefore, this experiment does not indicate whether the dithiolate complex is present in the original material.

Figure 4.21 The F.A.B. Mass Spectrum of the product isolated in Section 4.2.1

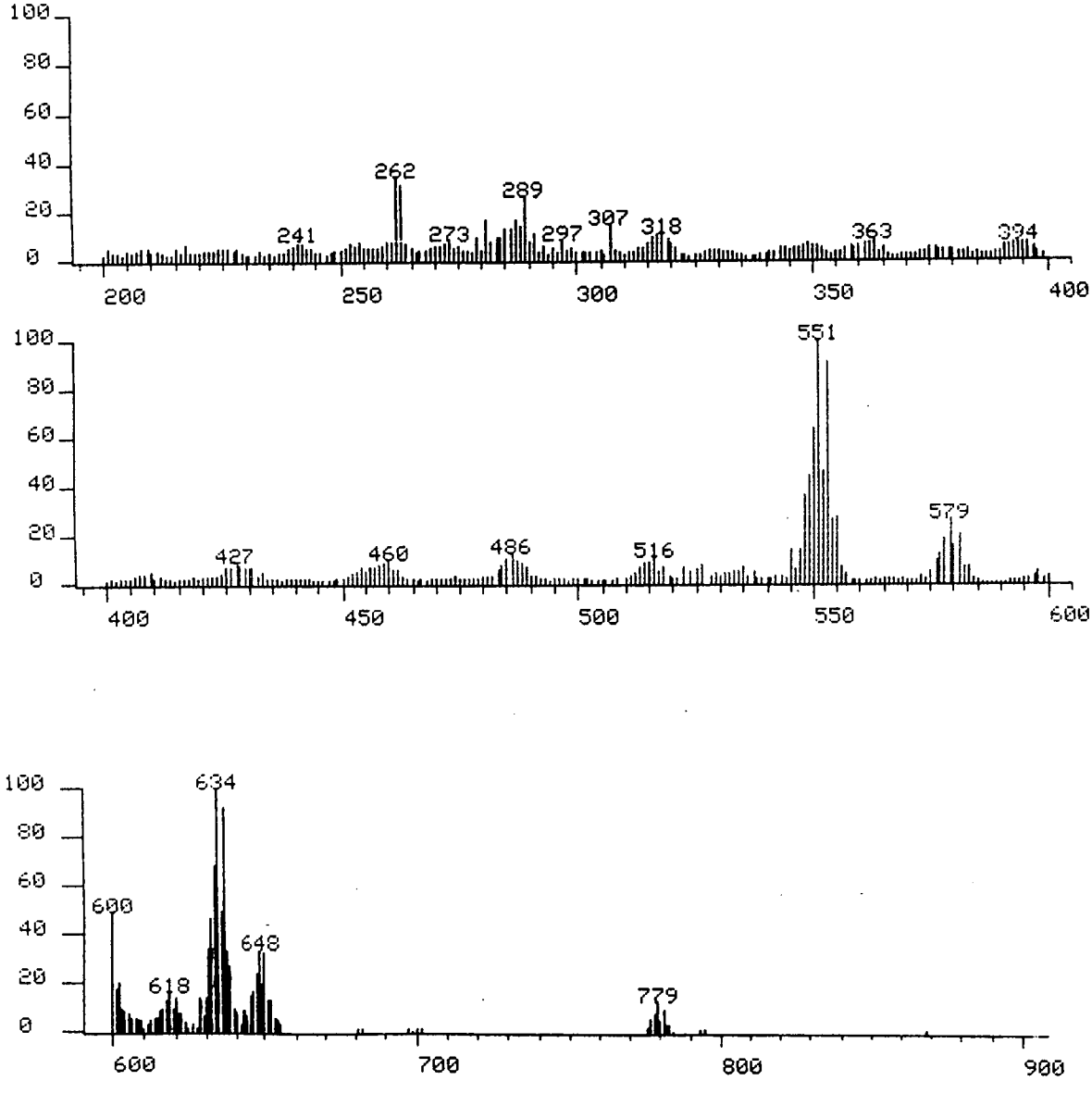

Ethylene loss from thioethers has been extensively studied by Sellman and co-workers[320-323]. They demonstrated that $\{S(C_6H_4)S(CH_2)_2S(C_6H_4)S\}^{2-}$ (L_4) can lose ethylene in both Fe and Mo complexes[320, 321]. Recently this work has been extended to the $[RuCl(PPh_3)(L_4)]$ complex and other Ru thioether complexes[322, 323]. The loss of ethylene may occur during the formation of the mixture of compounds, $[RuCl(C_4H_3O)(PPh_3)([9]aneS_3)]$ and $[RuCl(Z(CH_2CH_3)_n)(PPh_3)([9]aneS_3)](PF_6)_m$. However, the F.A.B. mass spectra of analogous pure complexes, such as $[RuCl_2(PPh_3)([9]aneS_3)]$, $[RuCl(L)(PPh_3)([9]aneS_3)]^+$ (L = $NCCH_3$, NCPh)[241], $[RuCl(SC_4H_8)(PPh_3)([9]aneS_3)]^+$ (Chapter 5), $[Ru(PPh_3)([9]aneS_3)(\mu\text{-}Cl)]_2(PF_6)_2$ and $[Ru(PPh_3)([9]aneS_3)(\mu\text{-}Cl)_2Tl](PF_6)_2$, (Chapter 3) all contain the m/e = 551 peak. It would appear therefore that ethylene loss from complexes of the type $[RuCl(L)(PPh_3)([9]aneS_3)]^{n+}$ occurs relatively easily during the fast atom bombardment in the experiment. Hence, it seems unlikely that the dithiolate forms during the reaction of $[RuCl_2(PPh_3)([9]aneS_3)]$ with $TlPF_6$.

4.2.5 Summary

The reaction of $[RuCl_2(PPh_3)([9]aneS_3)]$ with $TlPF_6$ in CH_3NO_2 seems to produce a mixture of a C-bound furyl complex, $[RuCl(C_4H_3O)(PPh_3)([9]aneS_3)]$ and an ethyl complex, $[Ru(Z(CH_2CH_3)_n)Cl(PPh_3)([9]aneS_3)](PF_6)_m$ (Figure 4.22). The N.M.R. spectral data for these complexes are presented in Tables 4.4 and 4.5. The F.A.B. mass spectrum of the mixture has peaks assignable to the C–bound furyl coupled and peaks at m/e = 779 and 634. The complex $[RuCl(C_4H_3O)(PPh_3)([9]aneS_3)]$ has been characterised by X-ray crystallography as its HPF_6 adduct.

However, a number of anomalies are associated with this assignment. In the X-ray crystal structure of the product, the location of the proton could not be determined, and was thought to reside on the O atom. However, the ^1H N.M.R. (CD_3NO_2) spectra of this product did not show any resonances associated with this missing proton. The resonances of the C–bound furyl group at δ = 6.5, 8.26 and 8.95

are significantly altered from those of free furan (δ = 6.3, 7.4). In the F.A.B. mass spectrum, there remains a problem in assigning the peaks at m/e = 779, 634, and 551.

It also appeared that a very unusual reaction was taking place. The only species containing four carbon atoms and an oxygen atom which is added to the reaction mixture is Et_2O. This suggests that Et_2O is being converted to a C-bound furyl group! This prospective conversion is highly unusual and unexpected since it would involve both C–H activation and C–C bond formation. However, despite considerable reservations about the unusual nature of this reaction a study of the factors influencing the formation of these products was undertaken in order to verify the exact nature of the product and to elucidate a possible pathway for this reaction.

Figure 4.22 The Synthesis of the Furyl and Ethyl Complexes

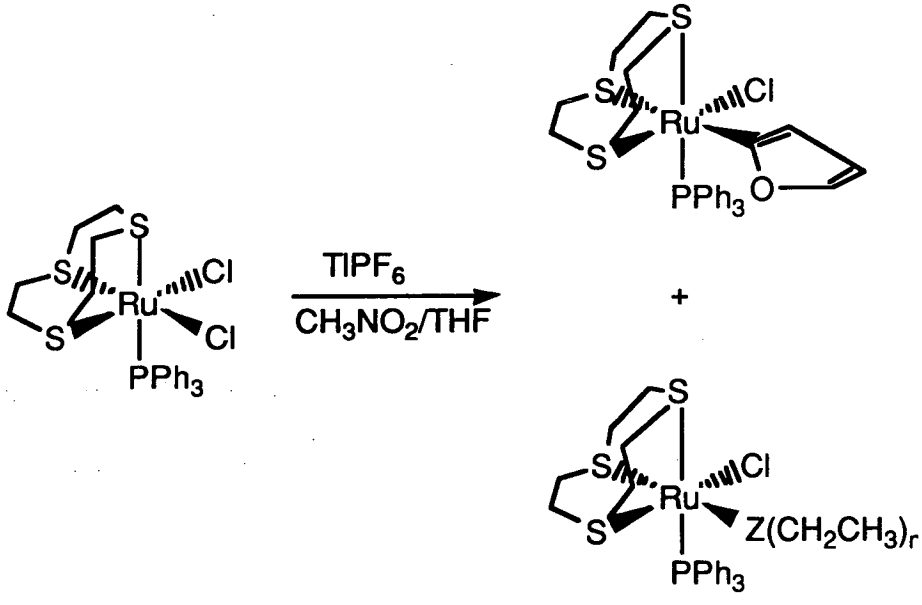

4.3 Factors Influencing the Formation of the Ethyl and Furyl Complexes

All the reactions of $[RuCl_2(PPh_3)([9]aneS_3)]$ with $TlPF_6$ in CH_3NO_2 (4 cm^3) and a proposed furyl source (1 cm^3), discussed in this Section, are carried out in a standard way (Scheme 4.3). No recrystallisation is carried out since this may alter the % composition. Control reactions, using the same solvents and run simultaneously with one in which a factor is varied, are also undertaken.

Scheme 4.3 The Reaction of $RuCl_2(PPh_3)[9]aneS_3$ with $TlPF_6$ in CH_3NO_2 in the Presence of a Proposed Furyl Source.

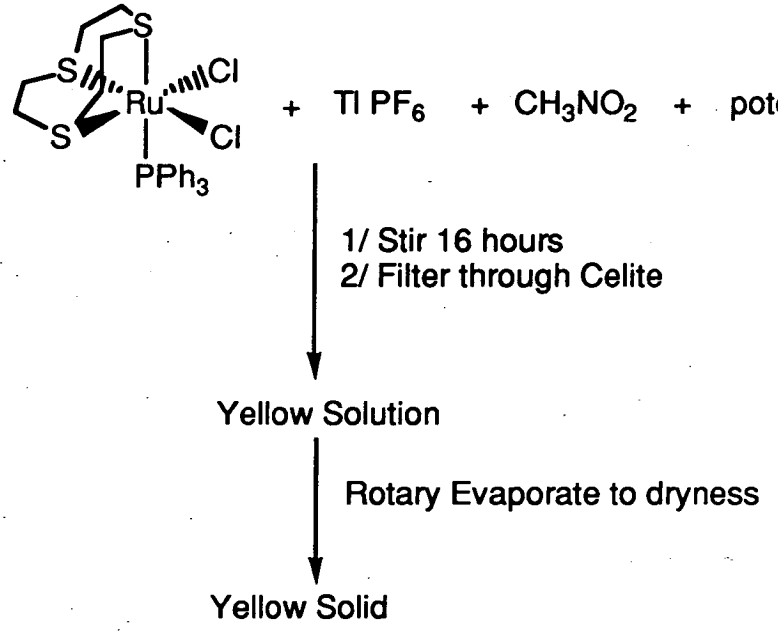

4.3.1 Possible Intermediates

The formation of the unusual ethyl complex, $[Ru(Z(CH_2CH_3)_n)Cl(PPh_3)([9]aneS_3)](PF_6)_m$ and C–bound furyl complex, $[RuCl(C_4H_3O)(PPh_3)([9]aneS_3)]$ from the reaction of $[RuCl_2(PPh_3)([9]aneS_3)]$ with $TlPF_6$ in the presence of Et_2O suggests that the furyl group may come from the Et_2O. This in turn would suggest that the ethyl complex is $[RuCl(O(CH_3CH_2)_2)(PPh_3)([9]aneS_3)](PF_6)$. A number of possible intermediates could be involved in this reaction (see Figure 4.23).

Figure 4.23 Possible Intermediates in the Conversion of Et_2O to a Furyl Ligand

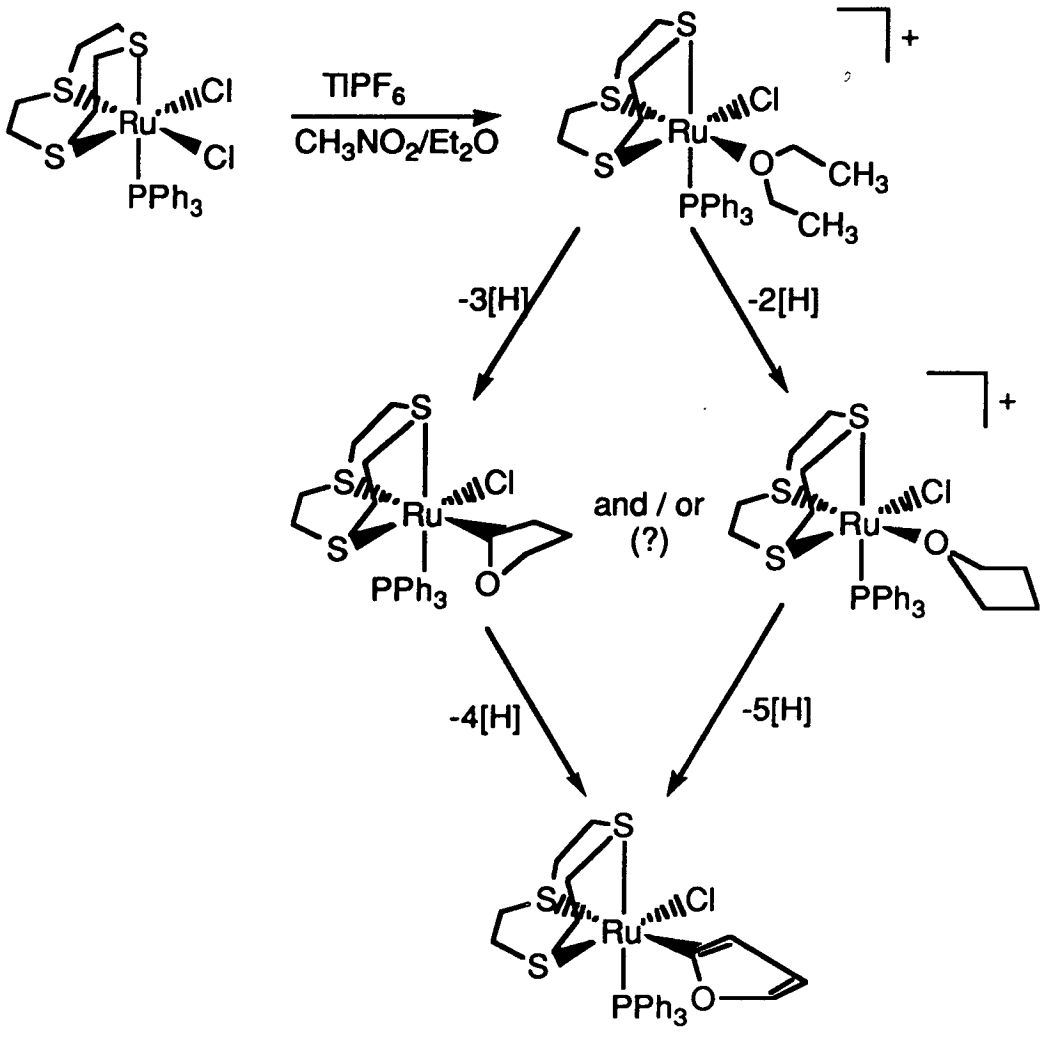

If any of the intermediates , shown in Figure 4.23 are present , it would be expected that THF, 2,5-dihydrofuran, 2,3-dihydrofuran [Figure 4.24] and furan would react to form the C-bound furyl complex.

Figure 4.24 Representations of Dihydrofurans

2,3 Dihydrofuran
2,3 DHF

2,5 Dihydrofuran
2,5 DHF

A yellow product can be isolated by reacting $[RuCl_2(PPh_3)([9]aneS_3)]$ with $TlPF_6$ in CH_3NO_2 and in the presence of THF, furan, 2,5-dihydrofuran or 2,3-dihydrofuran, using the method shown in Scheme 4.3. The ir, ^1H N.M.R., ^{31}P N.M.R. and F.A.B. mass spectra of the yellow product are the same in each case, and confirm the presence of the C-bound furyl complex. This indicates that the possible furyl source can be changed from Et_2O to THF, furan, 2,5-dihydrofuran or 2,3-dihydrofuran. However, the spectral data of the product also confirms that the ethyl species, $[Ru(Z(CH_2CH_3)_n)Cl(PPh_3)([9]aneS_3)](PF_6)_m$ is also present. This suggests that cyclic ethers can be surprisingly converted to an acyclic ethyl species. The conversion of THF to the C-bound furyl and the ethyl complex received most of the attention, during the work on this thesis.

The % composition of the two species, $[RuCl(C_4H_3O)(PPh_3)([9]aneS_3)]$ and $[Ru(Z(CH_2CH_3)_n)Cl(PPh_3)([9]aneS_3)](PF_6)_m$, which are formed by reaction of $[RuCl_2(PPh_3)([9]aneS_3)]$ with $TlPF_6$ in CH_3NO_2 in the presence of THF, is independent of the atmosphere used(N_2, argon or air), temperature and incident sunlight.

The conversion of cyclic ethers to the acyclic ethyl complex, together with the % composition being independent of temperature, increased the concern over the possible nature of the reaction, since it is even harder to envisage a pathway for this type of reaction.

4.3.2 The Possble Disproportionation of THF to a Et_2O Complex and the C-bound furyl Complex.

If the ethyl group in the complex, $[Ru(Z(CH_2CH_3)_n)Cl(PPh_3)([9]aneS_3)](PF_6)_m$ is Et_2O (Z = O, n = 2, m = 1) then it would appear that the novel disproportionation reaction of THF to furan and Et_2O (Figure 4.25) may be occurring. However, there should also be a 2 : 1 ratio in favour

of the Et_2O complex, but this has never been consistently observed, despite the care taken to ensure the integrity of the samples. The dispropotionation of THF would also suggest that there are at least two different reactions occurring since the formation of Et_2O from furan and vice versa could not to proceed via this reaction. Furthermore, Et_2O is an extremely weak ligand and therefore it seems unlikely that the complex $[Ru(O(CH_2CH_3)_2)Cl(PPh_3)([9]aneS_3)](PF_6)_m$ is present. Thus, it seems unlikely that the disproportionation route is responsible for the formation of $[RuCl(C_4H_3O)(PPh_3)([9]aneS_3)]$ and $[Ru(Z(CH_2CH_3)_n)Cl(PPh_3)([9]aneS_3)](PF_6)_m$.

Figure 4.25 The Disproportionation Reaction of THF

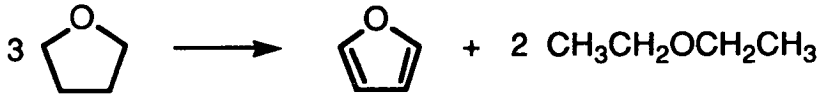

4.3.3 The Role of Tl in the Reaction of $[RuCl_2(PPh_3)([9]aneS_3)]$ with $TlPF_6$ in CH_3NO_2 in the presence of THF

Thallium complexes of furan are known[324], and such a species may have been partly responsible for the bond activation. However, when the dehalogenating agent is changed from $TlPF_6$ to $AgPF_6$ in the reaction shown in Scheme 4.3, no change is seen in the % compositions of $[RuCl(C_4H_3O)(PPh_3)([9]aneS_3)]$ and $[Ru(Z(CH_2CH_3)_n)Cl(PPh_3)([9]aneS_3)](PF_6)_m$. Furthermore, when the Ru dimer, $[Ru(PPh_3)([9]aneS_3)(\mu\text{-}Cl)]_2(PF_6)_2$ is dissolved in CH_3NO_2 and THF both species are formed, thus indicating that the dehalogenating agent is not responsible for the conversion of THF to the C-bound furyl complex.

4.3.4 C–H and C–C Bond Activation of Cyclic Ethers

The conversion of THF and diethyl ether to the C–bound furyl complex, [RuCl(C_4H_3O)(PPh_3)([9]aneS_3)] (Figure 4.12) involves C–H bond activation of five C–H bonds and C–C bond formation. The C–H activation of cyclic ethers to form C-bound metal complexes was discussed in Section 4.2.2.

The catalytic activation of C–H, C–C and C–O bands by a 'Cp*Ru^+' (Cp* = C_5Me_5) moiety has recently been reported by Chaudret *et al* [325]. The 'Cp*Ru^+' moiety is synthesised by reacting [Cp*Ru(OMe)]$_2$ with CF_3SO_2H in CH_2Cl_2 or THF. The 'Cp*Ru^+' fragment has catalysed the conversion of C_6 alkenes, dienes, alcohols, ketones, enone and dione to yield aromatic derivatives. The by-products of this reaction are H_2, H_2O, CH_4 and C_2H_6. The proposed mechanism for these reactions is shown in Scheme 4.4 [325].

Scheme 4.4 The Conversion of Methylhexene to Benzene and Toluene.

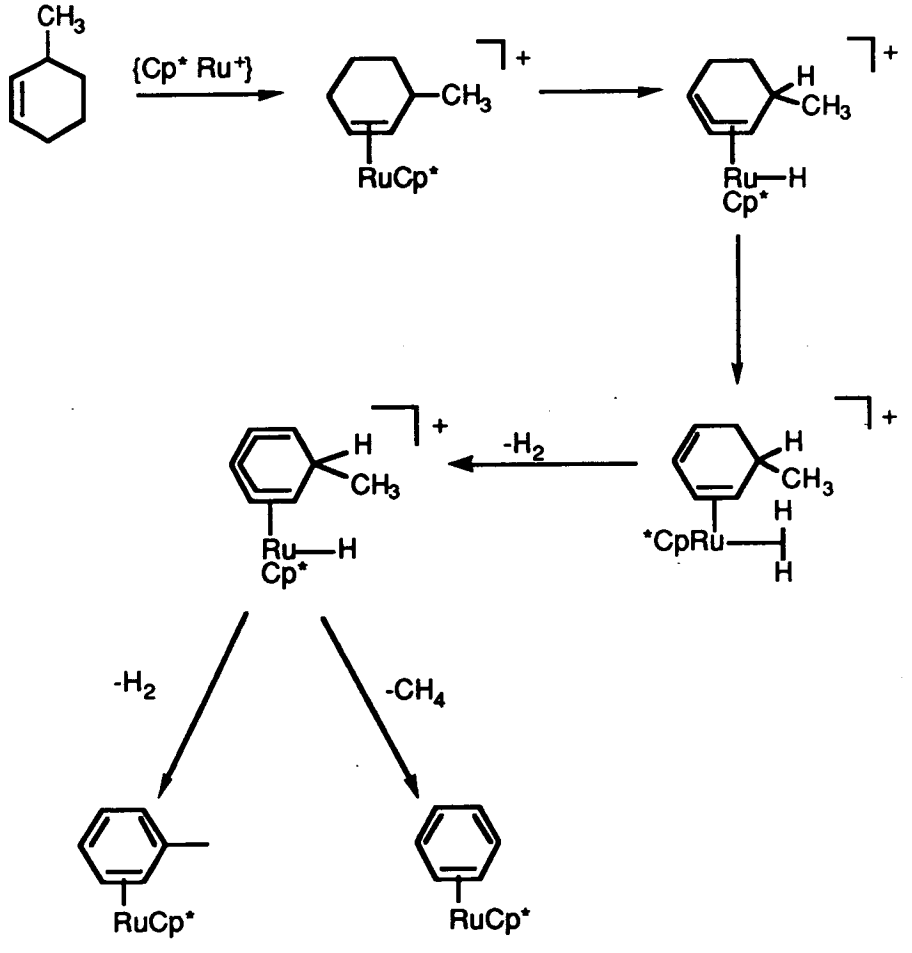

The cyclisation of ethers has been previously reported[318, 326] The photochemical cyclisation of unsaturated ethers has been catalysed by $Cu(CF_3SO_2)$ and these reactions are shown in Figure 4.26[326]. Pannel *et al* [318] reported that the complex $[MoCp(CO)_2(C_4H_3O)(PPh_3)]$ (Figure 4.15) can be formed by reacting $[CpMo(CO)_3]^-$ with $BrCH_2CHOCH_2$ in the presence of PPh_3. The mechanism for this reaction is shown in Scheme 4.5, and involves $BrCH_2CHOCH_2$ coupling with a CO ligand rearranging to form a substituted dihydrofuran complex, followed by elimination of H_2O to form the Mo C–bound furyl complex[318]. These mechanisms all require two vacant sites to be present in the metal complex.

Figure 4.26 The Photochemical Cyclisation of Unsaturated Ethers Catalysed by $Cu(CF_3SO_2)$

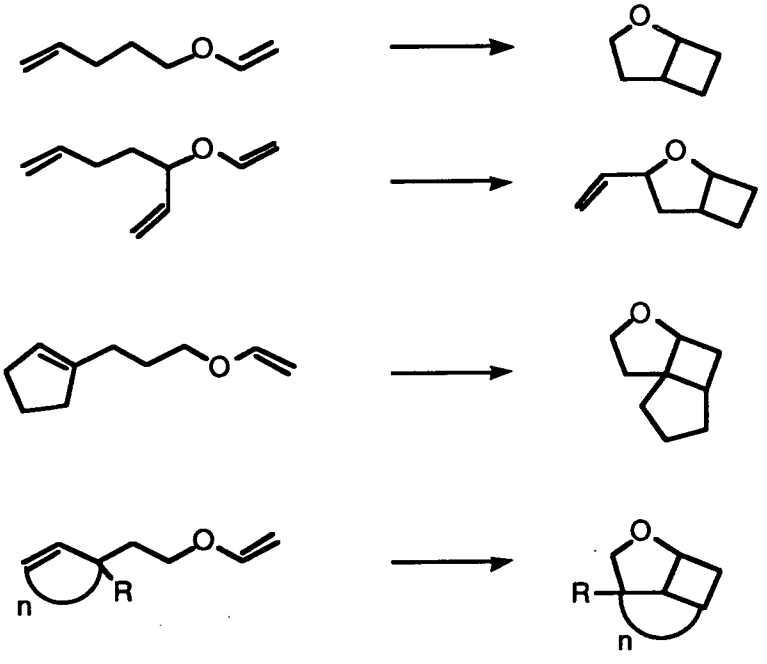

Scheme 4.5 The Proposed Mechanism for the Synthesis of $[CpMo(CO)_2(PPh_3)(C_4H_3O)]$

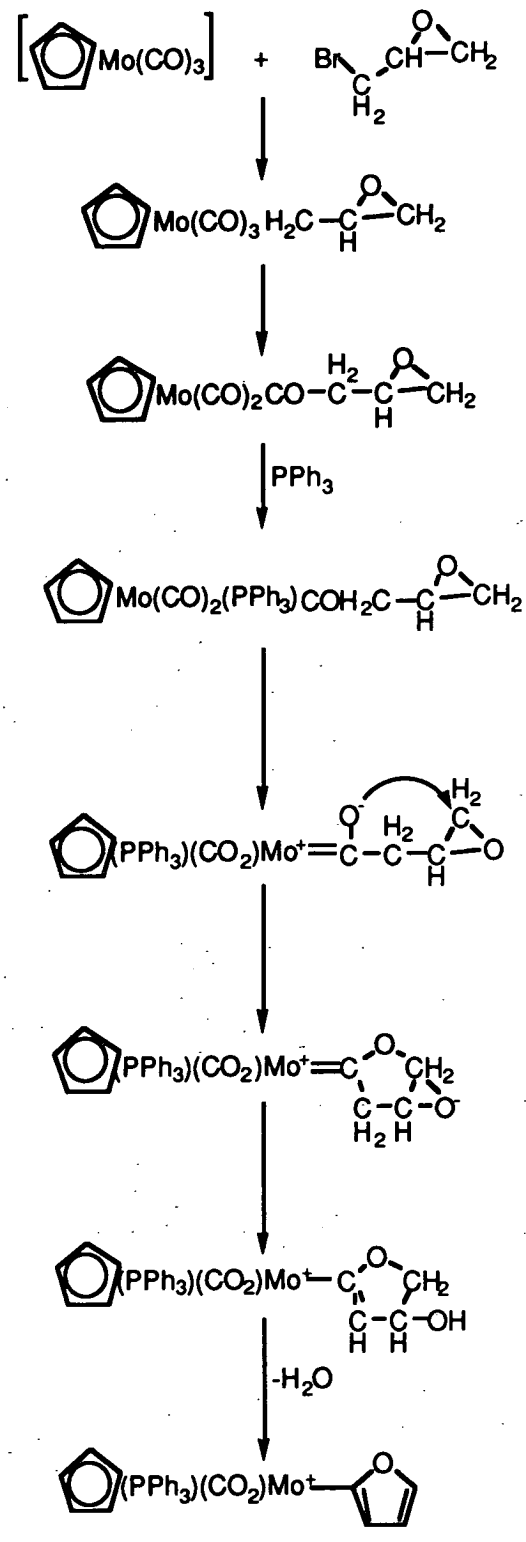

NB A representation of the final product is shown in Figure 4.15

Most catalytic reactions involve two sites, and it is difficult to envisage the C–H bond activation of THF or Et_2O by our Ru complex proceeding without two vacant sites. There is some tentative evidence for the loss of the second Cl^- during the reaction, since in the F.A.B. mass spectrum peaks at m/e =779, 634 are observed. These signals can be assigned to $[Ru(OH_2)(THF)(PPh_3)([9]aneS_3)PF_6+H]^+$ and $[Ru(OH_2)(THF)(PPh_3)([9]aneS_3)+H]^+$ respectively, although the isotopic distribution is <u>not</u> correct.

When $[RuCl_2(PPh_3)([9]aneS_3)]$ in CH_3NO_2 and THF are reacted with an excess $TlPF_6$, to remove any free Cl^- from solution, no change in chemical shifts nor composition of the mixture is observed. Furthermore, when a sample of the product is refluxed overnight with $TlPF_6$ in CH_3NO_2, no change is observed in the ^1H N.M.R. spectrum. This implies that the second Cl^- is strongly bound {as is the case for $[RuCl(NCCH_3)(PPh_3)([9]aneS_3)]PF_6$ } or that the species solution does not contain Cl^-, and the X-ray structure is of a 'rogue' crystal. However, evidence for the presence of Cl^- in the product comes from the F.A.B. mass spectrum which shows peaks at m/e = 579, 551, which can be assigned as $\{RuCl(PPh_3)([9]aneS_3)\}^+$ and $\{RuCl(PPh_3)(S(CH_2)_2S(CH_2)_2S)\}^+$ respectively. The loss of Cl^- from the second peak is also observed, indicating that the second Cl^- is strongly bound, since ethene is lost from $[9]aneS_3$ more readily than Cl^- is displaced from the Ru(II) ion.

All the evidence suggests that the fragment responsible for the reaction is $\{RuCl(PPh_3)([9]aneS_3)\}^+$, and that the mass spectrum peaks at m/e = 779 and 634 are due to the species $[RuCl(L)(PPh_3)([9]aneS_3)]PF_6$, where L has a weight of 55 mass units. The second vacant site required by most mechanisms for the cyclisation and dehydrogenation of THF of Et_2O may occur by $[9]aneS_3$ changing its co-ordination from tridentate to bidentate, although no evidence supporting this possibility has been found.

No evidence has been found for two free sites being present in any intermediate in the reaction of $[RuCl_2(PPh_3)([9]aneS_3)]$ with $TlPF_6$ in CH_3NO_2.

Therefore, the problem of how the complexes, $[RuCl(C_4H_3O)(PPh_3)([9]aneS_3)]$ and $[Ru(Z(CH_2CH_3)_n)Cl(PPh_3)([9]aneS_3)](PF_6)_m$ are formed still remains unresolved.

4.3.5 The Nature of the Solvent

(i) The Reaction of $[RuCl_2(PPh_3)([9]aneS_3)]$ with $TlPF_6$ in neat THF

The reaction of $[RuCl_2(PPh_3)([9]aneS_3)]$ with $TlPF_6$ in THF in air affords a blue solution and a white precipitate. After filtration, and removal of the solvent, a blue solid is isolated. No high frequency resonances associated with the C–bound furyl complex are observed in the ^1H N.M.R. spectrum of the blue product (Figure 4.27). However, the ^1H N.M.R. spectrum is broadened, which may indicate the presence of a Ru(III) complex, or some paramagnetic complex. The ir spectrum reveals strong bands at υ cm^{-1} = 1761, 1711 (br), 1615, 1572 and 1122, which are not present in the mixture of the C-bound furyl and ethyl complexes. The F.A.B. mass spectrum exhibits peaks at m/e = 836, 725, 644, 631, 594, 568, 550 and 530 (Figure 4.28). The peaks at 594, 550 and 530 show isotopic distributions which suggest that both Ru and Cl are present; the peaks at 594 and 550 can be assigned as $\{RuCl(PPh_3)O([9]aneS_3)\}^+$ and $\{RuCl(PPh_3)(S(CH_2)S(CH_2)_2S)\}^+$ respectively. This may indicate the presence of a species such as $[Ru(O)Cl(PPh_3)([9]aneS_3)]^{n+}$.

On exposure to air, the compound becomes yellow and both the ^1H N.M.R. and ir spectra broaden. No features can be distinguished in the F.A.B. mass spectrum. The nature of this yellow complex remains unknown. However, it is clear that the reaction of $[RuCl_2(PPh_3)([9]aneS_3)]$ with $TlPF_6$ in neat THF does not yield either the ethyl species or the C-bound furyl complex.

Figure 4.27 The ^1H N.M.R. Spectrum of the product of $[RuCl_2(PPh_3)([9]aneS_3)]$ and $TlPF_6$ in THF

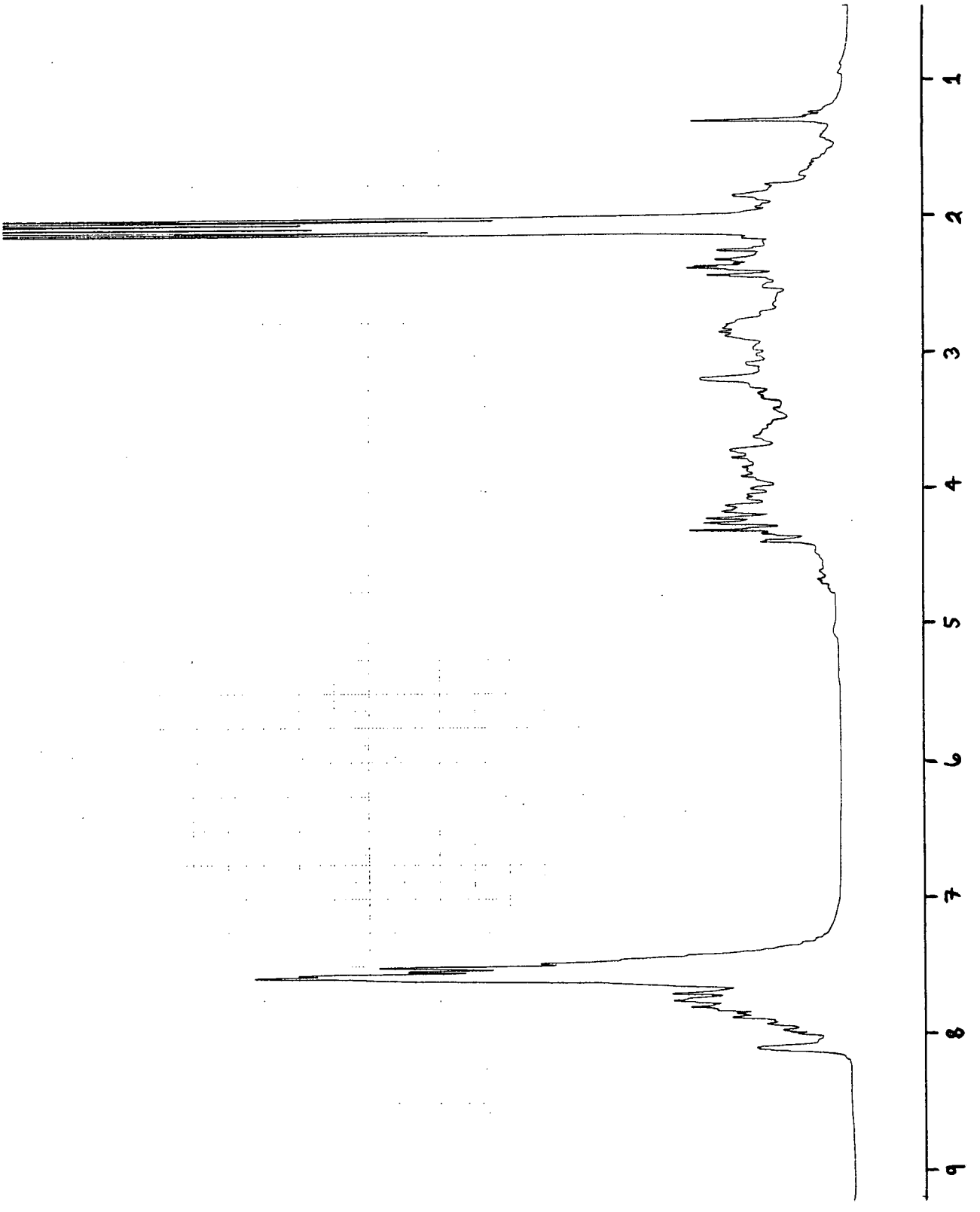

Figure 4.28 The F.A.B. Mass Spectrum of the Product of $[RuCl_2(PPh_3)([9]aneS_3)]$ and $TlPF_6$ in THF

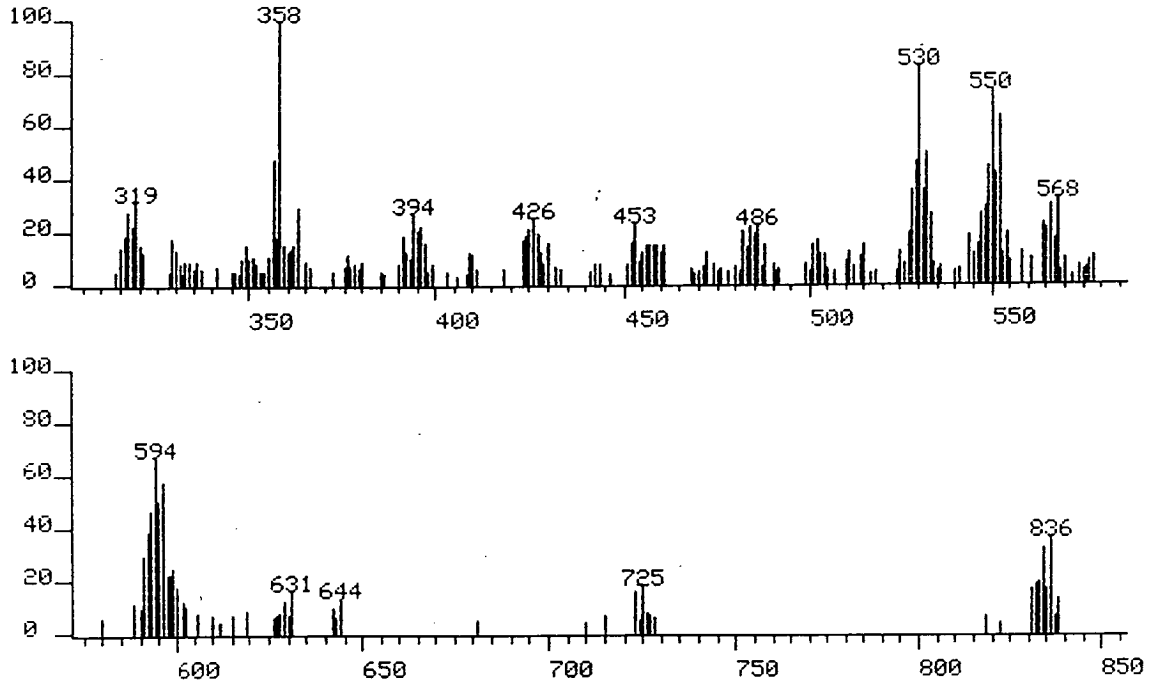

(ii) The Reaction of $[RuCl_2(PPh_3)([9]aneS_3)]$ with $TlPF_6$ in neat DHF

When $[RuCl_2(PPh_3)([9]aneS_3)]$ and $TlPF_6$ are added to neat 2,5-dihydrofuran or 2,3-dihydrofuran (no CH_3NO_2) a yellow solution forms. Reducing the solvent yields a yellow 'sticky' solid, whose F.A.B. mass spectrum shows peaks at m/e = 1122, 1052, 982, 841, 771, 701, 631, 561, 491, 421, 351, 281, 211, 141 and 72. This implies that a polymer has formed with at least sixteen units of DHF (16 x 71 = 1121). A possible structure of the polymer is shown in Figure 4.29. Hence, the reaction of $[RuCl_2(PPh_3)([9]aneS_3)]$ with $TlPF_6$ in DHF does not result in the formation of $[Ru(Z(CH_2CH_3)_n)Cl(PPh_3)([9]aneS_3)](PF_6)_m$ and $[RuCl(C_4H_3O)(PPh_3)([9]aneS_3)]$, suggesting that in order to form these complexes a solvent is required.

Figure 4.29 A Possible Structure of the 2,3- or 2,5- DHF Polymer

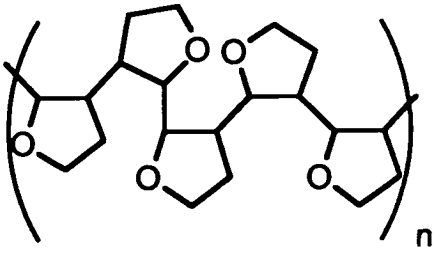

(iii) The Reaction of $[RuCl_2(PPh_3)([9]aneS_3)]$ with $TlPF_6$ and THF in a RNO_2 (R = Et, Ph)

When the solvent is changed from CH_3NO_2 to $CH_3CH_2NO_2$ or $PhNO_2$ in the reaction shown in Scheme 4.3, no C–bound furyl complex nor ethyl complex is observed in the ^1H N.M.R. spectrum. The light orange solid which can be isolated has been identified as the Ru dimer, $[Ru(PPh_3)([9]aneS_3)(\mu\text{-}Cl)]_2(PF_6)_2$ and the Ru/Tl ladder, $[Ru(PPh_3)([9]aneS_3)(\mu\text{-}Cl)_2Tl]_2(PF_6)_2$ described in Chapter 3. This indicates that only specific solvents may react to form the C- bound furyl and ethyl complexes.

(iv) The Reaction of $[RuCl_2(PPh_3)([9]aneS_3)]$ with $TlPF_6$ and THF in a Deuterated Solvents

The reaction of $[RuCl_2(PPh_3)([9]aneS_3)]$ with $TlPF_6$ in CD_3NO_2 and in either d^8-THF or 'normal' THF in the conditions shown in Scheme 4.3 results in a product the ^1H or ^2D N.M.R spectra of which does not show any resonances associated with the C-bound furyl or ethyl complexes. Yellow and orange crystals form from the solution, which are identified as the Ru dimer, $[Ru(PPh_3)([9]aneS_3)(\mu\text{-}Cl)]_2(PF_6)_2$ and the Ru_2Tl_2 ladder, $[Ru(PPh_3)([9]aneS_3)(\mu\text{-}Cl)_2Tl]_2(PF_6)_2$ discussed in Chapter 3.

The reaction of $[RuCl_2(PPh_3)([9]aneS_3)]$ with $TlPF_6$ in CH_3NO_2 in the presence of d^8-THF in the conditions shown in Scheme 4.3 leads to the isolation of a product, the ^1H N.M.R. spectrum of which shows the presence of both the C-bound furyl complex and ethyl species. However, no incorporation of the deuterium label into the C–bound furyl complex is seen in the ^2D N.M.R. This may indicate that the

d^8-THF undergoes deuterium/proton exchange with the CH_3NO_2. To check whether this occurs in the absence of the Ru complex, a mixture of d^8-THF/CH_3NO_2 (0.2 ml : 0.8 ml) was left for two days. The results show that little or no deuterium has been incorporated into the CH_3NO_2 nor have any protons been incorporated into the d^8-THF. When this was repeated with THF and CD_3NO_2 in the absence of any Ru complexes, similar results are observed. Thus d^8-THF only appears to undergo deuterium/proton exchange in the presence of $[RuCl_2(PPh_3)([9]aneS_3)]$ and $TlPF_6$. If this exchange occurs *after* the reaction has been completed i.e. between the C–bound furyl complex and the solvent rather than during the reaction to form this complex, then exchange should occur between the C–bound furyl complex and CD_3NO_2. To investigate this, a sample of the mixture of the C-bound complex and the ethyl species was prepared according to Scheme 4.3 in non-deuterated solvents and was dissolved in CD_3NO_2 for eight days, whereupon its ^1H N.M.R. spectra (CD_3NO_2) was recorded. No change in the spectrum is observed. However, this may be because the exchange was slow. The sample was then refluxed for two days and the spectrum retaken in CD_3NO_2 but the ^1H N.M.R spectrum still remains unchanged. To check whether any deuterium has been incorporarated into the furyl group, the sample was evaporated to dryness, and dissolved in CH_3NO_2, and the ^2D N.M.R. spectrum run. No incorporation of the ^2D label is seen in the ^2D N.M.R. spectrum. The only ^2D signal is of $CH_xD_yNO_2$, which could be due either to incompletely drying the compound, or to the naturally occurring deuterium in CH_3NO_2. Thus, when $[RuCl_2(PPh_3)([9]aneS_3)]$ and $TlPF_6$ is reacted in CH_3NO_2 and d^8-THF, no incorporation of the label is observed in the complex, $[RuCl(C_4H_3O)(PPh_3)([9]aneS_3)]$. However, it is unclear whether the deuterium label undergoes exchange **during** the reaction.

If THF and CH_3NO_2 do exchange protons then it could account for the fact that no other solvent displays this phenomenon, since any other solvent would have different proton exchange characteristics. It has been reported that the action

of acids or bases on THF leads to polymerisation[327]. Hence the reaction may occur only within a very specific pH range and if this is the case then it would explain the difference in reactivity between non deuteurated and deuterated CH_3NO_2. The solvent may also be responsible for prevention of dimerisation. If the solvent is not sufficiently ligating, then it cannot prevent dimerisation (e.g. acetone, CD_3NO_2, $CH_3CH_2NO_2$, $PhNO_2$, CH_2Cl_2). Likewise, if it has too great a co-ordinating ability (e.g. CH_3CN), then the solvated complex $[RuCl(Solv)PPh_3[9]aneS_3]PF_6$ will be formed. This may explain why the only solvent in which the reaction occurs is CH_3NO_2.

An alternative explanation for the lack of the ^2D label being incorporated into the C-bound furyl complex, $[RuCl(C_4H_3O)(PPh_3)([9]aneS_3)]$ in the reaction of $[RuCl_2(PPh_3)([9]aneS_3)]$ with $TlPF_6$ in CH_3NO_2 and d^8-THF is that the furyl complex does <u>not</u> come from THF. This suggests that another species, possibly an impurity, may be responsible for the reaction.

(v) <u>The Presence of Impurities in CH_3NO_2</u>

While the novel acid/base and proton exchange characteristics of CH_3NO_2 may explain why the reaction only occurs in this solvent, an alternative reason may be that an impurity is present in the CH_3NO_2 . The impurity may account for the reactivity in two main ways. Firstly, the impurity may react with the $[RuCl_2(PPh_3)([9]aneS_3)]$ to form a very reactive species, which could then go on to react with the potential furyl source to form the C-bound furyl complex and the ethyl species. Secondly, the impurity may react directly with the Ru complex to form both the ethyl and C-bound furyl complex. In order to determine whether the impurities have any effect on the formation of the C–bound furyl complex and the ethyl species, both distilled and non-distilled CH_3NO_2 can be used in a series of reactions.

CH_3NO_2 is purified by refluxing it with activated charcoal under N_2 for twenty-four hours, filtering it to remove the charcoal and then distilling it, discarding H_2O/CH_3NO_2 azeotrope (at 83° C). The distilled solvent is then passed

down an alumina column and redistilled. It is stored over $CaCl_2$ and redistilled before use.

No significant effect is observed in the composition of $[Ru(Z(CH_2CH_3)_n)Cl(PPh_3)([9]aneS_3)](PF_6)_m$ and $[RuCl(C_4H_3O)(PPh_3)([9]aneS_3)]$ when $[RuCl_2(PPh_3)[9]aneS_3]$ is reacted with $TlPF_6$ in freshly distilled CH_3NO_2 and THF.

4.3.6 Summary

The reaction of $[RuCl_2(PPh_3)([9]aneS_3)]$ with $TlPF_6$ in CH_3NO_2 in the presence of THF or Et_2O leads to the isolation of a product which has been assigned as a mixture of a C-bound furyl complex and an ethyl species. The reaction is independent of the dehalogenating agent used, the prospective furyl source, the Ru starting material and temperature. The only factor that cannot be changed is the solvent, CH_3NO_2. Changing the solvent to $EtNO_2$ or to CD_3NO_2 prevents the formation of the two complexes, $[Ru(Z(CH_2CH_3)_n)Cl(PPh_3)([9]aneS_3)](PF_6)_m$ and $[RuCl(C_4H_3O)(PPh_3)([9]aneS_3)]$. This indicates that CH_3NO_2 is crucial for the formation of the products. The reason for the key role of CH_3NO_2 is discussed in the next section.

It should be noted that the reservations expressed about the unusual nature of the the reaction in Section 4.2 and the lack of any logical explanation of the reactivity have not been clarified. Indeed, after the work described in this Section the problem seems to have become more complex, since it appears that not only does Et_2O convert to C-bound furyl complex, $[RuCl(C_4H_3O)(PPh_3)([9]aneS_3)]$ but that cyclic ethers are unexpectedly and uncharacteristically converted to the acyclic ethyl species, $[Ru(Z(CH_2CH_3)_n)Cl(PPh_3)([9]aneS_3)](PF_6)_m$. This confusing and complex reaction presents a number of problems in trying to account for it. However, towards the end of the research time available, an important break through was made, which totally explained the nature of this reaction, and this is the focus of Section 4.4.

4.4 The Key Role of Nitromethane

The normal supplier of CH_3NO_2 used in this work was May and Baker. When the reaction of $[RuCl_2(PPh_3)([9]aneS_3)]$ with $TlPF_6$ in CH_3NO_2 and THF is repeated as shown in Scheme 4.3, using Aldrich CH_3NO_2, no C–bound furyl complex is observed. The only product is the ethyl complex $[Ru(Z(CH_2CH_3)_n)Cl(PPh_3)([9]aneS_3)](PF_6)_m$ (80% composition). When a third source of CH_3NO_2 (Prolabo) is used in the reaction, the C–bound furyl species is once again observed. However, both Prolabo and May and Baker probably use the same manufacturing process, since both are owned by Rhône-Poulenc. **Thus, the use of Aldrich CH_3NO_2 in the reaction of $[RuCl_2PPh_3[9]aneS_3]$ with $TlPF_6$ in CH_3NO_2 : THF prevents the formation of the C–bound furyl species, and assists in the formation of the ethyl complex. However, when Prolabo or May and Baker CH_3NO_2 is used in the reaction both the C–bound furyl species and the ethyl complex form.**

The difference in the reactivity of the CH_3NO_2 from the different manufacturers again alerted us to the possibility that very low concentrations of impurities† are possibly responsible for the reaction. However, any impurity must have a similar boiling point to CH_3NO_2 , as no difference in the % composition of the C–bound furyl and the ethyl complexes is observed when CH_3NO_2 is distilled (Section 4.3). CH_3NO_2 is usually manufactured by gas-phase nitration of methane. The common impurities found are higher nitroalkanes, aldehydes, ketones and alcohols, all of which can be removed by distillation[328]. The presence of another impurity has also been identified, and provided us with a major insight into the process[329]. Propionitrile (ethyl cyanide) is present in low concentrations (less than 10^{-1} M) in commercial CH_3NO_2 [292]. Its physical properties make it very difficult to remove it by distillation[292]. The recommended method for its removal is by crystallisation of a CH_3NO_2 / Et_2O (1 : 1) mixture at -60° C[292, 330-332].

† 500 p.p.m. contamination level of an impurity would be a stoichiometric concentration with respect to the Ru starting material

Reacting $[RuCl_2(PPh_3)([9]aneS_3)]$ directly with $TlPF_6$ in propionitrile ($NCCH_2CH_3$) results in a white precipitate of TlCl and a yellow solution. Removing the TlCl and reducing the solvent to dryness affords a yellow product, which is identified as $[RuCl(NCCH_2CH_3)(PPh_3)([9]aneS_3)]PF_6$. The ir spectrum of the product is similar to the one observed for the mixture of products formed from Scheme 4.3, except that there is a weak stretch at $\upsilon = 2212\ cm^{-1}$, which can be assigned as a CN stretch. The ^1H N.M.R. (Figure 4.30), ^{13}C N.M.R. (Dept) (Figure 31) and ^{31}P N.M.R. spectra were recorded. They confirm that $[RuCl(NCCH_2CH_3)(PPh_3)([9]aneS_3)]PF_6$ is part of the product mixture which is formed when $TlPF_6$ is added to $[RuCl_2(PPh_3)([9]aneS_3)]$ in CH_3NO_2. This complex, $[RuCl(NCCH_2CH_3)(PPh_3)([9]aneS_3)]PF_6$ also explains the F.A.B. mass spectrum peaks at m/e = 779, 634, which can now be assigned as $\{RuCl(NCCH_2CH_3)(PPh_3)([9]aneS_3)PF_6\}^+$ and $\{RuCl(NCCH_2CH_3)(PPh_3)([9]aneS_3)\}^+$, respectively.

The reaction is therefore not a disproportionation reaction, but a competition between the formation of the C–bound furyl complex, $[RuCl(C_4H_3O)(PPh_3)([9]aneS_3)]$ and the reaction with the EtCN impurity. The reaction to form the C–bound furyl complex may not have occurred in Aldrich CH_3NO_2 because the concentration of propionitrile was sufficiently high to impede totally the formation of the C–bound furyl complex. The reaction of $[RuCl_2(PPh_3)([9]aneS_3)]$ in Aldrich CH_3NO_2 (purified by crystallisation) in the presence of THF, undertaken as shown in Scheme 4.3 results in a yellow/orange material containing the Ru dimer $[Ru(PPh_3)([9]aneS_3)(\mu\text{-}Cl)]_2(PF_6)_2$ and a small amount of $[RuCl(NCCH_2CH_3)(PPh_3)([9]aneS_3)]PF_6$. This indicates that only Rhône-Poulenc CH_3NO_2 could form the C–bound furyl complex, which may be due to another impurity activating the complex to C–H bonds.

Figure 4.30 The ^{1}H N.M.R. Spectrum of $[RuCl(NCCH_2CH_3)(PPh_3)([9]aneS_3)](PF_6)$

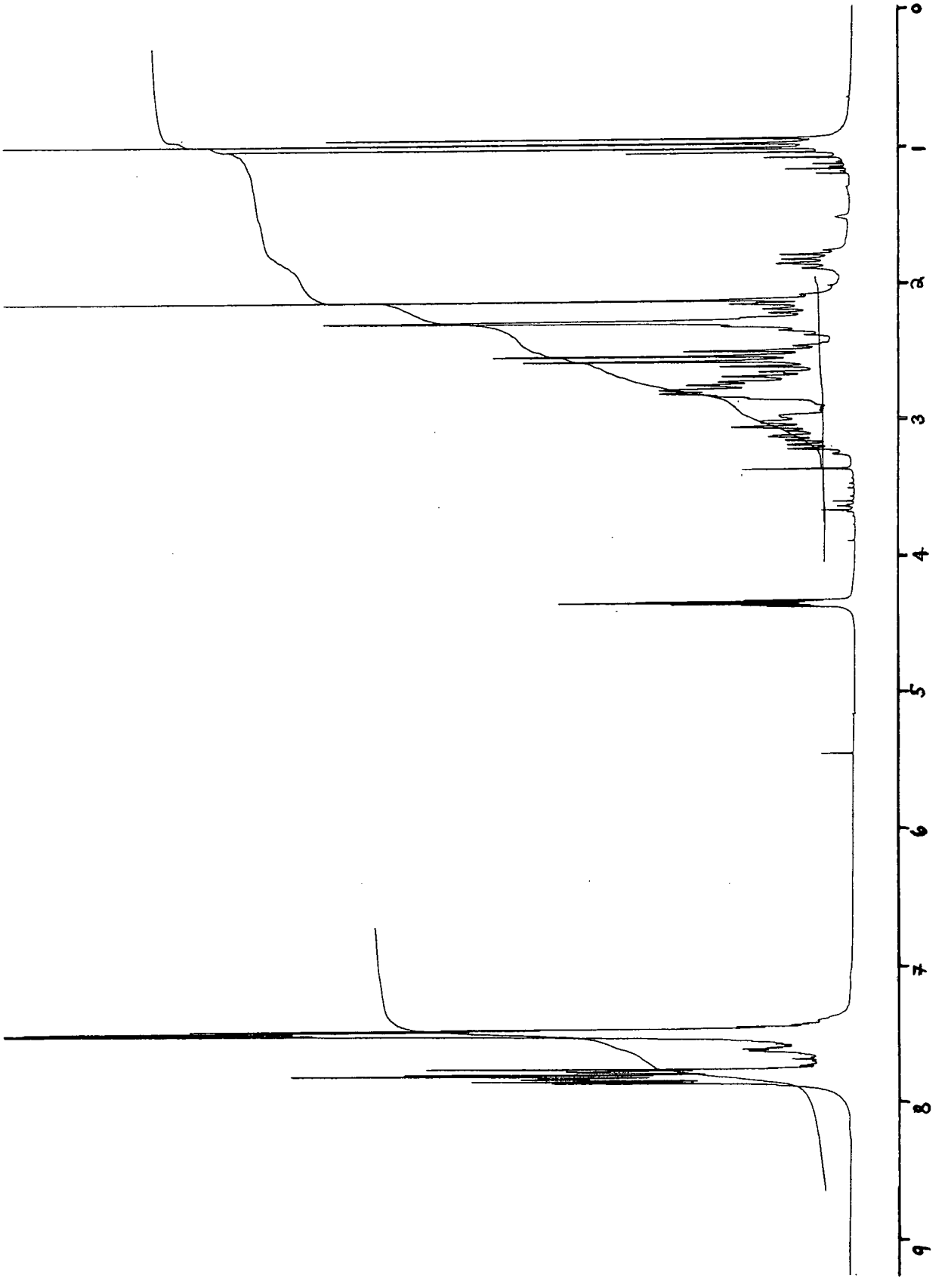

Figure 4.31 The ^{13}C N.M.R. Spectrum of
$[RuCl(NCCH_2CH_3)(PPh_3)([9]aneS_3)](PF_6)$

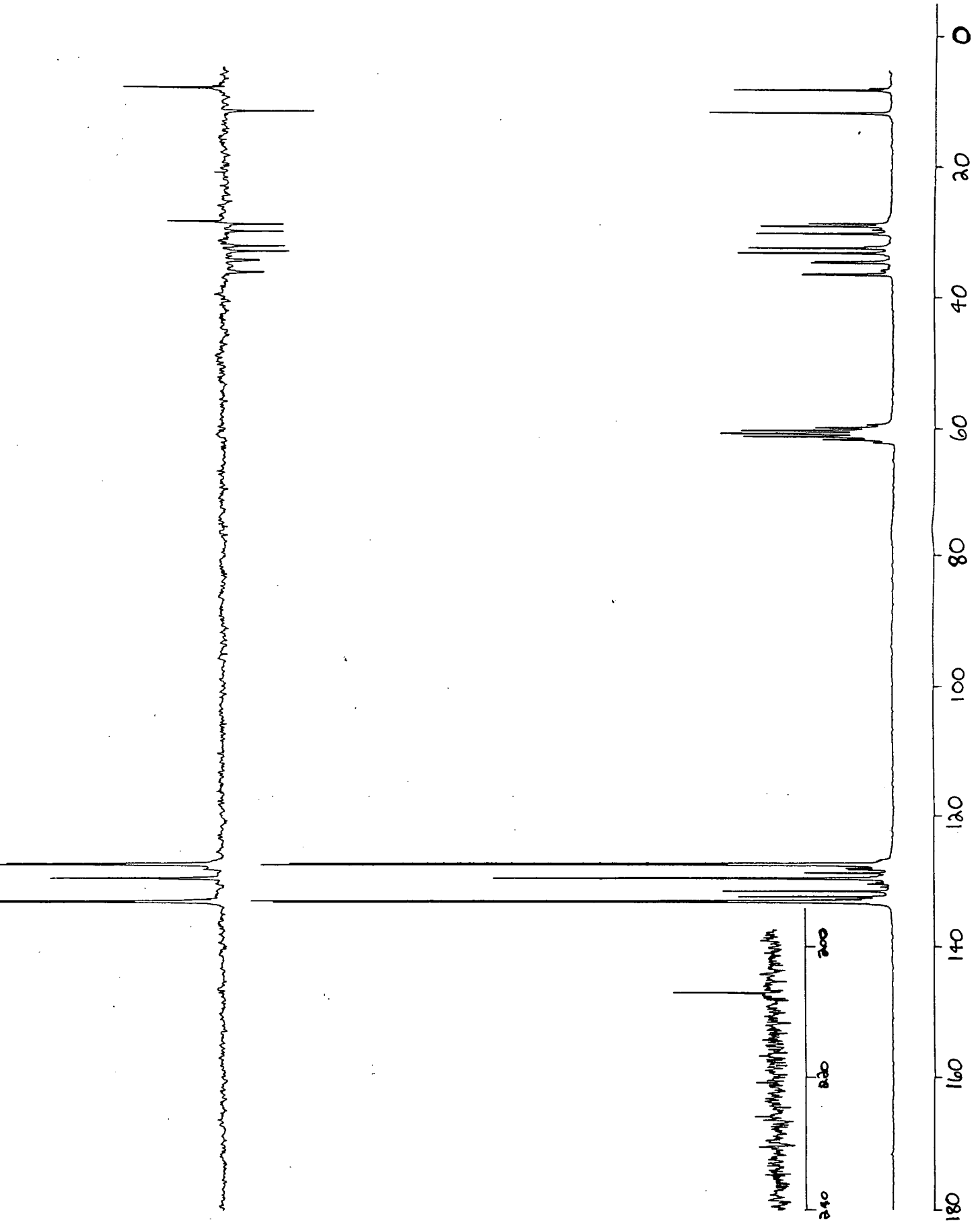

In order to demonstrate that the C–bound furyl complex is formed from THF, labelled THF could be used in the reaction described in Scheme 4.3. As has already been discussed, deuterium labelled THF did not incorporate the label into the product. However, this could be due to H/D exchange, and ^{13}C labelled THF would avoid this problem. The cost of commercially produced ^{13}C labelled THF is prohibitive, so the synthesis of ^{13}C labelled THF from labelled K*CN has to be undertaken. The method used is based on the previously reported preparations of labelled $HO_2{}^*CCH_2CH_2{}^*CO_2H$[333], the conversion of this labelled species into $HO^*CH_2CH_2CH_2{}^*CH_2OH$[334] and the reported dehydration of unlabelled $HOCH_2CH_2CH_2CH_2OH$ into THF[335] (see Scheme 4.6).

Scheme 4.6 The Synthesis of THF

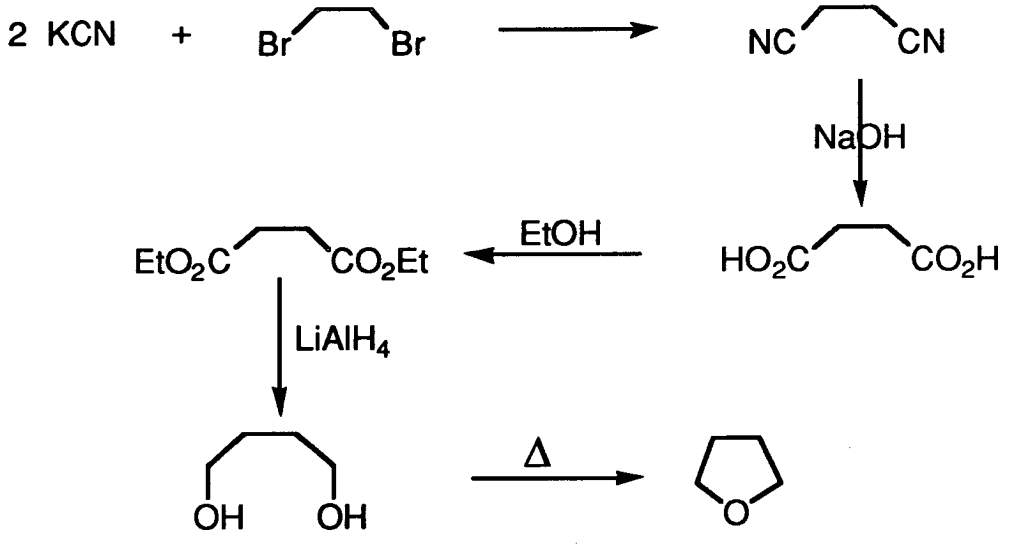

A mixture of K*CN, Br–CH_2–CH_2–Br and a trace amount of KI in H_2O and EtOH (1 : 3) was refluxed for one hour. The resulting light brown solution was diluted with H_2O and extracted with Et_2O to separate the excess dibromide starting material. The aqueous solution was then acidified with H_2SO_4 and left to stand for thirty minutes. KOH was added until the pH = 10, and then the system was refluxed for one day. The diacid, $HO_2{}^*CCH_2CH_2{}^*CO_2H$ was isolated by continous ether extraction of the aqueous solution for three days. The ether was then removed to yield a white solid of $HO^*CH_2CH_2CH_2{}^*CH_2OH$.

$HO^*CH_2CH_2CH_2{}^*CH_2OH$ was dissolved in EtOH/Benzene (1 : 4, v/v) and the solution saturated with $HCl_{(g)}$. This solution was refluxed for fifteen hours and the water that formed was removed by a water trap. The excess EtOH, the remaining water and the bulk of the benzene was removed by distillation at room temperature. This solution of diethyl succinate was diluted with Et_2O and then slowly added to a rapidly stirring solution of $LiAlH_4$ in Et_2O and refluxed for one hour. The excess $LiAlH_4$ was then destroyed by the carefull addition of H_2O, followed by the addition of HCl (6M) until a clear solution was obtained. The diol, $HO^*CH_2CH_2CH_2{}^*CH_2OH$ was isolated by continous Et_2O extraction of the aqueous solution for three days. Removing the Et_2O resulted in a cream solid.

The dehydration of this labeled diol, $HO^*CH_2CH_2CH_2{}^*CH_2OH$ in refluxing DMSO at 160°C did not result in the isolation of THF, the first time it was attempted. Before another attempt was undertaken, our attention turned again to the idea that impurities were responsible for the reaction.

Representatives from both Aldrich and Rhône-Poulenc stated that apart from H_2O and higher nitroalkanes, there are no significant impurities in their CH_3NO_2. However, a number of studies have revealed the presence of CH_3CH_2CN[330-332]. A gas chromatographic study by Osa *et al* [332] showed that, apart form H_2O, there were four organic components in commercial CH_3NO_2 (including CH_3NO_2 itself). These impurities† were identified by J.-C. Bardin[331] as CH_3CH_2CN ($\approx 2.2 \times 10^{-2}$M)‡, nitroethane ($\approx 1.8 \times 10^{-2}$ M)‡, and nitro–2–propane (1.5×10^{-1} M)‡. Three other impurities were also identified as NO_2, acetone and CH_3CN. However, none of these could explain the formation of the C-bound furyl complex.

It was therefore decided to check whether any further impurities are present in CH_3NO_2. A sample of Prolabo CH_3NO_2 in $CDCl_3$ was placed in the ^1H N.M.R. spectrometer and the spectrum accumulated over twenty four hours. The resulting spectrum confirms the presence of propionitrile and H_2O, and also shows the presence of a third very minor impurity with resonances in the aromatic region at

† For Aldich, Prolabo and Eastman Kodak CH_3NO_2
‡ Concentrations were only quoted for Aldrich CH_3NO_2

δ = 6.2 (t), 8.25 (broad) and 8.4 (d) p.p.m. (Figure 4.32). The guestimated concentration of the aromatic impurity is 300 p.p.m. The ^{1}H N.M.R. of Aldrich CH_3NO_2 was also accumulated over twenty four hours, however, no aromatic resonances were observed in the spectrum. This indicates that the C–bound furyl complex may come from an impurity in nitromethane.

It would seem that this impurity is an aromatic species, since it has a small coupling constant of 2 Hz associated with the triplet and the doublet, and also because of the high frequency of the chemical shifts. Due to the splitting pattern it seems probable that this complex is substituted at the 2-position. No monosubstituted furan seems capable of achieving such high frequencies of chemical shifts (8.25 and 8.44 p.p.m.). Nitrofuran has one of the highest frequencies associated with monosubstituted furans with d = 7.54, 6.88 and 7.89 p.p.m. for the 3,4,5 – H's, respectively. The presence of nitrofurans would not be unexpected due to the method of manufacture of nitromethane.

Since no 2–substituted furyl species has chemical shifts in the desired region, it must be due to a different heterocycle. One such heterocycle, with chemical shifts in approximately the correct area is isoxazole, which has chemical shifts in the ^{1}H N.M.R. ($CDCl_3$) at δ = 6.41 , 8.51 and 8.34 p.p.m. or at 6.53, 8.64 and 8.44p.p.m. There are two values for the chemical shift in the literature, since the exact position is variable, due to hydrogen bonding with the nitrogen of isoxazole.

Figure 4.32 The ^{1}H N.M.R. Spectrum of Prolabo CH_3NO_2

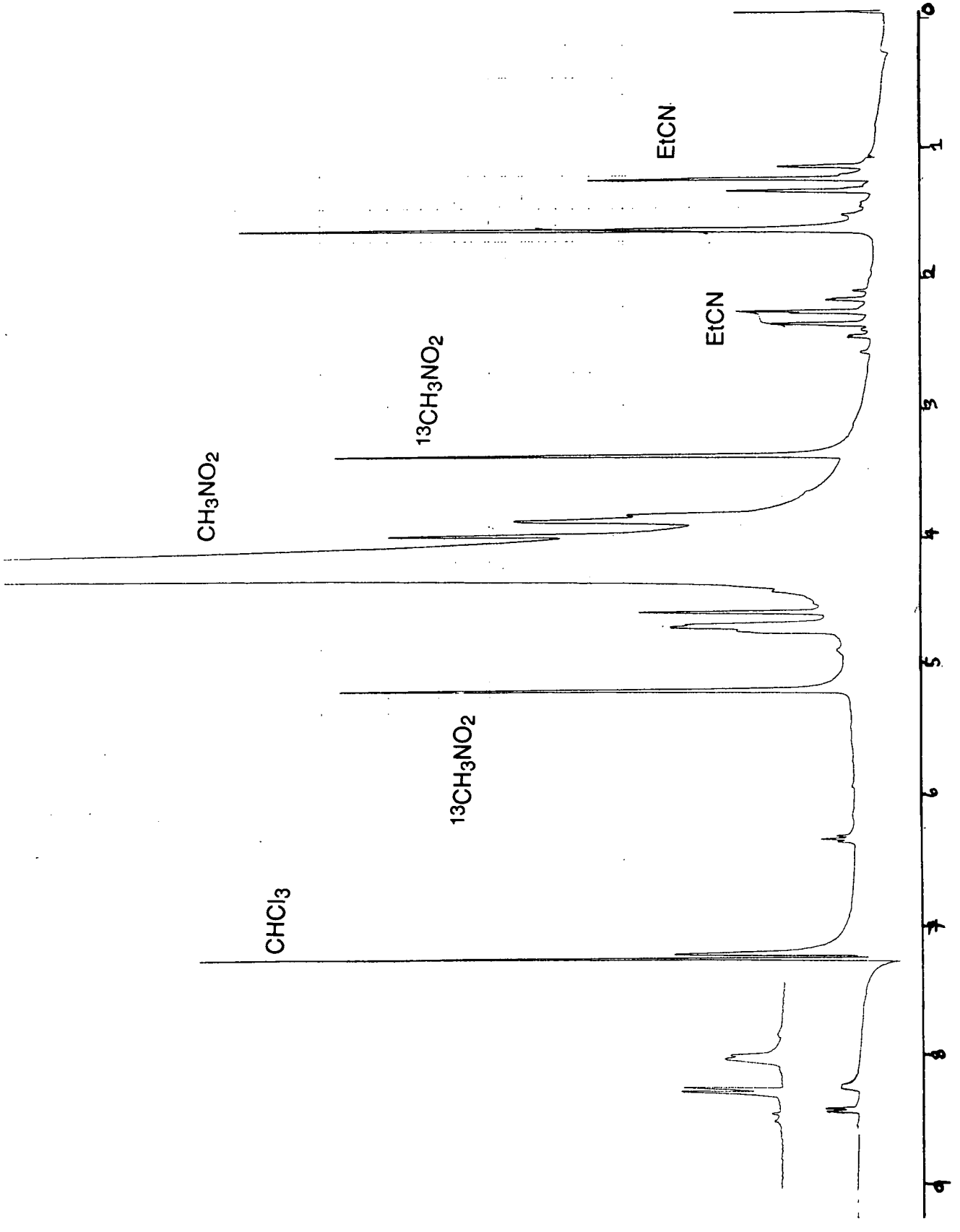

If isoxazole is present in Rhône-Poulenc nitromethane, the complex produced would not be the C–bound furyl but an N-donor isoxazole, the complex being $[RuCl(NC_3H_3O)(PPh_3)([9]aneS_3)](PF_6)$. The broadening of the resonance at $\delta = 8.25$ p.p.m. could be explained by N quadropolar coupling, and so it leaves unexplained only the extra quaternary carbon resonance in the ^{13}C N.M.R. spectrum at 206.9 p.p.m. This resonance, however, can now be explained by the CN group of the $[RuCl(NCCH_2CH_3)(PPh_3)([9]aneS_3)]PF_6$ complex, which is present in the product mixture. The $^{13}C\{^1H\}$ N.M.R. spectrum of the ethyl cyanide complex, $[RuCl(NCCH_2CH_3)(PPh_3)([9]aneS_3)]PF_6$ (Figure 4.31) confirms that the resonance at $\delta = 206.9$ p.p.m. is due to the complex, $[Ru(NCCH_2CH_3)Cl(PPh_3)([9]aneS_3)](PF_6)$ rather than $[RuCl(C_4H_3O)(PPh_3)([9]aneS_3)]$. If the C-bound furyl group is present, there is a missing quaternary carbon resonance in the $^{13}C\{^1H\}$ N.M.R. spectrum. Consequently it would appear that an isoxazole group is present as opposed to a furyl ligand.

On spectroscopic evidence, the structures of the two complexes which form during the reaction shown in Scheme 4.3 are an ethyl cyanide complex $[RuCl(NCCH_2CH_3)(PPh_3)([9]aneS_3)]PF_6$ and an isoxazole complex $[RuCl(NC_3H_3O)(PPh_3)([9]aneS_3)](PF_6)$. The presence of the isoxazole complex implies that the X-ray structure (Figure 4.12) has been mis-assigned. Examining the bond lengths of the 'bound furyl species' (Table 4.1), the bond length C_2–C_3 is very short at 1.277Å, especially when compared to C_4–C_5 (1.368Å). It would be expected that the C_2–C_3 bond length would be longer than the C_4–C_5 bond length because of the co-ordinated Ru(II) ion, since the Ru would lower the electron density, and therefore lower the bond order.

Further supporting evidence is obtained from a G.C./M.S. study of Prolabo CH_3NO_2, which shows a peak at m/e = 69 ({Isoxazole}$^+$) (Figure 4.33). Although only a very small amount is present, no recorded peaks are labelled in the spectrum unless the signal is present in three consecutive scans. This procedure removes all 'noise', and hence the signal marked at m/e = 69 is present in Prolabo CH_3NO_2.

The small amount present would be enough to react with $[RuCl_2(PPh_3)([9]aneS_3)]$ and $TlPF_6$ to form the isoxazole complex.

Finally, conclusive evidence is obtained by reacting $[RuCl_2(PPh_3)([9]aneS_3)]$ with $TlPF_6$ in isoxazole. After filtration and removal of the solvent, a yellow solid is isolated, whose the ^1H N.M.R., ^{13}C N.M.R. and ^{31}P N.M.R. spectra confirms that the complex, $[RuCl(NC_3H_3O)(PPh_3)([9]aneS_3)](PF_6)$ is present in the product obtained when $[RuCl_2(PPh_3)([9]aneS_3)]$ is reacted with $TlPF_6$ in CH_3NO_2 and THF. The ^1H and ^{13}C N.M.R. spectra of $[RuCl(NC_3H_3O)(PPh_3)([9]aneS_3)](PF_6)$ are shown in Figures 4.34 and 4.35 respectively.

Distillation of Prolabo CH_3NO_2 does not remove the isoxazole impurity, since the reaction of $[RuCl_2(PPh_3)([9]aneS_3)]$ and $TlPF_6$ in distilled Prolabo CH_3NO_2 still results in the formation of $[RuCl(C_4H_3O)(PPh_3)([9]aneS_3)]$ (see Section 4.3.5). The physical properties of both ethyl cyanide and isoxazole are similar (Table 4.6) and both should be removed by recrystallisation of CH_3NO_2 in Et_2O at -60°C. The reaction of $[RuCl_2(PPh_3)([9]aneS_3)]$ with $TlPF_6$ in thoroughly recrystallised CH_3NO_2, in the conditions shown in Scheme 4.3, results in a light orange product the spectral properties of which are identical to the mixture of $[Ru(PPh_3)([9]aneS_3)(\mu\text{-}Cl)_2Tl]_2(PF_6)_2$ and $[Ru(PPh_3)([9]aneS_3)(\mu\text{-}Cl)]_2(PF_6)_2$ isolated in chapter 3.

Table 4.6 The Boiling and Freezing Points of CH_3NO_2 , EtCN and Isoxazole

Compound	Boiling point °C	Freezing Point °C
CH_3NO_2	100.8	-17
EtCN	97.3	-92.9
Isoxazole	95-96	<-80

Figure 4.33 The G.C. / Mass Spectrum of Prolabo CH_3NO_2

Gas Chromatogram

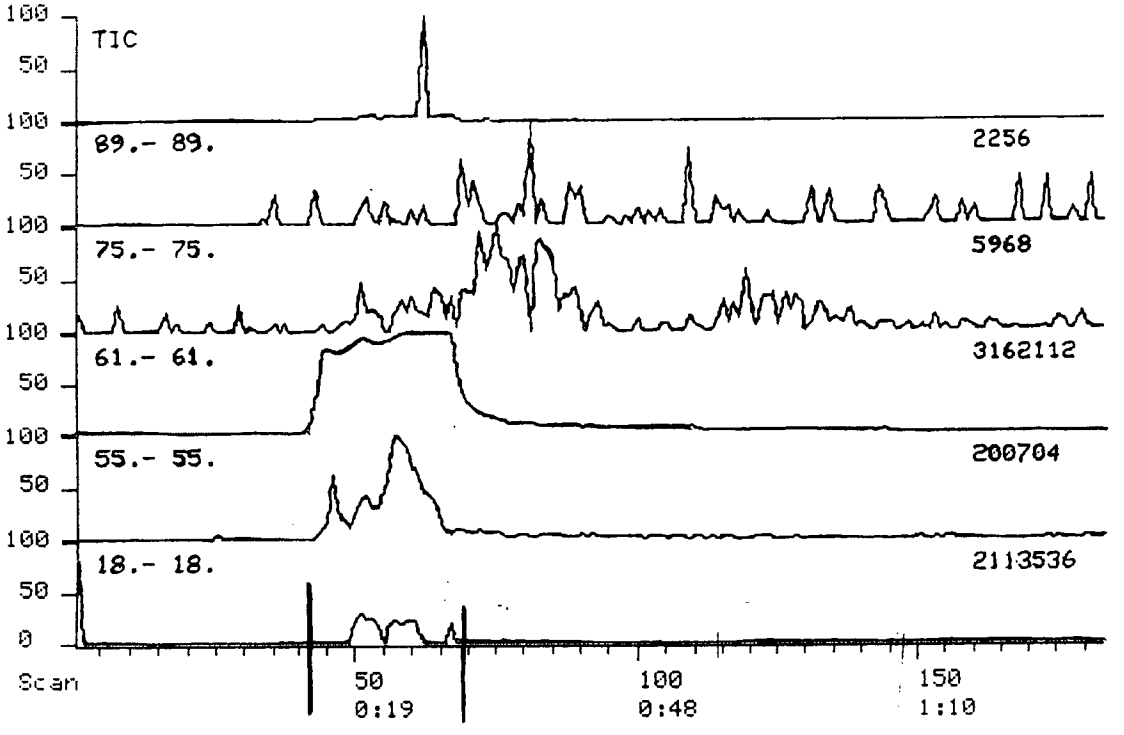

Area X

Mass Spectrum of Area X

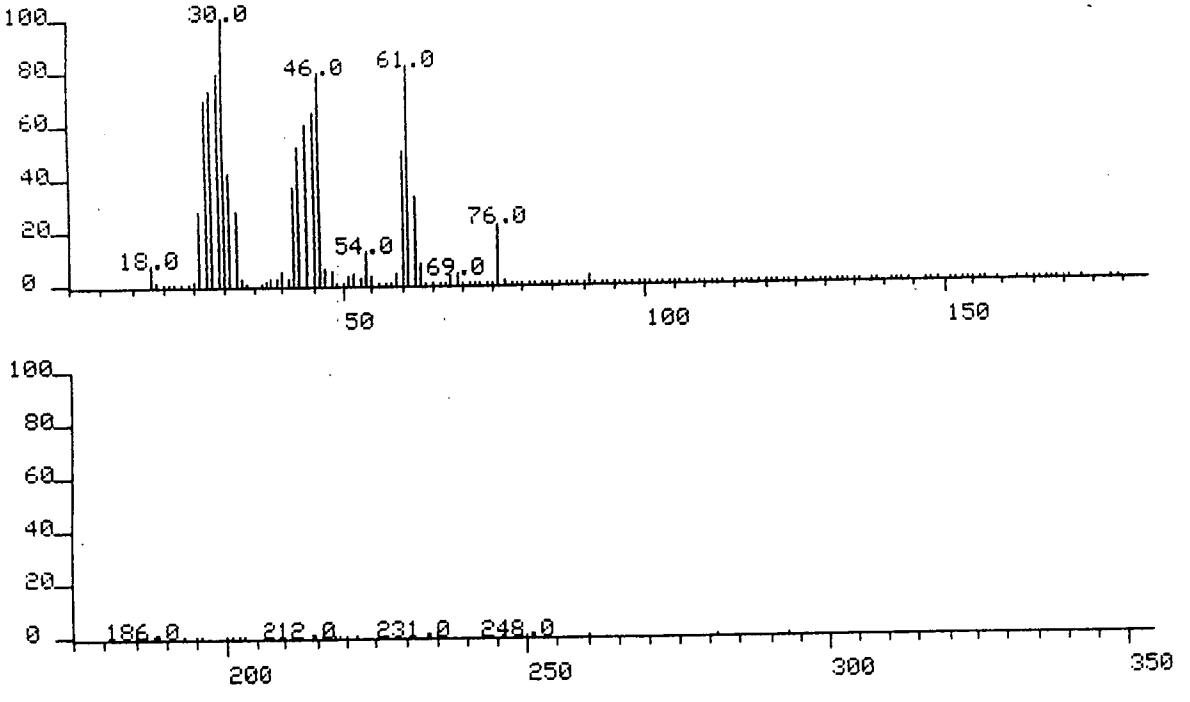

Figure 4.34 The ^1H N.M.R. Spectrum of
$[RuCl(NC_3H_3O)(PPh_3)([9]aneS_3)](PF_6)$

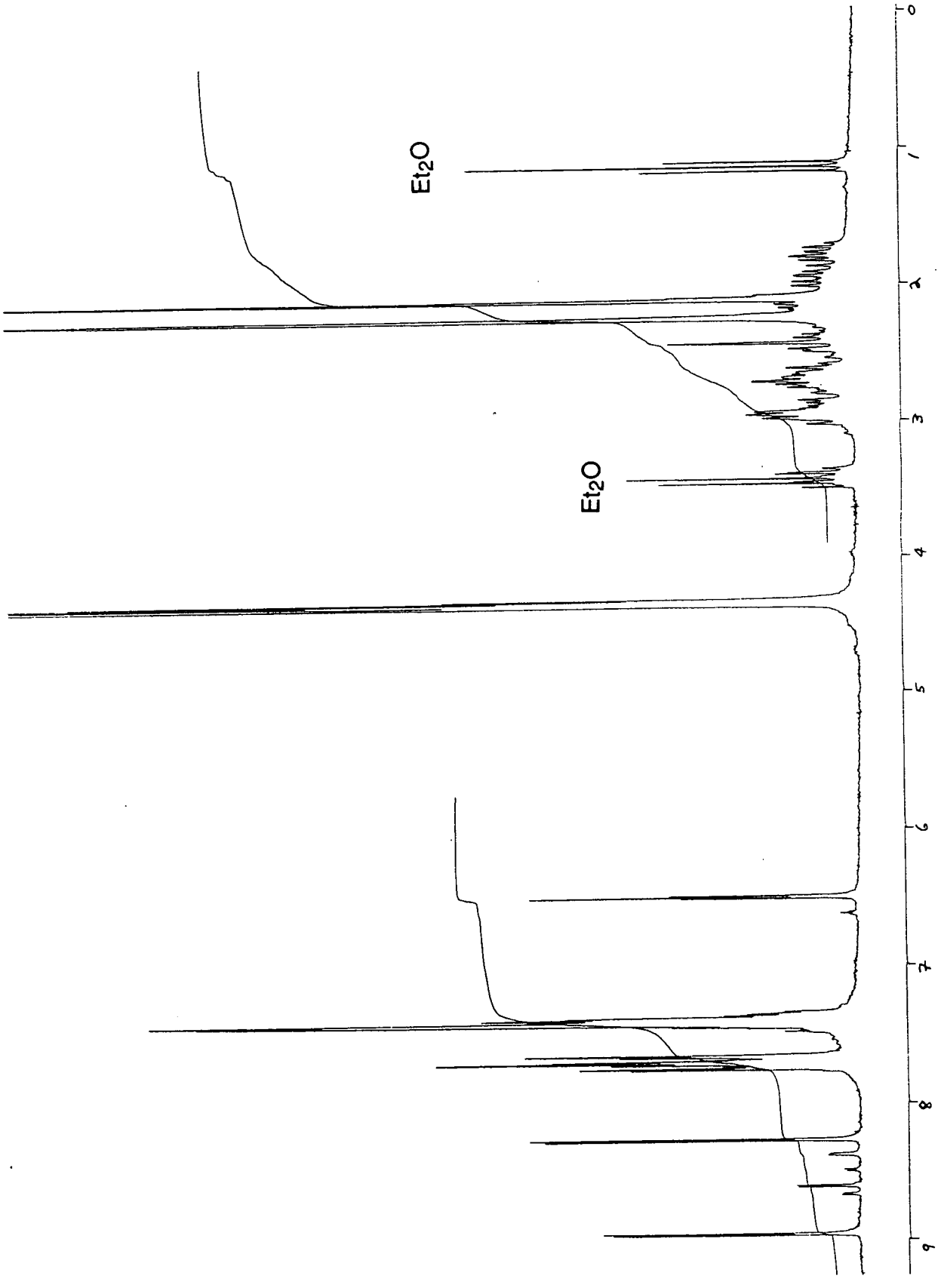

Figure 4.35 The ^{13}C N.M.R. Spectrum of
$[RuCl(NC_3H_3O)(PPh_3)([9]aneS_3)](PF_6)$

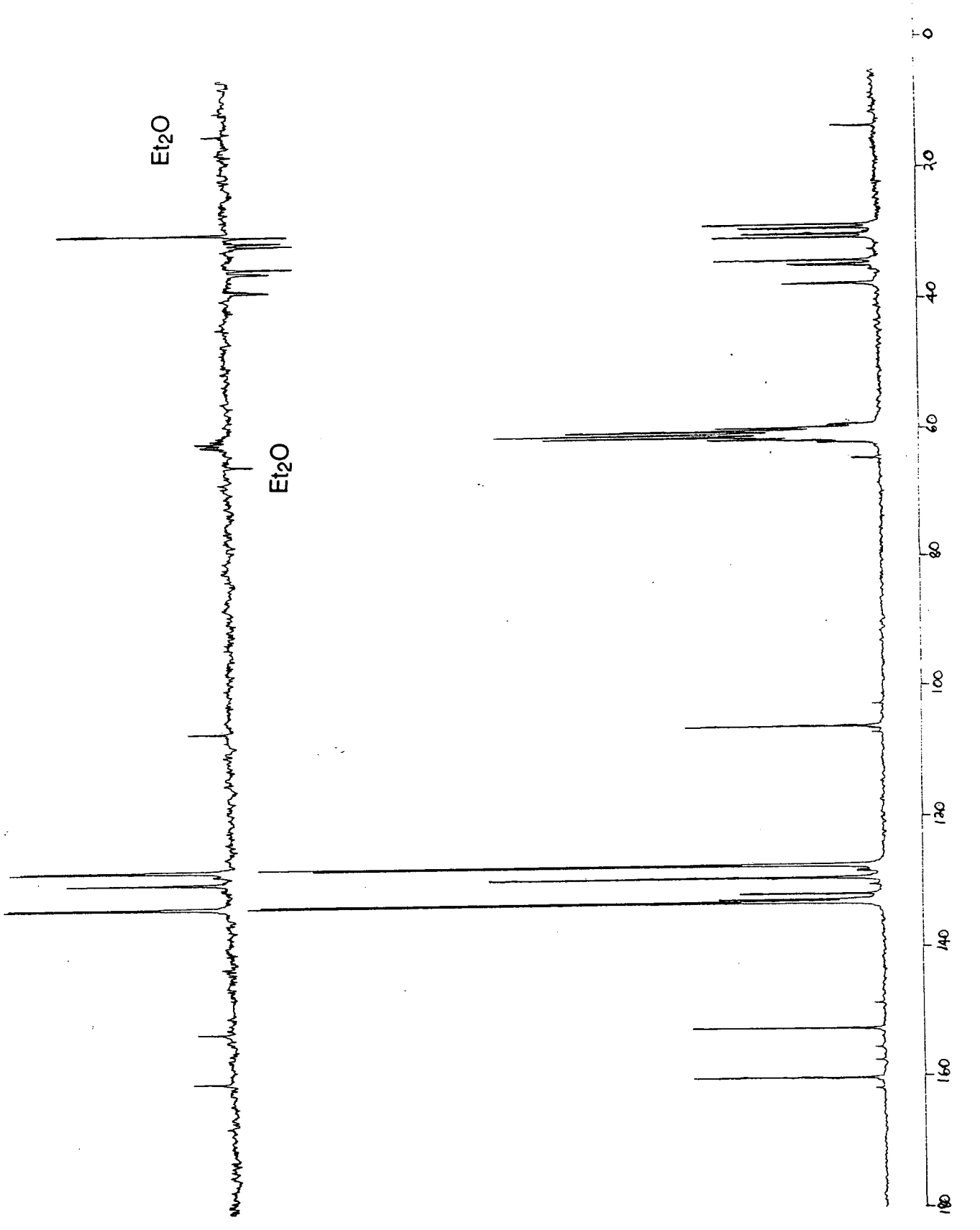

Re-interpreting the X-ray data in the light of the spectroscopic evidence results in a slight improvement in the R factor ($R_{(furyl)} = 0.477$, $R_{(isoxazole)} = 0.0459$). The bond lengths and angles of the isoxazole complex are shown in Table 4.7. A view of the revised structure is shown in Figure 4.36.

In summary, the reaction of $[RuCl_2(PPh_3)([9]aneS_3)]$ with $TlPF_6$ in CH_3NO_2 results in a mixture of $[Ru(NCCH_2CH_3)Cl(PPh_3)([9]aneS_3)](PF_6)$ and $[Ru(NCH_2CH_2CH_2O)Cl(PPh_3)([9]aneS_3)](PF_6)$ and all that we have been monitoring are the relative concentrations of these impurities and the factors influencing their relative rates of reaction. The novel conversion of Et_2O to the C-bound furyl complex, $[RuCl(C_4H_3O)(PPh_3)([9]aneS_3)]$ and an ethyl species, $[Ru(Z(CH_2CH_3)_n)Cl(PPh_3)([9]aneS_3)](PF_6)_m$ has been proven not to take place. Instead it is a simple matter of the fragment $\{RuCl(PPh_3)([9]aneS_3)\}$ reacting with the impurities. Our early reservations about the reaction, which prompted us to investigate the system in further detail, have been shown to be well founded and fully justified.

Table 4.7 Selected Bond Lengths (Å) and Angles (°) and Torsion Angles (°) with standard deviations for [RuCl(NC_3H_3O)(PPh_3)[9]aneS_3)](PF_6)

Ru–Cl	2.4519 (19)	C(6)–S(7)	1.837(8)
Ru–S(1)	2.3024 (20)	S(7)–C(8)	1.818 (8)
Ru–S(4)	2.2930 (18)	C(8)–S(9)	1.494 (12)
Ru–S(7)	2.3560 (20)	O(1i)–N(2i)	1.414 (8)
Ru–P(1)	2.3478 (20)	O(1i)–C(5i)	1.359 (11)
Ru–N(2i)	2.091 (5)	N(2i)–C(3i)	1.288 (10)
S(1)–C(2)	1.817 (9)	C(3i)–C(4i)	1.405 (12)
S(1)–C(9)	1.837 (9)	C(4i)–C(5i)	1.320 (13)
C(2)–C(3)	1.512 (12)	P(1)–C(11)	1.832 (5)
C(3)–S(4)	1.827 (8)	P(1)–C(21)	1.830 (5)
S(4)–C(5)	1.828 (8)	P(1)–C(31)	1.834 (5)
C(5)–C(6)	1.500 (11)		

Cl–Ru–S(1)	91.98 (7)	C(2)–S(1)–C(9)	101.2 (4)
Cl–Ru–S(4)	171.54 (7)	S(1)–C(2)–C(3)	115.0 (6)
Cl–Ru–S(7)	83.61 (7)	C(2)–C(3)–S(4)	113.3 (6)
Cl–Ru–P(1)	94.36 (6)	C(3)–S(4)–C(5)	100.1 (4)
Cl–Ru–N(2i)	89.16 (16)	S(4)–C(6)–S(7)	114.0 (5)
S(1)–Ru–S(4)	88.38 (7)	C(5)–C(6)–S(7)	111.1 (5)
S(1)–Ru–S(7)	87.61 (7)	C(6)–S(7)–C(8)	102.3 (4)
S(1)–Ru–P(1)	94.61 (7)	S(7)–C(8)–C(9)	114.0 (6)
S(1)–Ru–N(2i)	173.84 (16)	S(1)–C(9)–C(8)	112.7 (6)
S(4)–Ru–S(7)	87.97 (7)	N(2i)–O(1i)–C(5i)	107.5 (6)
S(4)–Ru–P(1)	94.04 (6)	O(1i)–N(2i)-C(3i)	104.9 (6)
S(4)–Ru–N(2i)	89.61 (16)	N(2i)–C(3i)–C(4i)	112.9 (7)
S(7)–Ru–P(1)	177.05 (7)	C(3i)–C(4i)–C(5i)	104.4 (8)
S(7)–Ru–N(2i)	86.51 (16)	O(1i)–C(5i)–C(4i)	110.4 (8)
P(1)–Ru–N(2i)	91.33 (16)	Ru–S(1)–C(2)	104.2 (3)
Ru–S(1)–C(9)	106.3 (3)	Ru–S(4)–C(3)	106.8 (3)
Ru–S(4)–C(5)	103.07 (25)	Ru–S(7)–C(6)	104.9 (3)
Ru–S(4)–C(8)	101.6 (3)	Ru–N(2i)–O(1i)	118.1 (4)
Ru–N(2i)–C(3i)	136.4 (5)	Ru–P(1)–C(1A)	111.76 (17)
Ru–P(1)–C(1B)	115.60 (16)	Ru–P(1)–C(1C)	119.45 (16)

C(9)–S(1)–C(2)–C(3)	74.1 (7)	C(6)–S(7)–C(8)–C(9)	64.5 (7)
C(2)–S(1)–C(9)–C(8)	-132.8 (6)	S(7)–C(8)–C(9)–S(1)	46.4 (8)
S(1)–C(2)–C(3)–S(4)	39.2 (8)	C(5i)–O(1i)–N(2i)–C(3i)	-1.2 (8)
C(2)–C(3)–S(4)–C(5)	-129.2 (6)	N(2i)–O(1i)–C(5i)–C(4i)	0.7 (9)
C(3)–S(4)–C(5)–C(6)	66.9 (6)	O(1i)–N(2i)–C(3i)–C(4i)	1.3 (8)
S(4)–C(5)–C(6)–S(7)	49.4 (7)	N(2i)–C(3i)–C(4i)–C(5i)	0.9 (10)
C(5)–C(6)–S(7)–C(8)	-135.6 (5)	C(3i)–C(4i)–C(5i)–O(1i)	0.1 (10)

Figure 4.36 A View of the X-Ray Structure of
[RuCl(NC_3H_3O)(PPh_3)([9]aneS_3)](PF_6)

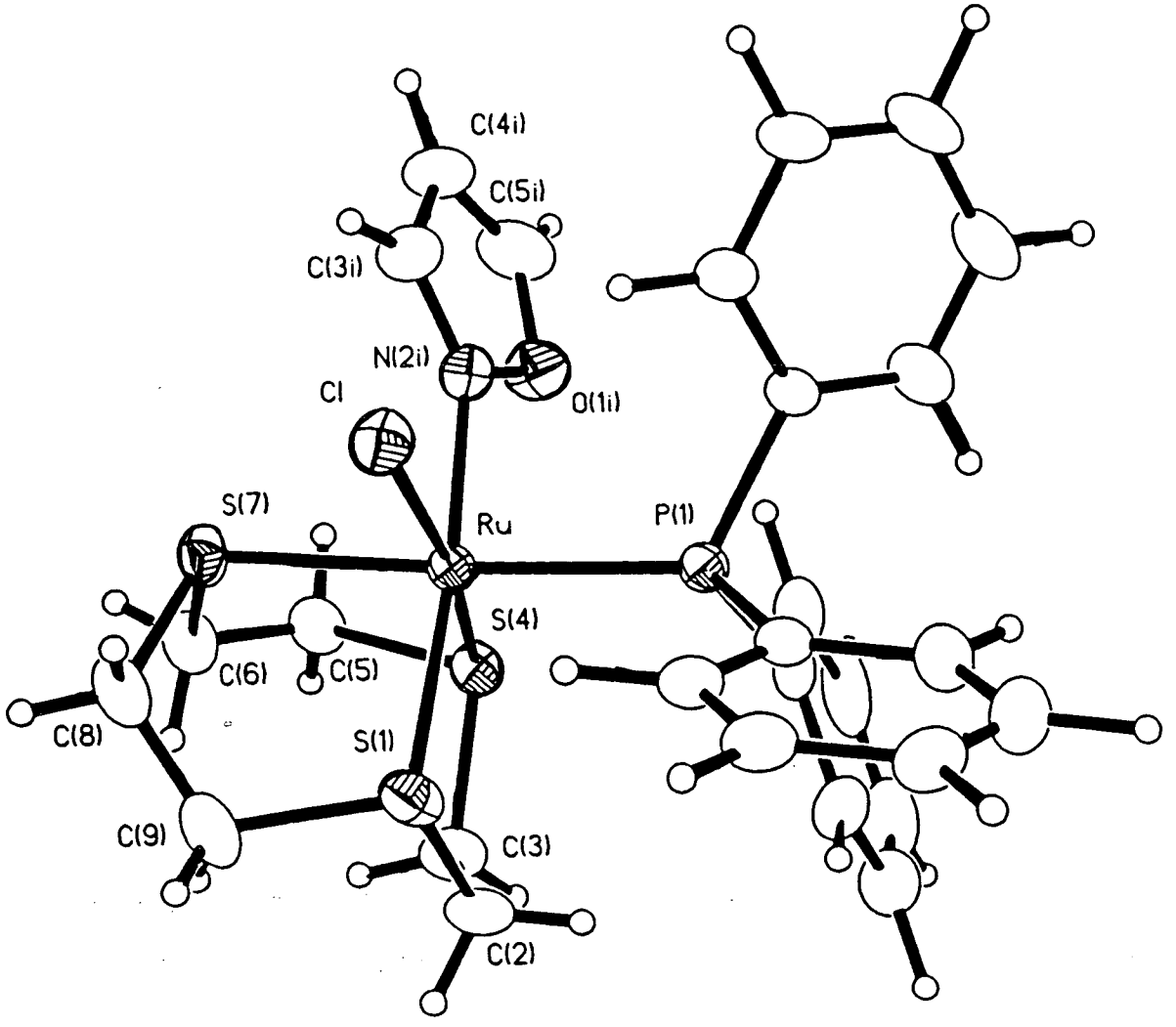

4.5 Summary and Conclusion

The reaction of $[RuCl_2(PPh_3)([9]aneS_3)]$ with $TlPF_6$ in CH_3NO_2 in the presence of THF for sixteen hours afforded a yellow solid after filtration and removal of the solvent. This yellow material was characterised by X-ray crystallography as $[RuCl(C_4H_3O)(PPh_3)([9]aneS_3)].HPF_6$. However, the presence of another complex was identified by ir, ^1H, ^{13}C and ^{31}P N.M.R. spectroscopy as $[Ru(Z(CH_2CH_3)_n)Cl(PPh_3)([9]aneS_3)](PF_6)_m$. After trying to elucidate a mechanism for this reaction, it was discovered that CH_3NO_2 contains propionitrile, which cannot be removed by distillation. The identity of the ethyl complex was confirmed as $[RuCl(NCCH_2CH_3)(PPh_3)([9]aneS_3)]PF_6$ by reacting $[RuCl_2(PPh_3)([9]aneS_3]$ with $TlPF_6$ in propionitrile.

On re–examination by spectroscopic methods, the C-Bound furyl complex, $[RuCl(C_4H_3O)(PPh_3)([9]aneS_3)]$ was re–assigned as a N–bound isoxazole complex, $[RuCl(NC_3H_3O)(PPh_3)([9]aneS_3)](PF_6)$. An isoxazole impurity in CH_3NO_2 has never been reported previously. Evidence for this impurity was obtained from a ^1H N.M.R. and by G.C./mass spectroscopic study of neat CH_3NO_2. The X-ray data were re–interpreted and were consistent with the isoxazole complex, $[RuCl(NC_3H_3O)(PPh_3)[9]aneS_3](PF_6)$. The isoxazole complex was confirmed by reacting $[RuCl_2(PPh_3)([9]aneS_3)]$ with $TlPF_6$ in neat isoxazole.

Results from the interpretation of X-ray data are usually taken to be extremely reliable. While this is generally the case, the correct identification of atom types is not a trivial matter. The difference between a C (6 electrons) and a N (7 electrons) is small, especially when it is bound to a transition metal ion. Therefore, care must be taken when assigning atom types in these types of systems and other spectroscopic evidence must be fully taken into account when assigning a complex.

4.6 Experimental

Physical Measurements

These were carried out as described in Section 3.4, except that ^1H N.M.R. were also run on a Brüker WP200 and a WH360 spectrometer operating at 200.13 MHz and 360 MHz. Selectively decoupled ^1H N.M.R. were also run on the WH360 instrument. ^2D N.M.R. were run on the Brüker WP200 operating at 30.722 MHz. Gas Chromatography/Mass Spectrometry were carried out on a KRATOS MS 50TC, using a OV101 column at an injection temperature of 100° C and a scan rate of 0.2 s^{-1}.

Reagents

The reagents and starting materials were used as described in Section 3.4. THF was purified by distillation over Na in the presence of benzophenone. CH_3NO_2 was purchased from May and Baker and was used without further purification, unless otherwise stated. Diethyl ether and hexane were purified by distillation over sodium wire and furan and the dihydrofurans were distilled before use. CD_3NO_2, d^8–THF and d^6-acetone were provided in sealed ampoules by Aldrich.

4.6.1 $[RuCl_2(PPh_3)([9]aneS_3)]$ with $TlPF_6$ in CH_3NO_2 : THF then diethyl ether

(i) $[RuCl_2(PPh_3)([9]aneS_3)]$ (51 mg, 8.3×10^{-5} M) and $TlPF_6$ (30 mg, 8.6×10^{-5} M) were added to CH_3NO_2 : THF (5 cm^3, 4 : 1 v/v) at 298K and stirred for sixteen hours. The white TlCl precipitate was removed by filtration through celite. The yellow solution was reduced in volume on a rotary evaporator and diethyl ether added. The yellow precipitate was collected and dried (Yield = 45 mg).
Ir spectrum $\upsilon(cm^{-1})$: 3650(mw), 3635(m), 3059(w), 2990(w), 2940(w), 2920(w), 1706(mw), 1623(w), 1587(w), 1557(w), 1484(m), 1436(s), 1410(ms), 1378(ms), 1318(w), 1293(w), 1225(w), 1189(w), 1132(m), 1092 (ms), 1045(m), 1027(w), 999(w), 839(vs, PF_6^-), 746(m), 699(s), 584(mw), 558(s, PF_6^-), 528(s), 517(ms), 501(s), 464(w), 446(w), 434(w), 301(w).

^{1}H N.M.R. spectrum (CD_3NO_2, 298K) δ = 0.96 (t, J = 7.5 Hz), 1.8–3.5 (m, [9]aneS_3), 6.49(t, J = 2 Hz), 7.35–7.85 (m, PPh_3), 8.26 (d, J = 2 Hz), 8.95 (d, J = 2 Hz) p.p.m.

^{1}H N.M.R.spectrum (d^6-acetone, 298K) δ = 0.97 (t, J = 7.5 Hz), 1.8–3.4 (m, [9]aneS_3), 6.56(t, J = 2 Hz), 7.4–7.85 (m, PPh_3), 8.52 (d, J = 2 Hz), 9.01 (d, J = 2 Hz) p.p.m.

When the ^{1}H N.M.R. spectrum (d^6-acetone) was irradiated at δ = 0.97 p.p.m. the spectrum was the same as above, except the quartet at δ = 2.61 p.p.m. became a singlet.

^{13}C N.M.R.spectrum (Dept) (CD_3NO_2) δ = 7.8, 11.4, 28 – 38([9]aneS_3), 106.1, 127 – 133 (PPh_3), 152.4, 160.1

^{13}C N.M.R.(Dept) spectrum (d^6-acetone) δ = 8.3, 11.4, 13.47 (diethyl ether), 28 – 40 ([9]aneS_3) , 63.1(diethyl ether), 108.1, 127 – 135, 153.5, 162.1 p.p.m.

^{31}P N.M.R.spectrum (CD_3NO_2) δ = –145 (septet, J = 710 Hz, PF_6^-), 34.7, 35.7 p.p.m.

^{31}P N.M.R.spectrum (d^6-acetone) δ = –145 (septet, J = 710 Hz, PF_6^-), 32.2, 33.4 p.p.m.

F.A.B. mass spectrum found m/e = 779, 648, 634, 579, 551, 516;

calculated for $\{RuCl(NCCH_2CH_3)(PPh_3)([9]aneS_3)PF_6\}^+$: 779, $\{RuCl(NOC_3H_3)(PPh_3)([9]aneS_3)\}^+$: 648, $\{RuCl(NCCH_2CH_3)(PPh_3)([9]aneS_3)\}^+$: 634, $\{RuCl(PPh_3)([9]aneS_3)\}^+$: 579, $\{RuCl(PPh_3)(S(CH_2)_2S(CH_2)_2S)\}^+$: 551, $\{Ru(PPh_3)(S(CH_2)_2S(CH_2)_2S)\}^+$: 516.

(ii) The reaction was repeated, but an aliquot of the solution was taken after sixteen hours stirring, filtered and its ^{1}H N.M.R. taken.

^{1}H N.M.R.spectrum (d^6-acetone capillary) δ = 0.96 (t), 122(t), 1.79 (m, THF), 3.62 (m, THF), 4.33 (s, CH_3NO_2), 5.24 (s), 6.5 (t), 7.3–8.0 (m, Ph), 8.26 (d), 8.9 (d) p.p.m.

4.6.2 The crystal structure of $[RuCl(L)((PPh_3)([9]aneS_3)](PF_6)$ (L = $[C_4H_3O]$ or $[NC_3H_3O]$)

A lemon column (0.077 x 0.59 mm) was obtained by recrystallisation from CH_3NO_2/ether.

Crystal data: (a) C–bound furyl complex(L = C_4H_3O); $C_{28}H_{30}ClOPRuS_3^+PF_6^-.CH_3NO_2$, Mwt = 852.22

(b) N–bound isoxazole complex(L = NC_3H_3O);

$C_{27}H_{30}ClOPRuS_3{}^+PF_6{}^-.CH_3NO_2$, Mwt = 854.15

Monoclinic, space group $P2_1/c$, a = 8.5779(12), b = 14.6221(17), c = 27.661(4)Å, β = 93.384(9), V = 3463Å [from 2θ values of 31 reflections measured at ±ω (2θ = 26→30, λ = 71073Å), T = 298K], Z = 4, D_e = 1.638 g cm^{-3}, μ(Mo–K_α) = 0.850 mm^{-1}, F(000) = 1.728.

Data Collection and processing: Stöe Stadi-4 four-circle diffractometer, graphite monochromated Mo–K_α X-radiation (λ = 0.71073Å), ω–2θ scans and the learnt-profile method[288] gave 4694 unique reflections (2θ max 45°, h = -9 →8, k = 0→15, l = 0→29), of which 3167 with $F \geq 4\sigma(F)$ were used in all calculations. A correction for isotropic crystal decay (4.5%) was incorporated in the data reduction.

Structure solution and refinement: following solution by heavy atom methods [330] the structure was refined by full-matrix least-squares on F. The usual disorder in the PF_6^- was modelled by two idealised octahedral with a common P atom: the occupancies of the major and minor components refined to 0.839(12) and 0.161(12) respectively. Two interpenetrating, half-occupied CH_3NO_2 solvent molecules were found in the lattice. Anisotropic thermal parameters were allowed for all non-H atoms except for solvent atoms and those F atoms of the minor disorder component. Non-solvent H atoms were included in fixed, calculated positions[289].

At final convergence, the C–bound furyl solution gave $\omega^{-1} = \sigma^2(F) + 0.000643(F)^2$, R = 0.0477, Rw = 0.0635, S = 1.054 for 379 parameters. For final ΔF synthesis, max and min residues were +0.78 and -0.53$Å^{-3}$.

At final convergence, the N–bound isoxazole solution gave R = 0.0459, Rw = 0.0578, S = 1.053 for 363 parameters and the ΔF synthesis showed no feature above 0.87e$Å^{-3}$. The final weighting scheme $\omega^{-1} = \sigma^2(F) + 0.00045(F)^2$ gave satisfactory agreement analysis and in the final cycle $(\Delta/\sigma)_{max}$ was 0.34.

The figures were prepared using SHELXTL PC[289] and the molecular geometry calculations utilised CALC[290]. Scattering factors were inlaid or taken from Ref. 291.

4.6.3 $[RuCl_2(PPh_3)([9]aneS_3)]$ + $TlPF_6$ in THF

$[RuCl_2(PPh_3)([9]aneS_3)]$ (49 mg, 8.0×10^{-5} M) and $TlPF_6$ (28 mg, 8.0×10^{-5} M) were added to THF (5 cm^3) and stirred for sixteen hours at 298K. The white precipitate of TlCl was removed by filtration through celite, revealing a blue solution. The solvent was removed on a Schlenk line, and a blue solid was isolated (Yield 30 mg), which turns green and then to yellow over three days.

Blue solid

^1H N.M.R.spectrum (d^6-acetone, 298K) δ = 1.8–3.5 (broad, $[9]aneS_3$), 7.2–8.0 (broad, PPh_3) p.p.m.

Ir spectrum $\upsilon(cm^{-1})$: 3654(mw), 3640(broad, m), 3055(w), 2980(mw), 2940(w), 2920(vw), 1764(ms), 1711(broad, m), 1615(s), 1572(s), 1486(m), 1432(s), 1410(ms), 1378(ms), 1318(w), 1295(w), 1225(w), 1189(m), 1122(s), 1092 (m), 1045(m), 1027(w), 999(w), 839(vs, PF_6^-), 748(m), 699(s), 586(mw), 558(vs, PF_6^-), 526(s), 517(ms), 510(s), 499(ms), 464(w), 446(vw)

F.A.B. Mass Spectrum found m/e = 836, 725, 644, 631, 594, 550, 530;
calculated for $\{RuCl(PPh_3)(O)([9]aneS_3)\}^+$: 594, $\{RuCl(PPh_3)(S(CH_2)_2S(CH_2)_2S)–H\}^+$: 550.

Light green/yellow compound (on prolonged exposure to air the solid turns green/yellow. In solution, the blue colouration rapidly turns green, and then slowly to yellow).

^1H N.M.R.spectrum (d^6-acetone, 298K) δ = 1.6–3.6 (v broad), 7.0–8.0 (v broad) p.p.m.

Ir spectrum $\upsilon(cm^{-1})$: 3650(mw, broad), 3050(w), 2980(w), 1760(broad, m), 1710(v broad, m), 1610(broad, m), 1570(broad, m), 1486(mw), 1432(m), 1410(mw), 1378(m), 1189(w), 1120(m), 1090(mw), 1045(w), 839(vs, PF_6^-), 749(mw), 699(m), 585(w), 555(s, PF_6^-), 526(m), 517(m), 510(mw), 499(mw).

F.A.B. Mass Spectrum found m/e = 363

F.A.B. Mass Spectrum(DMF/THIOGLYCEROL) found m/e = 363;
calculated for $\{Ru(PPh_3)\}^{+}$: 363

4.6.4 $[RuCl_2(PPh_3)([9]aneS_3)]$ + $TlPF_6$ in CH_3NO_2 and DHF or Furan

(i) $[RuCl_2(PPh_3)([9]aneS_3)]$ (51 mg, 8.3×10^{-5} M) was added to $TlPF_6$ in CH_3NO_2(4 cm^3) and 2,3- or 2,5- dihydrofuran (1 cm^3) and stirred at 298K for sixteen hours. The white precipitate was removed by filtration through celite, and the yellow solution was rotary evaporated to dryness; a light yellow sticky solid was found.

The solid was dissolved in acetone, and a light white solid was filtered and discarded, leaving a yellow solution which was evaporated to near dryness, and hexane added and the yellow precipitate collected and dried (Yield = 43 mg). The results were similar to 4.6.1.

(ii) The reaction was repeated as (i) above, except that Furan (1 cm^3, 6 µl, 18 µl, or 36 µl) was used. The results were also similar to (i) above, except that a light green sticky solid was formed. A yellow solid was obtained from recrystallisation in acetone/hexane. The results were similar to 4.6.1.

(iii) $[RuCl_2(PPh_3)([9]aneS_3)]$ (50 mg, 8.1×10^{-5} M) and $TlPF_6$ (29, 8.3×10^{-5} M) were added to 2,3- or 2,5- dihydrofuran(5 cm^3), a yellow solution formed on reducing the solvent, a yellow 'sticky' solid formed (Yield 0.75 g)
F.A.B. Mass Spectrum found m/e = 1122, 1052, 982, 911, 841, 771, 701, 631, 561, 491, 421, 351, 281, 211, 141 and 72

4.6.5 $[RuCl_2(PPh_3)([9]aneS_3)]$+ $TlPF_6$ in CH_3NO_2 andTHF

$[RuCl_2(PPh_3)([9]aneS_3)]$ (50 mg, 8.2×10^{-5} M) was added to CH_3NO_2 : THF (5 cm^3, 4 : 1 v/v) in the presence of a stoichiometric amount of $TlPF_6$ (29 mg, 8.3×10^{-5} M) and stirred for sixteen hours at 298K. The white precipitate of TlCl was then removed by filtration through celite, and the yellow solution rotary evaporated to dryness. The resulting yellow solid was transferred using excess acetone and care was taken to make sure ALL the solid was completely dissolved.

The acetone was then removed by evaporation. N.M.R. solutions were made by adding the yellow solid to the deuteurated solvent, ensuring that the solid had entirely dissolved. No excess solid was added and no filtration was required. None of these solutions were recrystallised.

The ir, ^{1}H N.M.R., ^{31}P N.M.R. and F.A.B. mass spectra were similar to 4.6.1, except that the relative integrals in the ^{1}H N.M.R. and the relative intensities of the ^{31}P N.M.R. resonances varied.

4.6.6 $[RuCl_2(PPh_3)([9]aneS_3)]$ + $TlPF_6$ in distilled CH_3NO_2 andTHF

The nitromethane used in (i) above (same batch and bottle) was purified by refluxing 450 cm^3 with activated charcoal under N_2 for twenty-four hours, and then filtering off the black charcoal. The clear solution was then distilled and the azeotrope (CN_3NO_2/H_2O) at 83° C was discarded and only the fraction at 100–102° C collected. This clear solution was then passed down a dry alumina column, and redistilled (again discarding the azeotrope at 83° C, and only collecting the fraction at 100–102° C). Finally, it was stored over dry CH_2Cl_2 and redistilled before use (yield ≈50%). This distilled nitromethane was then used in the reaction described in 4.6.5. The results were also similar to 4.6.1 above.

4.6.7 Other Factors Affecting the Reaction of $[RuCl_2(PPh_3)([9]aneS_3)]$ with $TlPF_6$

The reaction described in Table 4.8 were carried out as shown in Section 4.6.5. A control reaction was usually carried out in the same manner as 4.6.5, using the same solvents and at the same time as the other reactions. These are also indicated in Table 4.8.

Table 4.8 Experimental Conditions for the Reaction of $[RuCl_2(PPh_3)([9]aneS_3)]$ with $TlPF_6$

$[RuCl_2(PPh_3)([9]aneS_3)]$ added		$TlPF_6$ added		CH_3NO_2 added	THF added	Notes	Product
mg	(x 10^{-5} M)	mg	(x 10^{-5} M)	cm^3	cm^3		
50	(8.1)	28	(8.0)	4	1	Heated to 40° C	A
50	(8.1)	28	(8.0)	4	1	Reaction vessel covered in foil	A
49	(7.9)			4	1	24 mg $TlBF_4$ (8.3 x 10^{-5}M	B
50	(8.1)			4	1	21 mg $AgPF_4$ (8.3 x10^{-5}M	A
52	(8.5)	50	(14.3)	4	1		A
51	(8.3)	500	(143)	4	1		A
51	(8.3)	29	(8.3)	3	2		A
51	(8.3)	28	(8.0)	1	4		A
49	(7.9)	29	(8.3)	5	0.006		A
50	(8.1)	29	(8.3)	5	0.012		A
51	(8.3)	28	(8.0)	5	0.018		A
51	(8.3)	29	(8.3)	4	1	Under N_2 using Schlenk techniques	A
51	(8.3)	30	(8.6)	4	1	Compressed air bubbled through	A
51	(8.3)	28	(8.0)	4	1	Open to atmosphere. Workup using Schlenk techniques	A
50	(8.1)	28	(8.0)	4	1	Aldrich CH_3NO_2	C
51	(8.3)	28	(8.0)	4	1	Purified‡ Aldrich CH_3NO_2	D
49	(7.9)	28	(8.0)	4	1	Prolabo CH_3NO_2	A
50	(8.1)	29	(8.3)	4	1	Purified‡ Prolabo CH_3NO_2	D

Notes

Product A Ir, ^1H N.M.R., ^{31}P N.M.R. and F.A.B. mass spectra are similar to 4.6.5

Product B as product A except that no PF_6^- resonance was observed in the ^{31}P N.M.R. spectrum at δ = -145 p.p.m., nor ir peaks at 835 and 555 cm^{-1}. An extra stretch in the infrared spectrum is seen at ν = 1000 - 1150 cm^{-1}

Product C Ir spectrum $\upsilon(cm^{-1})$: 3650(mw), 3635(m),2940(m), 1484(m), 1436(s), 1410(ms), 1378(ms), 1132(m), 1092 (ms), 1045(m), 839(vs, PF_6^-), 746(m), 699(s), 583(mw), 556(s, PF_6^-), 527(s), 515(ms), 499(s), 303(w).

^1H N.M.R.spectrum (d^6-acetone, 298K) δ = 0.97 (t, J = 7.5 Hz), 1.8–3.4 (m, [9]aneS$_3$), , 7.4–7.85 (m, PPh_3) p.p.m.

^{31}P N.M.R.spectrum (d^6-acetone) δ = –145 (septet, J = 710 Hz, PF_6^-), 33.4 p.p.m.

F.A.B. mass spectrum found m/e = 779, 634, 579, 551, 516;

calculated for $\{RuCl(NCCH_2CH_3)(PPh_3)([9]aneS_3)PF_6\}^+$: 779, ,

$\{RuCl(NCCH_2CH_3)(PPh_3)([9]aneS_3)\}^+$: 634, $\{RuCl(PPh_3)([9]aneS_3)\}^+$: 579,

$\{RuCl(PPh_3)(S(CH_2)_2S(CH_2)_2S)\}^+$: 551, $\{Ru(PPh_3)(S(CH_2)_2S(CH_2)_2S)\}^+$: 516.

Product D Ir, ^1H N.M.R., ^{31}P N.M.R. and F.A.B. mass spectra as Section 3.4.1

‡ Purified by adding dry ice to 450 cm^3 CH_3NO_2 and 500 cm^3 ether till it was at -60°, filtering with a cold funnel (packed with dry ice), discarding the solution, and allowing the crystalline CH_3NO_2 to thaw. Distillation of the thawed CH_3NO_2, removing the CH_3NO_2 /H_2O azeotrope, and keeping the fraction at 100–102° C. This was repeated four times, before use (Yield 75 cm^3, 17%).

4.6.8 $[RuCl_2(PPh_3)([9]aneS_3)]$ + $TlPF_6$ in RNO_2 and THF

The reaction was carried out as descrided in 4.6.5, except that RNO_2 (4 cm^3, R= Et, Ph) was used instead of CH_2Cl_2 and the results were also similar to the complexes, $[Ru(PPh_3)([9]aneS_3)(\mu\text{-}Cl)]_2(PF_6)_2$ and $[Ru(PPh_3)([9]aneS_3)(\mu\text{-}Cl)_2Tl]_2(PF_6)_2$ discussed in Chapter 3

4.6.9 $[RuCl_2(PPh_3)([9]aneS_3)]$ + $TlPF_6$ in d^8–THF and CH_3NO_2

(i) $[RuCl_2(PPh_3)([9]aneS_3)]$ (35 mg, 5.7×10^{-5} M) was added to $TlPF_6$ (20 mg, 5.7×10^{-5} M) in d^8–THF (0.5 cm^3) andCH_3NO_2(2.5cm^3). The solution was stirred for sixteen hours at 298K, filtered through celite and reduced in volume to dryness. (Yield = 28 mg).

The results were similar to 4.6.6 and are shown in Table 4.15.
^2D N.M.R. spectrum (CH_3NO_2) δ = 4.33 ($CH_xD_yNO_2$) p.p.m.

(ii) A mixture of 0.2 cm^3 d^8–THF and 0.8 cm^3 CH_3NO_2 was left in a N.M.R. tube for two days.

^1H N.M.R. spectrum (d^8–THF) δ = 4.33. (CH_3NO_2) p.p.m.
^2D N.M.R. spectrum (CH_3NO_2) δ = 1.6 (s), 3.5 (s). (d^8–THF) p.p.m

(iii) A mixture of 0.2 cm^3 THF and 0.8 cm^3 CH_3NO_2 was left in an N.M.R. tube for fourteen days

^1H N.M.R. spectrum (CD_3NO_2) δ = 1.8 (m), 3.7 (m) (THF) p.p.m.
^2D N.M.R. spectrum (THF) δ = 4.31 (CD_3NO_2) p.p.m.

(iv) The product from the reaction 4.6.6 was dissolved in CD_3NO_2 (composition Furyl = 40% Ethyl = 45% composition) and left in solution for eight days. Its ^1H and ^{31}P N.M.R.spectra did not show any change.

The sample was then refluxed for 2 days. Its ^1H N.M.R. spectrum (CD_3NO_2) did not show any change. The sample then was then evaporated to dryness, dissolved in CH_3NO_2, and its ^2D spectrum taken immediately.

^2D N.M.R. spectrum δ = 4.33 (s) CD_3NO_2) p.p.m.

4.6.10 $[RuCl_2(PPh_3)([9]aneS_3)]$ + $TlPF_6$ in CD_3NO_2 and THF (d^8 or Normal)

(i) $[RuCl_2(PPh_3)([9]aneS_3)]$ (36 mg, 5.9×10^{-5} M) was added $TlPF_6$ (20 mg, 5.7×10^{-5} M) $TlPF_6$ THF (0.5 cm^3, d^8 or Normal) and CH_3NO_2 (1 cm^3), the sample was stirred for sixteen hours, and then filtered through celite to remove the TlCl, and the dark yellow solution was rotary evaporated to dryness. The resulting light orange solid was similar to the one described in Chapter 3, that contained $[Ru(PPh_3)([9]aneS_3)(\mu\text{-}Cl)]_2(PF_6)_2$ and $[Ru(PPh_3)([9]aneS_3)(\mu\text{-}Cl)_2Tl]_2(PF_6)_2$.

4.6.11 Synthesis of $[RuCl(NCCH_2CH_3)(PPh_3)([9]aneS_3)]PF_6$

$[RuCl_2(PPh_3)([9]aneS_3)]$ (75 mg, 1.2×10^{-4} M) and 45 mg (1.3×10^{-4} M) $TlPF_6$ was added to propionitrile (5 cm^3) and stirred for sixteen hours. The white precipitate of TlCl was removed by filtration through celite, and the yellow solution was reduced to dryness and recrystallised from acetone/hexane.

Ir spectrum $\upsilon(cm^{-1})$: 3050(w), 2940(w), 2920(w), 2212(w), 1730(w), 1587(w), 1555(mw), 1482(m), 1433(ms), 1408(m), 1380(w), 1310(w), 1225(vw), 1189(mw), 1092 (ms), 1045(m), 999(mw), 839(vs, PF_6^-), 746(m), 699(ms), 555(s, PF_6^-), 528(ms), 517(ms), 499(ms), 464(w), 446(w), 434(w), 301(w).

F.A.B. Mass Spectrum found m/e = 779, 634, 579, 551;

calculated for $\{RuCl(NCCH_2CH_3)(PPh_3)([9]aneS_3)PF_6\}$: 779, $\{RuCl(NCCH_2CH_3)(PPh_3)([9]aneS_3)\}$: 634, $\{RuCl(PPh_3)([9]aneS_3)\}$: 579, $\{RuCl(PPh_3)(S(CH_2)_2S(CH_2)_2S)\}$: 551

^1H N.M.R.spectrum (CD_3NO_2) δ = 0.97 (t, J = 7 Hz), 1.8–3.2 (m, $[9]aneS_3$), 2.73(t, J = 7 Hz), 7.2–8.0 (m, PPh_3) p.p.m.

^{31}P N.M.R.spectrum (CD_3NO_2) δ = –145 (PF_6^{-1}, J = 710 Hz), 35.8 p.p.m.

^{13}C N.M.R.spectrum (Dept) (CD_3NO_2) δ = 7.9(+), 11.5(–), 28 – 35 ($[9]aneS_3$), 126 – 133 (PPh_3) p.p.m.

^{13}C N.M.R. spectrum (CD_3NO_2) δ = as DEPT except extra resonance at 207 p.p.m.

4.6.12 Synthesis of $[[RuCl(NC_3H_3O)(PPh_3)([9]aneS_3)]PF_6$

$[RuCl_2(PPh_3)([9]aneS_3)]$ (70 mg, 1.1×10^{-4} M) and $TlPF_6$ (43 mg, 1.2×10^{-4} M) was added to isoxazole (5 cm^3) and stirred for sixteen hours. The white precipitate of TlCl was removed by filtration through celite, and the yellow solution was reduced to dryness and recrystallised from acetone/hexane.

Ir spectrum $\upsilon(cm^{-1})$: 3630(mw), 3059(mw), 2990(mw), 2940(mw), 1708(mw), 1587(w), 1625(mw), 1587(w), 1557(w), 1482(m), 1435(s), 1410(ms), 1132(m), 1090 (ms), 1045(m), 1027(vw), 999(mw), 839(vs, PF_6^-), 746(m), 699(s), 584(mw),558(s, PF_6^-) 434(w), 305(w).

F.A.B. mass spectrum found m/e = 648, 579, 551;

calculated for $\{RuCl(N(CH_2)_3O)(PPh_3)([9]aneS_3)\}^+$: 634, $\{RuCl(PPh_3)([9]aneS_3)\}$: 579, $\{RuCl(PPh_3)(S(CH_2)_2S(CH_2)_2S)\}^+$: 551.

^1H N.M.R.spectrum (CD_3NO_2) δ = 1012 (t, J = 7.5 Hz), 1.8–3.5 (m, $[9]aneS_3$), 3.36 (q), 6.49 (t, J = 2 Hz), 7.2–8.0 (m, PPh3). 8.25 (q, J = 2 Hz), 8.59 (d, wk), 8.95 (J = 2 Hz) p.p.m.

^{13}C N.M.R.spectrum (Dept) (CD_3NO_2) δ = 13.5(Et_2O), 28. - 37 ($[9]aneS_3$), 64.5(Et_2O), 106.2, 127 – 133 (PPh_3), 152.4, 160.1 p.p.m.

^{31}P N.M.R.spectrum (CD_3NO_2) δ = –145 (septet, J = 710 Hz, PF_6^-,)

4.6.13 Attempted synthesis of ^{13}C labelled THF

$K^{13}CN$ was purchased from Aldrich. The synthesis of 1,4 Succinic acid from KCN and ethylene bromide was performed as Ref. 333. The esterification with ethanol, and reduction by $LiAlH_4$ of the 1,4 succinic acid to form the 1,4 butanediol was carried out as described in Ref. 334. The results were identical to those described in the literature.

The unsuccessful condensation of the 1,4 butanediol was carried out in DMSO at 160° C[335].

4.6.14 The reaction of $[Ru(PPh_3)([9]aneS_3)(\mu\text{-}Cl)]_2(PF_6)_2$ with CH_3NO_2 and THF

$[Ru(PPh_3)([9]aneS_3)(\mu\text{-}Cl)]_2(PF_6)_2$ (40 mg, 0.028 mM) was added to CH_3NO_2 and THF (4 : 1 v/v, 5 cm^3) and stirred for 18 hours. The resulting yellow solution was reduced in volume to dryness. (Yield 30 mg).

Ir spectrum $\upsilon(cm^{-1})$: 3050(m), 2985(ms), 2940(mw), 2920(w), 1620(m), 1586(w), 1552(w), 1482(ms), 1435(s), 1410(ms), 1377(w), 1315(w), 1295(ms), 1225(mw), 1188(mw), 1090(s), 1047 (mw), 1028(m), 1000(m), 942(m), 910(m), 840(vs, PF_6^-), 785(br, m), 751(m), 700(ms), 580(ms), 517(ms), 558(s, PF_6^-), 528(ms), 517(ms), 501(ms), 468 (mw).

^1H N.M.R.spectrum (d^6-acetone) δ = 0.98 (t, ^3J_H = 7.5 Hz), 1.28 (s), 2.55 (q, ^3J_H = 7.5 Hz), 1.50–3.30 (m), 6.50 (t, ^3J_H = 2 Hz), 7.2–8.0 (m), 8.51 (d, ^3J_H = 2 Hz), 8.95 (d, ^3J_H = 2 Hz) p.p.m.

^{31}P N.M.R. spectrum (d^6-acetone) δ = 33.3, 32.2 + –145 (septet, J = 710 Hz, PF_6^-) p.p.m.

F.A.B. mass spectrum found m/e = 779, 648, 634, 614, 579, 551

Chapter 5

SYNTHESIS OF HALF SANDWICH Ru(II) COMPLEXES WITH [9]aneS$_3$ AND SULFUR AND NITROGEN ANALOGUES OF FURAN AND THF

5.1 Introduction

Pyrrole, thiophene, pyrrolidine and tetrahydrothiophene (THT) are N and S analogues of the five-membered heterocycles, furan and THF (Figure 5.1)[336-343] and can co-ordinate to metal ions via the lone pairs on the heteroatoms[221, 344]. The unsaturated heterocycles, furan, thiophene and pyrrole can also co-ordinate to metals through their C=C[221, 344, 345]. Thus, the complex $[Os(NH_3)_5(2,3\text{–}\eta^{*2}\text{–pyrrole})]^{2+}$ has recently been reported (Figure 5.2)[346].

Figure 5.1 Five Membered Heterocycles

Figure 5.1 Five Membered Heterocycles

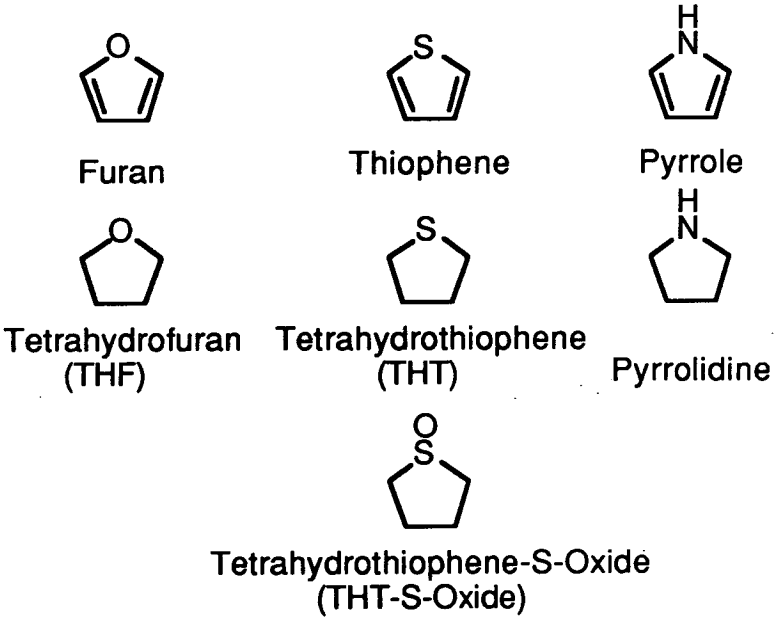

Relatively few S–bound thiophene complexes have been synthesised[345], since they usually co-ordinate to metals by their C=C bonds in a η^2, η^4, or η^5– manner (Figure 5.3)[345]. In 1985, the first structurally characterised S–bound thiophene complex, $[\{(C_4H_3S)CH_2Cp\}Ru(PPh_3)_2]^+$ was reported (Figure 5.4)[347].

Recently, the novel base hydrolysis of a co-ordinate thiophene in $[Cp^*Rh(C_4Me_4S)]^{2+}$ to form a furan (C_4Me_4O) and $[Cp^*RhS]_4$ has been reported. The proposed mechanism is shown in Scheme 5.1[348].

Porphyrin (polypyrrole) complexes have been discussed in Chapter 1.

Figure 5.2 A Representation of $[Os(NH_3)_5(2,3\text{–}\eta^{*2}\text{–pyrrole})]^{2+}$

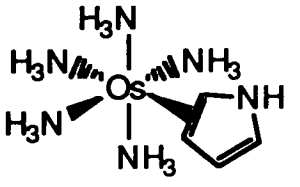

Figure 5.3 Possible Modes of Co-ordination of Thiophene

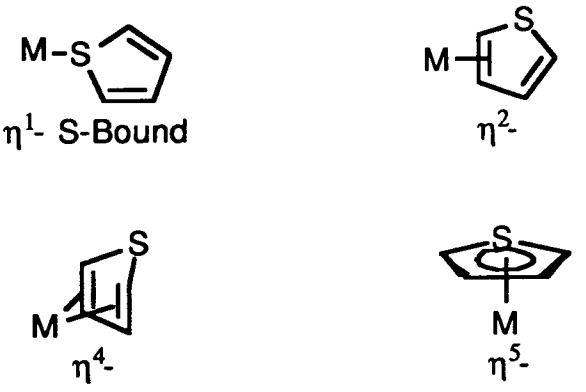

Figure 5.4 A Representation of $[\{(C_4H_3S)CH_2Cp\}Ru(PPh_3)_2]^+$

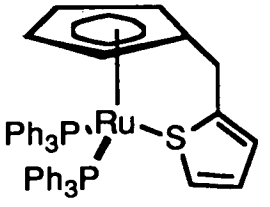

Scheme 5.1 The Conversion of Thiophene to Furan by $[Cp^*Rh(C_4Me_4S)]^{2+}$

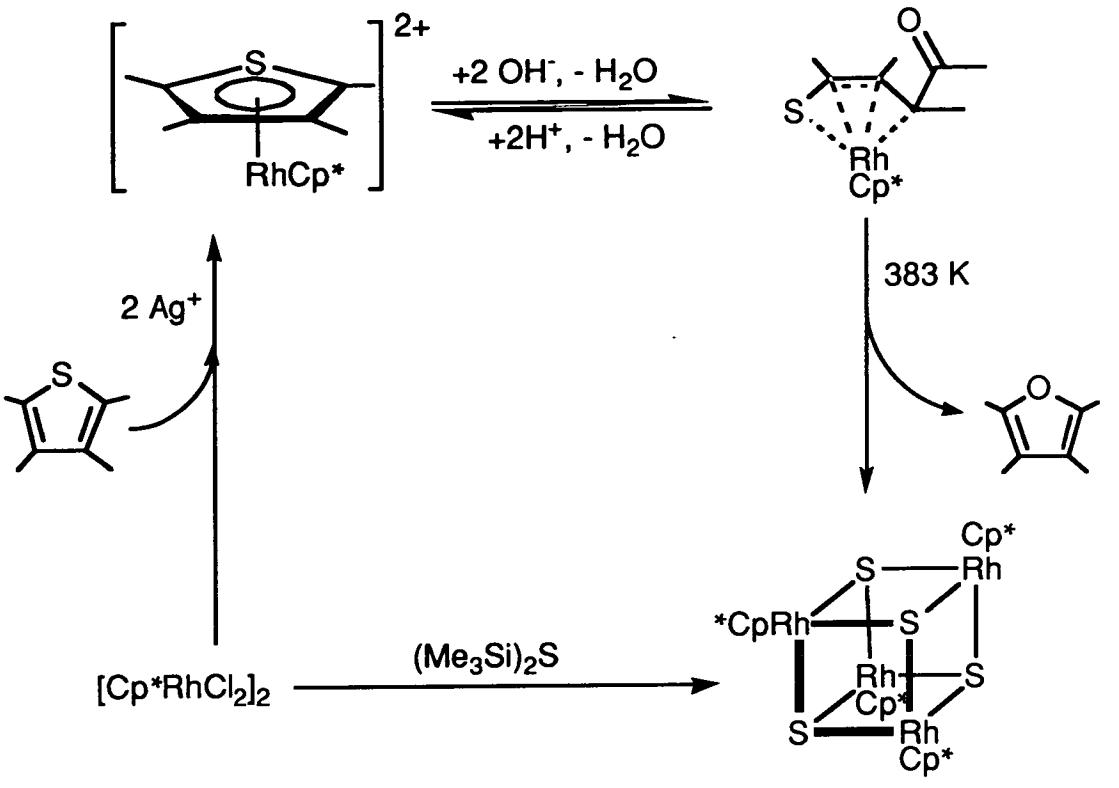

The reaction of $[RuCl_2(PPh_3)([9]aneS_3)]$ with $TlPF_6$ in CH_3NO_2 in the presence of THF or Furan was discussed in Chapter 4. This chapter extends this work to S and N heteroaromatic analogues of THF and furan. Originally this work was intended to help elucidate a possible mechanism for the formation of the C–bound furyl complex, $[RuCl(C_4H_3O)(PPh_3)([9]aneS_3)]$. The reaction of $[RuCl_2(PPh_3)([9]aneS_3)]$ with $TlPF_6$ with S and N heterocycles is also of interest, because of the possible formation of η^1, η^2, η^4 or η^5 complexes or the possible formation of C–bound heterocyclic complexes.

5.2 Results and Discussion

5.2.1 The Reaction of $[RuCl_2(PPh_3)([9]aneS_3)]$ with $TlPF_6$ and Thiophene and THT

The reaction of $[RuCl_2(PPh_3)([9]aneS_3)]$ and $TlPF_6$ with thiophene in CH_2Cl_2 affords a white precipitate of TlCl and a yellow solution. Filtration and evaporation of the solution to dryness results in yellow solid, which can be recrystallised from acetone/hexane. The ir spectrum of the product indicates that $[9]aneS_3$, PPh_3 and PF_6^- are all present and the ^1H N.M.R. spectrum (d^6-acetone) confirms the presence of $[9]aneS_3$ and PPh_3 with resonances at δ = 1.5–3.5 (m, $[9]aneS_3$) and 7.2–7.8 (m, PPh_3) p.p.m. The ^{31}P N.M.R. (d^6-acetone) spectrum exhibits resonances at δ = +33.5, +32.8 and -145 (septet, J = 710 Hz, PF_6^-) p.p.m. indicating that the Ru dimer $[Ru(PPh_3)([9]aneS_3)(\mu\text{-}Cl)]_2(PF_6)_2$ and the RuTl ladder species, $[Ru(PPh_3)([9]aneS_3)(\mu\text{–}Cl)_2Tl]_2(PF_6)_2$ are also present. This is confirmed by F.A.B. mass spectroscopy, which shows peaks at m/e = 819, 716, 614 and 579, which can be assigned to $\{Ru(PPh_3)([9]aneS_3)(\mu\text{-}Cl)_2Tl\}^+$, $\{Ru_2(PPh_3)([9]aneS_3)(\mu\text{-}Cl)\}^+$, $\{RuCl_2(PPh_3)([9]aneS_3)\}^+$ and $\{RuCl(PPh_3)([9]aneS_3)\}^+$ respectively. A similar mixture of products can be isolated from the reaction of $[RuCl_2(PPh_3)([9]aneS_3)]$ and $TlPF_6$ in the presence of thiophene in CH_3NO_2 . The spectral data for this product is nearly identical to the solid which is isolated from the CH_2Cl_2 solvent. The only differences are an extra resonance at δ = 0.97(t) in the ^1H N.M.R. (d^6-acetone) spectrum, and an extra signal at m/e = 634 in the F.A.B. mass spectrum in 3-NOBA, indicating that $[RuCl(NCCH_2CH_3)(PPh_3)([9]aneS_3)](PF_6)$ is also present (See Chapter 4).

Thus, the reaction of $[RuCl_2(PPh_3)([9]aneS_3)]$ with $TlPF_6$ in the presence of thiophene results in a mixture of the Ru dimer, $[Ru(PPh_3)([9]aneS_3)(\mu\text{–}Cl)]_2^{2+}$ and the RuTl ladder, $[Ru(PPh_3)([9]aneS_3)(\mu\text{–}Cl)_2Tl]_2^{2+}$, indicating that thiophene does not have sufficient co-ordinating ability to prevent dimerisation.

The addition of $TlPF_6$ to $[RuCl_2(PPh_3)([9]aneS_3)]$ in either CH_3NO_2 or CH_2Cl_2 in the presence of tetrahydrothiophene (THT) affords a yellow solution and a white precipitate of TlCl. Removal of TlCl and the solvent, followed by recrystallisation of the residue from acetone/hexane affords a bright yellow solid, the ir spectrum of which indicates that PF_6^-, PPh_3 and $[9]aneS_3$ are present. The ^1H N.M.R. spectrum (d^6-acetone) of this product shows resonances at δ = 2.0–3.5 (m) and 7.25–8.0 (m, PPh_3) p.p.m and the ^{31}P N.M.R. spectrum (d^6-acetone) exhibits resonances at δ = 27.2 and -145 (septet, J = 710 Hz, PF_6^-) p.p.m. The F.A.B. mass spectrum reveals signals at m/e = 812, 667, 579 and 551, which can be assigned to $\{RuCl(PPh_3)(THT)([9]aneS_3)PF_6\}^+$, $\{RuCl(PPh_3)(THT)([9]aneS_3)\}^+$ and $\{RuCl(PPh_3)([9]aneS_3)\}^+$ respectively, suggesting that the complex $[RuCl(PPh_3)(THT)([9]aneS_3)](PF_6)$ has been synthesised. To confirm this, crystals suitable for X-ray analysis were grown by vapour diffusion of hexane into d^6-acetone.

5.2.2 The crystal structure of $[RuCl(PPh_3)(THT)([9]aneS_3)](PF_6)$

The single crystal X-ray structure of $[RuCl(PPh_3)(THT)([9]aneS_3)](PF_6)$ shows the $[9]aneS_3$ ligand to be facially bound to an octahedral Ru(II) centre [$Ru\text{-}S_{([9]aneS_3)}$ = 2.3636(14), 2.3150(13) and 2.3335(13)Å] . The co-ordination shell is completed by a Cl^- donor [Ru-Cl = 2.4148(12)Å] , a PPh_3 ligand [Ru-P = 2.3575(13)Å] and a THT ligand [Ru-S = 2.3700(14)Å] (see Figure 5.5 and Table 5.1). Interestingly, the co-ordinated THT has been partially oxidised to a sulfoxide. The occupancy of the O on the sulfur was refined to 50%, indicating that **in the crystal structure** there is a 1 : 1 mixture of the THT complex, $[RuCl(PPh_3)(THT)([9]aneS_3)](PF_6)$ and the THT–S–Oxide complex, $[RuCl(PPh_3)(THT\text{–}S\text{–}Oxide)([9]aneS_3)](PF_6)$. The two species could not be distinguished crystallographically, and therefore the bond lengths and angles obtained are an average of the two complexes. The thermal parameters for the carbons in the heterocycle are only slightly larger than the carbons in the

[9]aneS$_3$ or PPh$_3$ ligands (Table 5.2). This suggests that the conformation of the heterocycle does not significantly alter, when it is oxidised from a thioether to a sulfoxide. This contrasts with the change in conformation when free [9]aneS$_3$ is oxidised to O$_6$[9]aneS$_3$ (See Chapter 7).

The sulfoxide is not formed during the reaction of [RuCl$_2$(PPh$_3$)([9]aneS$_3$)] with TlPF$_6$ in either CH$_3$NO$_2$ or CH$_2$Cl$_2$ in the presence of THT, since the ir, ^{1}H N.M.R., ^{31}P N.M.R. and F.A.B. mass spectra do not contain any features attributable to the sulfoxide **before** the crystals were grown by vapour diffusion. However, **after** vapour diffusion, the product shows an extra band at υ = 1048(m) cm^{-1} in the ir spectrum, which can be assigned as a υ_{SO} sulfoxide stretch. Furthermore, after recystallisation of the product, the ^{31}P N.M.R. spectrum shows two resonances at δ = 27.2 and 23.7 p.p.m. in the PPh$_3$ region while the F.A.B. mass spectrum shows an extra signal at m/e = 683, assignable as {Ru(THT–S–Oxide)Cl(PPh$_3$)([9]aneS$_3$)]}$^+$, **thus indicating that the sulfoxide must form during the crystal growth by vapour diffusion** (see Scheme 5.2).

Scheme 5.2 The Reaction of [RuCl$_2$(PPh$_3$)([9]aneS$_3$)] with TlPF$_6$ and THT

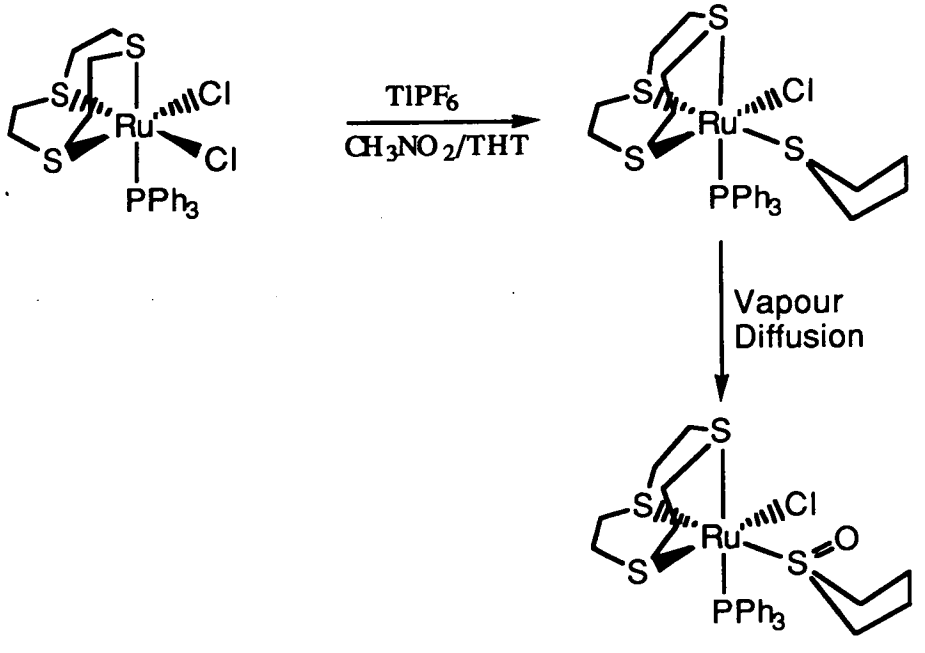

Figure 5.5 The Single Crystal X-Ray Structure of $[RuCl(C_4H_8S)(PPh_3)([9]aneS_3)](PF_6)$

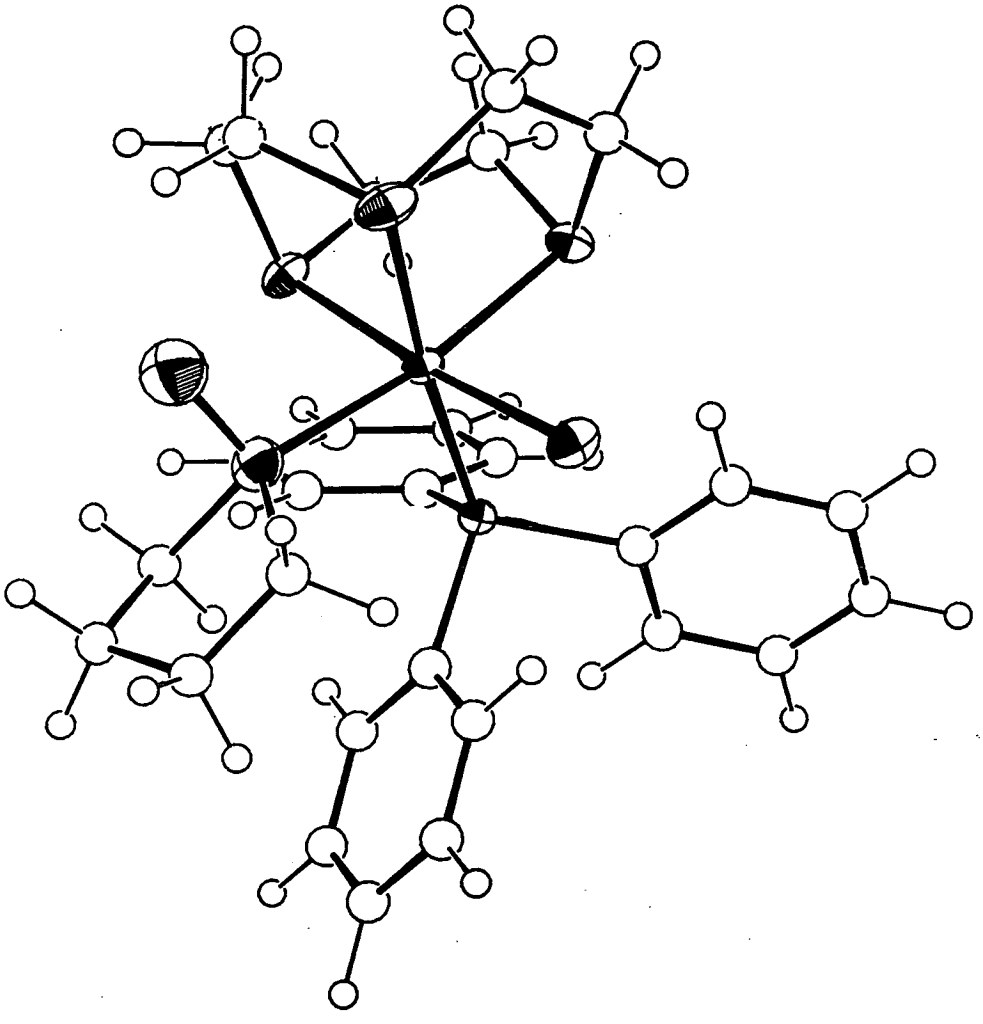

Table 5.1 Selected Bond Lengths (Å), Angles (°) and Torsion Angles (°) with standard deviations for $[RuCl(PPh_3)(THT)([9]aneS_3)](PF_6)$

Ru–Cl	2.4148(12)	C(6)–S(7)	1.846(6)
Ru–S(1)	2.3636(14)	S(7)–C(8)	1.818(7)
Ru–S(4)	2.3150(13)	C(8)–S(9)	1.440(11)
Ru–S(7)	2.3335(13)	S–O	1.495(8)
Ru–S	2.3700(14)	S–C(1t)	1.802(7)
Ru–P(1)	2.3573(12)	S–C(4t)	1.813(7)
S(1)–C(2)	1.828(8)	C–(1t)–C(2t)	1.538(10)
S(1)–C(9)	1.821(8)	C–(2t)–C(3t)	1.469(11)
C(2)–C(3)	1.417(10)	C–(3t)–C(4t)	1.502(10)
C(3)–S(4)	1.840(6)	P(1)–C(11)	1.843(3)
S(4)–C(5)	1.825(6)	P(1)–C(21)	1.843(3)
C(5)–C(6)	1.470(8)	P(1)–C(31)	1.855(3)

Cl–Ru–S(1)	85.92(5)	C(3)–S(4)–C(5)	99.2(3)
Cl–Ru–S(4)	173.14(4)	S(4)–C(5)–C(6)	114.5(4)
Cl–Ru–S(7)	91.03(4)	C(5)–C(6)–S(7)	114.1(4)
Cl–Ru–S	90.75(5)	Ru–S(7)–C(6)	105.81(19)
Cl–Ru–P(1)	89.62(4)	Ru–S(7)–C(8)	103.01(22)
S(1)–Ru–S(4)	87.36(5)	C(6)–S(7)–C(8)	100.4(3)
S(1)–Ru–S(7)	86.89(5)	S(7)–C(8)–C(9)	116.5(5)
S(1)–Ru–S	83.51(5)	S(1)–C(9)–C(8)	115.9(6)
S(1)–Ru–P(1)	174.51(5)	Ru–S–O	110.5(3)
S(4)–Ru–S(7)	87.23(5)	Ru–S–C(1t)	120.46(22)
S(4)–Ru–S	89.86(5)	Ru–S–C(4t)	119.95(21)
S(4)–Ru–P(1)	97.01(4)	O–S–C(1t)	106.4(4)
S(7)–Ru–S	170.08(5)	O–S–C(4t)	103.4(4)
S(7)–Ru–P(1)	89.99(4)	C(1t)–S–C(4t)	93.7(3)
S–Ru–P(1)	99.78(5)	S–C(1t)–C(2t)	103.0(5)
Ru–S(1)–C(2)	103.33(24)	C(1t)–C(2t)–C(3t)	108.6(6)
Ru–S(1)–C(9)	105.2(3)	C(2t)–C(3t)–C(4t)	111.8(7)
C(2)–S(1)–C(9)	102.2(4)	S–C(4t)–C(3t)	107.3(5)
S(1)–C(2)–C(3)	118.2(5)	Ru–P(1)–C(11)	112.72(10)
C(2)–C(3)–S(4)	116.7(5)	Ru–P(1)–C(21)	118.04(11)
Ru–S(4)–C(3)	106.43(19)	Ru–P(1)–C(31)	118.61(10)
Ru–S(4)–C(5)	105.18(19)		

C(9)–S(1)–C(2)–C(3)	78.6(6)	S(7)–C(8)–C(9)–S(1)	38.3(8)
C(2)–S(1)–C(9)–C(8)	-125.1(6)	O–S–C(1t)–C(2t)	-73.1(6)
S(1)–C(2)–C(3)–S(4)	31.6(7)	C(4t)–S–C(1t)–C(2t)	32.0(5)
C(2)–C(3)–S(4)–C(5)	-124.5(5)	O–S–C(4t)–C(3t)	92.4(6)
C(3)–S(4)–C(5)–C(6)	73.7(5)	C(1t)–S–C(4t)–C(3t)	-15.5(5)
S(4)–C(5)–C(6)–S(7)	41.3(6)	S–C(1t)–C(2t)–C(3t)	-41.3(7)
C(5)–C(6)–S(7)–C(8)	-132.2(5)	C(1t)–C(2t)–C(3t)–C(4t)	32.0(8)
C(6)–S(7)–C(8)–C(9)	70.7(6)	C(2t)–C(3t)–C(4t)–S	-7.2(8)

Table 5.2 Anisotropic Thermal Parameters in Å^2 for [RuCl(PPh$_3$)(THT)([9]aneS$_3$)](PF$_6$)

Atom	U_{11}	U_{22}	U_{33}	U_{23}	U_{13}	U_{12}
Ru	0.01877(23)	0.01752(23)	0.01545(22)	-0.0063(15)	0.00353(16)	-0.00232(15)
Cl	0.0251(6)	0.0301(7)	0.0257(6)	-0.0026(5)	-0.0003(5)	-0.0078(5)
S(1)	0.0395(7)	0.0272(7)	0.0285(7)	0.0063(6)	0.0037(6)	-0.0089(6)
C(2)	0.084(5)	0.056(5)	0.072(5)	0.034(4)	-0.44(4)	-0.019(4)
C(3)	0.041(3)	0.038(3)	0.053(4)	0.021(3)	0.001(3)	-0.002(3)
S(4)	0.0257(7)	0.0264(7)	0.0232(6)	0.0030(5)	0.0000(5)	-0.0009(5)
C(5)	0.049(4)	0.045(4)	0.027(3)	-0.012(3)	-0.002(3)	0.000(3)
C(6)	0.051(4)	0.057(4)	0.033(3)	-0.024(3)	0.013(3)	-0.010(3)
S(7)	0.0318(7)	0.0342(7)	0.0219(6)	-0.0006(5)	0.0119(5)	0.0026(6)
C(8)	0.052(4)	0.069(5)	0.065(4)	-0.003(4)	0.038(3)	-0.008(3)
C(9)	0.111(6)	0.060(5)	0.093(6)	0.003(4)	0.075(5)	-0.020(5)
S	0.0408(8)	0.0285(7)	0.0338(7)	-0.0023(6	0.0100(6)	0.0055(6)
C(1t)	0.052(4)	0.034(3)	0.088(5)	-0.002(3)	0.033(4)	0.009(3)
C(2t)	0.075(5)	0.075(5)	0.073(5)	-0.008(4)	0.044(4)	0.012(4)
C(3t)	0.085(6)	0.120(7)	0.058(4)	-0.033(5)	0.013(4)	0.043(5)
C(4t)	0.053(4)	0.054(4)	0.057(4)	-0.023(3)	0.011(3)	0.004(3)
P(1)	0.0176(6)	0.0176(6)	0.0170(6)	-0.0007(5)	0.0055(5)	-0.0012(5)
C(11)	0.0188(24)	0.027(3)	0.0179(23)	-0.0019(21)	0.0066(19)	-0.0069(21)
C(12)	0.024(3)	0.026(3)	0.0247(25)	0.0003(22)	0.0078(21)	-0.0034(22)
C(13)	0.023(3)	0.036(3)	0.026(3)	-0.0001(23)	0.0072(21)	-0.0064(23)
C(14)	0.037(3)	0.035(3)	0.028(3)	-0.0035(23)	0.0078(23)	-0.013(3)
C(15)	0.039(3)	0.026(3)	0.030(3)	-0.0053(24)	0.0101(23)	-0.007(3)
C(16)	0.033(3)	0.022(3)	0.027(3)	-0.0020(22)	0.0134(22)	-0.0014(22)
C(21)	0.027(3)	0.023(3)	0.0179(24)	0.0011(20)	0.0072(20)	0.0042(22)
C(22)	0.029(3)	0.033(3)	0.023(3)	-0.0013(22)	0.0080(22)	0.0005(23)
C(23)	0.041(3)	0.048(4)	0.027(3)	-0.009(3)	0.0080(25)	-0.002(3)
C(24)	0.041(3)	0.065(4)	0.023(3)	-0.005(3)	0.0157(25)	0.001(3)
C(25)	0.043(3)	0.062(4)	0.040(3)	0.002(3)	0.024(3)	-0.002(3)
C(26)	0.031(3)	0.041(3)	0.026(3)	0.0008(24)	0.0132(22)	-0.004(3)
C(31)	0.028(3)	0.022(3)	0.0192(23)	-0.0043(20)	0.0051(20)	0.0027(21)
C(32)	0.038(3)	0.022(3)	0.025(3)	0.0008(22)	0.0016(22)	0.0006(24)
C(33)	0.059(4)	0.018(3)	0.032(3)	0.0001(23)	0.002(3)	0.003(3)
C(34)	0.043(3)	0.032(3)	0.027(3)	-0.0102(24)	-0.0041(24)	0.012(3)
C(35)	0.030(3)	0.040(3)	0.029(3)	-0.0072(25)	0.0035(22)	0.012(3)
C(36)	0.025(3)	0.033(3)	0.0152(22)	-0.0025(21)	0.0032(20)	0.0057(23)
P	0.0322(8)	0.0394(8)	0.0279(7)	-0.0062(6)	0.0132(6)	-0.0030(6)
F(1)	0.099(3)	0.0428(22)	0.102(3)	-0.0097(21)	0.049(3)	0.0163(21)
F(2)	0.0767(25)	0.0602(23)	0.0480(20)	-0.0160(18)	0.0064(18)	-0.0249(20)
F(3)	0.0579(23)	0.109(3)	0.0560(21)	0.0034(22)	0.0388(19)	0.0052(22)
F(4)	0.0695(25)	0.131(4)	0.0485(21)	-0.0136(23)	0.0353(19)	-0.039(3)
F(5)	0.116(4)	0.083(3)	0.113(4)	0.044(3)	0.026(3)	0.049(3)
F(6)	0.074(3)	0.162(5)	0.0504(22)	-0.034(3)	0.0115(20)	-0.069(3)

Bound thioether ligands can be oxidised in a variety of ways. The reaction of $[RuCl_2(PPh_3)_3]$ with 2-(diphenylphosphino)-benzene thiol (DPPBT) yields $[Ru(DPPBT)_3]^-$, which can be oxidised to the neutral Ru(III) complex, [Ru(DPPBT)]. Further oxidation of the Ru(III) complex results in the complex, $[Ru(DPPBT)](2\text{–}Ph_2PC_6H_4S\text{–}OH)(2\text{–}Ph_2P\text{–}C_6H_4SO_2)]$, in which the co-ordinated thioether ligand has been oxidised to a sulphinic acid (S–OH) group, and a sulphinate (SO_2) group, both being ligated via the sulfur[349].

THT has been catalytically converted to THT–S–Oxides by Ru complexes[341-343]. Riley and co-workers have investigated the oxidation of $[RuX_2(DMSO)_4]$ (X = Cl, Br) in alcohol with a number of thioethers, including THT[350-353]. It has been found that trans-$[RuCl_2(DMSO)_4]$ is the best catalyst for the oxidation of thioethers, although a large number of Ru(II) and Ru(III) complexes are also active, including mer-$[RuCl_3(DMSO)_3]$, cis-$[RuCl_2(DMSO)_4]$ and $K_2[RuCl_5(OH_2)]$[354]. The 'all *trans*' relationship of thioether, sulfoxide and halide (Figure 5.6) is thought to be the active species, in the catalytic conversion of thioethers to sulfoxides in the presence of O_2[351, 354]. The oxidation of thioethers to sulfoxides and sulfones by chemical oxidation is discussed in chapter 7.

Figure 5.6 The Proposed Active Species in the Catalytic Oxidation of Thioethers to Sulfoxides by $[RuCl_2(DMSO)_4]$

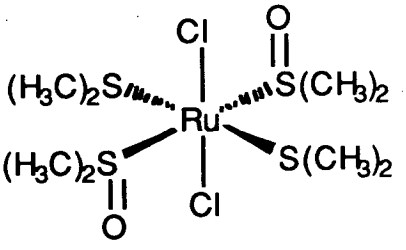

A number of THT complexes of transition metal ions have been reported[221, 350-367]. THT co-ordinates to metal ions in a variety of ways, usually via the sulfur lone pairs. THT can also co-ordinate via the α-carbon

(Figure 5.7)[361] and can also bridge two metals, as shown in Figure 5.8[367]. The reaction of $[Pt(H)(acetone)(PEt_3)_2]^+$ with 2,3-dihydrothiophene (2,3-DHT) results in the formation of the novel complex $[Pt(PEt_3)_2(SC_4H_7)]$ shown in Figure 5.9[361]. 2,3-DHT can also bridge two metals, and this is illustrated in the Os_3 cluster shown in Figure 5.10, the structure of the Os_3 cluster was confirmed by X-ray diffraction[361].

Figure 5.7 A Representation of $[CpFe(CO)(C_4H_3S)]$

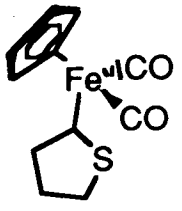

Figure 5.8 A Representation of $[Cp_2Mo_2(CO)_4(C_4H_4S)]$

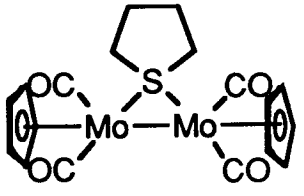

Figure 5.9 A Representation of $[Pt(PEt_3)_2(SC_4H_7)]$

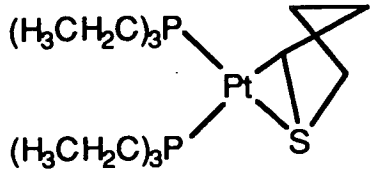

Figure 5.10 A Representation of $[Os_3(CO)_9(H)(PPh_3)(SC_4H_3)]$

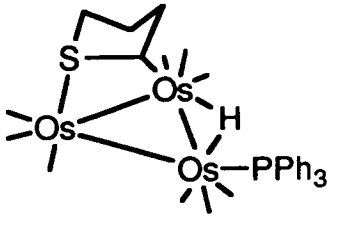

The Fe(II) porphyrin complexes [Fe(TPP)(THT–S–Oxide)$_2$] and [Fe(TPP)(THT)$_2$] have been prepared, and characterised by X-ray crystallography[350, 360, 366]. In [Fe(TPP)(THT)$_2$], the Fe(II) is co-ordinated to the porphyrin and two THT ligands [Ru–S = 2.336Å][362, 366]. In the THT–S–Oxide complex, [Fe(TPP)(THT–S–Oxide)], the Fe(II) is again co-ordinated to the porphyrin, but is also co-ordinated through the O donors of the THT–S–Oxide ligand[360].

A number of Ru complexes containing THT or THT–S–Oxide are known[221, 349-358]. The Ru(III) complexes, $[Ru(NH_3)_5(THT)]^{3+}$[357] and mer-$[RuCl_3(THT)_3]$[356] have been prepared, and their single crystal X-ray structures determined. The Ru–S bond length in $[Ru(NH_3)_5(THT)]^{3+}$ is 2.3666Å[357], which is very similar to the ones reported for mer-$[RuCl_3(THT)_3]$ [Ru–S = 2.393(1), 2.386(1) and 2.381(1)Å] [356]. The Ru(IV) complex, $[Ru(Cp^*)Cl_2(THT)_2]ClO_4$ has been synthesised and its crystal structure shows the Ru to be co-ordinated to two THT ligands [Ru–S = 2.422(1), 2.409(1)Å].

The Ru(II) complex, cis-$[RuCl_2(THT–S–Oxide)_4]$ has been synthesised and characterised by X-ray crystallography. In this complex, the Ru co-ordinates to all four S–donors [Ru–S = 2.74(1) and 2.341(1)Å][356]. This contrasts with cis-$[RuCl_2(DMSO)_4]$ which is co-ordinated to three S-donors and an O-donor[356]. In the complex, cis-$[RuCl_2(THT–S–Oxide)_4]$ the Ru–S bond length is 2.341(1)Å for the S *trans* to a THT–S–Oxide ligand. This is comparable to the $Ru–S_{(THT/THT\text{-}S\text{-}Oxide)}$ bond length of 2.3700(14) Å in the crystal structure of the mixture, $[RuCl(L)(PPh_3)([9]aneS_3)](PF_6)$ (L = THT or THT–S–Oxide). The complex, [RuCl(THT)(1,5–DTCO)(1,5–DTCO–O)](BPh_4) (Figure 5.11) has been synthesised. The Ru(II) metal ion co-ordinates to the two S donors of 1,5-DTCO [Ru–S = 2.361(2), 2.349(2)Å] , the S–donor of THT [Ru–S = 2.398(4)Å] , two S–donors of 1,5–DTCO–O [Ru–S = 2.353(2) $Ru–S_{(sulfoxide)}$ = 2.269(2)Å] , and a Cl^- donor [Ru–Cl = 2.455(2)Å][355]. The sulfoxide is *trans* to the Cl donor. The remaining S-donors are all *trans* to sulfur and have a comparable length

[Ru–S = 2.349(2) – 2.398(2)Å] to the Ru–S bond length in $[RuCl(L)(PPh_3)([9]aneS_3)](PF_6)$ (L = THT and THT–S–Oxide). This suggests that there is very little structural change when a bound THT is oxidised to a S–bound THT–S–Oxide .

Figure 5.11 A Representation of $[RuCl(THT)(1,5\text{–}DTCO)(1,5\text{–}DTCO\text{–}O)BPh_4$

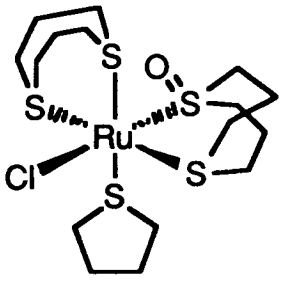

The reaction of $[RuCl_2(PPh_3)[9]aneS_3)]$ with $TlPF_6$ in the presence of sulfur heterocycles, THT and thiophene results in the formation of $[RuCl(L)(PPh_3)([9]aneS_3)](PF_6)$ (L = THT) or the Ru dimers $[Ru(PPh_3)([9]aneS_3)(\mu\text{–}Cl)_2]_2(PF_6)_2$ and $[Ru(PPh_3)([9]aneS_3)(\mu\text{–}Cl)_2Tl]_2(PF_6)$ (L = thiophene). The difference in reactivity can be attributed to the weaker co-ordination ability of the S in thiophene, since the sulfur in thiophene contributes two electrons to the aromatic π-electron cloud, and is less basic.

5.2.3 The Reaction of $[RuCl_2(PPh_3)([9]aneS_3)]$ with $TlPF_6$ and Pyrrole and Pyrrolidine

The reaction of $TlPF_6$ with $[RuCl_2(PPh_3)([9]aneS_3)]$ in CH_3NO_2 and pyrrolidine for sixteen hours results in the formation of a dark yellow solution and a white precipitate of TlCl. Removing the TlCl and reducing the solution to dryness affords an orange solid which can be recrystallised from acetone and hexane. The ir spectrum of the product indicates that PPh_3, $[9]aneS_3$ and PF_6^- are present [ν cm^{-1} = 1484(ms), 1435(s), 1410(ms), 1090(s), 835(vs), 557(s), 528(s), 513(ms), 499(m)]. The ^1H N.M.R. spectrum (d^6-acetone) of the product shows resonances at δ = 0.97(t), 1.5–3.5(m), 7.3–8.0(m) p.p.m. Its F.A.B. mass spectrum

shows peaks at m/e = 819, 716, 634, 614, 579 which can be assigned to $\{TlCl_2Ru([9]aneS_3)(PPh_3)\}^+$, $\{Ru_2Cl_2(PPh_3)([9]aneS_3)\}^+$, $\{Ru(NCCH_2CH_3)(PPh_3)Cl([9]aneS_3)\}^+$, $\{RuCl_2(PPh_3)([9]aneS_3)\}^+$, $\{RuCl(PPh_3)([9]aneS_3)\}^+$ respectively. Thus, the product formed is a mixture of the RuTl ladder, $[Ru(PPh_3)([9]aneS_3)(\mu\text{–}Cl)_2Tl]_2(PF_6)_2$, the Ru dimer, $[Ru(PPh_3)([9]aneS_3)(\mu\text{-}Cl)]_2(PF_6)_2$, (Chapter 3), and the ethyl cyanide complex, $[RuCl(NCCH_2CH_3)(PPh_3)([9]aneS_3)](PF_6)$ (EtCN is an impurity in CH_3NO_2 (see Chapter 4). Undertaking an identical reaction in CH_2Cl_2 results in a similar product. The only differences are that no resonance is observed at δ = 0.97(t) p.p.m. in the ^1H N.M.R. spectrum (d^6-acetone), and no peak at m/e = 634 is seen in the F.A.B. mass spectrum. Thus, the product formed when $[RuCl_2(PPh_3)([9]aneS_3)]$ reacts with $TlPF_6$ in CH_2Cl_2 in the presence of pyrrolidine, is a mixture of the Ru dimer, $[Ru(PPh_3)([9]aneS_3)(\mu\text{–}Cl)]_2(PF_6)$ and the RuTl ladder species $[Ru(PPh_3)([9]aneS_3)(\mu\text{–}Cl)_2Tl]_2(PF_6)_2$.

Addition of $TlPF_6$ to $[RuCl_2(PPh_3)([9]aneS_3)]$ in CH_3NO_2 or CH_2Cl_2 in the presence of pyrrole, and stirring for sixteen hours results in a white precipitate of TlCl and a light green solution. Removal of TlCl followed by reduction of solution to dryness affords a light green solid which is recrystallised from acetone/hexane. The ^1H N.M.R. spectrum (d^6-acetone) of the green solid is very broad, possibly indicating the presence of Ru(III) complex. The ir spectrum indicates that PPh_3, [9]$aneS_3$ and PF_6^- are present and the F.A.B. mass spectrum shows peaks at m/e = 819, 715, (634), 614, 579 (m/e = 634, only when undertaken in CH_3NO_2). This suggests that a mixture of the Ru dimer, $[Ru(PPh_3)([9]aneS_3)(\mu\text{–}Cl)]_2(PF_6)_2$, RuTl complex $[Ru(PPh_3)([9]aneS_3)(\mu\text{–}Cl)_2Tl]_2(PF_6)_2$, and another unidentified product possibly a Ru(III) complex are formed when the reaction of $[RuCl_2(PPh_3)([9]aneS_3)]$ with $TlPF_6$ is undertaken in the presence of pyrrole.

The presence of the dimeric Ru complexes suggests that these five-membered N-heterocycles do not have sufficient co-ordinating ability to prevent the dimerisation. It is also interesting to note that in CH_3NO_2, no isoxazole complex, $[RuCl(NC_3H_3O)(PPh_3)([9]aneS_3)]^+$ (another impurity in CH_3NO_2 see Section 4.4) was found. This could be due either to the N-heterocycles preventing the formation of the isoxazole complex, or to the batch of nitromethane used in these experiments being free from the trace isoxazole impurity.

Deprotonation of five-membered N-heterocycles improves their co-ordinating ability[344]. Therefore, reactions were undertaken with pyrrole and pyrrolidine, in the presence of base (either NEt_3 or proton sponge). Addition of $TlPF_6$ to $[RuCl_2(PPh_3)([9]aneS_3)]$ in CH_2Cl_2 or CH_3NO_2 in the presence of pyrrole along with NEt_3 or proton sponge forms a red solution and a white precipitate of TlCl. Removing the TlCl and evaporating the solution to dryness affords a red sticky solid. This product can be recrystallised from acetone/hexane. It is known that when a strong acid is added to pyrrole a red polymeric compound (polypyrrole) forms. However, the ir spectrum of this red sticky material shows that PF_6^- , PPh_3 and a thioether are all present. The ^1H N.M.R. spectrum (d^6-acetone) of the product is broad showing resonances at δ = 1.3–3.5(m, broad), 7.3–8.0(m, PPh_3) p.p.m, and a weak resonance at δ = 6.3(m) p.p.m. No significant peaks are observed in the F.A.B. mass spectra in either a 3-NOBA or a DMF/thioglycerol matrix. The reaction of $[RuCl_2(PPh_3)([9]aneS_3)]$ with $TlPF_6$ in CH_2Cl_2 or CH_3NO_2 and pyrrolidine in the presence of base also forms a red solution and a white precipitate of TlCl. Removing the TlCl, reducing the solution to dryness and recrystallising the resulting solid from acetone/hexane yields a similar sticky red solid. From this one can conclude that the product from both these reactions is not a pyrrole polymer. Furthermore, when base is added to neat pyrrole or pyrrolidine there is no change in colour after 2 days. The weak resonance at δ = 6.3 p.p.m., along with

its physical appearance may suggest that the co-ordinated [9]aneS$_3$ macrocycle ring-opened, to form a vinyl thioether moiety (see the Appendix and Figure 5.12). When pyrrole and pyrrolidine are deprotonated, they form quite powerful bases, which could easily deprotonate bound [9]aneS$_3$. However, the nature of this red Ru complex is not fully understood.

Figure 5.12 A Representation of a Possible Ru Vinyl Thioether Complex.

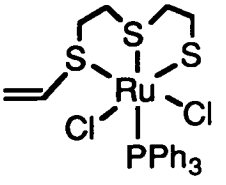

5.3 Summary

The reaction of [RuCl$_2$(PPh$_3$)([9]aneS$_3$)] with TlPF$_6$ in the presence of S and N heterocyclic analogues of furan or THF in CH_3NO_2 or CH_2Cl_2 has been investigated. Pyrrole, pyrrolidine and thiophene do not afford a heterocylic complex, instead the dimeric complexes, [Ru(PPh$_3$)([9]aneS$_3$)(μ–Cl)]$_2$(PF$_6$)$_2$ and [Ru(PPh$_3$)([9]aneS$_3$)(μ–Cl)$_2$Tl]$_2$(PF$_6$) are formed. Tetrahydrothiophene reacts with [RuCl$_2$(PPh$_3$)([9]aneS$_3$)] and TlPF$_6$ to form the complex [RuCl(THT)(PPh$_3$)([9]aneS$_3$)]PF$_6$, which is oxidised in air to form [RuCl(THT–S–Oxide)(PPh$_3$)([9]aneS$_3$)]PF$_6$.

5.4 Experimental

All physical measurements were recorded as described in Chapters 3 and 4.

Reagents

The reagents, solvents and starting materials were prepared as described in Chapters 3 and 4. Tetrahydrothiophene was purchased from Aldrich and distilled before use. All reactions involving CH_2Cl_2 were carried out on a Schlenk line under N_2.

5.4.1 $[RuCl_2(PPh_3)([9]aneS_3)]$ and $TlPF_6$ with pyrrolidine

(a) $[RuCl_2(PPh_3)([9]aneS_3)]$ (50 mg, 8.1×10^{-5}M) and $TlPF_6$ (30 mg, 8.5×10^{-5}M) were added to CH_3NO_2 (4 cm^3) and pyrrolidine (1 cm^3) and stirred for sixteen hours. The white precipitate TlCl was removed by filtration and the solvent evaporated to dryness on a rotary evaporator. The light orange solid was recrystallised from acetone/hexane.

Ir spectrum $\upsilon(cm^{-1})$: 3600(broad, m), 3051(w), 3059(w), 2920(mw), 1630(broad, mw), 1585(w), 1484(ms), 1435(s), 1410(ms), 1364(w), 1291(mw), 1090(s), 1025(w), 998(mw), 835(vs), 750(ms), 696(s), 557(s), 528(s), 513(ms), 499(m)

^1H N.M.R.spectrum (d^6-acetone, 298K) δ = 0.97 (t), 1.28(s), 1.5–3.5(m) , 7.3–8.0 (m) p.p.m.

F.A.B. mass spectrum found m/e = 819, 716, 634, 614, 579;

calculated for $\{^{205}Tl^{35}Cl_2{}^{102}Ru[9]aneS_3PPh_3\}^+$: 819, $\{^{102}Ru^{35}Cl_2(PPh_3)([9]aneS_3)\}^+$: 716, $\{^{102}Ru(NCCH_2CH_3)^{35}Cl(PPh_3)([9]aneS_3)\}^+$: 634, $\{^{102}Ru^{35}Cl_2(PPh_3)([9]aneS_3)\}^+$: 614, $\{^{102}Ru^{335}Cl(PPh_3)([9]aneS_3)\}^+$: 579

(b) The reaction was repeated as (a) above, but NEt_3 (0.1 cm^3) was added. A red solution formed after sixteen hours of stirring, which was filtered to remove a white precipitate, and the solvent removed by a rotary evaporator. The red sticky solid was recrystallised from acetone/hexane.

Ir spectrum $\upsilon(cm^{-1})$: 3580(broad, ms), 3052(w), 2980(w), 2920(w), 1635(broad, m), 1555(mw), 1475(ms), 1442(s), 1410(ms), 1365(w), 1290(w), 1090(s), 1035(w), 999(mw), 835(vs), 750(ms), 698(s), 557(vs), 528(s), 513(ms), 499(m)

^1H N.M.R.spectrum (d^6-acetone, 298K) δ = 1.28(s), 1.3–3.5(m, broad) , 7.3–8.0 (m, PPh_3) p.p.m.

F.A.B. mass spectrum(3-NOBA or DMF/Thioglycerol matrixes) : only showed peaks associated with the matrix.

(c) The reaction was carried out as described in (a) above, except that CH_2Cl_2 (8 cm^3) was used as a solvent, instead of CH_3NO_2.
Ir spectrum $\upsilon(cm^{-1})$: 3600(broad, ms), 3051(w), 2920(w), 1630(broad, m), 1587(mw), 1485(ms), 1435(ms), 1410(ms), 1290(mw), 1090(s), 1025(w), 999(mw), 835(vs), 750(ms), 695(s), 558(vs), 527(s), 510(ms), 499(m)
^1H N.M.R.spectrum (d^6-acetone, 298K) δ = 1.28(s), 1.3–3.5(m) , 7.3–8.0 (m) p.p.m.
F.A.B. mass spectrum found m/e = 819, 716, 614, 579;
calculated assignments see 5.4.1 (a)

(d) The reaction was repeated, in the conditions shown in Table 5.3.1, and, as indicated on the table, the resulting products spectra were similar to (a), (b) or (c) above.

5.4.2 $[RuCl_2(PPh_3)([9]aneS_3)]$ and $TlPF_6$ with pyrrole

A similar series of experiments was undertaken in an identical manner as 5.4.1, except that pyrrole (1 cm^3) was used in place of pyrrolidine. The conditions and results are shown in Table 5.3.2.

5.4.3 $[RuCl_2(PPh_3)([9]aneS_3)]$ and $TlPF_6$ with thiophene

The experiments were carried out as described in Section 5.4.1, except that thiophene (1 cm^3) was used in place of pyrrolidine. The conditions and results are shown in Table 5.3.3. In addition a ^{31}P N.M.R. was recorded.
^{31}P N.M.R.spectrum (d^6-acetone, 243K) δ = 33.5, 32.8, -145 (septet, J = 710 Hz, PF_6^-) p.p.m.

5.4.4. Synthesis of $[RuCl(PPh_3)(THT)([9]aneS_3)](PF_6)$

$[RuCl_2(THT)(PPh_3)([9]aneS_3)]$ (51 mg, 8.3 x 10^{-5} M) and $TlPF_6$ (30 mg, 8.6 x 10^{-5} M) was added to CH_3NO_2 (4 cm^3) (or CH_2Cl_2 (8 cm^3) under N_2) and

THT (1 cm^3) , and the solution stirred for sixteen hours. The white precipitate of TlCl was removed by filtration through celite, and the solvent removed by rotary evaporation. The bright product was recrystallised from acetone/hexane (yield = 60 mg, 86%).

(a) Before Crystallisation

Ir spectrum $\upsilon(cm^{-1})$: 3640(broad, w), 3052(mw), 2934(mw), 1705(ms), 1482(ms), 1434(s), 1410(s), 1363(w), 1263(w), 1223(w), 1188(w), 1091(ms), 1027(w), 999(w), 840(vvs), 746(ms), 698(s), 528(s), 558(vs), 527(s), 513(ms), 500(ms), 466(w), 425(w).

^1H N.M.R.spectrum (d^6-acetone, 298K) δ = 1.28(s), 1.8–3.5(m) , 7.25–8.0 (m) p.p.m.

^{31}P N.M.R.spectrum (d^6-acetone, 298K) δ = 27.2. -145 (septet, J = 710 Hz, PF_6^-) p.p.m.

F.A.B. mass spectrum found m/e = 812, 667, 579, 551;

calculated for $\{^{102}Ru([9]aneS_3)^{35}Cl(PPh_3)(THT)PF_6\}^+$: 812,

$\{^{102}Ru([9]aneS_3)^{35}Cl(PPh_3)(THT)\}^+$: 667, $\{^{102}Ru^{35}Cl(PPh_3)([9]aneS_3)\}$: 579,

$\{^{102}Ru(S(CH_2)_2S(CH_2)_2S)^{35}Cl(PPh_3)\}$: 551.

C.H.N. Expect 41.3%C 4.31%H 0%N for $[RuCl(PPh_3)(THT)([9]aneS_3)](PF_6)$

Found 39.6%C 4.25%H 0.0%N

(b) After Crystallisation

Crystals were grown by vapour diffusion of hexane into acetone (both d^6- or normal)

Ir spectrum $\upsilon(cm^{-1})$: 3450(broad, w), 3052(mw), 2926(w), 1711(m), 1482(m), 1436(ms), 1409(m), 1223(w), 1092(m), 1047(m), 1000(w), 840(vs), 779(m), 700(ms), 558(s), 528(s), 515(m), 499(mw), 431(w).

^1H N.M.R.spectrum (d^6-acetone, 298K) δ = 1.28(s), 1.7–3.5(m) , 7.25–8.0 (m) p.p.m.

^{31}P N.M.R.spectrum (d^6-acetone, 298K) δ = 27.2, 23.7, -145 (septet, J = 710 Hz, PF_6^-) p.p.m.

F.A.B. mass spectrum found m/e = 683, 667, 579, 351;

calculated assignment as (a) above except

for $\{^{102}Ru(THT–S–Oxide)^{35}Cl(PPh_3)([9]aneS_3)\}$: 683

5.4.5 The X-ray crystal structure of the 1 : 1 mixture of [RuCl(PPh$_3$)(THT)([9]aneS$_3$)](PF$_6$) and [RuCl(PPh$_3$)(THT-S-Oxide)([9]aneS$_3$)](PF$_6$)

Crystal data $C_{29}H_{35}S_4ClPRuOPF_6$, M = 840.23, monoclinic, $P2_{1/n}$, a = 12.9373(26), b = 16.710(5), c = 16.609(4)Å, β = 108.909(20); V = 3397Å^3 [from 2θ values of 65 reflections measured at ±ω ($30 \leq 2\theta \leq 32°$), T = 150 ± 0.1K, λ = 0.71073Å], De = 1.643 gcm^{-1}, Z = 4, F(000) = 1704, yellow column, 0.35 x 0.39 x 0.74 mm, μ(Mo–K$_\alpha$) = 9.17 cm^{-1}

Data Collection and processing: Stöe Stadi-4 diffractometer, graphite monochromated Mo–K$_\alpha$ radiation, ω–2θ scans, 4226 unique data collected measured ($2\theta_{max} = 45°$, h = -13 → 13, k = 0 → 15, l = 0 → 17), giving 3699 data with $F \geq 4\sigma(F)$. No significant crystal decay or movement was observed. Absorption correction (NPM) was applied, min = 0.625, max = 0.7226.

Structure solution and refinement: The Ru position was located by Patterson synthesis[288]. Non-H atoms were located and refined by interactive least squares refinement and Fourier transformations. All non-H atoms with an occupancy greater than 50% were refined anisotropically. The occupancy of the oxygen was refined and then set to 50%. The solvent fragment (C_2O) was also refined to an occupancy of 50%. H-atoms were included at fixed calculated positions with a fixed U_{iso}. Phenyl rings were constrained as idealised, planar hexagons. At convergence, $\omega^{-1} = \sigma^2(F) + 0.000256(F)^2$, R = 0.0349 and Rw = 0.0494, S = 1.281 for 360 parameters. For final ΔF synthesis, max and min residues were +0.78 and -0.52eÅ^3. Views of the cation were generated using XP[289], and tables utilised CALC[290]. Scattering factors were inlaid, or taken from Ref. 291.

Table 5.3 Experimental Conditions

Table 5.3.1 The reaction of $[RuCl_2(PPh_3)([9]aneS_3)]$ with $TlPF_6$ in the presence of pyrrolidine.

Amount of $[RuCl_2(PPh_3)[9]aneS_3)]$ added		Amount of $TlPF_6$ added		Solvent	Base	Product see section
mg	$x10^{-5}$ M	mg	$x10^{-5}$ M		Added	
50	8.1	30	8.6	CH_3NO_2 (4 cm^3)		5.4.1a
49	7.9	29	8.3	CH_3NO_2 (4 cm^3)	NEt_3 (0.1 cm^3)	5.4.1.b
51	8.3	30	8.6	CH_3NO_2 (4 cm^3)	Proton sponge	5.4.1.b
50	8.1	28	8.0	CH_2Cl_2 (8 cm^3)		5.4.1.c
50	8.1	29	8.3	CH_2Cl_2 (8 cm^3)	NEt_3 (0.1 cm^3)	5.4.1.b
49	7.9	30	8.6	CH_2Cl_2 (8 cm^3)	Proton sponge (100 mg, 0.41 cm^3)	5.4.1.b

Table 5.3.2 The reaction of $[RuCl_2(PPh_3)[9]aneS_3)]$ with $TlPF_6$ in the presence of pyrrole.

Amount of $[RuCl_2(PPh_3)[9]aneS_3)]$ added		Amount of $TlPF_6$ added		Solvent	Base	Product see section
mg	$x10^{-5}$ M	mg	$x10^{-5}$ M		Added	
50	8.1	31	8.9	CH_3NO_2 (4 cm^3)		5.4.1a
49	7.9	30	8.6	CH_3NO_2 (4 cm^3)	NEt_3 (0.1 cm^3)	5.4.1.b
49	7.9	30	8.6	CH_3NO_2 (4 cm^3)	Proton sponge(100 mg, 0.41 cm^3)	5.4.1.b
50	8.1	29	8.3	CH_2Cl_2 (8 cm^3)		5.4.1.c
50	8.3	31	8.9	CH_2Cl_2 (8 cm^3)	NEt_3 (0.1 cm^3)	5.4.1.b
51	8.3	31	8.9	CH_2Cl_2 (8 cm^3)	Proton sponge (100 mg, 0.41 cm^3)	5.4.1.b

Table 5.3.3 The reaction of $[RuCl_2(PPh_3)[9]aneS_3)]$ with $TlPF_6$ in the presence of thiophene.

Amount of $[RuCl_2(PPh_3)[9]aneS_3)]$ added		Amount of $TlPF_6$ added		Solvent	Product see section
mg	$x10^{-5}$ M	mg	$x10^{-5}$ M		
50	8.1	30	8.6	CH_3NO_2 (4 cm^3)	5.4.1a
48	7.7	28	8.0	CH_2Cl_2 (8 cm^3)	5.4.1.c

Chapter 6

RHODIUM AND RUTHENIUM COMPLEXES OF [n]aneS$_4$ (n = 12, 14, 16)

6.1 Introduction

The greater part of this thesis has been concerned with Ru complexes of [9]aneS$_3$, and in particular the reaction of [RuCl$_2$(PPh$_3$)([9]aneS$_3$)] with TlPF$_6$ (Chapters 3, 4 and 5). In this chapter, there is a change of emphasis to Ru and Rh complexes of [n]aneS$_4$ (n = 12, 14, 16). The complexes, [RuCl$_2$(L)] (L = [13]aneS$_4$, [14]aneS$_4$, benzo-[15]aneS$_4$, Me$_4$[14]aneS$_4$ and Me$_8$[14]aneS$_4$) have been reported and prepared by refluxing K$_2$[RuCl$_5$(OH$_2$)] with the tetrathioether macrocycle[26, 181, 368-372]. The structure of [RuCl$_2$([14]aneS$_4$)] has been confirmed by X-ray crystallography, as an octahedral Ru(II) complex with the Cl$^-$ donors in a *cis*-conformation [Ru–Cl = 2.471(1)Å, Ru–S$_{(trans\ to\ Cl^-)}$ = 2.262(1)Å, Ru–S$_{(trans\ to\ S)}$ = 2.333(1)Å] (Figure 6.1)[368-371]. The complexes [RuCl$_2$(L)] (L = Me$_4$[14]aneS$_4$ and Me$_8$[16]aneS$_4$) react with a large excess of NaBH$_4$ in CH$_3$OH at 298K to give the *trans* complexes [Ru(H)(Cl)(L)] [373]. Other complexes of the type [RuXY([14]aneS$_4$)]$^{x+}$ (X,Y = Br, I, NCS, NO$_2$, N$_3$, OH$_2$; x = 0, 1) have been prepared and their electrochemistry studied[368-372]. Ali *et al* have proposed that the reaction of RuCl$_3$.3H$_2$O with [14]aneS$_4$ in ethanol yields the complex [RuCl$_3$([14]aneS$_3$)], in which the [14]aneS$_4$ is proposed to be tridentate[245]. This complex reacts with LiBr to form the analogous Br complex [RuBr$_3$[14]aneS$_4$][245]. The addition of [12]aneS$_4$ to [RuCl$_2$(CO)$_2$(DMF)(PPh$_3$)] affords the complex [Ru(CO)(PPh$_3$)([12]aneS$_4$)]$^{2+}$, whose crystal structure shows the octahedral Ru(II) ion to be co-ordinated to tetrathioether macrocycle [Ru-S$_{(trans\ to\ P)}$ = 2.3757(11) Å, Ru-S$_{(trans\ to\ C)}$ = 2.3986(10) Å and Ru-S = 2.3819(10), 2.3913(10) Å] , a phosphine ligand [Ru-P = 2.3880(10) Å] and a carbonyl ligand [Ru-C = 1.889(4) Å] (Figure 6.2)[242, 268].

Figure 6.1 A View of the Single Crystal X-Ray Structure of $[RuCl_2([14]aneS_4)]$

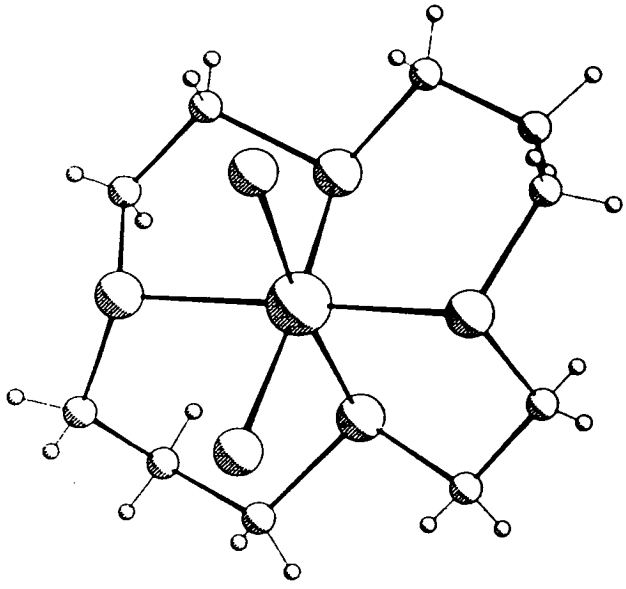

Figure 6.2 A View of the Single Crystal X-Ray Structure of $[Ru(CO)(PPh_3)([12]aneS_4)]^{2+}$

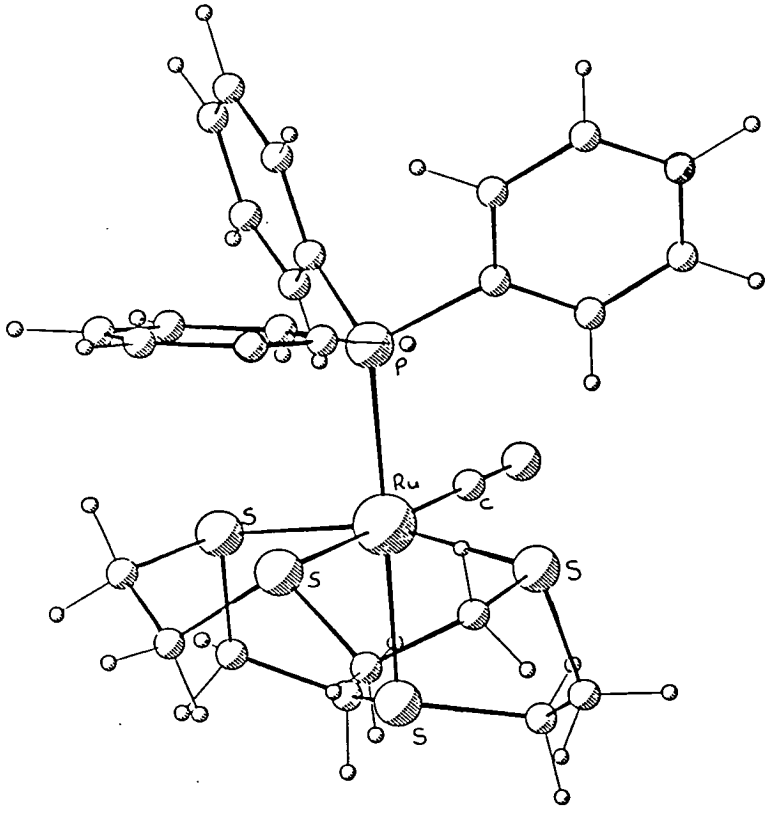

The Rh complexes $[RhCl_2(L)]^+$ (L = [12]aneS$_4$, [14]aneS$_4$ or [16]aneS$_4$) have also been prepared by refluxing $RhCl_3.3H_2O$ and L in CH_3OH[26, 374, 375]. The single crystal structures of $[RhCl_2([14]aneS_4)](PF_6)$ and $[RhCl_2([16]aneS_4)](PF_6)$ have been determined, and their structures are shown in Figures 6.3 and 6.4[374, 375]. The complex $[RhCl_2([14]aneS_4)](PF_6)$ shows that the Cl^- donors adopt a *cis* orientation [Rh-Cl = 2.3836(12) Å] and that the octahedral Rh(III) ion is co-ordinated to the tetrathioether macrocycle [Rh-S $_{(trans\ to\ Cl^-)}$ = 2.2870(12)Å and Rh-S$_{(\ trans\ to\ S)}$ = 2.3275(12)Å]. In contrast, the [16]aneS$_4$ complex $[RhCl_2([16]aneS_4)]PF_6$ adopts a *trans-* configuration [Rh-Cl - 2.3391(22)Å and Rh-S = 2.3483(25)Å]. This demonstrates that changing the ring size of [n]aneS$_4$ macrocycles can alter the stereochemistry of the metal ion, and is consistent with the increase in the hole size of a [16]aneS$_4$ macrocycle as compared to the [12] and [14] membered tetrathioethers.

Rh(I) complexes of tetrathioether macrocycles have also been reported. The complexes, $[Rh^{(I)}(L)]^+$ (L = [14]aneS$_4$, Me$_4$[14]aneS$_4$, Benzo[15]aneS$_4$) [26, 181, 375, 376] have been synthesised by electrochemically reducing $[RhCl_2([n]aneS_4)]^+$. The resultant complexes are dimeric (Figure 6.5), and undergo oxidative additions with CH_2Cl_2, CH_3I, $C_6H_5CH_2Br$, and CH_3NO_2Cl[376]. $[Rh([14]aneS_4)]^+$ can also combine with SO_2, BF_3, NO^+, O_2, tcne and H^+[26, 181]. $[Rh_2(Cp^*)_2Cl_4]$ reacts with [14]aneS$_4$ to form the dimeric species $[Rh_2(Cp^*)_2Cl_2([14]aneS_4)]$, shown in Figure 6.6[26, 181].

Figure 6.3 A View of the Single Crystal X-Ray Structure of $[RhCl_2([14]aneS_4)](PF_6)$

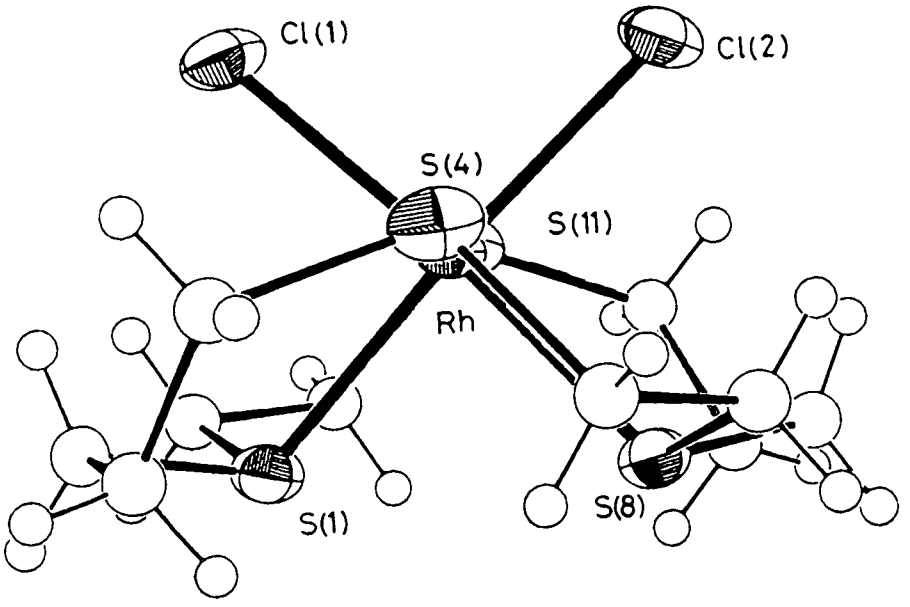

Figure 6.4 A View of the Single Crystal X-Ray Structure of $[RhCl_2([16]aneS_4)](PF_6)$

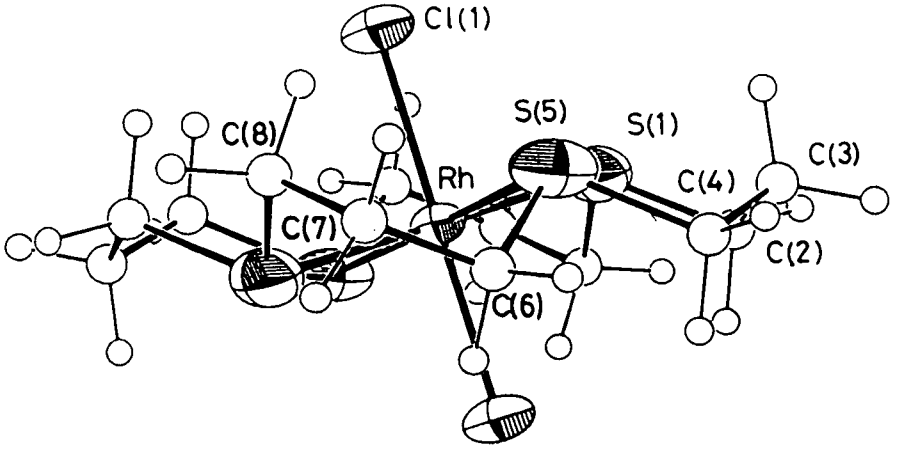

Figure 6.5 A View of the Single Crystal X-Ray Structure of $[Rh_2([14]aneS_4)_2](PF_6)_2$

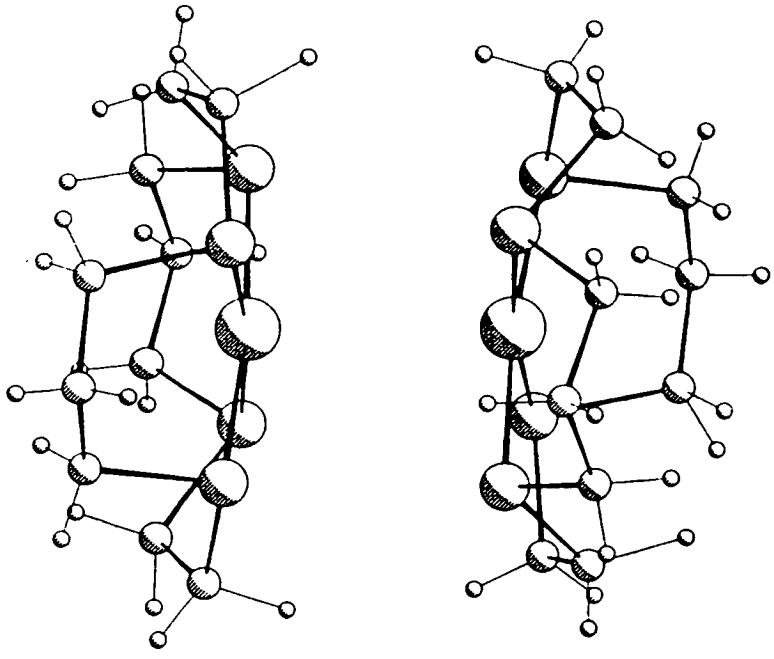

Figure 6.6 A View of the Single X-Ray Crystal Structure of $[Rh_2Cl_2(Cp^*)_2([14]aneS_4)](PF_6)_2$

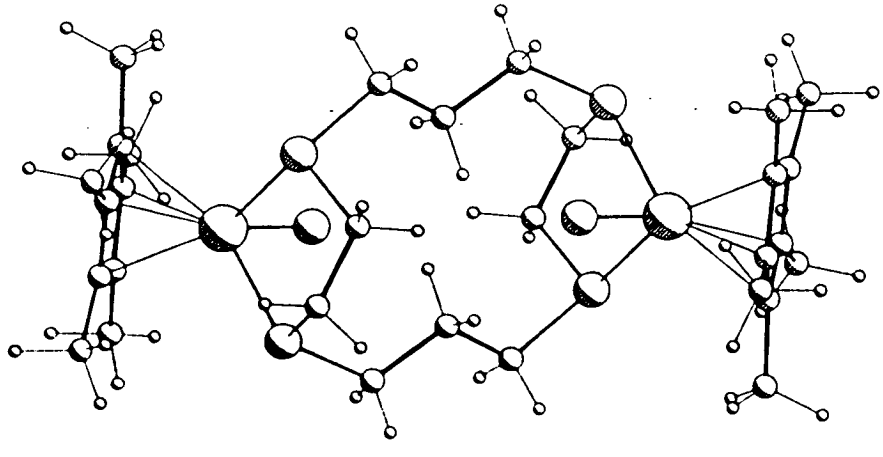

The aim of this work was to prepare $[RuCl_2([14]aneS_4)]$ and also the previously uncharacterised complexes,$[RuCl_2([n]aneS_4)]$ (n = 12, 16). Originally, one of the aims of this work was to help elucidate a possible mechanism for the synthesis of the 'C–bound furyl complex' from $[RuCl_2(PPh_3)([9]aneS_3)]$ with $TlPF_6$ in the presence of THF and CH_3NO_2 which was discussed in Chapter 4. The complexes $[MCl_2([n]aneS_4)]^{x+}$ (M = Rh, x = 1, n = 12, 14, 16; M = Ru, x = 0, n = 12, 14, 16) may have revealed whether the $\{MCl_2\}$ moiety was necessary for the formation of the 'C–bound furyl complex', and the complexes $[MCl(PR_3)([n]aneS_4)]^{x+}$ (M = Ru, Rh, x = 1, 2, PR_3 = PPh_3, n = 12, 14, 16) would have revealed whether the $\{MCl(PPh_3)\}$ moiety was necessary. However, it was discovered that the reaction of $[RuCl_2(PPh_3)([9]aneS_3)]$ with $TlPF_6$ in CH_3NO_2 and THF was a simple substitution of the impurities present in CH_3NO_2 (isoxazole and propionitrile). At the outset of the work described in this chapter, the explanation of the 'C–bound furyl complex' was not known. For the sake of brevity, the results will be discussed in the light of the impurities found in CH_3NO_2, which were presented in Section 4.4.

6.2 Ruthenium Complexes of [n]aneS$_4$ (n = 12, 14, 16)

6.2.1 The synthesis and reactivity of $[RuCl_2([n]aneS_4)]$ (n = 12, 14, 16)

The complex $[RuCl_2([14]aneS_4)]$ has been previously prepared by reaction of $K_2[RuCl_5(OH_2)]$ with $[14]aneS_4$ in 2-methoxyethanol for two days[369, 370]. This procedure was repeated and results in a yellow solid which is collected and dried. The complex is insoluble in CH_3OH , acetone, and CH_3NO_2, but is soluble in refluxing 2M HCl. The ir spectrum shows a broad band at $\upsilon_{c\text{-}s}$ = 1450 cm^{-1}, which could be assigned to $[14]aneS_4$, the absorbances in the $\upsilon_{c\text{-}c}$ 'fingerprint' region at 925, 908, 856, 843 and 814 cm^{-1} being the same as the literature values[368-371]. The F.A.B. mass spectrum of $[RuCl_2([14]aneS_4)]$ shows m/e = 404

and 369, which can be assigned to $\{RuCl([14]aneS_4)-H\}^+$, and $\{Ru([14]aneS_4)\}^+$. However, no parent ion is observed in either a 3-NOBA or a DMF/thioglycerol matrix.

The addition of [12]aneS$_4$ to $K_2[RuCl_5(OH_2)]$ in 2-methoxyethanol forms a similar yellow product, the ir spectrum of which is similar to $[RuCl_2([14]aneS_4)]$. The ir spectrum of the yellow product shows absorbances, in the υ_{c-c} 'fingerprint' region, at υ_{c-c} cm^{-1} = 925, 911, 860, 840, 820 , suggesting that the configuration of the [12]aneS$_4$ and [14]aneS$_4$ macrocycles are similar. Thus, the stereochemistry of $[RuCl_2([12]aneS_4)]$ is assigned as a *cis*-complex (Figure 6.1). The F.A.B. mass spectrum of $[RuCl_2([12]aneS_4)]$ shows peaks at m/e = 377, 345 which correspond to $\{RuCl([12]aneS_4)+H\}^+$ and $\{Ru[12]aneS_4]+H\}^+$ respectively.

Reaction of $K_2[RuCl_5(OH_2)]$ with [16]aneS$_4$ affords a pink solid after refluxing in 2-methoxyethanol for two days. The ir spectrum shows stretches at υ cm^{-1} = 1435, 926, 884, 873, 842 and 769 , which are quite different from both $[RuCl_2([n]aneS_4)]$ (n = 12, 14) complexes. The F.A.B. mass spectrum confirms the product to be $[RuCl_2([16]aneS_4)]$ with peaks at m/e = 470, 433, 397, which correspond to $\{RuCl([16]aneS_4)+3H^+\}$, $\{RuCl[16]aneS_4+H\}^+$, and $\{Ru([16]aneS_4)\}^+$ respectively. The ir spectrum and colour of the [16]aneS$_4$ complex are quite different from the [12]aneS$_4$ and [14]aneS$_4$ analogues, suggesting that $[RuCl_2([16]aneS_4)]$ adopts a *trans* configuration rather than a *cis* one. A similar change in stereochemistry has been observed from the complexes $[RhCl_2([n]aneS_4)]PF_6$ (n = 14, 16) (Figures 6.3 and 6.4).

The reaction of $[RuCl_2([n]aneS_4)]$ (n = 12, 14, 16) with $TlPF_6$ and THF in CH_3NO_2 results in the slow formation of a white solid (TlCl) and a coloured solution (n = 12, 14, yellow; n = 16 orange). Removing the precipitate, reducing the solution in volume to dryness, and recrystallising the resulting solid from acetone/hexane yields a yellow (n = 12, 14) or light orange (n = 16) solid. The F.A.B. mass spectra for all three compounds shows a peak at 55 mass units greater than $[RuCl([n]aneS_4)]$ (n = 12, 14, 16) which corresponds to the ethyl

cyanide complexes, $[RuCl(NCCH_2CH_3)([n]aneS_4)]^{n+}$. Ir spectroscopy confirms the presence of a CN group, with a stretch near υ = 2220 cm^{-1} for all three systems. In the $[12]aneS_4$ and $[16]aneS_4$ cases, no high frequency resonances assignable to an isoxazole complex are observed in the ^1H N.M.R. (d^6-acetone) spectrum . However, in the case of $[14]aneS_4$, a series of weak resonances are observed in the ^1H N.M.R. (d^6-acetone) spectrum (Figure 6.7), which possibly indicates the presence of an isoxazole complex, $[RuCl(NC_3H_3O)[14]aneS_4]PF_6$. As discussed in Section 4.4, CH_3NO_2 contains both ethyl cyanide and trace isoxazole impurities. The resulting complexes from the reaction of $[RuCl_2([n]aneS_4)]$ (n = 12, 14, 16) with $TlPF_6$ in CH_3NO_2 : THF are $[RuCl(NCCH_2CH_3)([n]aneS_4)]PF_6$ (n = 12, 14, 16) and possibly a small amount of $[RuCl(NC_3H_3O)([14]aneS_4)]PF_6$ (n=14).

6.2.2 The reactivity of $[RuCl(PPh_3)([n]aneS_4)](PF_6)$ complexes

The complexes $[RuCl(PPh_3)([n]aneS_4)](PF_6)$ (n = 12, 14, 16) have been synthesised, in the Edinburgh group by reacting $[RuCl_2(PPh_3)_3]$ with $[n]aneS_4$ in refluxing EtOH. The crystal structures of the complexes $[RuCl(PPh_3)([14]aneS_4)]^+$ and $[RuCl(PPh_3)([16]aneS_4)]^+$ have also been determined (Figures 6.8 and 6.9)[242].

The addition of $TlPF_6$ to $[RuCl(PPh_3)([n]aneS_4)]PF_6$ in CH_3NO_2 and THF does not result in any precipitation of TlCl, after stirring for sixteen hours at 298K, or after refluxing for eight hours. This implies that this Cl^- ligand is much more difficult to remove from the complex $[RuCl(PPh_3)([n]aneS_4)]PF_6$ than in $[RuCl_2([n]aneS_4)]$; This is probably due in part to the difference in charge between the complexes. It is interesting to note that $[RuCl(PPh_3)([n]aneS_4)](PF_6)$ (n = 12, 16) reacts with $TlPF_6$ in CH_3CN to afford the complexes $[Ru(NCCH_3)(PPh_3)([12]aneS_4)](PF_6)_2$ and $[Ru(NCCH_3)_2([16]aneS_4)](PF_6)_2$ (Figures 6.10, 6.11)[242], thus indicating that $TlPF_6$ can remove a Cl^- from the complexes $[RuCl(PPh_3)[n]aneS_4)]PF_6$ (n = 14, 16), but only in strongly co-ordinating solvents.

Figure 6.7 The ^{1}H N.M.R. Spectrum (d^{6}-acetone) of the yellow product isolated when $[RuCl_2([n]aneS_4)]$ reacts with $TlPF_6$ in CH_3NO_2

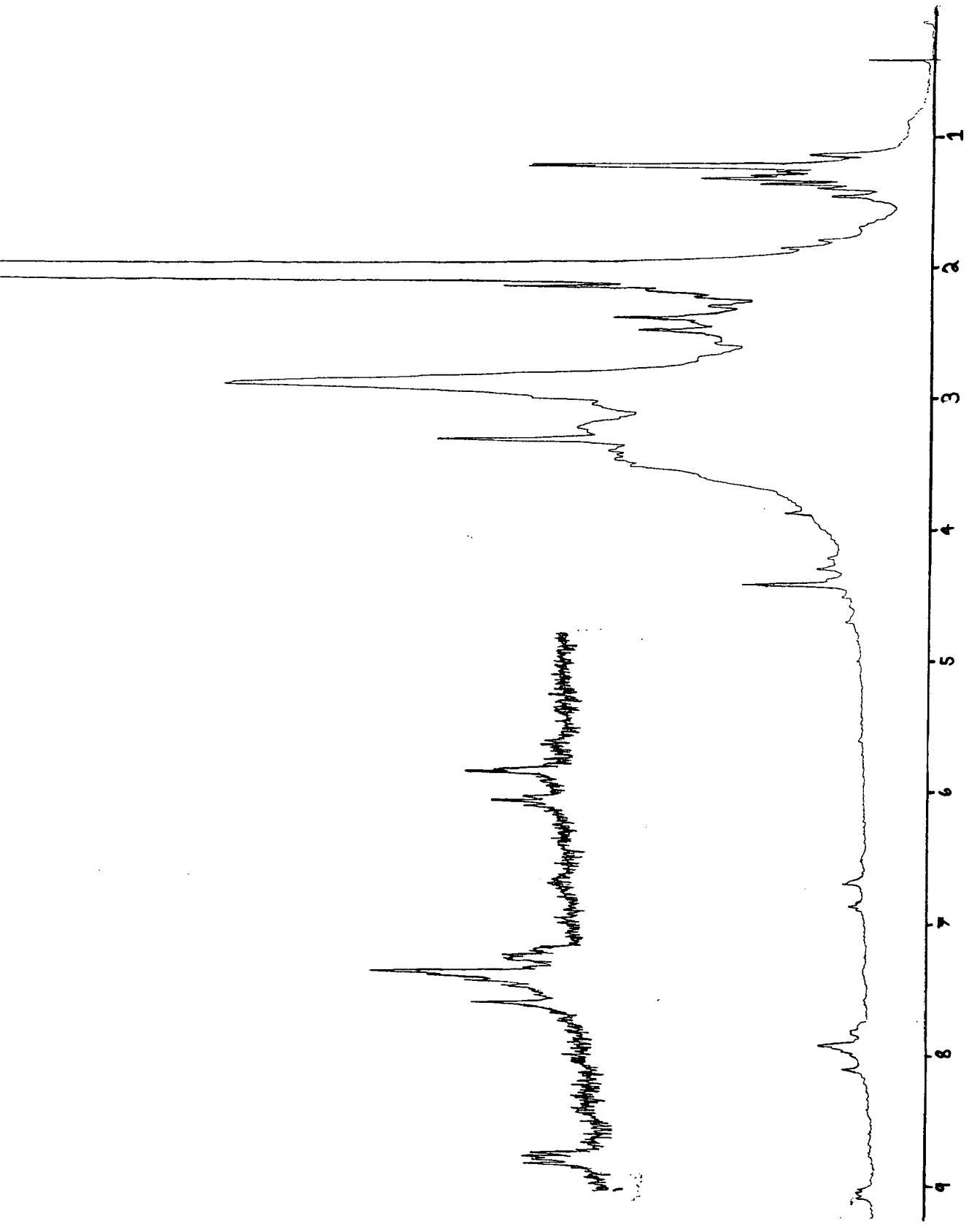

Figure 6.8 A View of the Single Crystal X-Ray Structure of [RuCl(PPh$_3$)([14]aneS$_4$)](PF$_6$)

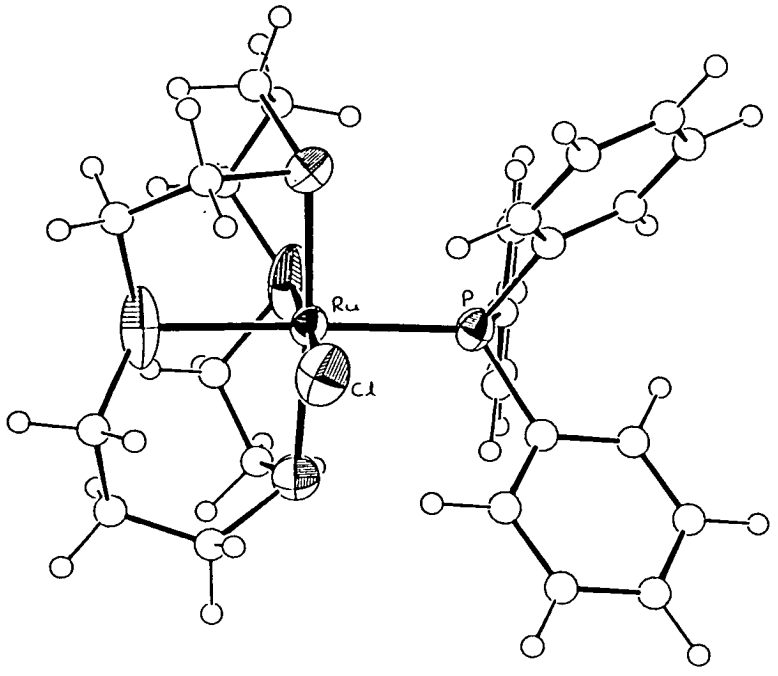

Figure 6.9 A View of the Single Crystal X-Ray Structure of [RuCl(PPh$_3$)([16]aneS$_4$)](PF$_6$)

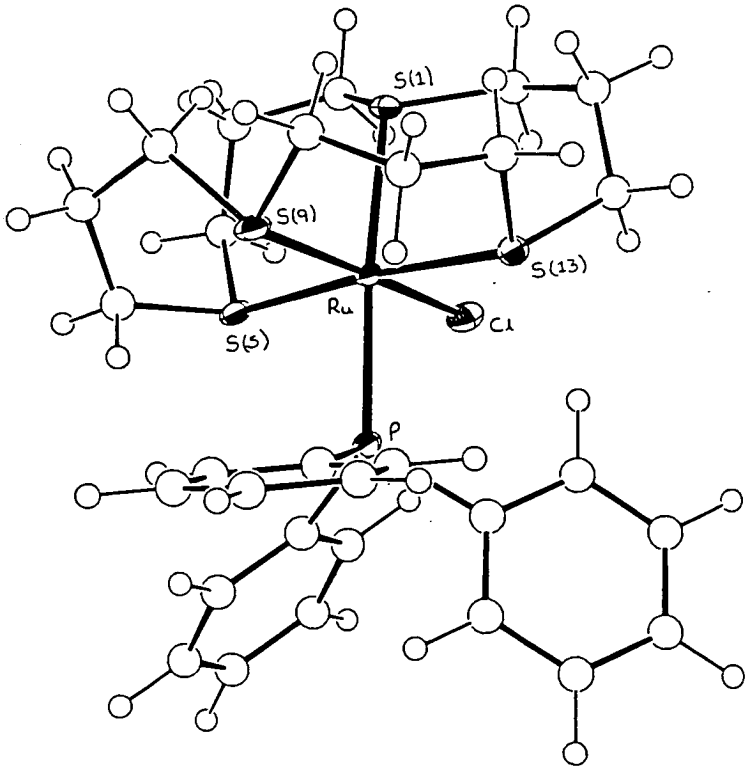

Figure 6.10 A View of the Single Crystal X-Ray Structure of $[Ru(NCCH_3)(PPh_3)([12]aneS_4)](PF_6)_2$

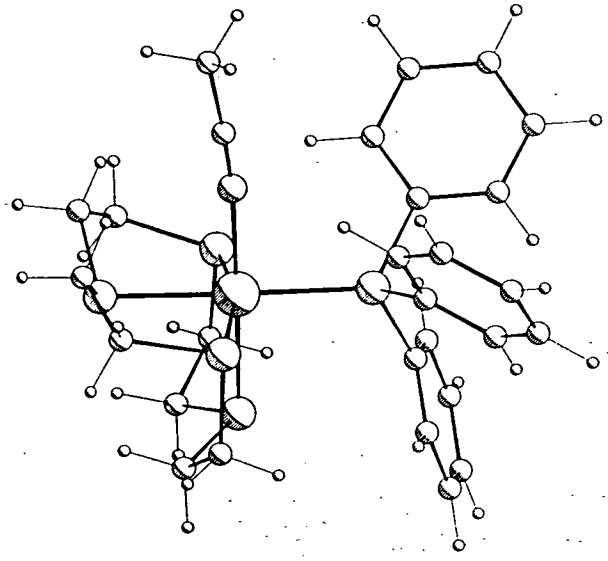

Figure 6.11 A View of the Single Crystal X-Ray Structure of $[Ru(NCCH_3)_2([16]aneS_4)](PF_6)_2$

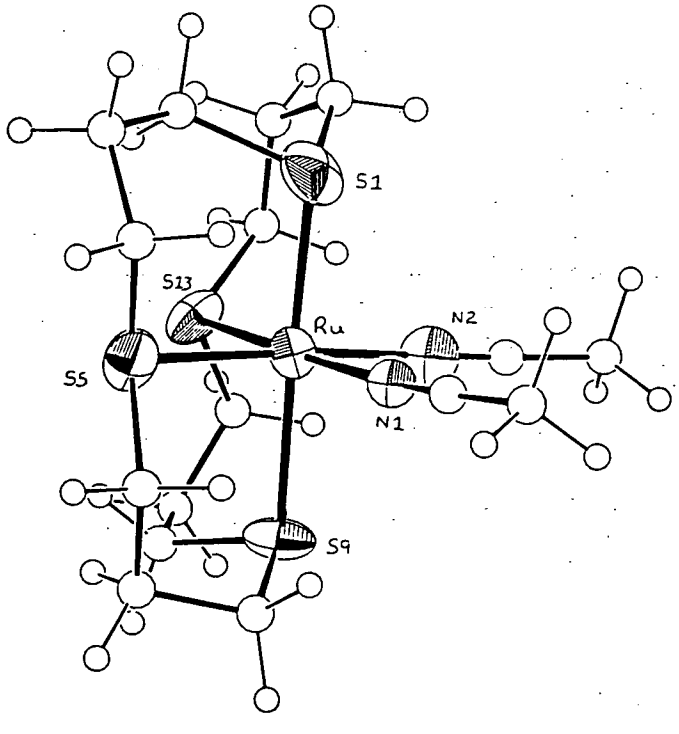

6.3 Rhodium Complexes of [n]aneS$_4$

6.3.1 The reactivity of [RhCl$_2$([n]aneS$_4$)]PF$_6$ complexes (n = 12, 14, 16)

The complexes [RhCl$_2$([n]aneS$_4$)]PF$_6$ (n = 12, 14, 16) have been synthesised, by Busch *et al* and also by the Edinburgh group, by reacting RhCl$_3$.xH$_2$O with [n]aneS$_4$ in refluxing CH$_3$OH under N$_2$, and then adding NH$_4$PF$_6$[374, 375]. Reaction of [RhCl$_2$([n]aneS$_4$)]PF$_6$ (n = 12, 14, 16) with TlPF$_6$ in CH$_3$OH and THF at 298K for sixteen hours results in a white precipitate of TlCl, and a yellow solution. Evaporating the solution to dryness, and recrystallising the residue from acetone/hexane affords a yellow solid which shows resonances in the ^{1}H N.M.R. spectrum (d^6-acetone) at δ = 1.1(m), 2.2–3.5 (m, [n]aneS$_4$) p.p.m., indicating that [n]aneS$_4$ is still present in the product. The F.A.B. mass spectrum of the yellow product shows a peak at 55 mass units greater than [RuCl([n]aneS$_4$)] and the ir spectrum reveals a stretch at υ = 2230cm^{-1} , indicating that the ethyl cyanide, present in CH$_3$NO$_2$, is co-ordinated to the Rh(III) ion. Thus, on reacting [RhCl$_2$([n]aneS$_4$)](PF$_6$) with TlPF$_6$ in CH$_3$NO$_2$ and THF, the complex [RhCl(NCCH$_2$CH$_3$)([n]aneS$_4$)](PF$_6$)$_2$ (n = 12, 14, 16) is formed and can be isolated.

6.3.2 The Synthesis of [RhCl(PR$_3$)([n]aneS$_4$)](PF$_6$)$_2$ Complexes, (n = 12, 14, 16; PR$_3$ = PMe$_2$Ph, PPh$_3$, PCy$_3$)

The reaction of [RhCl$_3$(PR$_2$Ph)$_3$] (R = Et, Me) with [12]aneS$_4$ in refluxing MeOH/EtOH (1 : 2 v/v) for six hours, followed by addition of NH$_4$PF$_6$ yields a yellow solid, which can be recrystallised from CH$_3$CN/diethyl ether. The ir spectrum indicates the presence of [12]aneS$_4$, PF$_6^-$ and PR$_2$Ph. However, the F.A.B. mass spectrum shows signals at m/e = 661, 515, 413, 378, and 343 (for R = Me) which can be assigned to {RhCl(PMe$_2$Ph)([12]aneS$_4$)PF$_6$}$^+$, {RhCl(PMe$_2$Ph)([12]aneS$_4$)}$^+$, {RhCl$_2$([12]aneS$_4$)}$^+$, {RhCl[12]aneS$_4$}$^+$ and {Rh[12]aneS$_4$}$^+$ respectively, indicating that the product is a mixture of

$[RhCl(PR_2Ph)([12]aneS_4)](PF_6)_2$ and $[RhCl_2([12]aneS_4)]PF_6$. Reacting $[RhCl_3(PR_2Ph)_3]$ with $[12]aneS_4$ in a series of solvents results in the desired complex, $[RhCl(PR_2Ph)([12]aneS_4)](PF_6)_2$, together with a significant amount of $[RhCl_2([12]aneS_4)]PF_6$. When two equivalents of $TlPF_6$ are added to the reaction mixture of $[RhCl_3(PR_2Ph)_3]$ and $[12]aneS_4$, $[RhCl_2([12]aneS_4)](PF_6)$ is still formed.

The presence of this $[RhCl_2([12]aneS_4)]PF_6$ and the shortage of suitable starting materials, led us to develop an alternative strategy, which involves reacting $[RhCl_2([n]aneS_4)]PF_6$ with $TlPF_6$ in the presence of an excess of PR_3. The reaction of $[RhCl_2([12]aneS_4)]PF_6$ with $TlPF_6$ and PPh_3 (2 equivalents) under N_2 in refluxing acetone affords a white precipitate of TlCl and a yellow solution. Removal of the TlCl and reduction of the volume of solution, followed by the addition of Et_2O results in a yellow precipitate, which can be collected and recrystallised from CH_3CN/Et_2O. The ir spectrum of the product shows bands at υ cm^{-1}= 1483, 1438, 1416, 833, 558, 526, 511 and 499 indicating the presence of PPh_3, PF_6^- and $[12]aneS_4$ while the ^1H N.M.R spectrum (CD_3CN) confirms the presence of $[12]aneS_4$ and PPh_3 with resonances at δ = 2.5–4.5(m, $[12]aneS_4$) and 7.4–8.0 (m, PPh_3) p.p.m. (Figure 6.12). The F.A.B. mass spectrum of the product shows peaks at m/e = 785, 640 and 378, which are assigned to $\{RhCl(PPh_3)([12]aneS_4)PF_6\}^+$, $\{RhCl(PPh_3)([12]aneS_4)\}^+$, $\{RhCl([12]aneS_4)\}^+$, respectively. The ^{13}C N.M.R. spectrum (CD_3CN) shows resonances in the $[12]aneS_4$ and PPh_3 region, some of which show coupling to ^{103}Rh (Figure 6.13), and in the ^{31}P N.M.R. spectrum (CD_3CN) a doublet at δ = 29.0 (d, J = 96 Hz) p.p.m. and a septet at δ = -145 (septet, J = 710 Hz, PF_6^-) p.p.m. are observed (Figure 6.14), confirming that this complex is $[RhCl(PPh_3)([12]aneS_4)](PF_6)_2$.

The reaction of $[RhCl_2([12]aneS_4)]PF_6$ with PCy_3 or PMe_2Ph and $TlPF_6$ in acetone also results in a white precipitate and a yellow solution from which a yellow solid can be isolated. The resulting yellow products exhibit similar spectral properties to $[RhCl(PPh_3)([n]aneS_4)](PF_6)_2$, which are summarised in Table 6.1

Figure 6.12 The ^1H N.M.R. Spectrum (CD_3CN) of $[RhCl(PPh_3)([12]aneS_4)](PF_6)_2$

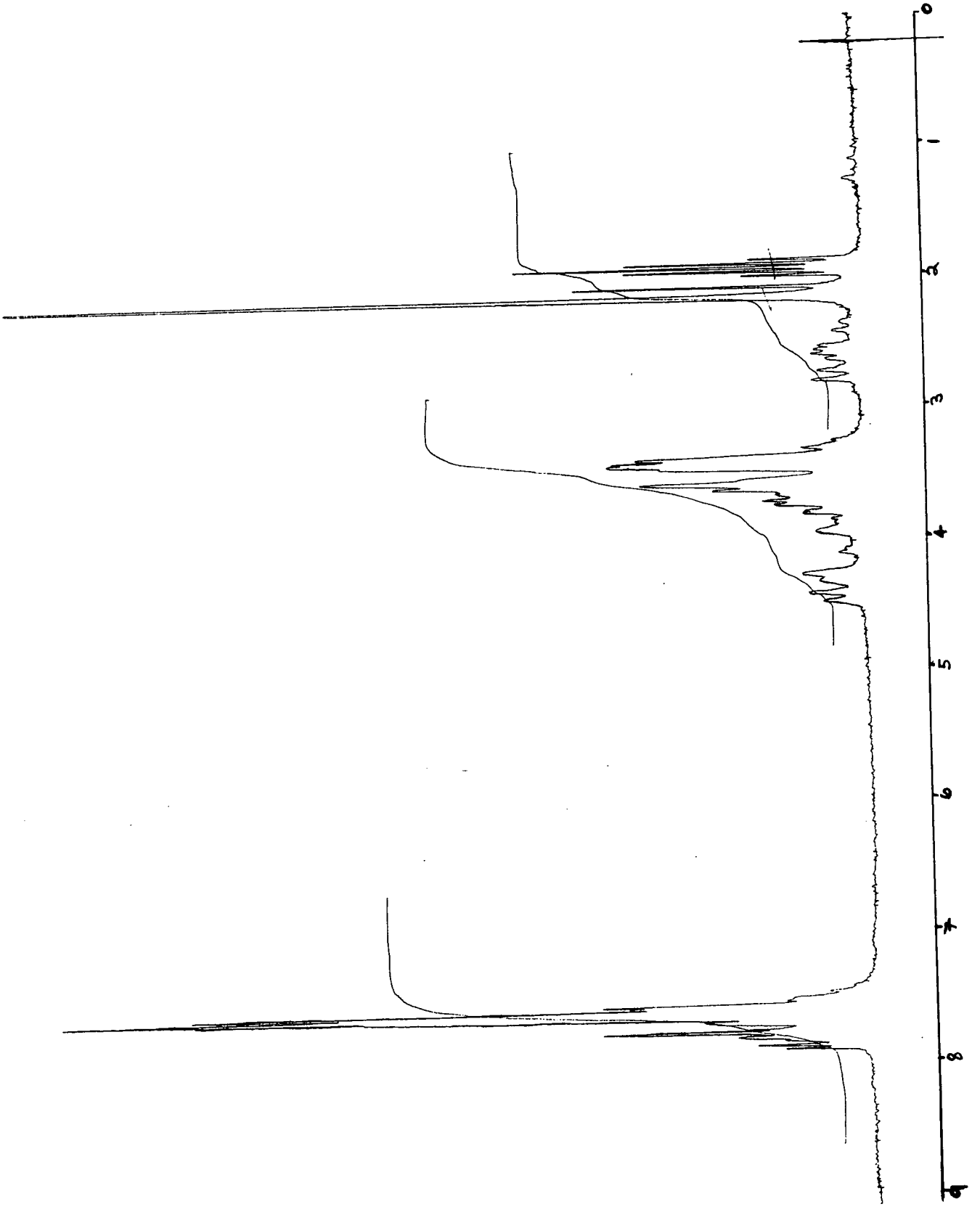

Figure 6.13 The ^{13}C N.M.R. Spectrum (CD_3CN) of $[RhCl(PPh_3)([12]aneS_4)](PF_6)_2$

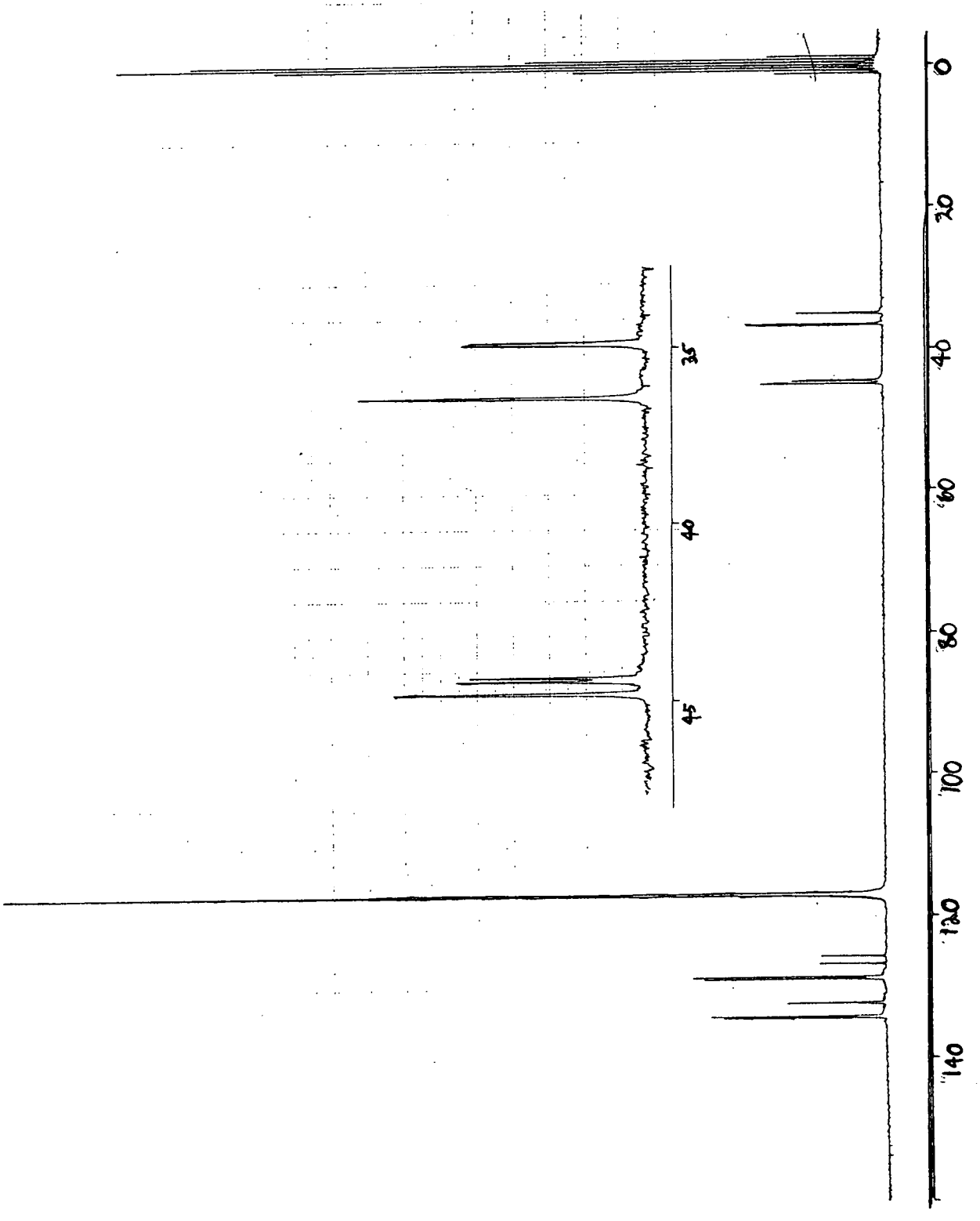

Figure 6.14 The ^{31}P N.M.R. Spectrum (CD_3CN) of $[RhCl(PPh_3)([12]aneS_4)](PF_6)_2$

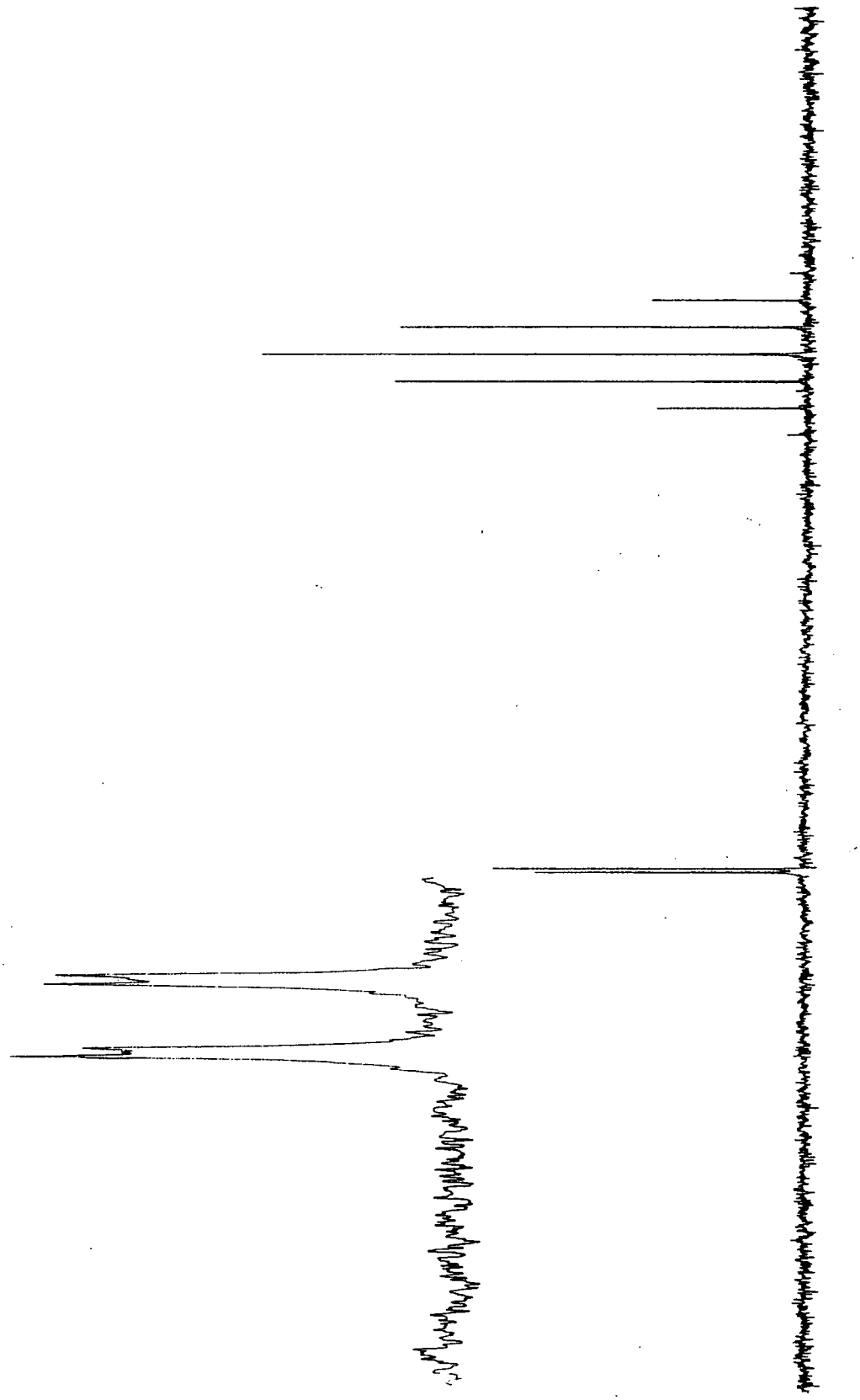

Table 6.1 Selected Spectroscopic Properties of $[RhCl(PR_3)([12]aneS_4)](PF_6)_2$

PR_3	PCy_3	PPh_3	PMe_2Ph
F.A.B. mass spectrum m/e =	803	785	661
	$\{Rh([12]aneS_4)(PCy_3)Cl\ PF_6\}^+$	$\{Rh([12]aneS_4)Cl(PPh_3)PF_6\}^+$	$\{Rh([12]aneS_4)Cl(PMe_2Ph)PF_6\}^+$
m/e =	658	640	515
	$\{Rh([12]aneS_4)(PCy_3)Cl\}^+$	$\{Rh([12]aneS_4)Cl(PPh_3)\}^+$	$\{Rh([12]aneS_4)Cl(PMe_2Ph)\text{-}H\}^+$
^{31}P N.M.R. (CD_3CN) δ = (p.p.m.)	41(d, J = 92 Hz)	29(d, J = 96 Hz)	14(d, J = 90 Hz)

The reaction of $[RhCl_2([14]aneS_4)]PF_6$ with $TlPF_6$ in the presence of two equivalents of PMe_2Ph in refluxing acetone under N_2 results in a white precipitate and a yellow solution. Removing the TlCl, reducing the solvent in volume and adding Et_2O yields a yellow precipitate, which can be collected and recrystallised from CH_3CN/Et_2O. The ir spectrum of the product shows absorbances assignable to $[14]aneS_4$, PMe_2Ph and PF_6^-. The N.M.R. (CD_3CN) spectra confirms the presence of $[14]aneS_4$, PMe_2Ph with the ^1H N.M.R. spectrum showing resonances at δ = 1.1(m), 2.5–3.5(m), 7.5–7.8(m) p.p.m. and the ^{31}P N.M.R. spectra revealing resonances at δ = -145 (septet, J = 710 Hz, PF_6^-) and 13(d, J = 94 Hz) p.p.m. The F.A.B. mass spectrum shows peaks at m/e = 669, 554 and 405, corresponding to $\{RhCl(PMe_2Ph)([14]aneS_3)PF_6\}^+$, $\{Rh([14]aneS_4)Cl(PMe_2Ph)\}^+$ and $\{RhCl([14]aneS_4)\}^+$, respectively.

However, the reaction of $[RhCl_2([14]aneS_4)]PF_6$ with $TlPF_6$ in refluxing acetone in the presence of PR_3 (PR_3 = PPh_3, PCy_3) did not afford a phosphine containing complex. The material isolated seems to be a mixture of starting material and another uncharacterised complex, perhaps $[Rh(solv)Cl([14]aneS_4)](PF_6)_2$. This can be attributed to the steric crowding

around the Rh(III) ion due to the increased size of the PR_3 group[377]. If this is the case, one does not expect that $[RhCl_2([16]aneS_4)](PF_6)$ would react with these phosphines. However, since $[RhCl_2([16]aneS_4)](PF_6)$ is a *trans* isomer, the synthesis of $[RhCl(PR_3)([16]aneS_4)](PF_6)$ may be possible.

The reaction of $[RhCl_2([16]aneS_4)]PF_6$ with $TlPF_6$ in the presence of PR_3 (PR_3 = PPh_3, PCy_3, PMe_2Ph) in refluxing acetone does not yield a phosphine containing complex, and the product is a mixture of the starting material and another complex, possibly $[RhCl(solv)([16]aneS_4)](PF_6)_2$.

To confirm the cis-stereochemistry of the new complexes $[RhCl(PR_3)([n]aneS_4)](PF_6)_2$ (n = 12, PR_3 = PPh_3, PCy_3, PMe_2PH; n = 14, PR_3 = PMe_2PH) crystals of $[RhCl(PPh_3)([12]aneS_4)](PF_6)_2$, suitable for X-ray analysis, were grown by vapour diffusion of Et_2O into an CH_3CN solution of the complex.

6.3.3 The Crystal Structure of $[RhCl(PPh_3)(12]aneS_4)](PF_6)_2$

Selected bond lengths and angles are shown in Table 6.2, and a view of the cation is shown in Figure 6.15.

The X-ray crystal structure shows the Rh(III) ion to be bound octahedrally to the tetrathioether macrocycle [$Rh–S_{(trans\ to\ Cl)}$ = 2.2955(14) Å , $Rh–S_{(trans\ to\ PPh_3)}$ = 2.3712(15), Rh–S = 2.3626(15) and 2.3673(15)Å] , a Cl^- donor [Rh-Cl = 2.3675(14) Å] and PPh_3 ligand [Rh-P = 2.3719(15) Å]. The Cl^- and PPh_3 ligands are in a *cis*-orientation with respect to each other.

In parallel with this work, the Edinburgh group have determined the structure of $[RhCl(PEt_2Ph)([12]aneS_4)](PF_6)_2$ (Figure 6.16). This similar complex also has a cis-configuration of the phosphine and Cl^- donors [Rh–Cl = 2.3567(19)Å, Rh–P = 2.3494(17)Å] , with the Rh(III) ion also co-ordinated to the macrocycle [$Rh–S_{(trans\ to\ Cl)}$ = 2.2869(16), $Rh–S_{(trans\ to\ PR_3)}$ = 2.3825(17)Å , Rh–S = 2.3402(17), 2.3507(17)Å] [286].

A comparison of bond lengths between various Rh(III) structures is shown in Table 6.3 It is interesting to note that in all the complexes studied in this thesis the M–S bond length is shortened when it is trans to a Cl^- donor (see Tables 4.2 and 6.3, as well as the crystal structures discussed in chapters 3 and 5). This implies that M→S π-back-donation occurs in thioether macrocyclic complexes.

Table 6.2 Selected Bond Lengths (Å), Angles (°) and Torsion Angles (°) with standard deviations for $[RhCl(PPh_3)([12]aneS_4)](PF_6)_2$

Rh–Cl	2.3675(14)	C(5)–C(6)	1.525(8)
Rh–S(1)	2.2955(14)	C(6)–S(7)	1.818(8)
Rh–S(4)	2.3673(15)	S(7)–C(8)	1.829(6)
Rh–S(7)	2.3712(15)	C(8)–C(9)	1.505(8)
Rh–S(10)	2.3626(15)	C(9)–S(10)	1.848(6)
Rh–P(1)	2.3719(15)	S(10)–C(11)	1.837(6)
S(1)–C(2)	1.821(6)	C(11)–C(12)	1.503(6)
S(1)–C(12)	1.811(6)	P(1)–C(11)	1.837(3)
C(2)–C(3)	1.515(8)	P(1)–C(21)	1.814(3)
C(3)–S(4)	1.836(6)	P(1)–C(31)	1.828(4)
S(4)–C(5)	1.857(6)		
Cl–Rh–S(1)	178.72(5)	Rh–S(4)–C(3)	100.94(19)
Cl–Rh–S(4)	92.29(5)	Rh–S(4)–C(5)	104.26(19)
Cl–Rh–S(7)	89.67(5)	C(3)–S(4)–C(5)	100.3(3)
Cl–Rh–S(10)	93.56(5)	S(4)–C(5)–C(6)	112.8(4)
Cl–Rh–P(1)	86.58(5)	C(5)–C(6)–S(7)	105.4(4)
S(1)–Rh–S(4)	87.27(5)	Rh–S(7)–C(6)	99.32(20)
S(1)–Rh–S(7)	91.47(5)	Rh–S(7)–C(8)	98.30(20)
S(1)–Rh–S(10)	87.12(5)	C(6)–S(7)–C(8)	106.7(3)
S(1)–Rh–P(1)	92.28(5)	S(7)–C(8)–C(9)	105.9(4)
S(4)–Rh–S(7)	83.31(5)	C(8)–C(9)–S(10)	113.5(4)
S(4)–Rh–S(10)	166.52(5)	Rh–S(10)–C(9)	103.27(19)
S(4)–Rh–P(1)	97.16(5)	Rh–S(10)–C(11)	101.02(19)
S(7)–Rh–S(10)	84.59(5)	C(9)–S(10)–C(11)	99.9(3)
S(7)–Rh–P(1)	176.24(5)	S(10)–C(11)–C(12)	113.6(4)
S(10)–Rh–P(1)	95.30(5)	S(1)–C(12)–C(11)	105.5(4)
Rh–S(1)–C(2)	101.42(19)	Rh–P(1)–C(11)	117.18(12)
Rh–S(1)–C(12)	101.87(19)	Rh–P(1)–C(21)	108.64(12)
C(2)–S(1)–C(12)	106.5(3)	Rh–P(1)–C(31)	115.37(12)
S(1)–C(2)–C(3)	105.1(4)	Rh–P(1)–C(31)	115.37(12)
C(2)–C(3)–S(4)	113.7(4)		
C(12)–S(1)–C(2)–C(3)	161.9(4)	C(5)–C(6)–S(7)–C(8)	163.9(4)
C(2)–S(1)–C(12)–C(11)	-160.8(4)	C(6)–S(7)–C(8)–C(9)	-163.6(4)
S(1)–C(2)–C(3)–S(4)	-59.5(4)	S(7)–C(8)–C(9)–S(10)	55.9(5)
C(2)–C(3)–S(4)–C(5)	-74.9(4)	C(8)–C(9)–S(10)–C(11)	-125.2(4)
C(3)–S(4)–C(5)–C(6)	123.1(4)	C(9)–S(10)–C(11)–C(12)	72.9(5)
S(4)–C(5)–C(6)–S(7)	-54.2(5)	S(10)–C(11)–C(12)–S(1)	59.4(5)

Figure 6.15 The Single Crystal X-Ray Structure of $[RhCl(PPh_3)([12]aneS_4)](PF_6)_2$

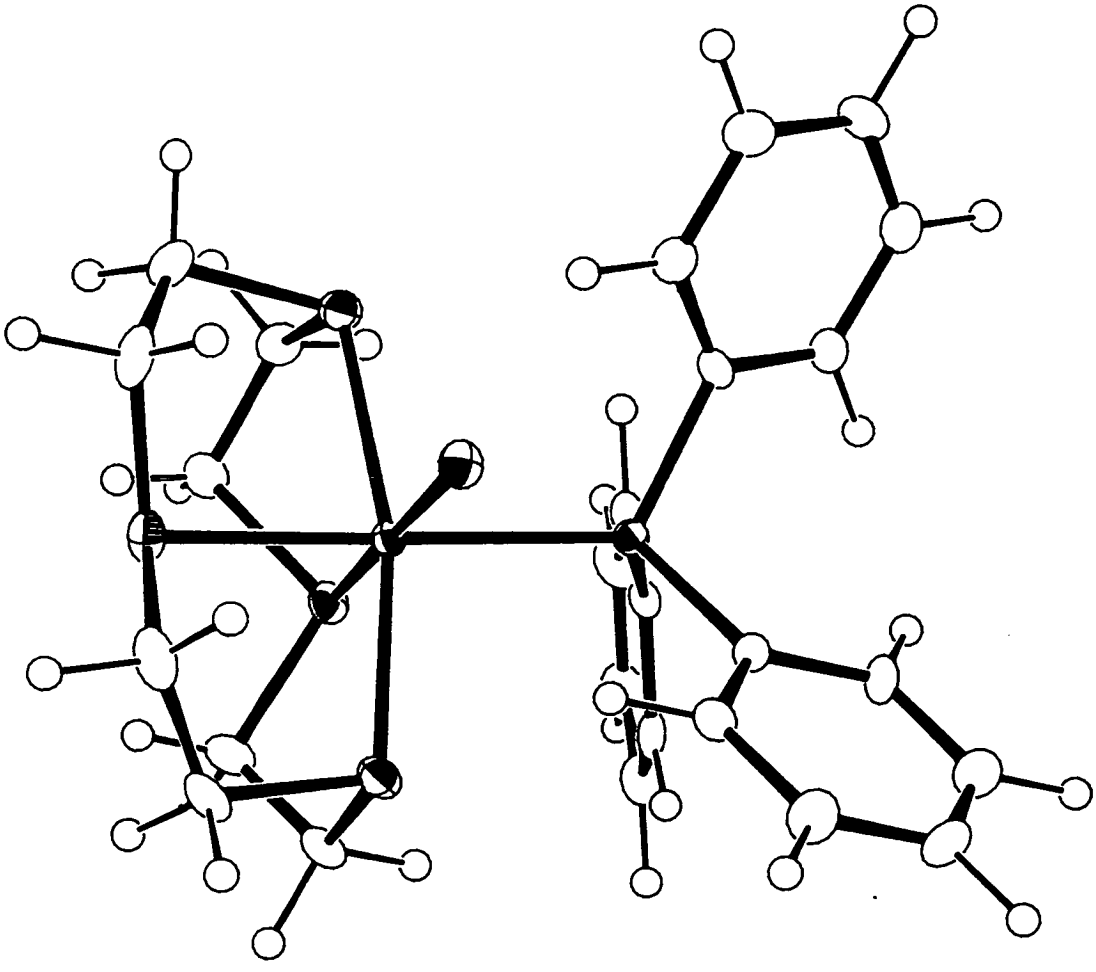

Figure 6.16 The Single Crystal X-Ray Structure of $[RhCl(PEt_2Ph)([12]aneS_4)](PF_6)_2$

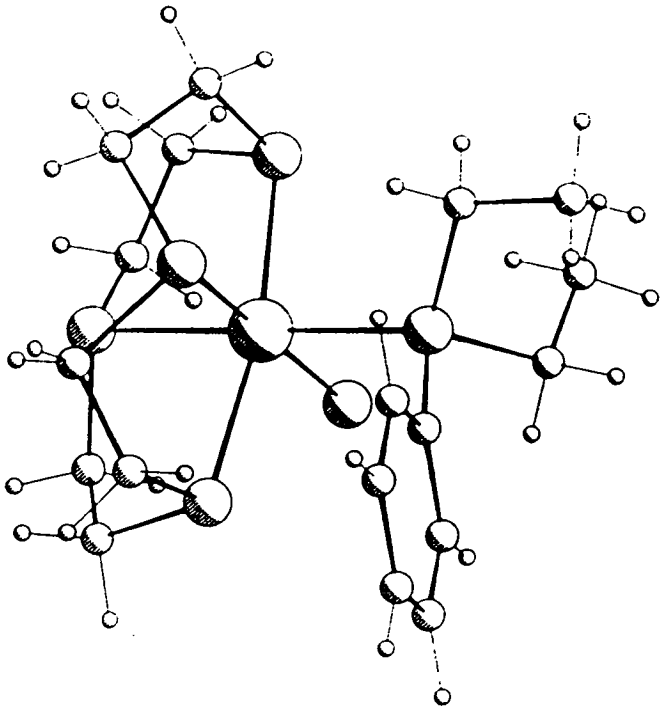

6.3.4 The Reactivity of $[RhCl(PR_3)([n]aneS_4)](PF_6)_2$ with $TlPF_6$

No TlCl precipitate is observed when $[RhClPR_3)([n]aneS_4)](PF_6)_2$ (n = 12, $PR_3 = PPh_3$, PCy_3, PMe_2Ph; n = 14, $PR_3 = PMe_2Ph$) is treated with $TlPF_6$ in CH_3NO_2 and THF at 298K for sixteen hours, nor after refluxing the same mixture for forty eight hours. The removal of a Cl^- from $[MCl(PR_3)([n]aneS_4)](PF_6)_z$ (z = 1, M = Ru, $PR_3 = PPh_3$, n = 12, 14, 16; z = 2, M = Rh, $PR_3 = PPh_3$, PCy_3, PMe_2Ph, n = 12; $PR_3 = PMe_2Ph$, n = 14) does not occur with excess $TlPF_6$ in refluxing CH_3NO_2. This may be due to the difficulty of removing the negatively charged Cl^- from a 1+ or 2+ charged complex. However, it has been shown, in the Edinburgh group, that $[RuCl(PPh_3)([n]aneS_4))]PF_6$ will react with $TlPF_6$ in CH_3CN to form $[Ru(NCCH_3)(PPh_3)([12]aneS_4)]PF_6$ and $[Ru(NCCH_3)_2(PPh_3)([16]aneS_4)]PF_6$[286], this is probably due to CH_3CN being a strongly co-ordinating ligand.

Table 6.3 A Comparison of the Bond Lengths in Rh(III) Tetrathioether Macrocyclic Complexes

	$[RhCl_2([14]aneS_4)]PF_6$	$[RhCl_2([16]ane\ S_4)]PF_6$	$[RhCl(PEt_2Ph)([12]ane\ S_4)](PF_6)_2$	$[RhCl(PPh_3)([12]ane\ S_4)](PF_6)_2$
	Å	Å	Å	Å
Ru–Cl_1	2.3826(12)	2.3391(22)	2.3567(19)	2.3675(14)
Ru–PR_3	—	—	2.3494(17)	2.3917(15)
Ru–S trans to Cl	2.2870(12)	—	2.2869(16)	2.2955(14)
Ru–S trans to P	—	—	2.3825(17)	2.3712(15)
Ru–S trans to S	2.3275(12)	2.3483(25)	2.3402(17)	2.3673(15)
			2.3505(17)	2.3626(15)

6.4 Summary

The synthesis of $[RuCl_2([n]aneS_4)]$ (n = 12, 14, 16) has been achieved by reacting $K_2[RuCl_5(OH_2)]$ with $[n]aneS_4$ in refluxing 2-methoxyethanol for two days. The complexes $[RuCl_2([n]aneS_4)]$ (n = 12, 14) adopt *cis*-configurations, whereas it is proposed that $[RuCl_2([n]aneS_4)]$ adopts a *trans*-configuration. The reaction of $[MCl_2([n]aneS_4)](PF_6)_z$ (z = 0, M = Ru, n = 12, 14, 16; z = 1, M = Rh; n = 12, 14, 16) with $TlPF_6$ in CH_3NO_2 and THF for sixteen hours leads to the formation of $[MCl(NCC_2H_5)([12]aneS_4)](PF_6)_{z+1}$. The only high frequency resonances observed in the ^1H N.M.R. spectra is in the reaction with $[RuCl_2([14]aneS_4)]$ (Figure 6.12) which may indicate that a small amount of $[RuCl(NC_3H_3O)([14]aneS_4)](PF_6)$ is present. The synthesis of $[RhCl(PR_3)([n]aneS_4)](PF_6)_2$ (n = 12, PR_3 = PPh_3, PCy_3, PMe_2PH; n = 14, PR_3 = PMe_2PH) has been achieved by reacting $[RhCl_2([n]aneS_4)](PF_6)$ with $TlPF_6$ and excess PR_3 in refluxing acetone under N_2. No reaction of $[MCl(PR_3)([n]aneS_4)](PF_6)_r$ (r = 1, M = Ru, PR_3 = PPh_3, n = 12, 14, 16; r = 2, M = Rh, n = 12, PR_3 = PPh_3, PCy_3, PMe_2PH; n = 14, PR_3 = PMe_2Ph) was observed with $TlPF_6$ in CH_3NO_2 in the presence of THF, even at reflux, confirming that the second Cl^- is more difficult to remove than the first one.

6.5 Experimental

The physical measurements were carried out as described in Chapters 3 and 4.

Reagents

The reagents were used as described in Chapters 3, 4 and 5. Generous loans of $RhCl_3.nH_2O$ were provided by Johnson-Matthey, PLC. $K_2[RuCl_5(OH_2)]$ was synthesised from of $RhCl_3.nH_2O$ by literature methods[378, 379] and $[RhCl_2([n]aneS_4)](PF_6)$ (n = 12, 14, 16)[374, 375] and $[RuClPPh_3([n]aneS_4)PF_6$ (n = 12, 14, 16)[242] were prepared using previously published procedures. [12]$aneS_4$, [14]$aneS_4$ and [16]$aneS_4$ were purchased from Aldrich, and used without further purification.

6.5.1 Synthesis of $[RuCl_2([14]aneS_4)]$

The complex was prepared as described in the literature[369, 370]. The resulting yellow complex was thoroughly washed with CH_3OH and acetone.

Ir spectrum $\upsilon(cm^{-1})$: 3630(broad, w), 2950(w), 2905(m), 1650(m, broad), 1450(broad, s), 1260(mw), 1241(mw), 1162(ms), 1143(w), 1090(w), 1169(w), 1006(mw), 994(mw), 971(m), 925(m), 905(m), 856(s), 843(m), 814(mw), 699(w), 665(w), 452(w), 430(w), 355(w), 270(mw).

F.A.B. mass spectrum found m/e = 404 and 369;

calculated for $\{^{102}Ru^{35}Cl([14]aneS_4)\}^+$: 404, $\{^{102}Ru([14]aneS_4)\}^+$: 369.

C.H.N.	Expect	27.3%C	4.55%H	0%N	for $[RuCl_2([14]aneS_4)]$
	Found	26.8%C	4.35%H	0.0%N	

6.5.2 The synthesis of $[RuCl_2([12]aneS_4)]$

The complex was synthesised in a similar manner to 6.5.1 except that $[12]aneS_4$ was used.

Ir spectrum $\upsilon(cm^{-1})$: 3630(broad, mw), 2920(ms), 1630(broad, w), 1435(s, broad), 1280(m), 1205(m), 1173(m), 1125(m), 1055(w), 1030(w), 925(mw), 911(mw), 860(ms), 840(mw), 820(m), 345(w), 249(mw).

F.A.B. mass spectrum found m/e = 377 and 345;

calculated for $\{^{102}Ru^{35}Cl([12]aneS_4)\}^+$: 376, $\{^{102}Ru([12]aneS_4)\}^+$: 341.

C.H.N.	Expect	23.3%C	3.88%H	0%N for $[RuCl_2([12]aneS_4)]$
	Found	23.8%C	3.95%H	0.0%N

6.5.3 The synthesis of $[RuCl_2([16]aneS_4)]$

The complex was synthesised in a similar manner to 6.5.1 except that $[16]aneS_4$ was used, and the final product was light pink in colour.

Ir spectrum $\upsilon(cm^{-1})$: 3420(broad, ms), 2904(m), 1652(ms), 1432(ms), 1310(w), 1264(w), 1158(w), 1101(mw), 1061(mw), 1017(ms), 926(m), 883(mw), 872(ms), 842(ms), 769(ms), 649(w), 495(w), 478(w), 340(w), 330(w), 298(mw).

F.A.B. mass spectrum found m/e = 470, 433 and 397;

calculated for $\{^{102}Ru^{35}Cl_2([16]aneS_4)\}^+$: 467$\{^{102}Ru^{35}Cl([16]aneS_4)\}^+$: 432, $\{^{102}Ru([16]aneS_4)\}^+$: 397.

C.H.N.	Expect	23.3%C	3.88%H	0%N for $[RuCl_2([16]aneS_4)]$
	Found	23.8%C	3.95%H	0.0%N

6.5.4 The Reactions of $[RuCl_2([n]aneS_4)]$ with $TlPF_6$ in CH_3NO_2

The reaction was carried out as described in Section 4.7.5, except that $[RuCl_2([n]aneS_4)]$ (n = 12, 14, 16) was used in place of $[RuCl_2(PPh_3)[9]aneS_3)]$.

(a) n = 12

Ir spectrum $\upsilon(cm^{-1})$: 3540(broad, m), 2980(w), 2930(m), 2222(w), 1650(br, mw), 1435(ms, broad), 1283(m), 1206(m), 1175(m), 1125(m), 1065(w), 928(mw), 911(mw), 835(vs, PF_6^-), 558(s), 345(w).

F.A.B. mass spectrum found m/e = 431, 376, 343;

calculated for $\{^{102}Ru(NCCH_2CH_3)^{35}Cl([12]aneS_4)\}^+$: 431,

$\{^{102}Ru^{35}Cl([12]aneS_4)\}^+$: 376, $\{^{102}Ru([12]aneS_4)\}^+$: 341.

^1H N.M.R.spectrum (CD_3CN, 298K) δ = 1.1 (m), 1.28(s), 2.4–3.8(m) p.p.m.

(b) n = 14

Ir spectrum $\upsilon(cm^{-1})$: 3640(broad, m), 2968(mw), 2911(m), 2225(w), 1650(br, mw), 1440(m, broad), 1250(br, m), 1168(ms), 1008(w), 995(w), 970(mw), 925(mw), 835(vs), 558(s), 270(w).

F.A.B. mass spectrum found m/e = 460, 405, 369;

calculated for $\{^{102}Ru(NCCH_2CH_3)^{35}Cl([14]aneS_4)\}^+$: 459,

$\{^{102}Ru^{35}Cl([14]aneS_4)\}^+$: 404, $\{^{102}Ru([14]aneS_4)\}^+$: 369

^1H N.M.R.spectrum (CD_3CN, 298K) δ = 1.2(m), 2.5–3.5(m) and weak resonances at 6.6(m), 6.9(m), 7.9(m), 8.1(m), 9.1(m) p.p.m.

(c) n = 16

Ir spectrum $\upsilon(cm^{-1})$: 3305(broad, ms), 2980(mw), 2906(w), 2235(w), 1650(br, mw), 1435(w), 1312(w), 1103(m), 926(mw), 835(vs), 768(m), 556(vs).

F.A.B. mass spectrum found m/e = 487, 433, 397;

calculated for $\{^{102}Ru(NCCH_2CH_3)^{35}Cl([16]aneS_4)\}^+$: 487,

$\{^{102}Ru^{35}Cl([16]aneS_4)\}^+$: 433, $\{^{102}Ru([16]aneS_4)\}^+$: 397

^1H N.M.R.spectrum (CD_3CN, 298K) δ = 1.08(m), 2.5–3.6(m) p.p.m.

6.5.5 The Reaction of $[RuCl(PPh_3)([n]aneS_4)]PF_6$ with $TlPF_6$ in CH_3NO_2 and THF

The reaction of $[RuCl(PPh_3)([n]aneS_4)]PF_6$ (n = 12, 14, 16) with $TlPF_6$ in CH_3NO_2 and THF was carried out in the same way as described in Section 4.7.5, except that $[RuCl(PPh_3)([n]aneS_4)]PF_6$ (n = 12, 14, 16) was used in place of $[RuCl_2(PPh_3)([9]aneS_3)]$. No white precipitate of TlCl was observed after stirring for sixteen hours at 298K. The mixture was then refluxed for eight hours, but still no precipitation of TlCl occurred. On removal of solvent and

recrystallisation from acetone/hexane the ir and ^1H N.M.R. spectra were identical to the starting material.

6.5.6 The Reaction of $[RhCl_2([n]aneS_4)]PF_6$ with $TlPF_6$ in CH_3NO_2 and THF

The reactions were carried out as described in Section 4.7.5, except that $[RhCl_2([n]aneS_4)]PF_6$ (n = 12, 14, 16) was used in place of $[RuCl_2(PPh_3)([9]aneS_3)]$.

(a) n = 12

Ir spectrum $\upsilon(cm^{-1})$: 3480(broad, m), 3005(sh), 2995(ms), 2930(s), 2228(w), 1630(broad, w), 1418(s), 1295(w), 1281(mw), 1264(mw), 1222(mw), 1096(mw), 995(mw), 929(ms), 908(ms), 835(vs), 695(w), 645(w), 610(w), 556(vs), 440(w), 365(w), 350(w), 295(m), 260(w)

^1H N.M.R.spectrum (CD_3CN, 298K) δ = 1.1 (m), 2.5–4.0(m) p.p.m.

F.A.B. mass spectrum found m/e = 613, 468, 413, 378, 343;

calculated for $\{Rh([12]aneS_4)(NCCH_2CH_3)ClPF_6\}^+$: 613,

$\{^{103}Rh([12]aneS_4)(NCCH_2CH_3)^{35}Cl\}^+$: 468, $\{^{103}Rh([12]aneS_4)^{35}Cl_2\}^+$: 413,

$\{^{103}Rh([12]aneS_4)^{35}Cl\}^+$: 378, $\{^{103}Rh([12]aneS_4)\}^+$: 343

(b) n = 14

Ir spectrum $\upsilon(cm^{-1})$: 3530(broad, ms), 3000(ms), 2932(s), 2230(mw), 1630(mw), 1430(ms), 1405(m), 1278(w), 1263(w), 1221(w), 1099(w), 996(w), 835(vs), 698(mw), 557(vs), 295(w).

^1H N.M.R.spectrum (CD_3CN, 298K) δ = 1.2(m), 2.2–3.9(m) p.p.m.

F.A.B. mass spectrum found m/e = 641, 496, 406;

calculated for $\{^{103}Rh^{35}Cl(NCCH_2CH_3)([14]aneS_4)PF_6\}^+$: 641,

$\{^{103}Rh^{35}Cl(NCCH_2CH_3)([14]aneS_4)\}^+$: 496, $\{^{103}Rh^{35}Cl([14]aneS_4)\}^+$: 406

(c) n = 16

Ir spectrum $\upsilon(cm^{-1})$: 3500(broad, ms), 2970(m), 2920(m), 2245(w), 1630(br, m), 1460(broad, m), 1399(mw), 1270(w), 1230(w), 1080(w), 996(w), 835(vs), 678(m), 557(s).

^1H N.M.R.spectrum (CD_3CN, 298K) δ = 1.25(m), 2.5–3.8(m) p.p.m.

F.A.B. mass spectrum found m/e = 669, 524, 469, 434;

calculated for $\{^{103}Rh([16]aneS_4)^{35}Cl(NCCH_2CH_3)PF_6\}^+$: 669,
$\{^{103}Rh([16]aneS_4)^{35}Cl(NCCH_2CH_3)\}^+$: 524, $\{^{103}Rh^{35}Cl_2([16]aneS_4)\}^+$: 469,
$\{^{103}Rh^{35}Cl([16]aneS_4)\}^+$: 434

6.5.7 The synthesis of $[Rh(PPh_3)Cl([12]aneS_4)](PF_6)_2$

$[RhCl_2([12]aneS_4)](PF_6)$ (60 mg, 1.1×10^{-4} M), $TlPF_6$ (40 mg, 1.1×10^{-4} M) and PPh_3 (59 mg, 2.3×10^{-4} M) was added to acetone (100 cm^3 , dry, degassed) at reflux. After sixteen hours the solution was filtered, reduced in volume and diethyl ether added. The yellow precipitate was collected and recrystallised from acetonitrile/diethyl ether.

Ir spectrum $\upsilon(cm^{-1})$: 3560(broad, ms), 2996(ms), 2942(m), 1701(mw), 1652(mw), 1579(w), 1568(w), 1483(ms), 1434(vs), 1406(vs), 1359(w), 1320(w), 1290(w), 1266(mw), 1255(mw), 1222(vw), 1190(w), 1161(w), 1095(vs), 1085(vs), 995(m), 953(m), 925(m), 835(broad, vs), 751(s), 699(s), 556(vs), 525(s), 518(s), 499(s), 448(m), 430(mw), 355(w), 343(w), 290(mw).

F.A.B. mass spectrum found m/e = 785, 640, 378, 343;
calculated for $\{^{103}Rh([12]aneS_4)(PPh_3)^{35}ClPF_6\}^+$: 785,
$\{^{103}Rh([12]aneS_4)(PPh_3)^{35}Cl\}^+$: 640, $\{^{103}Rh([12]aneS_4)^{35}Cl\}^+$: 378,
$\{^{103}Rh([12]aneS_4)\}^+$: 343

^1H N.M.R.spectrum (CD_3CN, 298K) δ = 3.5–4.5(m) , 7.5–7.8 (m) p.p.m.

^{13}C N.M.R.(DEPT)spectrum (CD_3CN, 298K) δ = 34-45 (CH_2, $[12]aneS_4$), 125-134 (CH, PPh_3) p.p.m.

^{31}P N.M.R.spectrum (CD_3CN, 298K) δ = 29(d, J = 96 Hz), -145(septet, J = 710 Hz, PF_6^-) p.p.m.

C.H.N.	Expect	33.6%C	3.35%H	0%N	for $[Rh(PPh_3)Cl([12]aneS_4)](PF_6)_2$
	Found	33.7%C	3.46%H	0%N	

6.5.8 The crystal structure of $[RhCl(PPh_3)([12]aneS_4)](PF_6)_2$

Crystals suitable for X-ray analysis were grown by vapour diffusion of diethyl ether into a solution of the compound in acetonitrile

Crystal data: $C_{26}H_{31}S_4ClPRh(PF_6)_2$, M = 930.91, monoclinic, $P_{21/c}$,

a = 8.403(4), b = 19.756(12), c = 20.055(13)Å, β = 92.19(4); V = 3327Å^3 [from 2θ values of 16 reflections measured at ±ω ($26 \leq 2\theta \leq 28°$), T = 150 ± 0.1K, λ = 0.710773Å], De = 1.858 gcm^{-3}, Z = 4, F(000) = 1864, pale yellow lath, 0.039 x 0.12 x 0.39 mm, μ(Mo–K_α) = 1.056 mm^{-1}

Data Collection and refinement: Stöe Stadi-4 diffractometer, graphite monochromated Mo–K_α radiation, ω–2θ scans, 4507 data measured ($2\theta_{max} = 45°$, $h = -9 \rightarrow 9$, $k = 0 \rightarrow 21$, $l = 0 \rightarrow 21$), giving 3146 data with $F \geq 4\sigma(F)$. No significant decay or movement of the crystal was observed.

Structure solution and refinement: The Rh position was located by Patterson synthesis[288]. Non-H atoms were located and refined by iterative least squares refinement and Fourier transformations. All non-H atoms with an occupancy greater than 50% were refined anisotropically. H-atoms were included at fixed calculated positions with a fixed μiso. Phenyl rings were constrained as idealised, planar hexagons. At final convergence, $\omega^{-1} = \sigma^2(F) + 0.000109(F)^2$, R = 0.0352 and Rw = 0.0405, S = 1.070 for 389 parameters. For final ΔF synthesis, max and min residues were 0.39 and -0.48eÅ^{-3}. Views of the cation were generated by XP[289], and tables utilised CALC[290]. Scattering factors were inlaid, or taken from Ref. 291.

6.5.9 The synthesis of [RhCl(PCy$_3$)([12]aneS$_4$)](PF$_6$)$_2$

The complex was synthesised as described in 6.5.7, but PCy$_3$ was used in place of PPh$_3$.

Ir spectrum υ(cm^{-1}) : 3500(broad, m), 2932(m), 2852(mw), 1453(mw), 1433(mw), 1418(mw), 1301(vw), 1279(vw), 1210(vw), 1183(vw), 1120(vw), 999(w), 835(vs), 740(w), 556(s).

F.A.B. mass spectrum found m/e = 803, 658, 378;

calculated for {^{103}Rh[12]aneS$_4$)(PCy$_3$)^{35}Cl]PF$_6$}$^+$: 803,

{^{103}Rh[12]aneS$_4$)(PCy$_3$)^{35}Cl]}$^+$: 658, {^{103}Rh[12]aneS$_4$)^{35}Cl]}$^+$: 378

^{1}H N.M.R.spectrum (CD$_3$CN, 298K) δ = 1.2–4.2(m) p.p.m.

^{13}C N.M.R.(DEPT)spectrum (CD_3CN, 298K) δ = 25–29 (CH_2, PCy_3) 33–45 (CH_2, [12]aneS_4) p.p.m.

^{31}P N.M.R.spectrum (d^6-acetone, 298K) δ = 41.0(d, J = 92 Hz), -145(septet, J = 710 Hz, PF_6^-) p.p.m.

C.H.N. Expect 32.9%C 5.10%H 0%N for [Rh(PCy_3)Cl([12]aneS_4)]$(PF_6)_2$

Found 33.5%C 4.98%H 0%N

6.5.10 The synthesis of [RhCl(PMe_2Ph)([12]aneS_4)]$(PF_6)_2$

The complex was synthesised as described in 6.5.7, but PMe_2Ph was used in place of PPh_3.

Ir spectrum $\upsilon(cm^{-1})$: 3500(broad, m), 2998(m), 2947(m), 1653(broad, m), 1433(m), 1290(m), 1110(mw), 952(m), 921(s), 835(vs), 750(m), 726(m), 699(m), 557(s), 490(m), 422(mw).

F.A.B. mass spectrum found m/e = 661, 515, 378;

calculated for $\{^{103}Rh[12]aneS_4)(PMe_2Ph)^{35}ClPF_6\}^+$: 661,

$\{^{103}Rh([12]aneS_4)(PMe_2Ph)^{35}Cl\}^+$: 516, $\{^{103}Rh[12]aneS_4)^{35}Cl\}^+$: 378

^1H N.M.R.spectrum (CD_3CN, 298K) δ = 2.13(s), 2.28(s), 3.0–4.5(m), 7.5–7.75(m) p.p.m.

^{13}C N.M.R.(DEPT) spectrum (CD_3CN, 298K) δ = 12.4 (CH_3, d, J = 38 Hz, PMe_2Ph), 29–45 (CH_2, [12]aneS_4), 128–132 (CH, PMe_2Ph) p.p.m.

^{31}P N.M.R.spectrum (CD_3CN, 298K) δ = 14(d, J = 90 Hz), -145(septet, J = 710 Hz, PF_6) p.p.m.

C.H.N. Expect 23.8%C 3.35%H 0%N for [Rh(PMe_2Ph)Cl([12]aneS_4)]$(PF_6)_2$

Found 23.1%C 3.28%H 0%N

6.5.11 The synthesis of [RhCl(PMe_2Ph)([14]aneS_4)]$(PF_6)_2$

The complex was synthesised as described in 6.5.10 above, except that [$RhCl_2$([14]aneS_4)]PF_6 was used as the Rh(III) starting material.

Ir spectrum $\upsilon(cm^{-1})$: 3510(broad, m), 3002(m), 2948(m), 1650(broad, ms), 1438(m), 1402(m), 1285(m), 1110(mw), 953(m), 920(s), 835(vs), 750(m), 728(m), 703(m), 556(s), 490(m), 422(mw).

F.A.B. mass spectrum found m/e = 669, 554, 405;

calculated for $\{^{103}Rh^{35}Cl(PMe_2Ph)([14]aneS_4)PF_6\}^+$: 669,

$\{^{103}Rh^{35}Cl(PMe_2Ph)([14]aneS_4)\}^+$: 554, $\{^{103}Rh^{35}Cl([14]aneS_4)\}^+$: 405

^1H N.M.R.spectrum (CD_3CN, 298K) δ = 2.05(s), 2.18(s), 2.6–4.1(m), 7.5–7.8(m) p.p.m.

^{13}C N.M.R.spectrum (CD_3CN) δ = 12.7(CH_3, d, J = 42Hz, PMe_2Ph) , 34–45 (CH_2, [14]aneS_4), 128–132 (CH, PMe_2Ph) p.p.m.

^{31}P N.M.R.spectrum (CD_3CN, 298K) δ = 13(d, J = 94 Hz), -145(septet, J = 710 Hz, PF_6^-) p.p.m.

C.H.N. Expect 36.5%C 3.81%H 0%N for $[Rh(PPh_3)Cl([12]aneS_4)](PF_6)_2$

Found 27.3%C 3.90%H 0%N

6.5.12 The Reaction of $[RhCl(PR_3)([n]aneS_4)](PF_6)_2$ with $TlPF_6$ in CH_3NO_2 and THF

$[RhCl(PPh_3)(12]aneS_4)](PF_6)_2$ (75 mg, 8.0×10^{-5} M) and $TlPF_6$ (55 mg, 1.5×10^{-4} M) was added to CH_3NO_2 : THF (5 cm^3 , 4 : 1, v/v) and stirred for sixteen hours. No white precipitate was observed. The system was then refluxed for a further forty-eight hours, but still no precipitate was seen. The solvent was removed, and the yellow solid recrystallised from acetonitrile and diethyl ether. The infrared and ^1H N.M.R. spectra were identical to the starting material, $[RhCl(PPh_3)(12]aneS_4)](PF_6)_2$.

When the reaction was repeated using $[Rh(PR_3)Cl([n]aneS_4)](PF_6)_2$ (PR_3 = PMe_2Ph, PCy_3, n = 12, n = 14, PR_3 = PMe_2Ph) similar results were observed.

6.5.13 Attempted synthesis of $[RhCl(PR_3)([12]aneS_4)](PF_6)_2$ from $[Rh(PR_3)_3Cl_3]$ ($PR_3 = PMe_2Ph, PEt_2Ph$)

(a) $[RhCl_3(PMe_2Ph)_3]$ (98 mg, 0.156 mM), $[12]aneS_4$ (42 mg, 0.156 mM) and $AgPF_6$ (98 mg, 0.390 mM) were added to EtOH ($50cm^3$) under N_2, refluxed for sixteen hours and the solvent reduced in volume. Diethyl ether was then added, the precipitate collected and recrystallised from acetonitrile/diethyl ether.
Ir spectrum $\upsilon(cm^{-1})$: 3600(broad, ms), 2970(mw), 2920(mw), 1650(broad, m), 1450(m), 1430(ms), 1406(m), 1262(mw), 1171(ms), 1098(mw), 935(m), 835(vs), 750(m), 626(mw), 557(s), 529(m), 508(mw), 427(w).
F.A.B. mass spectrum found m/e = 661, 515, 413, 378, 343,
$\{^{103}Rh^{35}Cl(PMe_2Ph)([12]aneS_4)PF_6\}^+$: 661, $\{^{103}Rh^{35}Cl(PMe_2Ph)([12]aneS_4)\}^+$: 516, $\{^{103}Rh^{35}Cl_2([12]aneS_4)\}^+$: 413, $\{^{103}Rh^{35}Cl([12]aneS_4)\}^+$: 378, $\{^{103}Rh([12]aneS_4)\}^+$: 343

(b) The reaction was carried out in the refluxing solvents under N_2 in conditions shown in Table 6.4, the results were similar to (a) above, and are shown in Table 6.4

Table 6.4 Experimental Conditions for the Reaction of $[12]aneS_4$ with $[Rh(PMe_2Ph)_3Cl_3]$

Solvent	Volume cm^3	Counter ion	Products $[RhCl_2[12]aneS_4]PF_6$	Products $[Rh(PMe_2Ph)Cl([12]aneS_4)](PF_6)_2$
MeOH	5	NH_4PF_6	√	×
EtOH	10	NH_4PF_6	√	×
MeOH	50	$AgPF_6$	√	√
MeOH/EtOH	100	NH_4PF_6	√	√
MeOH/EtOH	100	$AgPF_6$	√	√
Acetone	50	NH_4PF_6	√	√
CH_3NO_2	50	$TlPF_6$	√	√
Acetone	50	$TlPF_6$	√	√

(c) The reaction was carried out as described in (a) above, except that $[RhCl_3(PEt_2Ph)_3]$ (104 mg, 1.17×10^{-4} M) was used in place of $[RhCl_3(PMe_2Ph)_3]$. The results were similar to (a) above and are shown in Table 6.5.

F.A.B. mass spectrum found m/e = 689, 543, 413, 378, 343;

calculated for $\{^{103}Rh(PEt_2Ph)^{35}Cl[12]aneS_4)PF_6\}^+$: 689,

$\{^{103}Rh(PEt_2Ph)^{35}Cl[12]aneS_4)\}^+$: 543. For the assignment of the rest of the peaks see (a) above.

Table 6.5 Experimental Conditions for the Reaction of [12]aneS$_4$ with [Rh(PEt$_2$Ph)$_3$Cl$_3$]

			Products	
Solvent	Volume cm^3	Counter ion	$[RhCl_2[12]aneS_4]PF_6$	$[Rh[12]aneS_4PEt_2CyCl(PF_6)_2$
MeOH	10	NH_4PF_6	√	×
EtOH	50	$AgPF_6$	√	√
Acetone	50	$TlPF_6$	√	√
CH_3NO_2	50	$TlPF_6$	√	√
CH_3CN	50	$TlPF_6$	√	√

6.5.14 Attempted synthesis of [RhCl(PR$_3$)([14]aneS$_4$)](PF$_6$)$_2$ (PR$_3$ = PPh$_3$, PCy$_3$)

The reaction was carried out as described in 6.5.7, except that $[RhCl_2([14]aneS_4)]PF_6$ and PPh_3 or PCy_3 were used in the conditions shown in Table 6.6.

Table 6.6 Experimental Conditions for the Attempted Synthesis of [Rh(PR$_3$)Cl[14]aneS$_4$](PF$_6$)$_2$ from [RhCl$_2$([14]aneS$_4$)]PF$_6$

PR3	Solvent	Vol cm^3	Time hrs	Conditions	Dehalogenating agent	Product
PPh3	Acetone	100	16	Reflux/N_2	$TlPF_6$ (1 equiv)	A
PPh3	CH_3NO_2	100	16	Reflux/N_2	$TlPF_6$ (1 equiv)	A
PPh3	CH_3CN	100	16	Reflux/N_2	$TlPF_6$ (1 equiv)	A
PPh3	Acetone	25	24	Reflux/N_2	$TlPF_6$ (2 equiv)	A
PCy3	Acetone	100	16	Reflux/N_2	$TlPF_6$ (1 equiv)	A
PCy3	CH_3NO_2	100	16	Reflux/N_2	$TlPF_6$ (1 equiv)	A
PCy3	CH_3CN	100	16	Reflux/N_2	$TlPF_6$ (1 equiv)	A

Notes

Product A

Ir spectrum $\nu(cm^{-1})$: 3600(broad, s), 3010(w), 2996(w), 2920(w), 1650(broad, m), 1570(mw), 1440(broad, m), 1405(m), 1260(mw), 1178(m), 926(m), 835(vs), 750(m), 626(mw), 557(s), 499(w), 430(w).

F.A.B. mass spectrum found m/e = 405, 371;

calculated for $\{^{103}Rh^{35}Cl([14]aneS_4)\}^+$: 406, $\{^{103}Rh([14]aneS_4)\}^+$: 371

^1H N.M.R.spectrum (CD_3CN, 298K) δ = 2.8–3.9(m) p.p.m.

^{31}P N.M.R.spectrum (CD_3CN, 298K) δ = -145(septet, J = 710 Hz, PF_6^-) p.p.m.

6.5.17 Attempted synthesis of $[RhCl(PR_3)([16]aneS_4](PF_6)_2$ (PR_3 = PMe_2Ph, PPh_3, PCy_3)

The reaction was carried out as described in 6.5.7, except that $[RhCl_2([16]aneS_4]PF_6$ was used in the conditions shown in Table 6.7.

Table 6.7 Experimental Conditions for the Attempted Synthesis of $RhCl(PR_3)[16]aneS_4](PF_6)_2$ from $[RhCl_2([16]aneS_4)]PF_6$

PR_3	Solvent	Vol cm^3	Time hrs	Conditions	Dehalogenating agent	Product
PMe_2Ph	CH_3NO_2	100	16	Reflux/N_2	$TlPF_6$ (1 equiv)	B
PMe_2Ph	Acetone	100	16	Reflux/N_2	$TlPF_6$ (1 equiv)	B
PMe_2Ph	CH_3CN	50	24	Reflux/N_2	$TlPF_6$ (1 equiv)	B
PPh_3	CH_3NO_2	100	16	Reflux/N_2	$TlPF_6$ (2 equiv)	B
PPh_3	Acetone	100	24	Reflux/N_2	$TlPF_6$ (2 equiv)	B
PPh_3	CH_3CN	50	16	Reflux/N_2	$TlPF_6$ (1 equiv)	B
PCy_3	CH_3NO_2	100	24	Reflux/N_2	$TlPF_6$ (1 equiv)	B
PCy_3	Acetone	100	16	Reflux/N_2	$TlPF_6$ (1 equiv)	B
PCy_3	CH_3CN	50	16	Reflux/N_2	$TlPF_6$ (1 equiv)	B

Notes

Product B

Ir spectrum $\upsilon(cm^{-1})$: 3520(broad, m), 3005(w), 2940(w), 1650(mw), 1530(mw), 1435(m), 1410(m), 1261(mw), 1175(m), 945(m), 905(mw), 874(m), 835(vs), 773(m), 628(mw), 557(s), 499(w), 430(w).

F.A.B. mass spectrum found m/e = 435, 399;

calculated for $\{^{103}Rh^{35}Cl([16]aneS_4)\}$: 434, $\{^{103}Rh([16]aneS_4)\}$: 399

Chapter 7

THE OXIDATION OF [9]aneS$_3$

7.1 Introduction

This chapter describes the synthesis of the trisulfone, O$_6$[9]aneS$_3$ and the attempted synthesis of the trisulfoxide, O$_3$[9]aneS$_3$. These compounds are illustrated in Figure 7.1.

Figure 7.1 The Ligands Discussed in Chapter 7

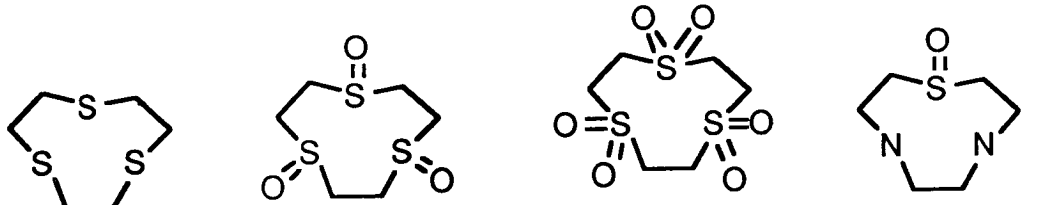

Trithioether Trisulfoxide Trisulfone

In cyclic sulfoxides, a number of isomers are possible which depend upon the orientation of the O-atom with respect to the conformation of the ring (Figure 7.2). These *cis* and *trans* isomers exhibit different chemical and spectroscopic properties. This is exemplified in the ^{1}H N.M.R. spectra for a series of thian-1-oxide derivatives ($C_5R_{10}SO$) in which an axially orientated S=O bond has been found to deshield the syn 1,3 axial hydrogens by as much as 1 p.p.m. compared to its equatorial isomer (see Table 7.1)[380]. N.M.R. spectroscopy has not proven to be a good method of detecting previously uncharacterised cyclic sulfoxides, since no reliable method for predicting the position of the ^{1}H or ^{13}C N.M.R. resonance exists. However, in ir spectroscopy, the position of the strong band at 1060–1030 cm^{-1} assigned to S=O stretching vibration , υ_{SO}, of a sulfoxide, is not affected by the conformation of the ring, and thus, ir spectroscopy is an excellent method for detecting the presence of a sulfoxide in a compound[381, 382].

Ir spectroscopy is also of great use in detecting sulfones, since a sulfone shows two strong bands in its ir spectrum at υ_{SO_2} = 1340 to 1400 cm^{-1} and 1160 to 1140 cm^{-1} assigned to the assymetric and symetric stretches of the SO_2 group, υ_{so_2}respectively.

Figure 7.2 Cis and Trans Isomerisation in Cyclic Sulfoxides.

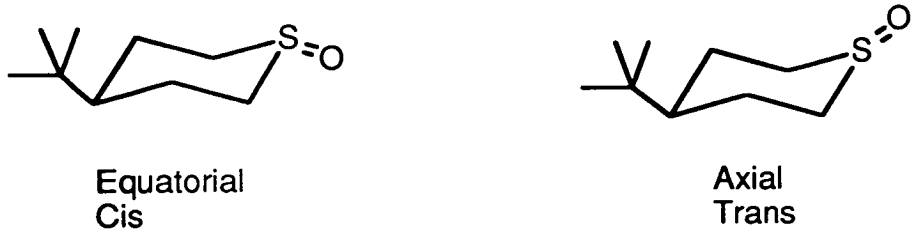

Equatorial
Cis

Axial
Trans

Table 7.1 ^1H and ^{13}C N.M.R. spectral data of t-butylthian-1-oxide

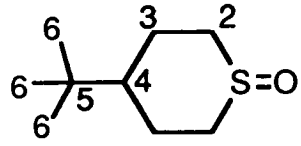

^1H N.M.R. (δ p.p.m.)

Atom	Cis compound	Trans compound	Difference δcis–δtrans
$H_2(ax)$	2.53	2.30	0.23
$H_2(eq)$	3.36	3.00	0.36
$H_3(ax)$	1.42	2.10	-0.68
$H_3(eq)$	2.06	1.70	0.36
H_4	1.30	1.14	0.16
H_6	0.86	0.90	-0.04

^{13}C N.M.R. (δ p.p.m.)

Atom	Cis compound	Trans compound	Difference δcis–δtrans
C_2	52.4	46.9	5.5
C_3	24.4	16.9	7.5
C_4	48.0	47.3	0.7
C_5	32.5	33.6	-0.5
C_6	27.6	27.3	0.3

The S=O bonds in sulfones are both shorter (1.43 Å Vs 1.49Å) and stronger (bond dissociation energy per S–O bond of 469 Vs 368 $kjmol^{-1}$) than those in sulfoxides. In fact, the S=O bond in a sulfone is one of the strongest bonds known[383]. The formation of a sulfone is consequently thermodynamically more likely than the formation of two sulfoxides. This situation creates

synthetic difficulties in oxidising thioethers to sulfoxides, since sulfones may also be synthesised (Figure 7.3).

Figure 7.3 The General Synthesis of Sulfoxides and Sulfones

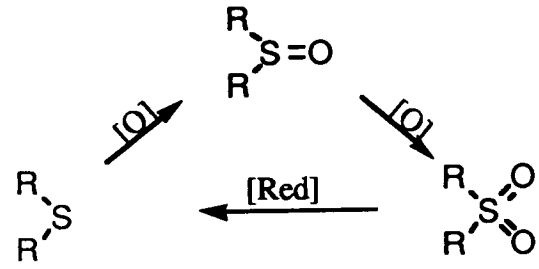

There are a number of reviews in the literature discussing the synthesis of sulfoxides, most of which involve the oxidation of a thioether[381, 383-385]. The methods for reducing sulfones have also been reviewed, but these usually only produce thioethers[386, 387]. A very wide range of oxidising agents have been used for the conversion of thioethers to sulfones, but the specific oxidation to a sulfoxide is synthetically difficult, and requires stoichiometric quantities of highly selective oxidising agents.

The problems encountered in the synthesis of linear polysulfoxides lie in the formation of sulfones and other unwanted products such as sulfoxides (Scheme 7.1) and problems may also arise in the separation of the different isomers and compounds formed during the oxidation[353]. Furthermore, in the synthesis of cyclic sulfoxides, ring opening has also proved to be a serious problem, especially in 3, 4 or 5 membered rings. For example, heating the 3-membered cyclic sulfoxide, C_2H_4SO results in bond cleavage to form an isomeric linear compound[353]. However, both in principle and in practice the properties and chemical behaviour of cyclic sulfoxides and sulfones with a ring size greater than 7 are usually similar to their acyclic analogues[381].

Scheme 7.1 Oxidation to Polysulfoxides

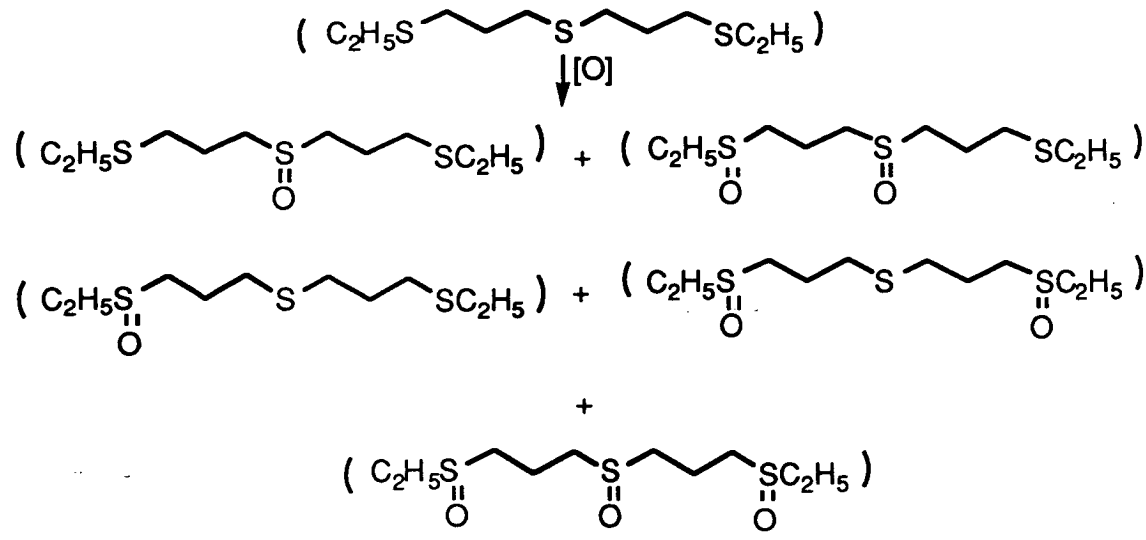

The presence of more than one thioether in a ring makes any selective oxidation intrinsically more difficult. In general, these cyclic polysulfoxides are generally much less stable and much more reactive to further oxidation than their open-chain analogues[383]. No general synthetic methods are available for the synthesis of pure sulfoxides, and during their synthesis sulfones are frequently generated (Scheme 7.2)[383]. However, in some cases, the synthesis of cyclic polysulfoxides can be achieved. Some examples are illustrated in Scheme 7.3.

Scheme 7.2 The Unselective Oxidation of Thioethers

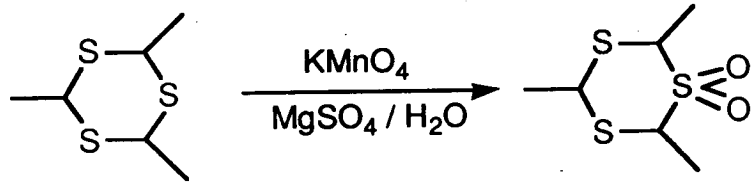

Scheme 7.3 The Selective Oxidation of Thioethers

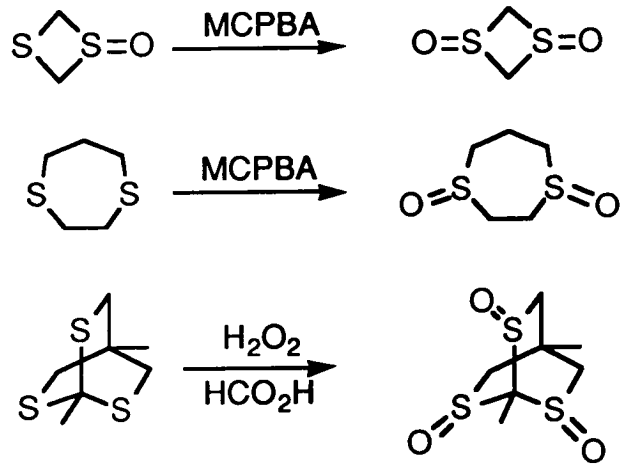

Cyclic polythioethers can be electrochemically oxidised to form a number of products, usually involving C–S bond cleavage and S···S bond formation, although sulfoxides have also been synthesised (Scheme 7.4)[388]. During photo-oxidation, similar C–S bond cleavage and S···S bond formation occurs (Scheme 7.5)[386].

Scheme 7.4 The Electrochemical Oxidation of Thioethers

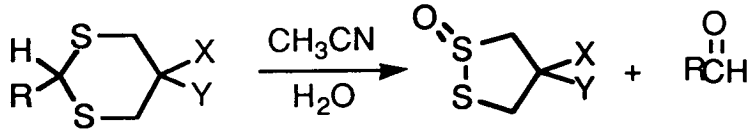

R = ^{t}Bu, p-$CH_3OC_6H_4$; X = H, OH, OCH_3, $OSi(CH_3)_2(^tBu)$
Y= H, OH, $OSi(CH_3)_3$, $OSi(CH_3)_2(^tBu)$; XY= OCH_2CH_2O

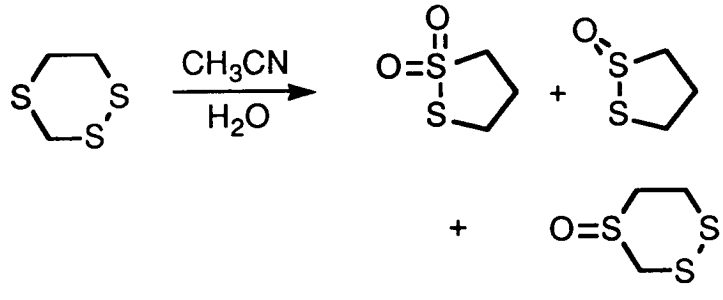

Scheme 7.5 The Photochemical Oxidation of Thioethers

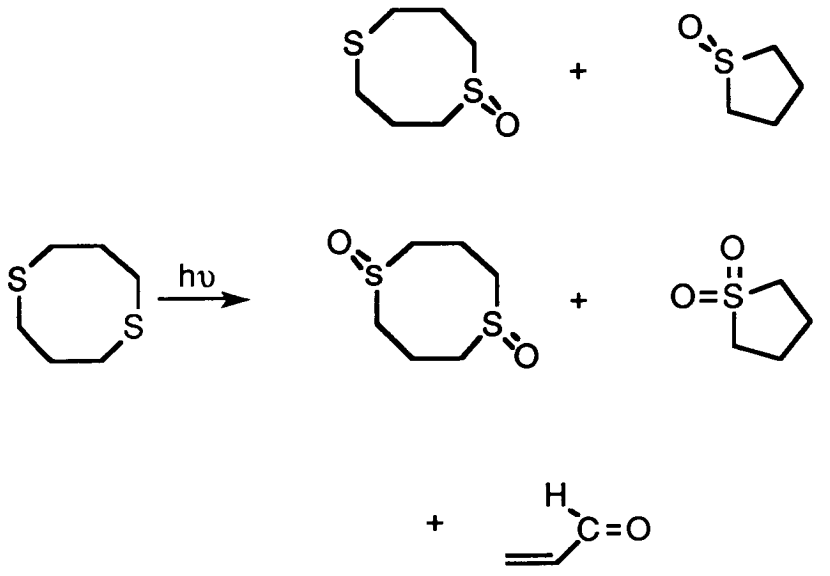

Oxidation of 9-membered thioether macrocycles has been previously studied . The compound, O[9]aneN_2S has been prepared by oxidation of [9]aneN_2S with $NaBrO_2$[389]. The oxidation of [9]aneS_3 in dry anaerobic conditions using one molar equivalent of $PhC^+PF_6^-$ in CH_3NO_2 results in the formation of a bicylclic sulfonium salt $[C_6H_{11}S_3]^+$, whose structure consists of a fused 5- and 6-membered ring, with the sulfonium S-atom at the bridgehead (Figure 7.4). This has been confirmed by X-Ray crystallography[390]. The electrochemical oxidation of [9]aneS_3 in CH_3CN (in 0.1 M $TBAPF_6$) shows an irreversible oxidation at Epa = +0.98V vs Fc/Fc^+, with a return wave being observed at Epc = 0.5 V. This electrochemical oxidation has been assigned as the formation of a dithioether dication (Figure 7.5)[390]. The trisulfone, O_6[9]aneS_3 has been synthesised by reacting [9]aneS_3 in refluxing H_2O_2 for 10 minutes, but the compound was only characterised on the basis of its ir spectrum.[391].

Figure 7.4 A Representation of the Sulfonium Salt, $[C_6H_{11}S_3]^+$

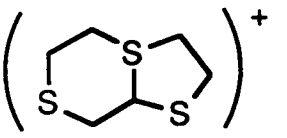

Sulfonium Salt
$[C_6H_{11}S_3]^+$

Figure 7.5 A Representation of the Dithioether Dication

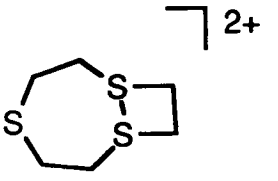

In recent years, great interest has been shown in mixed donor macrocycles, since they can exhibit unusual chemical properties. Since the target compound O_3[9]aneS_3 is a trisulfoxide, it could co-ordinate through either the O or the S atoms, in an ambivalent manner similar to DMSO.

Crystallographic studies on a series of DMSO complexes of transition metal ions show that the internal geometry of DMSO is largely unaffected on co-ordination (Table 7.2)[406]. When DMSO co-ordinates to a metal ion *through the S-donor*, the S–O bond length shortens from the free ligand value of 1.531Å[407] , however, when DMSO co-ordinates to a metal ion *through the O-donor*, the S–O bond length does not change appreciably. This is illustrated in the complex, $[Ru(DMSO)_6]^{2+}$ which clearly shows this trend in its DMSO bond lengths [$Ru–S_{(S\text{-bound})}$ = 1.482 Å and $R–S_{(O\text{-bound})}$ = 1.536 Å][265]

Table 7.2 The Internal Geometry of Free and Co-ordinated DMSO

	Free DMSO	Co-ordinated DMSO
<OSO	106.7°	≈ 107°
<CSC	97.4°	from 99.4(6)° to 104.5(7)°
C–S bond length	1.8Å	1.8Å

The effect on the metal-S bond length when a thioether is oxidised to a sulfoxide has been studied in the complexes $[Pt(H_2NCH(CO_2H)CH_2SMe)Cl_2]$ and $[Pt(H_2NCH(CO_2H)CH_2SMe)Cl_2]$. The Pt–S bond length is 2.26 Å in the thioether case and when the sulfur is oxidised to a sulfoxide Pt–S bond length shortens to 2.198Å[392, 393]. It would be interesting to compare the trisulfoxide, O_3[9]aneS_3 complexes of transition metal ions with their thioether ([9]aneS_3) analogues, to see what effect the oxidation of [9]aneS_3 has on its chemical, physical and co-ordinative properties.

A number of 9-membered sulfoxide-containing macrocyclic complexes have been reported[389, 391]. The complexes $[M(O[9]aneN_2S)_2]^{2+}$ (M = Co, Cu, Ni) have been synthesised in which the metal ion binds to the oxygen in the sulfoxide [389]. [9]aneS_3 has been oxidised to the monosulfoxide, in the complex $[Fe(O[9]aneS_3)([9]aneS_3)]^{2+}$ by reacting $[Fe([9]aneS_3)_2]^{2+}$ with $Na_2S_2O_8$ in H_2O. In this complex, $[Fe(O[9]aneS_3)([9]aneS_3)]^{2+}$, the sulfoxide is co-ordinated through the S-donor (Figure 7.6)[391].

The synthesis and characterisation of the trisulfone O_6[9]aneS_3 is described in section 7.2 and the attempted synthesis of the polysulfoxide O_3[9]aneS_3 using the common selective oxidisation methods is described in section 7.3.

Figure 7.6 A View of the Single Crystal X–Ray Structure of $[Fe(O[9]aneS_3)([9]aneS_3)]^{2+}$

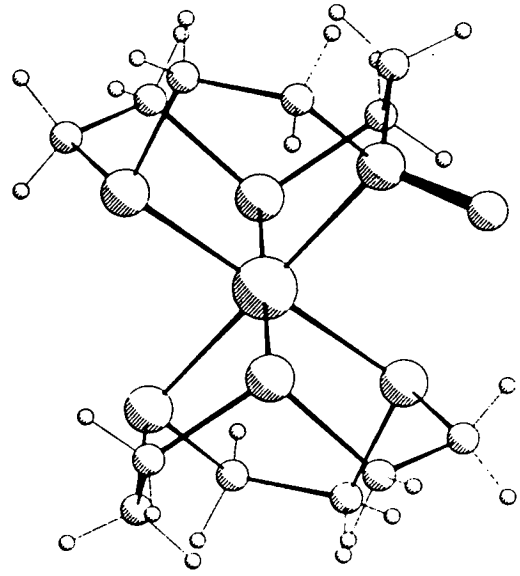

7.2 The Synthesis of $O_6[9]aneS_3$

Sulfones are chemically and thermodynamically very stable. They can be oxidised further, but only under extreme and forceful conditions, usually involving combustion at high temperatures[383]. The oxidation of thioethers to sulfones normally proceeds via a sulfoxide intermediate (Figure 7.3). The formation of a sulfoxide can generally be avoided by using an excess of a powerful oxidising agent at elevated temperatures. The compound $O_6[9]aneS_3$ has been previously synthesised by refluxing either $[Mo([9]aneS_3)(CO)_3]$ or $[9]aneS_3$ with H_2O_2 for ten minutes. This compound has been reported as

insoluble in all common solvents, and has been characterised purely on the basis of its ir spectrum[391].

Repeating the literature preparation of O_6[9]aneS_3 by refluxing the slurry of [9]aneS_3 and H_2O_2 for ten minutes only results in unreacted starting material. Refluxing the slurry for longer periods of time still shows no change from [9]aneS_3. This lack of reactivity may be due to [9]aneS_3 not being soluble in H_2O_2 or that H_2O_2 is not a powerful enough oxidising agent. It is known that the presence of acid catalyses the reaction of peroxides with thioethers[383]; therefore, to overcome both these potential problems the reaction was carried out in glacial acetic acid. The addition of H_2O_2 to [9]aneS_3 in glacial acetic acid at 60°C results, after stirring for six hours, in the formation of a white precipitate , which was collected and dried. The ir spectrum of this product shows two strong bands at υ = 1315 cm^{-1} and 1120 cm^{-1} which can be assigned as the $\upsilon_{(asymm)}$ and $\upsilon_{(symm)}$ stretching vibration of a SO_2 group, respectively. The ir spectrum is similar to the one that has been reported by Wieghardt *et al*[391]. The frequency of the symmetric stretch is lower than expected at 1120 cm^{-1}, as compared to the usual frequency for this stretch ($\upsilon_{(symm)}$ = 1140–1160 cm^{-1}). However, the elemental analysis agrees the formulation as $C_6H_{12}S_3O_6$ and the compound is assigned as the trisulfone.

The trisulfone compound is soluble in DMSO and refluxing H_2O. The ^1H N.M.R. spectrum (d^6–DMSO) of O_6[9]aneS_3 shows a resonance at δ = 3.96(s) p.p.m and the ^{13}C N.M.R. spectrum (d^6–DMSO) shows a resonance at δ = 43.3 p.p.m., confirming the symmetric nature of the compound.

The ^1H N.M.R. spectum of free [9]aneS_3 in d^6–DMSO shows a resonance at δ = 3.06 p.p.m., which is a lower frequency than the trisulfone compound. This shift can be attributed to the electron density being reduced at the sulfur due to the bonded oxygens. This in turn will lead to a reduction in the electron density around the C and H atoms, and hence to a deshielding the protons and an increase the frequency of the chemical shift. Neither E.I. nor F.A.B. (in

3-NOBA or DMF/thieglycerol matrices) mass spectrometroscopy is successful in locating the parent ion.

To confirm the structure of the compound, crystals suitable for X-ray analysis can be grown by vapour diffusion of CH_3OH into a DMSO solution of the compound. The structure is shown in Figure 7.7 and 7.8, and the bond lengths and angles are shown in Table 7.3. The S–O and the C–S bond lengths are typical of a sulfone [S–O = 1.4306(15) – 1.4431(14)Å , C–S = 1.7817(19) – 1.788(19)Å]. The C–S bond lengths are slightly shorter in the trisulfone than in [9]aneS_3 [C–S = 1.820(5)Å – 1.823(5)Å] , the structure of [9]aneS_3 is shown in Figure 2.6[16]. The C–C bond lengths of the two compounds O_6[9]aneS_3 and [9]aneS_3 are very similar [$C–C_{(trisulfone)}$ = 1.525(3)Å – 1.533(3)Å , $C–C_{([9]aneS_3)}$ = 1.510(6)Å]. Both compounds adopt the symmetric [333] conformation in the solid state. The conformations are related by a pseudo rotation of 40°.

Table 7.3 Selected Bond Lengths (Å), Angles (°) and Torsion Angles (°) with standard deviations for O_6[9]aneS_3

S(1)–O(1a)	1.4431(14)	S(4)–C(5)	1.7855(20)
S(1)–O(1b)	1.4370(14)	C(5)–C(6)	1.529(3)
S(1)–C(2)	1.7820(19)	C(6)–S(7)	1.7852(19)
S(1)–C(9)	1.7817(19)	S(7)–O(7a)	1.4306(15)
C(2)–C(3)	1.525 (3)	S(7)–O(7b)	1.4344(14)
C(3)–S(4)	1.7881(19)	S(7)–C(8)	1.7826(19)
S(4)–O(4a)	1.4373(15)	C(8)–C(9)	1.533(3)
S(4)–O(4b)	1.4306(15)		

O(1a)–S(1)–O(1b)	119.32(8)	O(4a)–S(4)–C(5)	107.96(9)
O(1a)–S(1)–C(2)	108.32(8)	O(4b)–S(4)–C(5)	107.73(9)
O(1a)–S(1)–C(9)	106.56(8)	S(4)–C(5)–C(6)	113.31(13)
O(1b)–S(1)–C(2)	106.93(8)	C(5)–C(6)–S(7)	115.921(13)
O(1b)–S(1)–C(9)	108.30(8)	C(6)–S(7)–O(7a)	106.49(9)
C(2)–S(1)–C(9)	106.81(8)	C(6)–S(7)–O(7b)	108.92(8)
S(1)–C(2)–C(3)	114.22(13)	C(6)–S(7)–C(8)	106.50(9)
C(2)–C(3)–S(4)	112.56(13)	O(7a)–S(7)–O(7b)	118.74(9)
C(3)–S(4)–O(4a)	106.45(8)	O(7a)–S(7)–C(8)	108.10(9)
C(3)–S(4)–O(4b)	108.06(9)	O(7b)–S(7)–C(8)	107.49(8)
C(3)–S(4)–C(5)	106.10(9)	S(7)–C(8)–C(9)	112.89(13)
O(4a)–S(4)–O(4b)	119.79(9)	S(1)–C(9)–C(8)	113.08(13)

O(1a)–S(1)–C(2)–C(3)	58.70(15)	O(4a)–S(4)–C(5)–C(6)	56.20(15)
O(1b)–S(1)–C(2)–C(3)	-171.51(13)	O(4b)–S(4)–C(5)–C(6)	-173.12(13)
C(9)–S(1)–C(2)–C(3)	-55.74(15)	S(4)–C(5)–C(6)–S(7)	133.28(12)
O(1a)–S(1)–C(9)–C(8)	-176.74(13)	C(5)–C(6)–S(7)–O(7a)	-170.91(14)
O(1b)–S(1)–C(9)–C(8)	53.73(15)	C(5)–C(6)–S(7)–O(7b)	59.92(16)
C(2)–S(1)–C(9)–C(8)	-61.12(15)	C(5)–C(6)–S(7)–C(8)	-55.72(16)
S(1)–C(2)–C(3)–S(4)	137.52(11)	C(6)–S(7)–C(8)–C(9)	-65.72(15)
C(2)–C(3)–S(4)–O(4a)	-179.80(13)	O(7a)–S(7)–C(8)–C(9)	48.37(15)
C(2)–C(3)–S(4)–O(4b)	50.33(15)	O(7b)–S(7)–C(8)–C(9)	177.67(13)
C(2)–C(3)–S(4)–C(5)	-64.98(15)	S(7)–C(8)–C(9)–S(1)	137.22(11)
C(3)–S(4)–C(5)–C(6)	-57.59(15)		

Figure 7.7 A View of the Single Crystal X-Ray Structure of O_6[9]aneS_3

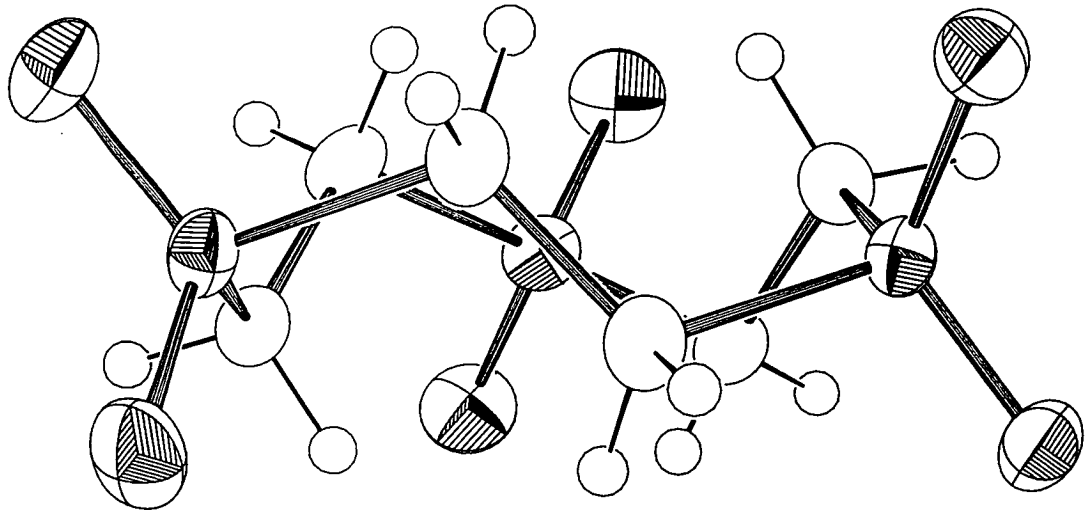

Figure 7.8 An Alternative View of the Single Crystal X-Ray Structure of O_6[9]aneS_3

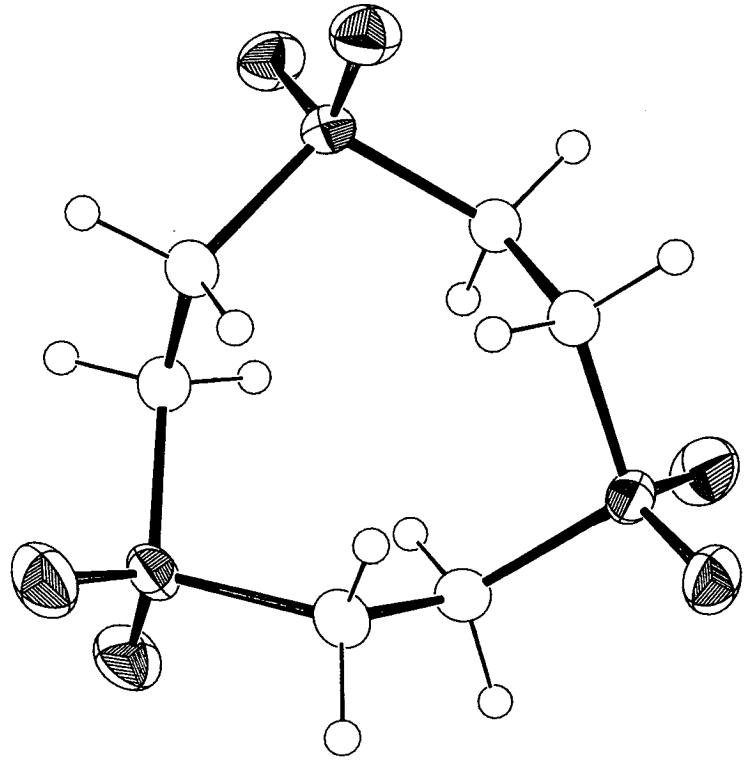

7.3 The attempted synthesis of O_3[9]aneS_3

Scheme 7.6 The Oxidation of Thioethers by ROOH

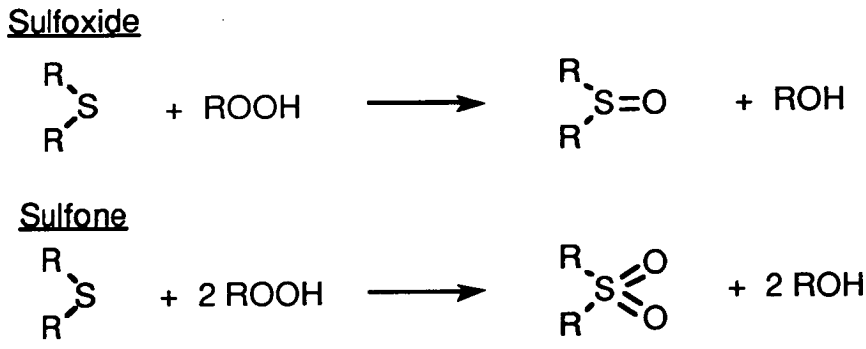

The reaction of ROOH (R = H, alkyl) with thioethers at 298K is one of the most widely used methods for forming sulfoxides[383, 384] (Scheme 7.6). However, [9]aneS_3 does not react with either H_2O_2 or t-BuOOH at 298K in H_2O , CH_3OH or acetone. [9]aneS_3 does react with H_2O_2 in glacial acetic acid when heated or after prolonged exposure resulting in a product which shows stretches in the ir spectrum indicating the presence of both sulfoxide and sulfone functional groups (see Table 7.4). It is unclear whether the product is a single compound, which contains both functional groups (for example the compound O_5[9]aneS_3 shown in Figure 7.9) or whether it is a mixture of compounds. Possible compounds, which may be present in the product are shown in Figure 7.9.

Table 7.4 The ir Spectra of the oxidised products

Oxidising conditions	ir spectrum $\upsilon(cm^{-1})$ Stretches		
	Sulfoxide	Sulfone	
H_2O_2/glacial acetic acid	1050–1020 (s, br)	1130 (s)	1330(s)
MCPBA	1000–1050 (s)	1120 (s)	1320(s)
MMPP	1045 (s)	1125 (s)	1325(s)
$NaIO_4$	1020 (mw)	1115 (s)	1325(s)
$NaBrO_2$	1040 (s)	1120 (s)	1325(s)
PhIO	1050 (s)	1120 (s)	1330(s)
$NaIO_4$/Si Gel	1040 (s)	1120 (s)	1340(s)
$(NBu_4)IO_4$/[TPPFeCl]	1050 (w)	1120 (w)	1350(w)

The ir spectrum generally shows bands at υ (cm^{-1}) = 2960(ms), 2920(w), 1445(s), 1285(ms), 1260(ms), 940(m), 890(m), 855(m), 720(m), 680(w), 480(w), and bands in the sulfoxide and sulfone regions as shown above

Figure 7.9 Possible Compounds Synthesised when Oxidising [9]aneS$_3$

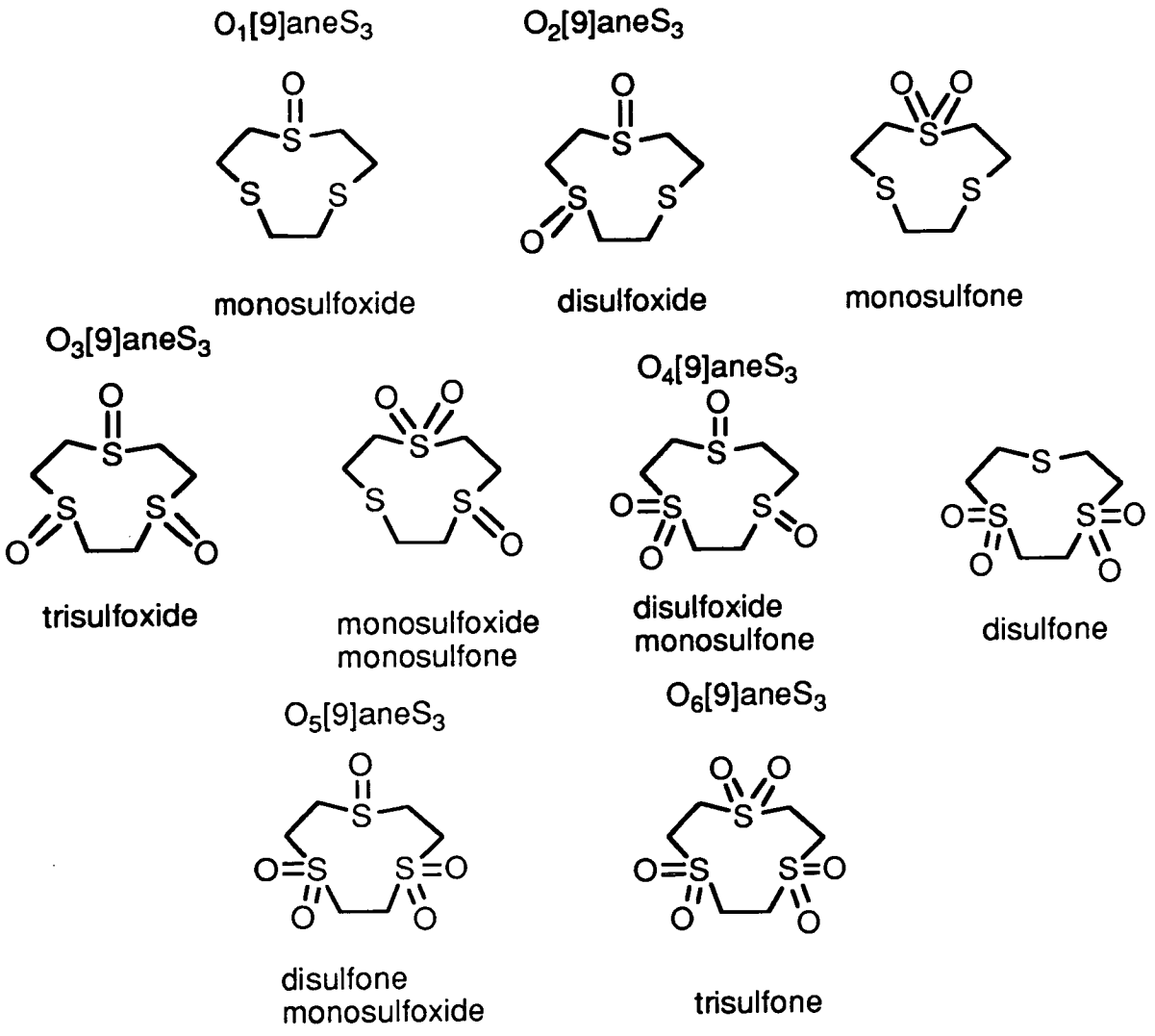

It is well known that the selective oxidation of thioethers requires gentle conditions. Organic peracids are stronger oxidising agents than peroxides and should react with thioethers in less forcing conditions. The mechanism for the oxidation of thioethers by peracids has been proposed and is shown in Scheme 7.7. One of the most selective oxidising agents for the conversion of thioethers to sulfoxides in metachloro perbenzoic acid (MCPBA). Unfortunately, this compound is unstable and highly explosive, and is no longer commercially available.

The addition of MCPBA to [9]aneS$_3$ in CH_2Cl_2, CH_3CN or CH_3NO_2 at 298K for six hours results in a clear solution. Subsequent addition of a saturated

solution of $NaHCO_3$ affords a two-phase mixture, which is separated and the aqueous layer extracted with Et_2O and then CH_3NO_2. Removing the solvent from the organic layers reveals a white solid which shows strong bands in both the sulfone and sulfoxide regions of the ir spectrum (see Table 7.4), suggesting that the product is a compound or a mixture of compounds shown in Figure 7.9.

Magnesium monophthalate (MMPP) is a more stable recent replacement for MCPBA[387]. [9]aneS_3 reacts with MMPP in EtOH and H_2O to afford a clear solution. Passing this solution down a column of Silica removes the oxidising agent and reducing the resulting solution to dryness yields a white sticky solid the ir spectrum of which reveals the presence of a sulfoxide and a sulfone functional groups. The F.A.B. mass spectrum of the white product shows peaks at m/e = 259 and 242, which may correspond to $\{O_5[9]aneS_3+H\}^+$ and $\{O_5[9]aneS_3-2H\}^+$. In general, F.A.B. mass spectroscopy is not suitable for detecting the presence of sulfoxides or sulfones. In the previous section (7.2) it was noted that O_6[9]aneS_3 did not exhibit a mass spectrum (either E.I. or F.A.B.), and so it is not be surprising that in the majority of cases, no satisfactory mass spectrum of the oxidised product is observed. It seems that the oxidation of [9]aneS_3 with MMPP or MCPBA is not selective.

Although the exact nature of the products which form when [9]aneS_3 is reacted with peroxides and peracids is unknown, it would seem that the probable mixture of products contains a sulfone functional group, demonstrating that the selective oxidation to the trisulfoxide has not been acheived.

Scheme 7.7 The Proposed Mechanism for the Oxidation of Thioethers by Peracids

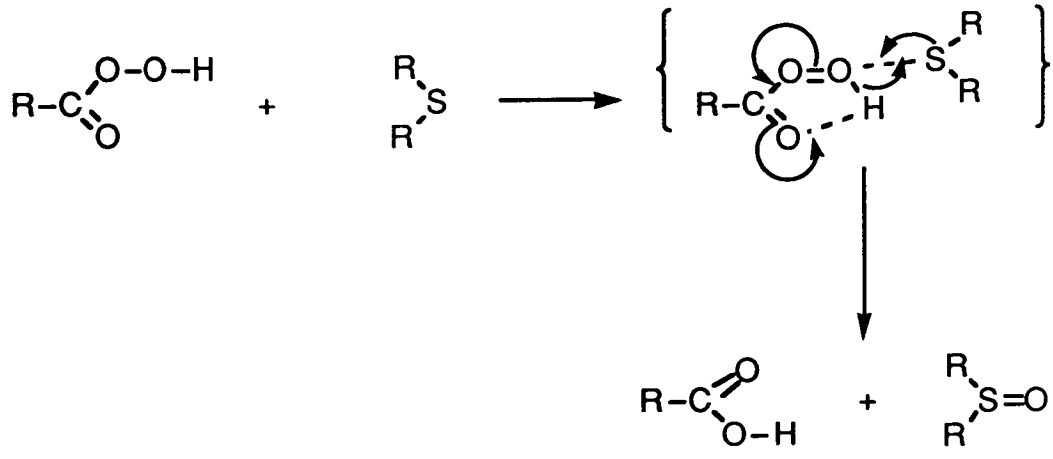

A second major class of oxidising agents used for the conversion of thioethers to sulfoxides are the halogen oxides. A wide variety of thioethers have been oxidised to sulfoxides by $NaIO_4$ (Scheme 7.8)[383, 384], and more recently by $NaBrO_2$[384, 394]. [9]aneS_3 reacts with $NaIO_4$ in CH_3OH/H_2O at 273K after four hours to afford a clear solution. Passing the solution down a Si Gel column, and then removing the solvent affords a white solid the ir spectrum of which indicates that a sulfone is present. A sulfoxide may also be present since a stretching vibration is observed in the ir spectrum at υ = 1200 (mw) cm^{-1}. This band is both weak and rather low for a sulfoxide [the normal range for a sulfoxide being υ cm^{-1}= 1060–1040 (s)] suggesting that if a sulfoxide is present then it is only in a small amount. However, there are a strong bands at υ = 1325 cm^{-1} and υ = 1115 cm^{-1} , which suggests that the compound is predominantly a sulfone. Since the white solid was soluble in CH_3CN, it could not be the trisulfone, because O_6[9]aneS_3 is soluble only in hot H_2O or DMSO. The product is probably a mono- or di- sulfone.

Scheme 7.8 The Oxidation of Thioethers by Periodate

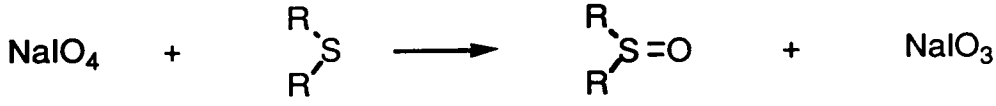

[9]aneS$_3$ is oxidised by NaBrO$_2$ when the reaction is carried out in H$_2$O/dioxane. A white solid could be isolated, the ir spectrum of which shows bands associated with both sulfoxide and sulfone. The product is probably a compound or a mixture of compounds illustrated in Figure 7.9.

Iodosobenzene (PhIO) and its diacetate derivative [PhI(OAC)$_2$] are frequently used to oxidise thioethers to sulfoxides (Scheme 7.9 and Scheme 7.10)[381, 383-385, 395]. However, [9]aneS$_3$ does not react with PhIO in either CH$_3$OH or dioxane . The reaction of [9]aneS$_3$ with PhI(OAC)$_2$ in MeOH yields a white solid, whose ir spectrum indicates that both a sulfoxide and sulfone functional group are present in the product . Consequently, it would appear that halogen oxides are not selective in their oxidation of [9]aneS$_3$ to O$_3$[9]aneS$_3$.

Scheme 7.9 The Oxidation of Thioethers by PhIO

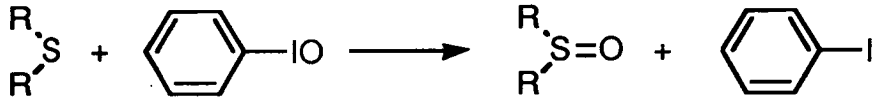

Scheme 7.10 The Proposed Mechanism for the Oxidation of Thioethers by PhI(OAc)$_2$

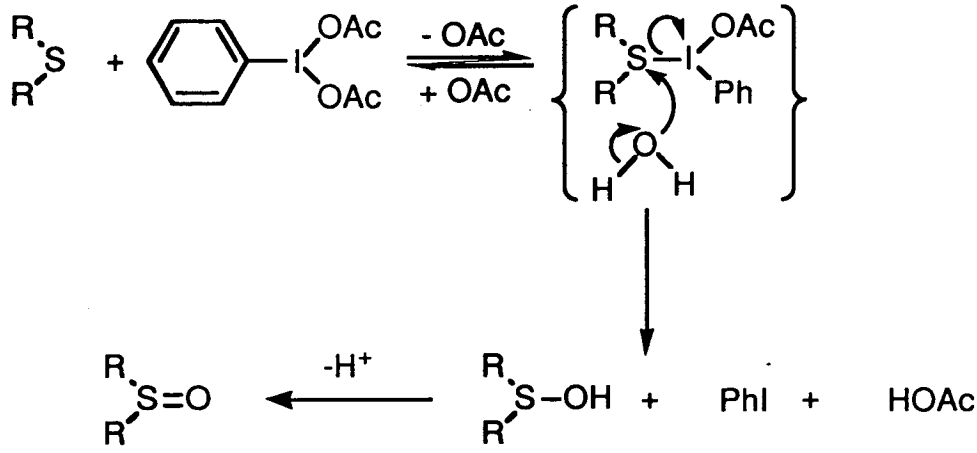

All the oxidising agents so far discussed have required H$_2$O as a solvent, or were only soluble in H$_2$O. A number of sulfoxides are hygroscopic, and so the presence of H$_2$O may lead to problems in isolating the complex. (NBu$_4$)IO$_4$ is an

oxidising agent soluble in organic media. Addition of $(NBu_4)IO_4$ to [9]aneS$_3$ in CH_2Cl_2 affords a clear solution, from which a white solid can be isolated. The ir spectrum of this product shows weak stretches in the regions associated with a sulfone functional group and no bands associated with a sulfoxide (Table 7.4). The presence of a sulfone suggests that $(NBu_4)IO_4$ is too powerful and unselective at oxidising [9]aneS$_3$. The reaction of $NaIO_4$ on Silica[396] with [9]aneS$_3$ in CH_2Cl_2 affords a slurry which is stirred for four days. Filtering the mixture and reducing the solvent to dryness results in a white solid, whose ir spectrum shows bands which can be assigned to a sulfoxide and a sulfone functional group. This indicates that periodate is not a selective enough oxidising agent

The highly selective oxidation of thioethers in biological systems may result in chiral sulfoxides[397]. The reaction is generally catalysed by Cytochrome P_{450}[398] (see Chapter 1) and this system has recently been modelled by using a 'twin coronet' Fe porphyrin to catalyse the chiral oxidation of a thioether to a sulfoxide[399]. In general [$Fe^{(III)}$(TPP)Cl] has been used to catalyse the oxidation of thioethers from sulfoxides[400].

No reaction is observed when PhIO is added to [9]aneS$_3$ at 298K in the presence of [$Fe^{(III)}$(TPP)Cl]. The more powerful oxidising agent $(NBu_4)IO_4$ reacts with [9]aneS$_3$ in the presence of a catalytic amount of [$Fe^{(III)}$(TPP)Cl] after three hours to yield a white solid, whose ir spectrum shows bands in both the sulfoxide and sulfone regions. While [$Fe^{(III)}$(TPP)Cl] catalyses the reaction of [9]aneS$_3$ with $(NBu_4)IO_4$, it does not do so selectively.

One possible method of avoiding the over oxidation of [9]aneS$_3$ is to co-ordinate it to a metal ion, and then chemically oxidise the complex. The metal ion will bind to [9]aneS$_3$ through three of the sulfur lone pairs and only the three remaining lone pairs should be available for oxidation (Scheme 7.11). The

partial oxidation of $[Fe([9]aneS_3)_2]^{2+}$ by NaS_2O_8 has been previously reported (Figure 7.6)[391].

Scheme 7.11 The Oxidation of Co-ordinated $[9]aneS_3$

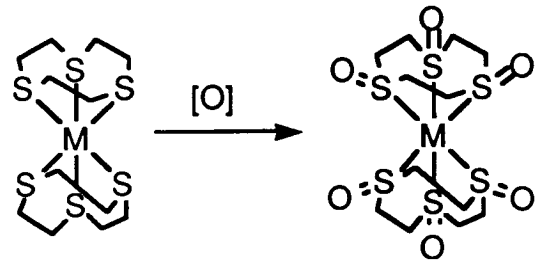

No reaction is observed when $[Co([9]aneS_3)_2](PF_6)_3$ is refluxed in neat H_2O_2, when $[Ni([9]aneS_3)_2](PF_6)_2$ is passed down a column of $NaIO_4$ loaded Silica, or when $[Ni([9]aneS_3)_2](PF_6)_2$ is stirred with MMPP in EtOH at 298K for eight hours. However, the addition of MMPP to $[Ni([9]aneS_3)_2](PF_6)_2$ in CH_3CN at reflux for two hours affords a precipitate. Collecting the precipitate and washing it with CH_3CN removes the remaining Ni complex. The resulting white solid is only soluble in DMSO and exhibits the same ir and ^1H N.M.R. spectra as the trisulfone $O_6[9]aneS_3$, thus indicating that $O_6[9]aneS_3$ has been prepared. The CH_3CN solvent and washings only contained unreacted starting material. The effect on co-ordinating $[9]aneS_3$ to a metal ion, and then oxidising it neither increases the selectivity of the oxidising agent, nor the ease of oxidation.

The reaction of a slurry of $O_6[9]aneS_3$ with $NaBH_4$ in dry refluxing CH_3OH for 24 hours results in unreacted $O_6[9]aneS_3$ and $[9]aneS_3$. No sulfoxide stretches are observed in any of the compounds isolated. It seems that $O_6[9]aneS_3$ behaves as a typical sulfone, since it is both difficult to reduce and a thioether is formed on reduction.

In general, the oxidation of $[9]aneS_3$ by the common oxidising agents discussed in this section either were not powerful enough, or were not selective enough in their oxidation. This resulted in products which showed the

presence of both sulfoxide and sulfone functional groups. The probable composition of the product is either a compound or a mixture of the compounds shown in Figure 7.9.

In the case of the oxidation shown in Scheme 7.1, the products have been separated by extracting the aqueous acetone with pentane. The pentane layer contained monosulfoxides and the aqueous acetone layer held the di- and tri-sulfoxides[353]. In our case, the solubility of the monosulfoxide should be similar to [9]aneS$_3$. However, the ir spectrum of any recovered product from the Et_2O or CH_2Cl_2 extractions did not show any sign of the presence of any sulfoxide. The oxidised product that was obtained by extracting the aqueous layer with CH_3NO_2 contained both sulfone and sulfoxide. It is possible that in these reactions, the di- or tri-sulfoxide may remain in the aqueous layer. However, removing the oxidising agents by column chromatography and reducing the resulting solution to dryness results in a product that still shows the presence of both sulfoxide and sulfone functional groups in the ir spectrum, suggesting that simple extraction is not suitable for separating the mixture of compounds.

The problem of separating the probable mixture of products could be overcome by thin layer chromotography (TLC). The monosulfoxide should be easily separated from the tri- and di-sulfoxides. The T.L.C. of the product isolated from the CH_3NO_2 extraction does not separate in the following solvent systems; MeOH/H_2O (various ratios), ethylacetate/H_2O, CH_3CN/H_2O and DMSO/H_2O.

The ^{1}H N.M.R. spectrum of the products containing both sulfoxide and sulfone is not very informative. A typical spectrum consists of a multiplet between δ = 2.8 and 4.0p.p.m. This indicates that the nature of the oxidation is non symmetric, that a mixture of isomers are present, or that a mixture of compounds of the type O_n[9]aneS$_3$ (n = 1 to 6) are present. Neither F.A.B. (in

3-NOBA or DMF/thioglycerol) nor E.I. Mass spectroscopy are informative, since no parent on peaks are observable for either sulfones or sulfoxides. Only in one case (MMPP) was a satisfactory mass spectrum obtained, which indicated that O_5[9]aneS_3 and O_4[9]aneS_3 may be present.

The problem in synthesising O_3[9]aneS_3 could be due to the selectivity of the oxidising methods employed. If there is no selectivity for the oxidation of thioether as compared to a sulfoxide, most of the product would be a compound with one sulfone and one sulfoxide functional group.

A number of other compounds, without sulfoxide or sulfone functional groups could also be formed in the reaction. The solid state crystal structure of [9]aneS_3 shows all three sulfur lone pairs point towards the centre of the cavity (Chapter 2). It should therefore be possible to form an internal oxy-bridged compound (Scheme 7.12). Attack of the oxidising agent on the oxy-bridge would probably result in the formation of the thermodynamically more stable mono sulfone as opposed to the disulfoxide (Scheme 7.13).

Scheme 7.12 The Formation of an Oxy-Bridged Species

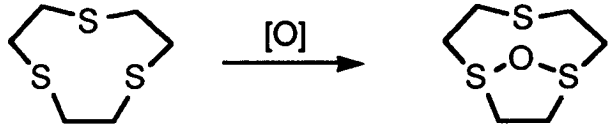

Scheme 7.13 The Oxidation of an Oxy-Bridged Species

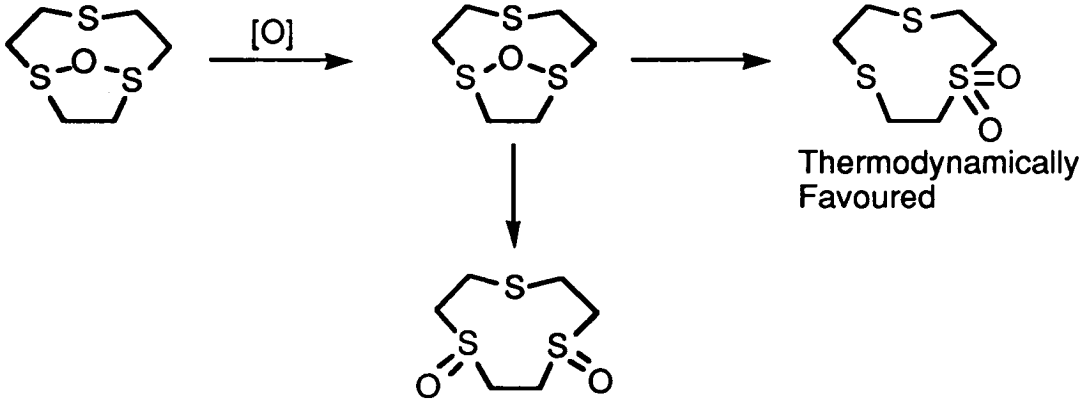

It is known that oxygen exchange between a thioether and a sulfoxide can occur (Scheme 7.14)[384]. Due to the geometry of [9]aneS$_3$, a sulfur lone pair is ideally placed to interact with another sulfur's oxygen, enabling exchange to take place internally. This in turn could form a sulfone (Scheme 7.15), since sulfones are thermodynamically more stable than disulfoxides and are resistant to reduction. Once a sulfone is formed, it is likely that they would remain inert to subsequent reaction.

Scheme 7.14 Sulfoxide/Thioether Oxygen Exchange

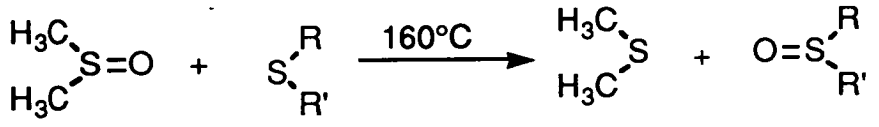

Scheme 7.15 The Interconversion of a Disulfoxide to a Sulfone

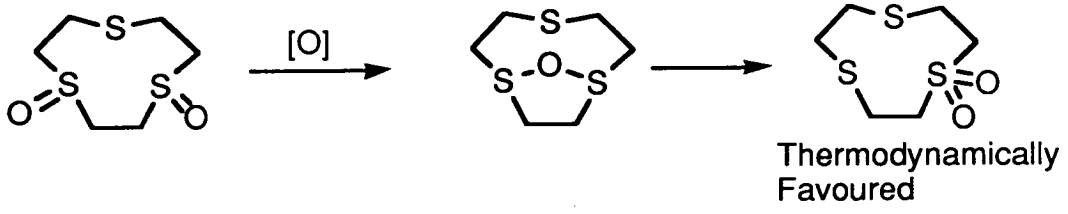

The synthesis of the trisulfoxide O$_3$[9]aneS$_3$ has not been successful. This could be due to problems associated with separating a large number of possible products obtained when oxidising [9]aneS$_3$, or that the nature of [9]aneS$_3$ leads to the isomerisation of di- or trisulfoxides to form a sulfone. The reduction of the trisulfone O$_6$[9]aneS$_3$ did not yield the trisulfoxide. The trisulfone behaves as a typical sulfone, being difficult to reduce, and producing the thioether [9]aneS$_3$ on reduction.

In contrast, in the complex [RuCl(PPh$_3$)(THT)([9]aneS$_3$)](PF$_6$), the THT ligand is easily oxidised in air to the sulfoxide THT-S Oxide. This is discussed in Chapter 5.

7.4 Summary

The chemical oxidation of [9]aneS$_3$ has been investigated. Since the trisulfoxide O$_3$[9]aneS$_3$ could not be synthesised, it was not possible to investigate the chemical and physical characteristics of both the free ligand and its complexes. The usual product on gentle oxidation of [9]aneS$_3$ was a compound or compounds containing both the sulfoxide and sulfone functional groups. The reason for the difficulties in synthesising O$_3$[9]aneS$_3$ is not known. However, the complete oxidation of [9]aneS$_3$ has been achieved, yielding the trisulfone O$_6$[9]aneS$_3$. This compound has been characterised by ir and N.M.R. spectroscopy, elemental analysis and X-ray diffraction.

7.5 Experimental

Reagents and physical measurements were used as discussed in Chapters 3 and 4. Most oxidising agents were commercially available, except lodosobenzene [401], $NaIO_4$ on silica (10% loaded by weight)[396] and [Fe$^{(III)}$(TPP)Cl][402] which were synthesised by literature methods. All the products in the reactions which exhibited an ir spectrum that indicated the presence of sulfones or sulfoxides were analysed by T.L.C. All the samples were thoroughly dried in a dessicator before use. The solvent systems used were MeOH/H_2O (10 : 1, 5 : 1, 3 : 1, 1 : 1) ethylacetate/H_2O (5 : 1), or DMSO/H_2O (3 : 1), depending on the product. No separation of the product in any of the cases was observed. The plates were developed in an iodine tank, after they had been dried in an oven.

7.5.1 Oxidation of [9]aneS$_3$ by H_2O_2 and t-BuOOH

(a) H_2O_2 (5 cm^3, 30% vol 0.09 mM) was added to [9]aneS$_3$ (50 mg, 0.29 mM) and stirred in a slurry at 298K for three hours, filtered and the white solid

dried. The ir spectrum was the same as [9]aneS$_3$. The aqueous layer was then extracted CH_3NO_2, but no solid was found in the CH_3NO_2 layer.

This procedure was repeated in the conditions shown in Table 7.5(i).

(b) [9]aneS$_3$ (52 mg, 0.29 mM) was added to H_2O_2 (0.1 cm^3, 30% vol 0.09 mM) in 5 cm^3 of solvent and stirred in the conditions shown in Table 7.5(ii). The solution was extracted by ether and then by CH_3NO_2. The ether extraction contained unreacted [9]aneS$_3$ and the CH_3NO_2 extraction the oxidised product. Both were isolated by removing the solvent on a rotary evaporator. The results of the ir spectrum of the oxidised product is shown in Table 7.4.

(c) The reaction was carried out as described in 7.5.1b, except that t-BuOOH replaced H_2O_2 as the oxidising agent. The results and conditions are shown in Table 7.5(iii).

Table 7.5 Experimental Conditions for the Oxidation of [9]aneS$_3$ by H_2O_2 and t-BuOOH

(i) [9]aneS$_3$ with neat H_2O

Volume (cm^3)	Temp (K)	Time (hours)	% [9]aneS$_3$ recovered
5	298	3	90
5	298	6	73
5	298	12	68
5	298	24	81
5	338	12	82
5	reflux	10 mins	91
5	reflux	20 mins	89
5	reflux	4	83
10	reflux	4	88

(ii) [9]aneS$_3$ with H_2O_2 in a solvent

Solvent	Temp (K)	Time (hours)	% [9]aneS$_3$ recovered	Result
acetone	reflux	2	80	[9]aneS$_3$
acetone	298	12 days	80	[9]aneS$_3$
glacial acetic acid	298	24	76	[9]aneS$_3$
glacial acetic acid	338	12	—	Table 7.4
glacial acetic acid	298	12 days	—	Table 7.4

(iii) [9]aneS$_3$ and t-BuOOH in a solvent

Volume t-BuOOH cm^3	(mM)	Solvent (cm^3)	Temp K	Time day	% [9]aneS$_3$ recovered
1.4	(1.02)	H_2O(3.5)	298	1	78
1.4	(1.02)	H_2O(3.5)	358	1	76
1.4	(1.02)	H_2O(3.5)	reflux	1	80
1.2	(0.87)	CH_3OH(3)	298	1	70
1.2	(0.87)	CH_3OH(10)	reflux	1	72
1.2	(0.87)	CH_3OH(10)	298	12	78
1.2	(0.87)	Acetone(10)	298	1	72
1.2	(0.87)	Acetone(15)	298	12	80

7.5.2.1 The synthesis of O_6[9]aneS$_3$

[9]aneS$_3$ (96 mg, 0.533 mM) was dissolved in glacial acetic acid (7.5cm^3) and heated to 60° C for six hours. The resulting white precipitate was collected by centrifuge, washed with H_2O_2, acetone and ether, and dried. (Yield = 133 mg, 90%).

Ir spectrum $\upsilon(cm^{-1})$: 2970(s), 2940(s), 1445(s), 1430(s), 1405(w), 1340(s), 1270(s), 1200(w), 1182(w), 1145(m), 1115(vs), 1055(m), 1040(w), 947(mw), 900(m), 890(mw), 850(mw), 780(vs), 750(m), 730(mw), 690(w), 650(w), 530(w), 510(m), 495(sh), 450(s), 430(m).

E.I. Mass Spectrum found m/e = 184, 156, 140, 120, 92, 91;

F.A.B. Mass Spectrum (DMF/Thioglycerol) found m/e = 279, 274, 257, 239, 197;

calculated for $\{O_6[9]aneS_3\}^+$: 276, $\{O_5[9]aneS_3\}^+$: 260, $\{O_4[9]aneS_3\}^+$: 244, $\{O[9]aneS_3\}^+$: 196, $\{[9]aneS_3\}^+$: 180

^1H N.M.R. spectrum (d^6–DMSO, 298K) δ = 3.96 p.p.m.

^{13}C N.M.R.spectrum. (d^6–DMSO, 298K) δ = 43.3 p.p.m.

C.H.N.	Expect	26.1%C	4.34%H	0%N for O_6[9]aneS$_3$
	Found	25.9%C	4.45%H	0%N

Sulfur analysis	Expect	34.8% for O_6[9]aneS$_3$
	Found	34.3%

7.5.2.2 Structural Determination of O_6[9]aneS_3

A colourless columnar crystal (0.18 x 0.21 x 0.42 mm) suitable for X-ray analysis was obtained by vapour diffusion of CH_3OH into DMSO.

Crystal data: $[C_{26}H_{12}S_3O_6]$, Mwt = 276.31, monoclinic, space group $P2_{1/n}$, a = 5.99785, b = 12.9947(12), c = 13.8201(12)Å, β = 101.244(8)°; V = 1056.3Å^3 [from setting angles for 18 centred reflections with 2θ = 30–32°, λ = 0.71073Å, Z = 4, D_c = 1.737 Mgm^{-3}, μ = 0.68 mm^{-1}, F(000) = 576.S

Data Collection and processing: Stöe Stadi-4 circle diffractometer, graphite monochromated Mo–K_α X-radiation, T = 298K, ω–2θ scans using the learnt profile method[403]. 1937 data measured ($2\theta_{max}$ = 50°, h = -6 → 6, k = 0 → 15, l = 0 → 16), giving 1672 data with F ≥ 6σ(F) for use in all calculations. No significant crystal decay was observed.

Structure solution and refinement: Automatic direct methods[404] located all non-H atoms were refined anisotropically[288]: H-atoms were refined freely with a common μ_{iso} of 0.0368(16)Å^2. At final convergence, R = 0.0246 and Rw = 0.0370, S = 1.322 for 173 parameters. The weighting scheme $\omega^{-1} = \sigma^2(F) + 0.000225(F)^2$ gave satisfactory agreement analysis and in the final cycle Δ/σ max 0.07.

7.5.3 The oxidation of [9]aneS_3 by MCPBA

[9]aneS_3 (50 mg, 0.28 mM) was dissolved in CH_2Cl_2 or CH_3CN or CH_3NO_2 (5 cm^3 in each case) at 273K for six hours with MCPBA (278 mg, 50% in H_2O, 0.802 mM). A saturated solution of sodium bicarbonate (10 cm^3) was then added and the resulting two-phase solution was separated, and worked up in the same way as 7.5.1(b). The ir spectrum was identical in all three cases and is shown in Table 7.4.

7.5.4 The oxidation of [9]aneS_3 by MMPP

[9]aneS_3 (54 mg, 0.30 mM) was dissolved in 6 cm^3 EtOH and 270 mg MMPP (0.42 mM) in 3 cm^3 H_2O (15 cm^3) was added and the solution stirred at

room temperature for six hours, passed down a Si Gel column, eluted with EtOH, and the resulting solution reduced in volume to dryness to reveal a white sticky solid (yield 38 mg).

Ir spectrum as shown in Table 7.5

F.A.B. Mass Spectrum found m/e = 259, 242;

calculated for $\{O_5[9]aneS_3\}^+$: 260, $\{O_4[9]aneS_3\}^+$: 244

7.5.5 The oxidation of [9]aneS_3 by IO_4^-

(i) [9]aneS_3 was added to three equivalents of the oxidising agent and in the conditions shown in Table 7.6. The resulting solution was passed down a column of silica gel, and then the solvent was removed. The resulting white solid was identified by ir spectroscopy.

(ii) [9]aneS_3 (48 mg, 0.27 mM) was dissolved in 10 cm^3 CH_2Cl_2 and stirred at 298K for four days with $NaIO_4$ on Si Gel (10% loaded), filtered and the solvent removed to reveal a white solid. The results are shown in Table 7.4.

Table 7.6 Experimental Conditions for the Oxidation of [9]aneS_3 by Periodate

Solvent	Method	Oxidising Agent	Temp	Time	Result
CH_3CN(5 cm^3)/H_2O (2 cm^3)	(i)	$NaIO_4$	273	8 hrs	No reaction
CH_3OH/H_2O (5 cm^3, 2 cm^3)	(i)	$NaIO_4$	273	4 hrs	Table 7.4
CH_2Cl_2 (4 cm^3)	(i)	N(Bu4)IO_4	298	24 hrs	Table 7.4
CH_2Cl_2 (10 cm^3)	(ii)	$NaIO_4$/Si Gel	298	4 days	Table 7.4

7.5.6 Oxidation of [9]aneS_3 with $NaBrO_2$

[9]aneS_3 (61 mg, 0.34 mM) was dissolved in the solvent and in the conditions shown in Table 7.7, and a solution of $NaBrO_2$ in H_2O added. The solvent was reduced in volume, and extracted with ether and the nitromethane. The ether extraction contained any unreacted [9]aneS_3, and the CH_3NO_2 extraction contained the oxidised products. The results with dioxane/H_2O were all the same, and their ir is shown in Table 7.4.

Table 7.7 Experimental Conditions for the Oxidation of [9]aneS$_3$ by NaBrO$_2$

Solvent	Temp K	Time	Result
Dioxane (20 cm^3)/H$_2$O (5 cm^3)	298	30 mins	Table 7.4
Dioxane (10 cm^3)/H$_2$O (10 cm^3)	298	1 hr	Table 7.4
Dioxane (30 cm^3)/H$_2$O (5 cm^3)	298	30 mins	Table 7.4
Dioxane (40 cm^3)/H$_2$O (1 cm^3)	298	30 mins	Table 7.4

7.5.7 Oxidation of [9]aneS$_3$ with PhIO and PhI(OAC)$_2$

[9]aneS$_3$ (45 mg, 0.25 mM) was added to three equivalents of the oxidising agent and in the conditions shown in Table 7.8. The solution was then passed through a Si Gel column, and the solvent removed to yield a white solid which was characterised by ir (Tables 7.4 and 7.8).

Table 7.8 Experimental Conditions for the Oxidation of [9]aneS$_3$ by PhIO or PhI(OAc)$_2$

Oxidising agent	Solvent	Temp	Time	Result
PhIO	CH$_3$OH (10 cm^3)/0.5 cm^3 H$_2$O	298	12 hrs	No reaction
PhIO	Dioxane (10 cm^3)/1cm^3 H$_2$O	298	12 hrs	No reaction
PhI(OAc)2	CH$_3$OH (20 cm^3)/1 cm^3 H$_2$O	298	12 hrs	Table 7.4

7.5.8 Oxidation of [9]aneS$_3$ using a [Fe(TPP)Cl] catalyst

[9]aneS$_3$ (45 mg, 0.25 mM) was added to the oxidising agent and in the conditions shown in Table 7.9, along with [Fe(TPP)Cl] (10 mg). The colour changed immediately to brown. After the solution had been stirred for the number of hours shown in Table 7.9, it was filtered through silica gel and the solvent removed. The results are shown in Table 7.9

Table 7.9 Experimental Conditions for the Oxidation of [9]aneS$_3$ Catalysed by [Fe(TPP)Cl]

Oxidising Agent	Solvent	Temp (K)	Time (hours)	Result
PhIO	CH$_2$Cl$_2$ (10 cm^3)	298	10	[9]aneS$_3$
(NBu$_4$)IO$_4$	CH$_2$Cl$_2$ (10 cm^3)	298	4	Table 7.4

7.5.9 Oxidation of [9]aneS$_3$ metal complexes

[Ni([9]aneS$_3$)$_2$](PF$_6$)$_2$[177] and [Co([9]aneS$_3$)$_2$](PF$_6$)$_3$[405] were prepared by literature methods.

(a) [Ni([9]aneS$_3$)$_2$](PF$_6$)$_2$ (70 mg, 0.098 mM) was added to 3 equivalents of MMPP and reacted in the conditions shown in Table 7.10. The white solid of O$_6$[9]aneS$_3$, which was found during the reaction was removed by filtration and identified by ir and ^{1}H N.M.R. The pink solution was passed down a Si Gel column, and eluted with CH$_3$CN until all the pink bond had been removed from the column. On reducing the solvent to dryness, a pink solid formed which had the same ir spectrum as the starting material [Ni([9]aneS$_3$)$_2$](PF$_6$)$_2$.

(b) [Ni([9]aneS$_3$)$_2$](PF$_6$)$_2$ (70 mg, 0.098 mM) was dissolved in CH$_3$CN and passed down a silica gel column with a 10% loading of NaIO$_4$ and eluted with CH$_3$CN. The pink bond obtained from the column was identified by ir as the starting material.

(c) [Co([9]aneS$_3$)$_2$](PF$_6$)$_3$ (50 mg, 0.058 mM) was added to H$_2$O$_2$ (10 cm^3, 30% vol) and refluxed in a slurry for six hours, filtered and dried. The H$_2$O$_2$ aqueous solutions was colourless, and the orange solid was identified as the Co starting material by its ir spectrum.

Table 7.10 Experimental Conditions for the Oxidation of [9]aneS$_3$ metal complexes

Metal Complex	Oxidising Agent	Temp (K)	Time (hours)	Solvent	Result
[Ni([9]aneS$_3$)$_2$]$^{2+}$	MMPP	reflux	2	CH$_3$CN	O$_6$[9]aneS$_3$
[Ni([9]aneS$_3$)$_2$]$^{2+}$	MMPP	298	8	CH$_3$CN	No reaction
[Ni([9]aneS$_3$)$_2$]$^{2+}$	NaIO$_4$/Si Gel	298	—	CH$_3$CN	No reaction
[Ni([9]aneS$_3$)$_2$]$^{2+}$	H$_2$O$_2$	reflux	6	—	No reaction

7.5.10 Reduction of O_6[9]aneS_3 by $NaBH_4$

O_6[9]aneS_3 (50 mg, 0.18 mM) was added to a solution of $NaBH_4$ (16 cm^3, 0.42 mM) in dry degassed CH_3OH and the white slurry stirred at reflux for one day under N_2. The mixture was filtered and the white solid dried (yield = 30 mg). The ir spectrum of this product was the same as the O_6[9]aneS_3.

The CH_3OH solvent was passed down a silica column, eluted with CH_3OH and all the fractions collected, reduced in volume to dryness and the resulting white solid had ir and ^1H N.M.R. spectra which were identical to [9]aneS_3.

Appendix

THE DEPROTONATION OF THIOETHER MACROCYCLES

Introduction

Co–ordinated thioether macrocycles are generally regarded as stable. However, when they are co–ordinated to transition metal ions, the macrocyclic ring may be cleaved to yield an open–chain vinyl thioether complex[408]. The addition of NEt_3 to $[M([9]aneS_3)_2]^{3+}$ (M = Co, Rh, Ir) leads to the deprotonation at a methylene carbon of [9]aneS$_3$. This is followed by a ring opening process to yield $[M([9]aneS_3)([9]aneS_3\text{-}H)]^{2+}$, as illustrated in Scheme A.1. The crystal structures of $[Rh([9]aneS_3)_2]^{3+}$ and $[Rh([9]aneS_3)([9]aneS_3\text{-}H)]^{2+}$ have been solved by the Edinburgh group and are shown in Figures 2.15 and A.1. During the course of this work, the double deprotonation of $[Ru(Cp^*)([9]aneS_3)]^{2+}$ was reported by Bennett *et al* [409]. The second deprotonation of bound [9]aneS$_3$ occurs on the same ring to yield a bound ethene thiol ligand, as illustrated in Scheme A.2. The final species $[Ru(\eta\text{–}Cp^*\text{–}CH_2\text{–}CH_2\text{–}S\text{–}CH_2\text{–}CH_2\text{–}S)(SCHCH_2)]$ has been characterised by X-ray Crystallography[409].

Figure A.1 A View of the Single Crystal X-Ray Structure of $[Rh([9]aneS_3)([9]aneS_3\text{-}H)]^{2+}$

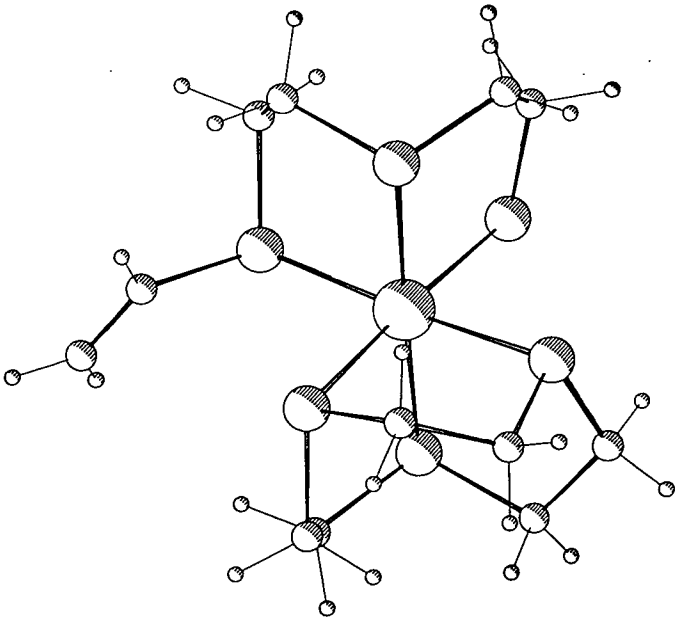

Scheme A.1 The Deprotonation of Co–ordinated [9]aneS_3

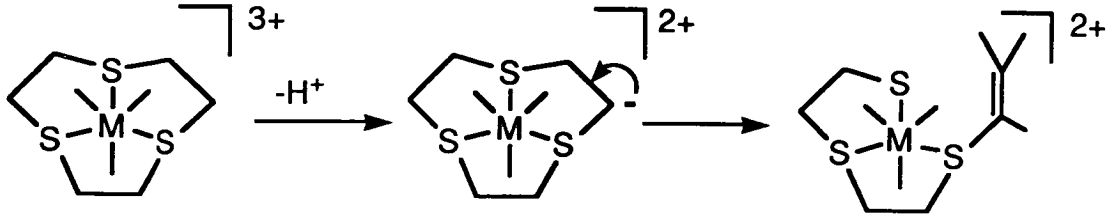

Scheme A.2 The Double Deprotonation of Co-ordinated [9]aneS_3

The formation of the Ethene thiol Complex

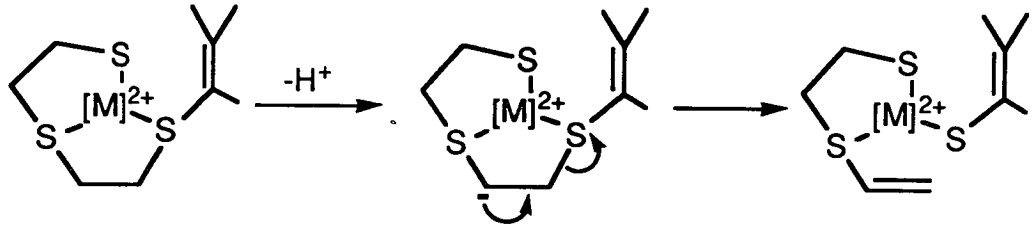

The Subsequent Reaction to form the Complex
[Ru(η–Cp*–CH_2–CH_2–S–CH_2–CH_2–S)(SCHCH_2)]

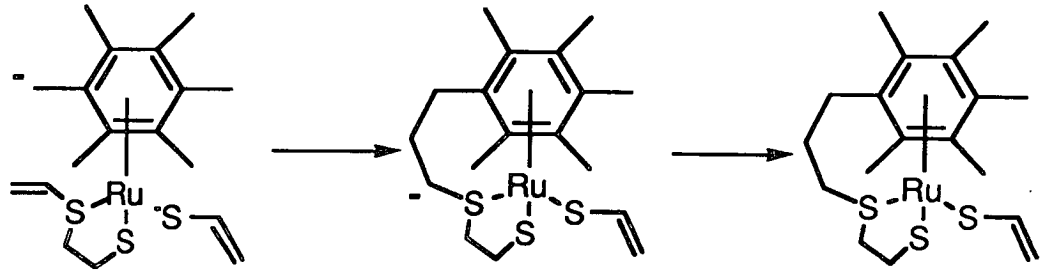

Sellman and co-workers have also reported the deprotonation of bound thioether macrocycles. The Ru complex, [$Ru^{(II)}(L_4)(PPh_3)_2$] (L_4- dication of 1,2–bis(mercaptophenylthio)ethane) ring opens to form a vinyl thioether moiety, which has been characterised by X-ray crystallography. This is illustrated in Scheme A.3[410]. Sevdic et al reported that [14]aneS_4 and [18]aneS_6 deprotonate in the complexes, [$MoCl_x(L)]_n$. The products were characterised by ir, ^{1}H N.M.R., ^{13}C N.M.R. and mass spectroscopy as well as elemental analysis

and magnetic measurements[411]. This appendix discusses the deprotonation reactions of $[Rh([9]aneS_3)_2](PF_6)_3$.

Scheme A.3 The Formation of a Vinyl-Thioether Moiety from $[Ru(L_4)(PPh_3)_2]$

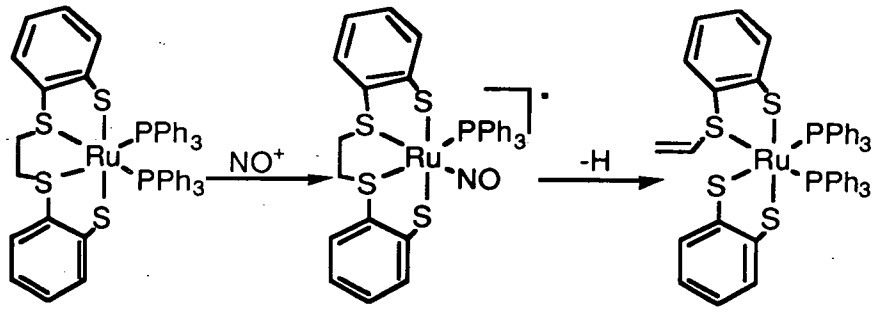

Results and Discussion

On addition of a stoichiometric amount of NEt_3 to $[Rh([9]aneS_3)_2](PF_6)_3$ in CH_3NO_2 , the solution turns from colourless to red. The ^1H N.M.R.spectrum (CD_3NO_2) shows resonances at δ = 2.9(m), 6.2(dd), and 6.9(dd) p.p.m. (Figure A.2), indicating that the complex, $[Rh([9]aneS_3)([9]aneS_3\text{-}H)]^{2+}$ is formed. The presence of a minor component can also be seen in the ^1H N.M.R. spectrum, since there is an extra resonance at δ = 6.75(dd) p.p.m. The presence of this minor product is confirmed by ^{13}C N.M.R. spectroscopy which shows resonances at δ = 30-42 ([9]aneS$_3$), 122.1, 124.3, 128,8, and 131.0 p.p.m.[286].

A variable temperature ^1H N.M.R. study, between 71°C and -18°C , of the deprotonated product did not show coalescence of the vinyl thioether resonances[286]. This suggests that the product is a mixture of two different products, which may be either isomers that do not easily interconvert, or two different complexes, one of which can be assigned as $[Rh([9]aneS_3)([9]aneS_3\text{-}H)]^{2+}$.

Figure A.2 The ^1H N.M.R. Spectrum (CD_3NO_2, 298K) of $[Rh([9]aneS_3)([9]aneS_3\text{-}H)]^{2+}$

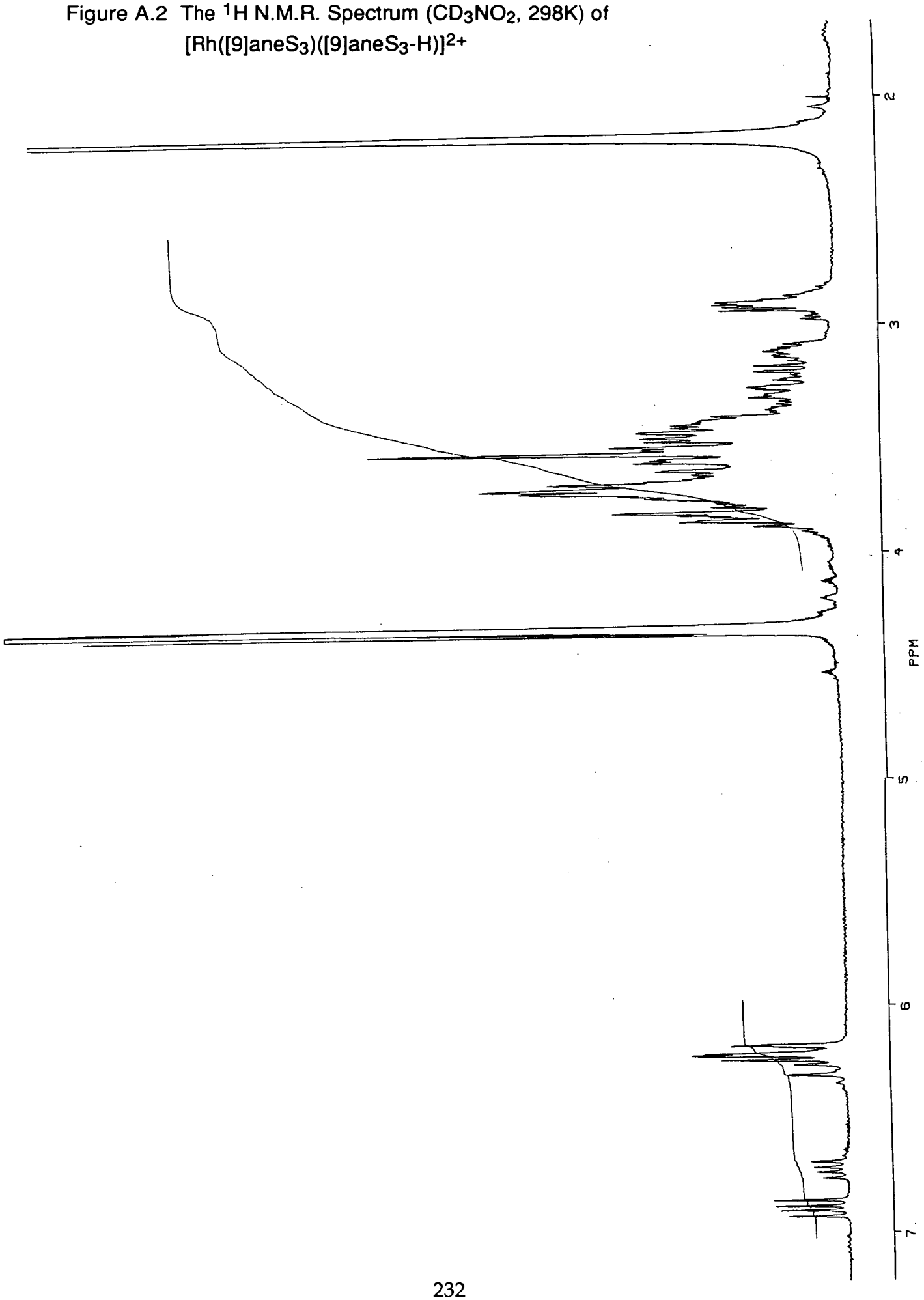

When a excess of NEt_3 is added to $[Rh([9]aneS_3)_2]^{3+}$ or to $[Rh([9]aneS_3)([9]aneS_3\text{-}H)]^{2+}$ in CH_3NO_2 , ir bands at 1549(mw) and 1590 (mw) cm^{-1} are observed. These stretches are not seen in either the ir spectrum of $[Rh([9]aneS_3)_2]^{3+}$ or of $[Rh([9]aneS_3)([9]aneS_3\text{-}H)]^{2+}$. The ratio of the intergrals of the two resonances at δ = 6.75 and 6.9 p.p.m. in the ^1H N.M.R.spectrum also changes, with a slight increase in the proportion of the minor component at δ = 6.75 (dd). Bennett *et al* described in their recent paper the ir spectrum of a bound ethene thiol, which showed an infrared stretch at υ = 1556 cm^{-1}. This suggests that the addition of excess of NEt_3 to $[Rh([9]aneS_3)_2]^{3+}$ results in the double deprotonation of $[9]aneS_3$ on the same ring to form a ethene thiol complex, $[Rh([9]aneS_3)(S\text{-}C_2H_4\text{-}S\text{-}C_2H_3)(SC_2H_3)]^+$ as opposed to the second $[9]aneS_3$ ring opening (Figure A.3).

Figure A.3 The Possible Structures Formed When Double Deprotonating $[Rh([9]aneS_3)_2]^{3+}$

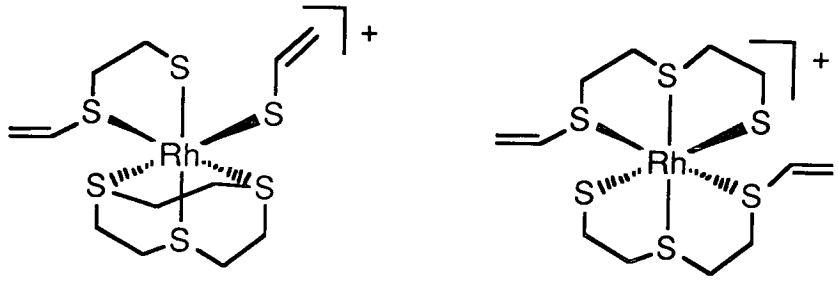

Cyclic voltammetry of $[Rh([9]aneS_3)([9]aneS_3\text{-}H)]^{2+}$ shows that the complex has no oxidation (to + 2V Vs Fc/Fc^+) but exhibits an irreversible reduction at E = -1.04V and a reversible reduction at -1.56 V (ΔE = 88mV) Vs Fc/Fc^+ (0.1M $TBAPF_6$ in CH_3CN at 12°C, scan speed = 181 V ms^{-1}) . Coulometric measurements on the first reduction at a constant potential of e = 1.2 V show that it is a 2 electron process.

The protonation of $[Rh([9]aneS_3)([9]aneS_3\text{-}H)]^{2+}$ can be achieved by using forcing conditions. The conversion occurs in refluxing HBF_4 after two hours, or in refluxing CH_3CN in the presence of an excess of HPF_6.

Summary

The deprotonation of $[Rh([9]aneS_3)_2]^{3+}$ results in the formation of $[Rh([9]aneS_3)([9]aneS_3\text{-}H)]^{2+}$ and another minor product. The formation of the minor product is favoured in excess NEt_3 and exhibits ir stretches at 1590 and 1549 cm^{-1}. By analogy with the double deprotonation of $[Ru(C_6Me_6)([9]aneS_3)]^+$, the complex $[Rh([9]aneS_3)(SCHCH_2)(SCH_2CH_2SCHCH_2)]^+$ is proposed as being the minor product. The electrochemistry of $[Rh([9]aneS_3)([9]aneS_3\text{-}H)]^{2+}$ shows a two electron reduction at E = -1.04 V Vs Fc / Fc^+ and a reversible reduction at $E_{1/2}$ = 1.54 V Vs Fc / Fc^+ in 0.1 M $TBAPF_6$ in CH_3CN. The conversion of $[Rh([9]aneS_3)([9]aneS_3\text{-}H)]^{2+}$ to $[Rh([9]aneS_3)_2]^{3+}$ has been acheived by refluxing $[Rh([9]aneS_3)([9]aneS_3\text{-}H)]^{2+}$ in HBF_4 or in CH_3CN in the presence of an excess of HPF_6.

Experimental

Physical measurements and reagents were used as descibed in Chapters 3 and $[Rh([9]aneS_3)_2]^{3+}$ was prepared as described in the literature[408], except that $NaBF_4$ was used in place of NH_4PF_6. An inert atmosphere was not used unless otherwise stated . This work was based upon the work of T.I. Hyde[286, 408].

The Synthesis of $[Rh([9]aneS_3)([9]aneS_3\text{-}H)]^{2+}$

(a) $[Rh([9]aneS_3)_2](BF_4)_3$ (95mg, 0.12 x 10^{-3}M) was added to CH_3NO_2 (3 cm^3) and NEt_3 (18.5 x 10^{-3} cm^3, 0.13 x 10^{-3}M). The resulting solution turned red very rapidly, and the mixture was stirred for one hour. Et_2O was then added and the red precipitate filtered, washed with Et_2O, and then recystallised from acetone/Et_2O

Ir spectrum $\upsilon(cm^{-1})$: 2990-2960(broad, s), 1630(m), 1449 (s), 1410(s), 1200-1000(vs, BF_4), 820(s), 621(m), 552(w)

^1H N.M.R.spectrum (CD_3NO_2 , 298K) δ = 2.7-3.7 (m), 6.2(m), 6.75 (dd, J = 9Hz), and 6.9 (dd, J = 9 Hz) p.p.m.

^{13}C N.M.R.(DEPT) spectrum (CD_3NO_2 , 298K) δ = 31-43 ([9]$aneS_3$), 122.1, 124.3, 128.8, 131.0 p.p.m.

F.A.B. mass spectrum found m/e = 549, 461;

calculated for $\{^{103}Rh([9]aneS_3)([9]aneS_3\text{-}H)BF_4\}^+ = 549$,

$\{^{103}Rh([9]aneS_3)([9]aneS_3\text{-}H)\}^+ = 461$

C H N Analysis

Expect	19.9%C	3.23%H	0%N	for $[Rh([9]aneS_3)([9]aneS_3\text{-}H)](BF_4)_2$
Found	20.4%C	3.29%H	0%N	

(b) The reaction was carried out as described in (a) above, except that 0.5 cm^3 of NEt_3 was added. The resulting red product was isolated as detailed above. The ^1H N.M.R. spectrum was similar to a above except that the intergral of the resonance at $\delta = 6.75$ was larger.

Ir spectrum $\upsilon(cm^{-1})$: 2995-2940(broad, s), 1630(w), 1590(mw),1550(mw),1445(s),1415(s),1405(s), 1285(s), 1200-1000(br,vs,BF_4), 940(ms), 910(ms), 820 (ms), 620(ms), 520(ms).

The Conversion of $[Rh([9]aneS_3)([9]aneS_3\text{-}H)](BF_4)_2$ to $[Rh([9]aneS_3)_2]$

(a) $[Rh([9]aneS_3)([9]aneS_3\text{-}H)](BF_4)_2$ (20mg) was added to refluxing HBF_4 and stirred for two hours. CH_3CN was added and then Et_2O to yield a cream precipitate which was isolated and dried.

^1H N.M.R.spectrum (CD_3CN, 298K) $\delta = 3.09$ ($[9]aneS_3$) p.p.m.

(b) $[Rh([9]aneS_3)([9]aneS_3\text{-}H)](PF_6)_2$ (20mg) was dissolved in refluxing CH_3CN and HPF_6 added. After stirring for two hours Et_2O was added to yield a cream precipitate which was isolated and dried.

^1H N.M.R.spectrum (CD_3CN, 298K) $\delta = 3.09$ ($[9]aneS_3$) p.p.m.

Electrochemistry

Electrochemical measurements were carried out on a Brüker E310 Universal Palorograph. All readings were taken using a three-electrode potentiastatic system in CH_3CN with 0.1M $TBABF_4$ as a supporting electrolyte. Cyclic Voltammetry measurements were performed under an argon atmosphere using a double Pt electrods and an Ag/AgCl reference electrode. All potentials are quoted Vs Fc / Fc^+.

References

1 'The Chemistry of Macrocyclic Ligand Complexes', L.F. Lindoy, Cambridge University Press, Cambridge, 1989.

2 G.A. Melson in 'Coordination Chemistry of Macrocyclic Compounds', Ed G.A. Melson, Plenum Press, New York, 1979, chapter 1

3 J.F. Endicott and D. Durham 'Coordination Chemistry of Macrocyclic Compounds', Ed G.A. Melson, Plenum Press, New York, 1979, chapter 6

4 V.L. Goedken in 'Coordination Chemistry of Macrocyclic Compounds', Ed G.A. Melson, Plenum Press, New York, 1979, chapter 10

5 L.J. Boucher in 'Coordination Chemistry of Macrocyclic Compounds', Ed G.A. Melson, Plenum Press, New York, 1979, chapter 8

6 L.J. Boucher in 'Coordination Chemistry of Macrocyclic Compounds', Ed G.A. Melson, Plenum Press, New York, 1979, chapter 9

7 (a) N.F. Curtis, *J. Chem. Soc.*, 1960, 4409
(b) N.F. Curtis and D.A. House, *Chem. Ind. (London)*, 1961, 1708

8 For example, M. de Sousa-Healy and A.J. Rest, *Adv. Inorg. Chem. Radiochem.*, 1978, **21**, 1

9 D. K. Cabbiness and D.W. Margerum, *J. Am. Chem. Soc.*, 1969, **91**, 6540

10 K. Henrick, P.A. Tasker, and L.F. Lindoy, *Prog. Inorg. Chem.*, 1983, **33**, 1

11 K.R. Adam, M. Antolovich, L.G. Brigden, A.J. Loeng, L.F. Lindoy, P.J. Baillie, D.K. Uppal, M. McPartlin, D. Prospero, L. Fabrizzi, and P.A. Tasker, *J. Chem. Soc., Dalton Trans.*, 1991, 2493

12 R.C. Luckay and R.D. Hancock, *J. Chem. Soc., Dalton Trans.*, 1991, 1491

13 'Stereochemistry of Organometallic and Inorganic Compounds Volume 2: Stereochemical and Stereophysical Behaviour of Macrocycles', Ed I. Bernal, Elsevier, Amsterdam, 1987

14 R.D. Hancock and A.E. Martel, *Comments in Inorg. Chem.*, 1988, **6**, 237

15 R.E. de Simone and M.D. Glick, *J. Am. Chem. Soc.*, 1976, **98**, 762

16 R.S. Glass, G.S. Wilson, and W.N. Setzer, *J. Am. Chem. Soc.*, 1980, **102**, 5068

17 G.F. Smith and D.W. Margerum, *J. Chem. Soc., Chem. Commun.*, 1975, 807

18 F.P. Minz and D.W. Margerum, *Inorg. Chem.*, 1978, **13**, 2941

19 V.J. Thoem, J.C.A. Bayern, and R.D. Hancock, *J. Am. Chem. Soc.*, 1984, **106**, 3198.

20 Y. Hung, L.Y. Martin, S.S. Jackels, A.M. Tait, and D.H. Busch, *J. Am. Chem. Soc.*, 1977, **99**, 4029

21 D.K. Cabbiness and D.W. Margerum, *J. Am. Chem. Soc.*, 1970, **92**, 2151

22 D.H Busch, K. Farmiery, V.L. Goedken, V. Katovic, A.C. Melnuk, C.R. Sperati, and N. Tokel, *Adv. Chem. Ser.*, 1971, **100**, 44

23 P. Chaudhuri and K. Wieghardt, *Prog. Inorg. Chem.*, 1987, **35**, 329

24 R. Bhula, P. Osvath, and D.C. Weatherburn, *Coord. Chem. Rev.*, 1988, **91**, 89

25 P.V. Bernhardt and G.A. Lawrance, *Coord. Chem Rev.*, 1990, **104**, 297

26 A.J. Blake and M. Schröder, *Adv. Inorg. Chem.*, 1990, **35**, 1

27 L. Sacconi, F. Mani, and A. Benchini in 'Comprehensive Coordination Chemistry', Ed G. Wilkinson, Pergamon Press, Oxford, 1987, vol 5, chapter 50

28 B.J. Hathaway in 'Comprehensive Coordination Chemistry', Ed G. Wilkinson, Pergamon Press, Oxford, 1987, vol 5, Chapter 53

29 P.S. Sheridan and F. Jardine in 'Comprehensive Coordination Chemistry', Ed G. Wilkinson, Pergamon Press, Oxford, 1987, vol 4, chapter 48

30 M.J.H. Russel and C.F.J. Bernard in 'Comprehensive Coordination Chemistry', Ed G. Wilkinson, Pergamon Press, Oxford, 1987, vol 5, chapter 51

31 D.M. Roundhill in 'Comprehensive Coordination Chemistry', Ed G. Wilkinson, Pergamon Press, Oxford, 1987, vol 5, chapter 52

32 T. Mashiko and T. Dolphin in 'Comprehensive Coordination Chemistry', Ed G. Wilkinson, Pergamon Press, Oxford, 1987, vol 2, chapter 21

33 A. Müller and E. Diemann in 'Comprehensive Coordination Chemistry', Ed G. Wilkinson, Pergamon Press, Oxford, 1987, Vol 2, chapter 16.2

34 M. Schröder and T.A. Stephenson in 'Comprehensive Coordination Chemistry', Ed G. Wilkinson, Pergamon Press, Oxford, 1987, vol 4, chapter 45

35 (a) K. Nay and A. Chakravorty, *Coord. Chem. Rev.*, 1980, **33**, 87
(b) R.I. Haines and A. McAuley, *Coord. Chem. Rev.*, 1981, **39**, 77

36 N.F. Curtis and D.F. Cook, *J. Chem. Soc., Chem. Commun.*, 1967, 962

37 D.C. Olsen and J. Vasilevskis, *Inorg. Chem.*, 1969, **8**, 1611

38 E.K. Barefield and T. Mocella, *Inorg. Chem.*, 1973, **12**, 2439

39 D.G. Pilsbury and D.H. Busch, *J. Am. Chem. Soc.*, 1976, **98**, 7836

40 A. Benchini, L. Fabrizzi, and A. Poggi, *Inorg. Chem.*, 1981, **20**, 2544

41 J.C. Brodovitch, A. McAuley, and T. Ostwald, *Inorg. Chem.*, 1982, **21**, 3442

42 R. Hay, H. Pizari, B. Korybut-Doszkiwicz, G. Ferguson, and B. Ruhl, *J. Chem. Soc., Dalton Trans.*, 1989, 85

43 G. de Santis, M.D. Casa, M. Mariani, B. Seghi, and L. Fabrizzi, *J. Am. Chem. Soc.*, 1989, **111**, 3422

44 D.P. Rillema, J.F. Endicott, and E. Papacostantinov, *Inorg. Chem.*, 1971, **10**, 1739

45 E.K. Barefield, F.V. Lovecchio, N.E. Tokel, E. Ochiai, and D.H. Busch, *Inorg. Chem.*, 1972, **11**, 283

46 (a) K. Wieghardt, W. Schmidt, W. Herman, and H.-J. Küppers, *Inorg. Chem.*, 1983, **22**, 2953

(b) K. Wieghardt, W. Walz, B. Nuber, J. Weiss, A. Ozarowski, H. Stratemaier, and D. Reiner, *Inorg. Chem.*, 1986, **25**, 1650

47 L. Fabrizzi, M. Mariano, B. Seghi, and F. Zanchi, *Inorg. Chem.*, 1989, **28**, 3362

48 A. McAuley, P.R. Norman and O. Olubuyide, *Inorg. Chem.*, 1984, **23**, 1939

49 (a) N. Jubran, G. Ginzberg, H. Cohen, and D. Meyerstein, *J. Chem Soc., Chem. Commun.*, 1982, 517;

(b) N. Jubran, G. Ginzberg, H. Cohen, and D. Meyerstein, *Inorg. Chem.*, 1985, **24**, 251

50 'The Bioinorganic Chemistry of Nickel', Ed J.R. Lancaster, V.C.H. Publishers, New York, 1988, chapters 1, 2, 5, 8, 9, 10

51 C. Fan, M. Teixeira, J. Moura, B.H. Huynh, J. le Gall, H.D. Peck Jr., and B.M. Hoffman, *J. Am. Chem. Soc.*, 1991, **113**, 20

52 G.J. Colpas, M.J. Maroney, C. Baginka, M. Kumar, W.S. Willis, S.L. Suib, N. Baidya, and P.K. Masharak, *Inorg. Chem.*, 1991, **30**, 920

53 D.C. Olsen and J. Vasilevskis, *Inorg. Chem.*, 1971, **10**, 463

54 R.L. Deming, A.L. Allred, A.E. Dahl, A.W. Merlinger, and M.O. Kostner, *J. Am. Chem. Soc.*, 1976, **98**, 4132

55 T.R. Felthouse, *Prog. Inorg. Chem.*, 1982, **29**, 73

56 K.J. Pandry, *Coord. Chem. Rev.*, 1992, **121**, 1

57 M. Hoshino, K. Yasufuku, S. Konishu and M. Imamura, *Inorg. Chem.*, 1984, **23**, 1982

58 (a) K.M. Kadish, C.-L. Yao, J.E. Anderson, and P. Cocollias, *Inorg. Chem.*, 1985, **24**, 4515

(b) J.E. Anderson, C.-L. Yao, and K.M. Kadish, *Inorg. Chem.*, 1986, **25**, 718

(c) J.E. Anderson, C.-L. Yao, and K.M. Kadish, *Organometallics*, 1987, **6**, 706

(d) J.E. Anderson, C.-L. Yao, and K.M. Kadish, *J. Am. Chem. Soc.*, 1987, **109**, 1106

59 A.E. Sherry and B.B. Wayland, *J. Am. Chem. Soc.*, 1989, **111**, 5010

60 B.R. James and D.V. Stynes, *J. Am. Chem. Soc.*, 1972, **94**, 6225

61 (a) B.B. Wayland and K.B. Rassi, *J. Organomet. Chem.*, 1984, **276**, C27

(b) K.J. Del Rossi and B.B. Wayland, *J. Am. Chem. Soc.*,1985, **107**, 7941

62 R. S. Paonessa, N.C. Thomas, and J. Halpern, *J. Am. Chem. Soc.*, 1985, **107**, 4333

63 Y.H. Tse, P. Seymour, N. Kobayashi, H. Lam, C.C. Leznoff, and A.B.P. Lever, *Inorg. Chem.*, 1991, **30**, 4453

64 J. MacB. Harrowfield, A.J. Herlt, P.A. Lay, A.M. Sargeson, A.M. Bond, W.A. Mulac, and J.C. Sullivan, *J. Am. Chem. Soc.*, 1983, **105**, 5503

65 H.A. Boucher, G.A. Lawrance, P.A. Lay, A.M. Sargeson, A.M. Bond, D.M. Sangster, and J.C. Sullivan, *J. Am. Chem. Soc.*, 1983, **105**, 4652

66 A.J. Blake, L.M. Gordon, T.I. Hyde, G. Reid, and M. Schröder, *J. Chem. Soc., Chem. Commun.*, 1988, 1452

67 D. Mandon, R. Weiss, M. Franke, E. Bill, and A.X. Trautwein, *Angew. Chem., Int. Ed. Engl.*, 1989, **28**, 1709

68 H. Fuji and K. Ichikawa, *Inorg. Chem.*, 1992, **31**, 110

69 A.L. Balch, C.R. Conman, L. Latos-Grazyñski, and M.W. Reiner, *J. Am. Chem. Soc.*, 1992, **114**, 2230

70 D. Mandon, R. Weiss, K. Tayaraj, A. Gold, J. Turner, and A.X. Trautwein, *Inorg. Chem.*, 1992, **31**, 4404

71 S. Ozawara, Y. Watanabe, and I. Morishama, *Inorg. Chem.*, 1992, **31**, 4043

72 S. Tsuchiya, *J. Chem. Soc., Chem. Commun.*, 1991, 716

73 W.R. Scheidz, H. Song, K.J. Haller, M.K. Safo, R.D. Osursz, C.A. Reed, P.G. Debrunner, and C.E. Schultz, *Inorg. Chem.*, 1992, **31**, 1991

74 (a) L.R. Milgrom, W.D. Flitter, and E.L. Short, *J. Chem. Soc., Chem. Commun.*, 1991, 788

(b) L.R. Milgrom and W.D. Flitter, *J. Chem. Soc., Chem. Commun.*, 1991, 1492

75 M.A. Petit, T. Thami and R. Even, *J. Chem. Soc., Chem. Commun.*, 1989, 1059

76 I.S. Butler and J.F. Harrod, 'Inorganic Chemistry, Principles and Applications', Benjamin/Cummings Publishers, New York, 1989, chapter 24

77 M.W. Makinen in 'Techniques and Topic in Bioinorganic Chemistry', Ed C.A. McAuliffe, MacCallum Press, New York, 1975, chapter 1

78 E. Frieden, *J. Chem. Educ.*, 1985, **62**, 917

79 T.D. P. Stack, T.B. Karpishin, and K.N. Raymond, *J. Am. Chem. Soc.*, 1992, **114**, 1512

80 S. Konnetschny-Rapp, G. Jung, K.N. Raymond, J. Meines, and H. Zähner, *J. Am. Chem. Soc.*, 1992, **114**, 2224

81 C.-W. Lee, D.J. Ecker, and K.N. Raymond, *J. Am. Chem. Soc.*, 1985, **107**, 6920

82 T.B. Karpishin, M.S. Gebherd, E.I. Soloman, and K.N. Raymond, *J. Am. Chem. Soc.*, 1991, **113**, 2977

83 Y. Tor, J. Libman, A. Shanzer, C.E. Felder, and E. Lifson, *J. Am. Chem. Soc.*, 1992, **114**, 6661

84 T.B. Karpishin and K.N. Raymond, *Angew. Chem., Int. Ed. Engl.*, 1992, **31**, 466

85 N.D. Chasteen, *Coord. Chem. Rev.*, 1977, **22**, 1

86 S.M. Heald, E.A. Stern, B. Bunner, E.M. Holt, and S.L. Holt, *J. Am. Chem. Soc.*, 1979, **101**, 67

87 S.M. Gorum and S.J. Lippard, *Nature*, 1986, **319**, 666

88 B.D. Berezin, 'Coordination Compoounds of Porphyrins and Phthalocyanines', (trans. V.G. Voplan), John Wiley and Sons, Chichester, 1982, chapters 1, 2 and 8

89 K.S Suslick and T.J. Reinart, *J. Chem. Educ.*, 1985, **62**, 974

90 B. Morgan and D. Dolphin, *Structure and Bonding*, 1987, **64**, 115

91 P.R.O. Montellano, *Acc. Chem. Res.*, 1987, **20**, 289

92 E. Tsuchida, T. Komatsu, E. Hasegawa, and H. Uishide, *J. Chem. Soc., Dalton Trans.*, 1990, 2713

93 C. Cartier, M. Momenteau, E. Dartyge, A. Fontaine, G. Tourillon, A. Michalowicz, and M. Verdaguer, *J. Chem. Soc., Dalton Trans.*, 1992, 609

94 G.E. Wuenschell, C. Teteau, D. Lavalette, and C.A. Reed, *J. Am. Chem. Soc.*, 1992, **114**, 3346

95 J.P. Collman, R.R. Gagné, T.R. Halbert, J.-C. Marchon, and C.A. Reed, *J. Am. Chem. Soc.*, 1973, **95**, 7868

96 J.P. Collman, *Acc. Chem. Res.*, 1977, **10**, 265

97 J.T. Groves, *J. Chem. Educ.*, 1985, **62**, 928

98 S. Kock, S.C. Tang, R.H. Holm, and R.B. Frankel, *J. Am. Chem. Soc.*, 1975, **97**, 914

99 D.L. Corina, S.L. Miller, J.N. Wright, and M. Ahtar, *J. Chem. Soc., Chem. Commun.*, 1991, 782

100 P.J. Toscano and L.G. Marzini, *Prog. Inorg. Chem.*, 1984, **31**, 105

101 J.M. Pratt, *Chem. Soc. Rev.*, 1985, **14**, 161

102 H.M. Marques, *J. Chem. Soc., Dalton Trans.*, 1991, 339

103 M.R. Tarasevich and K.A. Radyushkina, *Russ. Chem. Rev (Engl. Transl.)*, 1980, **49**, 718

104 E. Yeager, *Electrochim Acta*, 1984, **29**, 1527

105 F. Van den Brink, E. Barendrecht, and W. Visscher, *Recl. Trav. Chim, Pays-Buys*, 1980, **99**, 253

106 R.J.H. Chan, C. Ueda, and T. Kuwana, *J. Am. Chem. Soc.*, 1983, **105**, 3713

107 R.J.H. Chan, C. Ueda, and T. Kuwana, *Inorg. Chem.*, 1985, **24**, 3777

108 S. Fukuzumi, S. Mochizuki, and T. Tanaka, *J. Chem. Soc., Chem. Commun.*, 1989, 391

109 D. Sazov, A. McAdams, H.M.M. Franzen, and K.M. Kadish, *J. Am. Chem. Soc.*, 1990, **112**, 7879

110 J. P. Collman, P. Denisevich, Y. Konai, M. Marocco, C. Koval, and F.C. Anson, *J. Am. Chem. Soc.*, 1980, **102**, 6027

111 Y. Le Mest, M. L'Her, J. Courtot-Coupez, J.P. Collman, and E.R. Eritt, *J. Chem. Soc., Chem. Commun.*, 1983, 1286

112 H.-Y. Liu, I. Abdulmuhdi, C.K. Chang, and F.C. Anson, *J. Phys. Chem.*, 1985, **89**, 665

113 R. Karaman, S. Jean, Ö. Almersson, and T.C. Bruice, *J. Am. Chem. Soc.*, 1992, **114**, 4899

114 J.P. Collman, J.E. Hutchinson, M.A. Lopez, A. Tabord, R. Guillard, W.K. Seok, J.A. Ibers, and M. L'Her, *J. Am. Chem. Soc.*, 1992, **114**, 9869

115 J.P. Collman and K.Kim, *J. Am. Chem. Soc.*, 1986, **108**, 7847

116 O. Ikeda, S. Itoh, and H. Yoneyama, *Bull. Soc. Chem. Jpn.*, 1988, **61**, 1428

117 N. Kobayashi, K. Sudo, and T. Osa, *Bull. Soc. Chem. Jpn.*, 1990, **63**, 571

118 N. Kobayashi, P. Janda, and A.B.P. Lever, *Inorg. Chem.*, 1992, **31**, 5173

119 D. Chen, R.J. Motekaitis, and A. E. Martell, *Inorg. Chem.*, 1991, **30**, 1396

120 J.H. Cameron, and S. Graham, *J. Chem. Soc., Dalton Trans.*, 1992, 385

121 N. Shinohara, K. Ishii, and M. Hirose, *J. Chem. Soc., Chem. Commun.*, 1990, 701

122 E. Asato, S. Hashimote, N. Matsumate and S. Kida, *J. Chem. Soc., Dalton Trans.*, 1990, 1741

123 R.V. Gobi and R. Ramaraj, *J. Chem. Soc., Chem. Commun.*, 1992, 1436

124 (a) J.P. Collman, J.E. Hutchinson, P.S. Wagenknecht, N.S. Lewis, M.A. Lopez, and R. Guillard, *J. Am. Chem. Soc.*, 1990, **112**, 8206

(b) J.P. Collman, P.S. Wagenknecht, J.E. Hutchinson, N.S. Lewis, M.A. Lopez, R. Guillard, M. L'Her, A.A. Bothner-By, and P.K. Mishra, *J. Am. Chem. Soc.*, 1992, **114**, 5654

125 J.P. Collman, P.S. Wagenknecht, R.T. Hembre, and N.S. Lewis, *J. Am. Chem. Soc.*, 1990, **112**, 1294

126 J.P. Collman, P.S. Wagenknecht, and N.S. Lewis, *J. Am. Chem. Soc.*, 1992, **114**, 5665

127 J.W. Buchler and P.D. Smith, *Angew. Chem., Int. Ed. Engl.*, 1974, **13**, 745

128 M.J. Camenzind, B.R. James, and D. Dolphin, *J. Chem. Soc., Chem. Commun.*, 1986, 1137

129 J.P. Collman, J.I. Brauman, J.P. Fitzgerald, J.W. Sparapenny, and J.A. Ibers, *J. Am. Chem. Soc.*, 1988, **110**, 3486

130 M.J. Camenzind, B.R. James, D. Dolphin, J.W. Sparapenny, and J.A. Ibers, *Inorg. Chem.*, 1988, **27**, 3054

131 T. Yoshida, T. Adachi, M. Kaminaka, and T. Ueda, *J. Am. Chem. Soc.*, 1988, **119**, 4872

132 (a) J.P. Collman, J.E. Hutchinson, M.A. Lopez, R. Guillard, and R.A. Reid, *J. Am. Chem. Soc.*, 1991, **31**, 2795

(b) J.P. Collman, J.E. Hutchinson, M.A. Lopez, and R. Guillard, *J. Am. Chem. Soc.*, 1992, **114**, 8066

133 J.P. Collman, J.E. Hutchinson, M.S. Ennis, M.A. Lopez, and R. Guillard, *J. Am. Chem. Soc.*, 1992, **114**, 8074

134 M.H. Barley, K. Takeuchi, W.R. Murphy, and J. Meyer, *J. Chem. Soc., Chem. Commun*, 1985, 507

135 I. Taniguchi, N. Nakashima, and K. Yasukouchi, *J. Chem. Soc., Chem. Commun*, 1986, 1814

136 I. Taniguchi, T. Shimpuku, K. Yamashita, and H. Otaki, *J. Chem. Soc., Chem. Commun*, 1990, 915

137 (a) B.B. Wayland and B.A. Woods, *J. Chem. Soc., Chem. Commun*, 1981, 700

(b) B.B. Wayland, B.A. Woods, and V.L. Coffin, *Organometallics*, 1986, **5**, 1059

138 H.W. Bosch and B.B. Wayland, *J. Chem. Soc., Chem. Commun*, 1986, 900

139 A.E. Sherry and B.B. Wayland, *J. Am. Chem. Soc.*, 1989, **111**, 5010

140 R. Paonessa, N.C. Thomas, and J. Halpern, *J. Am. Chem. Soc.*, 1985, **107**, 4333

141 P.J. Brothers and J.P. Collman, *Acc. Chem. Res.*, 1986, **19**, 209

142 J.Y. Becker, B. Vaines, R. Eger (née Levin), and L. Kaufman (née Orenstein), *J. Chem. Soc., Chem. Commun.*, 1985, 1471

143 S. Meshitsuka, M. Ichikawa, and K. Tamaru, *J. Chem. Soc., Chem. Commun.*, 1974, 158

144 S. Kapusta and N. Hackerman, *J. Electrochem. Soc.*, 1984, **131**, 1511

145 C.M. Lieber and N.S. Lewis, *J. Am. Chem. Soc.*, 1984, **106**, 5033

146 T. Atoguchi, A. Aramata, A. Kazusaka, and M. Enyo, *J. Chem. Soc., Chem. Commun.*, 1991, 156

147 M. Hammouche, D. Lexa, M. Momenteau, and J.M. Saveant, *J. Am. Chem. Soc.*, 1991, **113**, 8455

148 B. Fisher and R. Eisenberg, *J. Am. Chem. Soc.*, 1980, **102**, 7361

149 M. Beley, J.-P. Collin, R. Ruppert, and J.P. Sauvage, *J. Am. Chem. Soc.*, 1986, **108**, 7461

150 M.G. Bradley, T. Tysak, D.J. Groves, and N.A. Vlachopoulos, *J. Chem. Soc., Chem. Commun.*, 1983, 349

151 D.A. Gangi and R.R. Durand Jr, *J. Chem. Soc., Chem. Commun.*, 1986, 697

152 E. Fujita, C. Creutz, N. Smith and D.J. Szalda, *J. Am. Chem. Soc.*, 1991, **113**, 343

153 (a) C. Creutz, H.A. Schwarz, J.F. Wishart, E. Fujita, and N. Sutin, *J. Am. Chem. Soc.*, 1989, **111**, 1153

(b) C. Creutz, H.A. Schwarz, J.F. Wishart, E. Fujita, and N. Sutin, *J. Am. Chem. Soc.*, 1991, **113**, 3361

154 S. Sakaki, *J. Am. Chem. Soc.*, 1992, **114**, 2055

155 E. Kumura, X. Bu, M. Shionaya, S. Wada, and S. Marayama, *Inorg. Chem.*, 1992, **31**, 4542

156 B. Mennier, *Chem. Rev.*, 1992, **92**, 1411

157 J.T. Groves and T.E. Nemo, *J. Am. Chem. Soc.*, 1983, **105**, 5786

158 T.G. Traylor, W.-P. Fann, and D. Bandyopadhay, *J. Am. Chem. Soc.*, 1989, **111**, 8009

159 S. O'Malley and T. Kodadek, *J. Am. Chem. Soc.*, 1989, **111**, 9116

160 J.P. Collman, X. Zhang, R.T. Hembre, and J.I. Brauman, *J. Am. Chem. Soc.*, 1990, **112**, 5356

161 J.P. Collman, X. Zhang, V.J. Lee, and J.I. Brauman, *J. Chem. Soc., Chem. Commun.*, 1992, 1647

162 Y. Naruta, F. Tani, N. Ishikara, and K. Maruyama, *J. Am. Chem. Soc.*, 1991, **113**, 6865

163 K. Konishi, K.-I. Oda, K. Nishida, T. Aida, and S. Inoue, *J. Am. Chem. Soc.*, 1992, **114**, 1313

164 L.-N. Chiang, K. Konishi, T. Aida, and S. Inoue, *J. Chem. Soc., Chem. Commun.*, 1992, 254

165 H. Ohtake, T. Higuchi, and M. Horobi, *J. Am. Chem. Soc.*, 1992, **114**, 10660

166 J.T. Groves and P. Viski, *J. Am. Chem. Soc.*, 1989, **111**, 8537

167 J.F. Bartoli, O. Brigand, P. Battioni, and D. Mansuy, *J. Chem. Soc., Chem. Commun.*, 1991, 440

168 (a) J.I. Setsume, X. Ishimara, T. Moriyama, and T. Kitao, *J. Chem. Soc., Chem. Commun.*, 1991, 555

(b) J.I. Setsume, X. Ishimara, T. Moriyama, and T. Kitao, *J. Chem. Soc., Chem. Commun.*, 1991, 556

169 (a) Y. Naruta, F. Tani, and K. Maruyama, *J. Chem. Soc., Chem. Commun.*, 1990, 1378

(b) Y. Naruta, F. Tani, and K. Maruyama, *J. Chem. Soc., Chem. CommunTetrahedron Assym.*, 1991, **2**, 533

170 (a) C.J. Pedersen, *J. Am. Chem. Soc.*, 1967, **89**, 2495

(b) C.J. Pedersen, *J. Am. Chem. Soc.*, 1967, **89**, 7017

(c) C.J. Pedersen, *J. Am. Chem. Soc.*, 1967, **92**, 386

(d) C.J. Pedersen, *J. Am. Chem. Soc.*, 1967, **92**, 391

171 W. Mansfield, *Ber.*, 1886, **19**, 696

172 P.C. Ray, *J. Chem. Soc.*, 1920, **117**, 1090

173 (a) G.M. Bennet, *J. Chem. Soc.*, 1922, **121**, 1279

(b) G.M. Bennet, *J. Chem. Soc.*, 1925, **127**, 910

174 J.R. Meadow and E.E. Reid, *J. Am. Chem. Soc.*, 1934, **56**, 2177

175 W. Rosen and D. H. Busch, *J. Chem. Soc., Chem. Commun.*, 1969, 148

176 D. Gerber, P. Changsawangvirod, A.K. Leung, and L.A. Ochrymowycz, *J. Org. Chem.*, 1977, **42**, 2644

177 W.N. Setzer, C.A. Ogle, G. Wilson, and R.S. Glass, *Inorg. Chem.*, 1983, **22**, 266

178 (a) D. Sellman and L. Zapf, *Angew. Chem., Int. Ed. Engl.*, 1984, **23**, 807

(b) D. Sellman and L. Zapf, *J. Organomet. Chem.*, 1985, **289**, 57

179 (a) J. Buter and R. M. Kellogg, *J. Chem. Soc., Chem. Commun.*, 1980, 466

(b) J. Buter and R. M. Kellogg, *J. Org. Chem.*, 1981, **46**, 4481

(c) J. Buter and R. M. Kellogg, *Org. Synth.*, 1987, **65**, 150

180 P.J. Blower and S. R. Cooper, *Inorg. Chem.*, 1987, **26**, 2009

181 S.R. Cooper and S.C. Rawle, *Structure and Bonding*, 1990, **72**, 1

182 B. De Groot, G.R. Giesbrecht, S.J. Loeb, and G.K. Shimuzu, *Inorg. Chem.*, 1991, **30**, 177

183 W.N. Stezer, E.L. Cacioppo, Q. Guo, G.J. Grant, D.D. Kim, J.L. Hubbard, and D.G. Van Derveer, *Inorg. Chem.*, 1990, **29**, 2672

184 J. Buter, R. M. Kellogg, and F. Van Bolhuis, *J. Chem. Soc., Chem. Commun.*, 1990, 282

185 J. Buter, R. M. Kellogg, and F. Van Bolhuis, *J. Chem. Soc., Chem. Commun.*, 1991, 910

186 J. Butter, R. M. Kellogg, and F. Van Bolhuis, *J. Chem. Soc., Chem. Commun.*, 1991, 911

187 R.J. Smith, G.D. Admans, A.P. Richardson, H.-J. Küppers, and P.J. Blower, *J. Chem. Soc., Chem. Commun.*, 1991, 475

188 P. Osvath, A.M. Sargeson, B.W. Skelton, and A.H. White, *J. Chem. Soc., Chem. Commun.*, 1991, 1036

189 (a) G.S. Hanan, J.E. Kickam, and S.J. Loeb, *J. Chem. Soc., Chem. Commun.*, 1991, 893

(b) G.S. Hanan, J.E. Kickam, and S.J. Loeb, *Organometallics*, 1992, **11**, 3063

190 B. De Groot and S.J. Loeb, *Inorg. Chem.* 1990, **29**, 4084

191 J. Casabó, L. Mestres, L. Eschriche, E. Teixidor, and C. Perez-Jimenez, *J. Chem. Soc., Dalton Trans.*, 1991, 1969

192 V. Ahsen, A. Gürek, A. Gül, and Ö. Bekâroglu, *J. Chem. Soc., Dalton Trans.*, 1990, 5

193 J.J. Edema, J. Buter, R.M. Kellog, A.L. Spek, and F. Van Bolhuis, *J. Chem. Soc., Chem. Commun.*, 1992, 1559

194 A. Gelling, J.C. Jeffery, D.C. Pouey, and M.J. Went, *J. Chem. Soc., Chem. Commun.*, 1991, 349

195 C.R. Lucas, S. Liu, M.J. Newlands, J.-P. Charland, and E.J. Gabe, *Can. J. Chem.*, 1989, **67**, 639

196 C.R. Lucas, S. Liu, M.J. Newlands, J.-P. Charland, and E.J. Gabe, *Can. J. Chem.*, 1988, **66**, 1506

197 H. Wu and C.R. Lucas, *Inorg. Chem.*, 1992, **31**, 2354

198 S. Liu, C.R. Lucas, M.J. Newlands, and J.-P. Charland, *Inorg. Chem.*, 1990, **29**, 4380

199 G. Reid and M. Schröder, *Chem. Soc. Rev.*, 1990, **19**, 239

200 Y. Angus, J. Gisselbrecht, R. Louis, and B. Metz, *J. Am. Chem. Soc.*, 1989, **111**, 1494

201 P.D. Beer, J.E. Nation, S.L.W. McWhinnie, M.E. Harman, M.B. Hursthouse, M.I. Ogden, and A.H. White, *J. Chem. Soc., Dalton Trans.*, 1991, 2485

202 A. Craig, R. Kataky, D. Parker, H. Adams, N. Bailey, and H. Schneider, *J. Chem. Soc., Chem. Commun.*, 1989, 1870

203 A.J. Blake, G. Reid, and M. Schröder, *J. Chem. Soc., Dalton Trans.*, 1991, 615

204 N. Atkinson, A.J. Blake, M.J.B. Drew, G. Forsyth, A.J. Lavery, G. Reid, and M. Schröder, *J. Chem. Soc., Chem. Commun.*, 1989, 984

205 N. Atkinson, A.J. Blake, M.J.B. Drew, G. Forsyth, R.O. Gould, A.J. Lavery, G. Reid, and M. Schröder, *J. Chem. Soc., Dalton Trans.*, 1992, 2993

206 A.J. Blake, G. Reid, and M. Schröder, *J. Chem. Soc., Dalton Trans.*, 1990, 3849

207 A.J. Blake, G. Reid, and M. Schröder, *J. Chem. Soc., Chem. Commun.*, 1992, 1074

208 R. Bonomo, F. Bottino, F. Fronczek, A. Mamo, and S. Pappalardo, *Inorg. Chem.*, 1989, **28**, 4593

209 V. Kallert and R. Mattes, *Polyhedron*, 1992, **11**, 617

210 A. McAuley and S. Subramanian, *Inorg. Chem.*, 1990, **29**, 2830

211 U. Heinzel and R. Mattes, *Polyhedron*, 1992, **11**, 597

212 U. Heinzel and R. Mattes, *Polyhedron*, 1991, **10**, 19

213 B.C. Westerby, K.L. Juntunen, G.H. Leggett, V.B. Pett, M.J. Koenigbauer, M.D. Purgett, M.J. Taschner, L.A. Ochrymowycz, and D.B. Rorabacher, *Inorg. Chem.*, 1991, **30**, 2109

214 D. Wakine, M.J. Heeg, J.F. Endicott, and L.A. Ochrymowcz, *Inorg. Chem.*, 1991, **30**, 3061

215 S. Chandrasekhar and A. McAuley, *J. Chem. Soc., Dalton Trans.*, 1992, 2967

216 A. Craig, D. Parker, and G. Ferguson, *Acta Cryst,Section C*, 1989, **45**, 1498

217 L. Escriche, M. Sanz, J. Casabó, F. Teixodor, E. Malin, and C. Miravitiles, *J. Chem. Soc., Dalton Trans.*, 1989, 1739

(b) R.J. Batchelor, F.W.B. Einstein, I.D. Gay, J.-H. Gu, B.D. Johnstone, B.M. Pinto and X.-M. Zhou, *J. Am. Chem. Soc.*, 1990, **112**, 3707

218 W.N. Setzer, B.R. Coleman, G.S. Wilson and R.S. Glass, *Tetrahedron*, 1981, **37**, 2743

219 R. Blom, D.W.H. Rankin, H.E. Robertson, M. Schröder, and A. Taylor, *J. Chem. Soc., Perkin Trans. 2*, 1991, 773

220 J.C. Lockhart and N.P. Tomkinson, *J. Chem. Soc., Perkin Trans 2*, 1992, 533

221 S.G. Murray and F.R. Hartley, *Chem. Rev.*, 1981, **81**, 365

222 M. Schröder, *Pure Appl. Chem.*, 1988, **60**, 517

223 S.R. Cooper, *Acc. Chem. Res.*, 1988, **21**, 141

224 C.G. Kuehn and S.S. Isied, *Prog. Inorg. Chem.*, 1980, **27**, 153

225 A.J. Blake, J.A. Greig, A.J. Holder, T.I. Hyde, A. Taylor, and M. Schröder, *Angew, Chem., Int. Ed. Engl.*, 1990, **29**, 197

226 A.J. Blake, R.O. Gould, J.A. Greig, A.J. Holder, T.I. Hyde, and M. Schröder, *J. Chem. Soc., Chem. Commun.*, 1989, 876

227 (a) A.J. Blake, A.J. Holder, T.I. Hyde, and M. Schröder, *J. Chem. Soc., Chem. Commun.*, 1987, 987

(b) A.J. Blake, A.J. Holder, T.I. Hyde, Y.V. Roberts, A.J. Lavery, and M. Schröder, *J. Organomet. Chem.*, 1987, **323**, 261

228 A.J. Blake, R.O. Gould, A.J. Holder, T.I. Hyde, M.O. Odulate, A.J. Lavery, and M. Schröder, *J. Chem. Soc., Chem. Commun.*, 1987, 118

229 K. Wieghardt, H.-J. Küppers, E. Raube, and C. Krüger, *Angew. Chem., Int. Ed. Eng.*, 1986, **25**, 1101

230 B. De Groot, G.S. Hanan, and S.J. Loeb, *Inorg. Chem.*, 1991, **30**, 4644

231 G.J. Grant, K.A. Sanders, W.N. Setzer, and D.G. Van Derveer, *Inorg. Chem.*, 1991, **30**, 4053

232 S. Chadrasekhar and A. McAuley, *Inorg. Chem.*, 1992, **31**, 2663

233 K. Wieghardt, H.-J. Küppers, and J. Weiss, *Inorg. Chem*, 1985, **24**, 3067

234 H.-J. Küppers, K. Wieghardt, B. Nuber, J. Weiss, E. Bill, and A.X. Trautwein, *Inorg. Chem.*, 1987, **26**, 3762

235 A.J. Blake, A.J Holder, T.I. Hyde, and M. Schröder, *J. Chem. Soc., Chem. Commun.*, 1989, 1433

236 D. Sellman, H.-P. Neuner, and F. Knoch, *Inorg. Chim. Acta*, 1991, **190**, 61

237 (a) A. Hills, D.L. Hughes, M. Jimenenez-Tenerio, J. Leigh, A. Houlton, and J. Silver, *J. Chem. Soc., Chem. Commun.*, 1989, 1774

(b) D.L. Hughes, M. Jimenenez-Tenerio, J. Leigh, A. Houlton, and J. Silver, *J. Chem. Soc., Dalton Trans.*, 1992, 2033

238 (a) D. Sellman and P. Frank, *Angew. Chem., Int. Ed. Engl.*, 1986, **25**, 1107

(b) D. Sellman, P. Frank, and F. Knoch, *J. Organomet. Chem.*, 1988, **339**, 345

239 M.N. Bell, A.J. Blake, A.J. Holder, T.I. Hyde, and M. Schröder, *J. Chem. Soc., Dalton Trans.*, 1990, 3841

240 M.N. Bell, Ph.D Thesis, Univ. of Edinburgh, 1987

241 R.M. Christie, Ph.D Thesis, Univ. of Edinburgh, 1989

242 Y.V. Roberts, Ph.D Thesis, Univ. of Edinburgh, 1991

243 D. Sellman, F. Knoch, and C. Wronna, *Angew. Chem., Int. Ed. Engl.*, 1988, **27**, 691

244 (a) S.C. Rawle and S.R. Cooper, *J. Chem. Soc., Chem. Commun.*, 1987, 308

(b) S.C. Rawle, T.J. Sewell, and S.R. Cooper, *Inorg. Chem.*, 1987, **26**, 3769

(c) M.N. Bell, A.J. Blake, M. Schröder, H.-J. Küppers, and K. Wieghardt, *Angew. Chem., Int. Ed. Eng.*, 1987, **26**, 250

(d) M.N. Bell, A.J. Blake, R.M. Christie, R.O. Gould, A.J Holder, T.I. Hyde, M. Schröder, and L.J. Yellowlees, *J. Chem. Soc., Dalton Trans.*, 1992, 2977

245 R. Ali, S.J. Higgins, and W. Levason, *Inorg. Chim. Acta*, 1984, **84**, 65

246 A.J. Edwards, B.F.G. Johnstone, F.K. Khan, J. Lewis, and P.R. Raithby, *J. Organomet. Chem.*, 1992, **426**, C44

247 W.N. Setzer, G.S. Wilson, and R.S. Glass, *Inorg. Chem.*, 1983, **22**, 266

248 G.S. Wilson, D. Swanson, and R.S. Glass, *Inorg. Chem.*, 1986, **25**, 3827

249 J.R. Hartman, E.R. Hinsta, and S.R. Cooper, *J. Am. Chem. Soc.*, 1986, **108**, 1208

250 D. Reinen, A. Ozarowski, B. Jakob, J. Pebler, H. Stratemaier, K. Wieghardt, and I. Tolksdorf, *Inorg. Chem.*, 1987, **26**, 4010

251 S. Chandrasekhar and A. McAuley, *Inorg. Chem.*, 1992, **31**, 480

252 H.-J. Küppers, K. Wieghardt, S. Stenken, B. Nuber, and J. Weiss, *Z. Anorg. Alle. Chem.*, 1989, **572**, 43

253 H. Doine and T.W. Swaddle, *Inorg. Chem.*, 1991, **30**, 1859

254 K. Travis and D.H. Busch, *Inorg. Chem.*, 1974, **13**, 2591

255 J. Jenkenson, W. Levason, R. Perry, and M. Spicer, *J. Chem. Soc., Dalton Trans.*, 1989, 453

256 S.C. Rawle, R. Yagbasan, K. Prout, and S.R. Cooper, *J. Am. Chem. Soc.*, 1987, **109**, 6181

257 A.J. Blake, R.O. Gould, T.I. Hyde, and M. Schröder, *J. Chem. Soc., Dalton Trans.*, 1988, 1861

258 S.R. Cooper, S.C. Rawle, R. Yagbasan, and D.J. Watkin, *J. Am. Chem. Soc.*, 1991, **113**, 1600

259 A.J. Blake, M.A. Halcrow, and M. Schröder, *J. Chem. Soc., Chem. Commun.*, 1991, 253

260 D.P. Riley and J.D. Oliver, *Inorg. Chem.*, 1983, **22**, 3361

261 A.J. Blake, R.O. Gould, A.J. Holder, T.I. Hyde, G. Reid, and M. Schröder, *J. Chem. Soc., Dalton Trans.*, 1990, 1759

262 A.J. Blake, R.O. Gould, G. Reid, and M. Schröder, *J. Organomet. Chem.*, 1988, **356**, 389

263 S. Saraullah, K. Kano, R.S. Glass, and G.W. Wilson, *J. Am. Chem. Soc.*, 1993, **115**, 592

264 M.J. Bruce and M.A. Bennet in 'Comprehensive Organometallic Chemistry', Ed. G. Wilkinson, 1982, Pergamon Press, Oxford, vol 4, Chapter 32

265 E.A. Seddon and K.R. Seddon, 'The Chemistry of Ruthenium', Elsevier, Oxford, 1984

266 K.R. Seddon, *Coord. Chem. Rev.*, 1982, **41**,112–114 and references therein

267 K.R. Seddon, *Coord. Chem. Rev.*, 1985, **67**, 220–221 and references therein

268 (a) A.F. Hill, N.W. Alcock, J.C. Cannadine, and G.R. Clarke, *J. Organomet. Chem.*, 1992, **426**, C40

(b) N.W. Alcock, J.C. Cannadine, G.R. Clarke, and A.F. Hill, *J. Chem. Soc., Dalton Trans.*, 1993, 1131

269 J.C. Cannadine, A. Hector and A.F. Hill, *Organometallics*, 1992, **11**, 2323

270 R. Mason, K.M. Thomas, D.F. Gill, and B.L. Shaw, *J. Organometallic Chem.*, 1972, 40, C67

271 A.J.F. Fraser and R.O. Gould, *J. Chem. Soc., Dalton Trans.*, 1974, 1139

272 B. Deschamps, F. Mathey, J. Fischer, and J.-H. Nelson, *Inorg. Chem.*, 1984, **23**, 3455

273 Tl···Mo interactions

(a) R.B. King, *Inorg. Chem.*, 1970, **9**, 1936

(b) J. Rajaram and J.A. Ibers, *Inorg. Chem.*, 1973, **12**, 1313

(c) R. Uson, A. Laguna, A. Abada, and E. de Jesus, *J. Chem. Soc., Dalton Trans.*, 1983, 1127 and references therein

(d) R. Guilard, A. Zrinch, M. Ferhart, A. Tabard, P. Mitaine, C. Swistak, P. Richard, C. Leconte, and K.M. Kadish, *Inorg. Chem.*, 1988, **27**, 697 and references therein

(e) A.B. Vishnikin, L.P. Tsyganok, V.A. Omelchenko, and I.G. Glushko, *Ukr. Khim. Zh., (Russ. Ed)*, 1987, **53**, 35 from *Chem. Abs.*, 1987, **107**, 48107

274 Ru···Fe interactions

(a) K.H. Whitmire, R.R. Ryan, J.J. Wasserman, T.A. Albright, and S.-K. Kary, *J. Am. Chem. Soc.*, 1986, **108**, 6831

(b) K.H. Whitmire, J.M. Cassidy, A.L. Rheingold, and R.R. Ryan, *Inorg. Chem.*, 1988, 27, 1347 and references therein

(c) J.M. Cassidy and K.H. Whitmire, *Inorg. Chem.*, 1989, **28**, 1432 and 1435 and references therein

275 Tl···Pt interactions

(a) J.K. Nagle, A.L. Balch, and M.M. Olmstead, *J. Am. Chem. Soc.*, 1988, **110**, 319

(b) T. Ziegler, J.K. Nagle, J.G. Snijders, and E.J. Baerend, *J. Am. Chem. Soc.*, 1989, **111**, 5631 and references therein

(c) A.L. Balch and S.P. Rowley, *J. Am. Chem. Soc.*, 1990, **112**, 6139 and references therein

276 Tl···Au interactions

(a) S. Wang, J.P. Fackler Jr, C. King, and J.C. Wang, *J. Am. Chem. Soc.*, 1988, **110**, 3309

(b) S. Wang, G. Garzon, C. King, J.-C. Wang, and J.P. Fackler Jr, *Inorg. Chem.*, 1989, **28**, 4623 and references therein

(c) Z. Assefa, F. de Stefano, M.A. Garepapaghi, J.H. La Casce Jr, S. Ovellette, M.R. Corson, J.K. Nagle, and H.H. Patterson, *Inorg. Chem.*, 1991, **30**, 2868

277 Tl···Ir interactions

(a) P.I. Van Vliet and K. Vrieze, *J. Organomet. Chem.*, 1977, **139**, 337

(b) A.L. Balch, J.K. Nagle M.M. Olmstead, and P.E. Reedy Jr, *J. Am. Chem. Soc.*, 1987, **109**, 4123

(c) A.L Balch, F. Nere, and M.M. Olmstead, *J. Am. Chem. Soc.*, 1991, **113**, 2995 and references therein

278 Tl···Cu interactions

A.V. Ivanov, P.M. Solozhenkin and V.B. Klyashtornyi, *Koord. khim.*, 1990, **16**, 1240. From *Chim. Abs.*, 1991, **114**, 34612

279 Tl···Ru interaction

G.B. Ansell, M.A. Modrick, and J.S. Bradley, *Acta Crystall., Section C.*, 1984, **40**, 1315

280 Bridging Sulphides

N. Bett, A. Sucheta, F.A. Armstrong, J. Breton, A.J. Thomson, and E.C. Hatchikian, *J. Am. Chem. Soc.*, 1991, **113**, 8948

281 Bridging thiolates

(a) W.A.W.A. Baker, J.L. Davidson, E. Lindsell, K.J. McCullough, and K.W. Muir, *J. Organomet. Chem.*, 1987, **322**, C1

(b) W.A.W.A. Baker, J.L. Davidson, E. Lindsell, K.J. McCullough, and K.W. Muir, *J. Chem. Soc., Dalton Trans.*, 1989, 991 and references therein.

(c) J.L. Davidson, K. Davidson and E. Lindsell, *J. Chem. Soc., Chem. Commun.*, 1983, 452

282 For bridging SCN and SeCN

P.P. Singh, R.C. Verma and G.S. Singh, *Ind. J. Chem., Section A.*, 1982, **21**, 431 and references therein

283 For bridging (C_4BMe_4H)

K. Strumpf, H. Pritzkow, and W. Siebert, *Angew. Chem., Int. Ed. Engl.*, 1985, **24**, 71

284 O.J. Ezomo, M.P. Mingos, and I.D. Williams, *J. Chem. Soc., Chem. Commun.*, 1987, 924

285 H. Schmidbauer, W. Bublak, J. Riede, and G. Müller, *Angew. Chem., Int. Ed. Engl.*, 1985, **24**, 414

286 T.I. Hyde and M. Schröder, Unpublished Results

287 T.A. Stephenson and G. Wilkinson, *J. Inorg. Nucl. Chem.*, 1966, **28**, 945

288 SHELX-76,program for crystal refinement, G.M. Sheldrick, Univ. of Cambridge, England, 1976

289 SHELXTL , P.C. Version 4.2, G.M.Sheldrick, Univ. of Göttingen, Germany, 1990. Siemons Analytical X-ray Instrumentation Inc., Madison, Wisconsin, USA, 1990

290 CALC, program for molecular geometry calculations, R.O. Gould and P. Taylor, Univ. of Edinburgh, 1985

291 D.T. Cromer and J.B. Mann, *Acta Crystallogr., Section A*, 1968, **24**, 321

292 J.F. Coetzee and T.-H. Chang, *Pure Appl. Chem.*, 1986, **58**, 1541 and references therein

293 R.W. Jones and R.H. Staley, *J. Am. Chem. Soc.*, 1982, **104**, 2296

294 (a) B.J. Hathaway and D.G. Holah, *J. Chem. Soc.*, 1964, 2408

(b) W.L. Driessen and W.L. Greoneveld, *Rec. Trav. Chim. Pays-Bas*, 1969, **88**, 491

295 P. Legzdins and J.C. Oxley, *Inorg. Chem.*, 1984, **23**, 1053

296 (a) G. Wu, A.L. Rheingold, and R.F. Heck, *Organometallics*, 1986, **5**, 1922

(b) G. Wu, A.L. Rheingold, and R.F. Heck, *Organometallics*, 1987, **6**, 2386

297 T. Easton, G.A. Heath, T.A. Stephenson and M. Bochmann, *J. Chem. Soc., Chem. Commun.*, 1985, 154

298 K.M. Kadish, and D. Chang, *Inorg. Chem.*, 1982, **21**, 3614

299 (a) J. Lorberth, J. Pebler, and G. Lange, *J. Organometallic Chem.*, 1973, **54**, 177

(b) D.J. Cole-Hamilton and G. Wilkinson, *Nouv. J. Chem.*, 1977, **1**, 141

300 (a) M.A. Bennett and T. Yoshida, *J. Am. Chem. Soc.*, 1978, **100**, 1750

(b) J. F. Almeida, and A. Pidcock, *J. Organomet. Chem.*, 1981, **209**, 415

(c) M.A. Cairns, K.R. Dixon, and M.A.R. Smith, *J. Organomet. Chem.*, 1977, **135**, C33

(d) D.P. Arnold, and M.A. Bennett, *J. Organometallic Chem.*, 1980, **199**, 119

(e) F. Caballero and P Roys, *J. Organometallic Chem.*, 1977, **137**, 229

301 (a) P.S. Pregosin, R. Favez, R. Roulet, T. Bosch, R.A. Michelin and R. Ros, *Inorg. Chim. Acta*, 1980, **45**, L7

(b) L. Randaccio, N. Bresciani-Pahor, P.J. Toscano, and L.G. Marzillo, *Inorg. Chem.*, 1981, **20**, 2722

302 L.G. Marzillo, F. Bayo, M.F. Summers, L.B. Thomas, E. Zangrando, N. Bresciani-Pahor, M. Mari, and L. Randaccio, *J. Am. Chem. Soc.*, 1987, **109**, 6045

303 H.C. Knachel, D.S. Dudis, and J.P. Fackler, *Organometallics*, 1984, **3**, 1312

304 M.D. Fryzuk, C.D. Montgomery, and S.J. Rettig, *Organometallics*, 1991, **10**, 467

305 P. Diversi, G. Ignosso, A. Lucherini, F. Marchetti, V. Adavasio and M. Nardello, *J. Chem. Soc., Dalton Trans.*, 1991, 203

306 D.J. Cole-Hamilton and G. Wilkinson, *J. Chem. Soc., Dalton Trans.*, 1977, 797

307 J.-I. Setsune, Y. Ishimaru, t. Marigama, and T. Kitoa, *J. Chem. Soc., Chem. Commun.*, 1991, 555 and 556

308 T. Faure and P. Braunstein, Poster No 40, 29th International Conference in Co-ordination Chemistry, Lausanne, 1992

309 (a) A. Monge, O. Boutry, E. Carmone, E. Guitterez-Puebla, M.C. Nicasio, P.J. Perez, M.L. Poveda and C. Riva, Poster No 284, 29th International Conference in Co-ordination Chemistry, Lausanne, 1992

(b) O. Boutry, E. Guitterez-Puebla, A. Monge, M.C. Nicasio, P.J. Perez, and E. Carmona, *J. Am. Chem. Soc.*, 1987, **109**, 6045

310 (a) I.T. Horvath, G. Payli, L. Marka, and G. Andreetti, *J. Chem. Soc., Chem. Commun.*, 1979, 1054

(b) I.T. Horvath, G. Payli, L. Marka, and G. Andreetti, *Inorg. Chem.*, 1983, **22**, 1049

311 P.C. Bevan, J. Chatt, A. Diamantis, R.A. Head, G.A. Heath and G.J. Leigh, *J. Chem. Soc., Dalton Trans.*, 1977, 1711

312 (a) T.V. Ashworth, M. Berry, J.A.K. Howard, M. Lugano, and F.G.A. Stone, *J. Chem. Soc., Chem. Commun.*, 1979, 43

(b) M. Berry, J.A.K. Howard, and F.G.A. Stone, *J. Chem. Soc., Dalton Trans.*, 1980, 1601

313 C.P. Casey, R.A. Boggs, D.F. Marter, and J.C. Calabrese, *J. Chem. Soc., Chem. Commun.*, 1973, 243

314 'Comp. Organometallic Chem.', Ed. G. Wilkinson, Pergamon Press, Oxford, 1982, Vol 7, pp 80, 329, 499 and references therein

315 F.M. Dean, *Adv. in Heterocyclic Chem.*, 1982, **30**, 167

316 Y. Kojima, S. Wakita, and N. Kato, *Tetrahedron Lett.*, 1979, 4577 and 4667

317 (a) C. Ullenius, *Acta Chem., Scand.*, 1972, **26**, 3382
(b) F.D. King and D.R.M. Walton, *Synthesis*, 1976, 40
(c) D.W. Knight and G. Pattenden, *J. Chem. Soc., Perkin I*, 1975, 641

318 K.H. Pannell, R. Lea-Olivares, R.A. Toscano, and R.N. Kapoor, *Organometallics*, 1987, **6**, 1821

319 B. Chaudret, and F.A. Jalon, *J. Chem. Soc., Chem. Commun.*, 1988, 711

320 (a) D. Sellman, U. Kleine Kleffmann, L. Zapf, G. Hunter, and L. Zsolnai, *J. Organometallic Chem.*, 1984, **263**, 321
(b) D. Sellman and W. Reissner, *J. Organometallic Chem.*, 1985, **294**, 333

321 D. Sellman and W. Reissner, *J. Organometallic Chem.*, 1985, **297**, 319

322 (a) D. Sellman, P Lechner, M. Moll and F. Knoch, *Z. Naturfursch, Section B*, 1991, **46**, 209
(b) D. Sellman, H.-P. Neuner, M. Moll, and F. Knoch, *Z. Naturfursch, Section B*, 1991, **46**, 303
(c) D. Sellman, P Lechner and M. Moll, *Z. Naturfursch, Section B*, 1991, **46**, 1459
(d) D. Sellman, P Lechner, F. Knoch and M. Moll, *Z. Naturfursch, Section B*, 1991, **46**, 1585

323 (a) D. Sellman, Unpublished Results
(b) I. Barth, disseration, Erlangen, 1989 (student in D. Sellman's laboratories)

324 (a) H. Gilman and G.F. Wright, *J. Am. Chem. Soc.*, 1933, **55**, 3302
(b) M. Sikirica, D. Grdeniç, and S. Gimas, *Acta Cryst. Section B*, 1986, **28**, 926
(c) P.W. Jennings, S.K. Reeder, J.C. Hurley, C.N. Caughan, and G.D. Smith, *J. Org. Chem.*, 1974, **39**, 3392

325 D. Randon, B. Chaudret, X.-D. He, and D. Labroue, *J. Am. Chem. Soc.*, 1991, **113**, 5671

326 S.R. Radchaudhuri, S. Ghosh, and R.S. Solomon, *J. Am. Chem. Soc.*, 1980, **104**, 6841

327 (a) F.M. Dean and M.V. Sargeant in 'Comprehensive Heterocyclic Chemistry', Ed. A.R. Katritzky and C.W. Rees, Pergamon Press, Oxford, 1984, vol 3, chapter 3.10, 3.11
(b) ' Chemistry of Carbon Compounds ', Rodd, Volume iv, Part A, 1973, Elsevier Publishing Co. and References therein.

328 'The Purification of Laboratory Chemicals', D.D. Perrin, W.L.F. Armarego, and D.R. Perrin, 1980, Pergamon Press, Oxford

329 (a) My thanks to L.R. Hanton, University of Otago, Dunedin, New Zealand, for fruitful discussions.

(b) A.J. Down, L.R. Hanton, and T. Kemmitt, Poster No 660, 29th International Conference on Co-ordination Chemistry, Lausanne, 1992

330 (a) F.W. Parett, and M.S. Sun, *J. Chem. Educ.*, 1977, **54**, 448

(b) J.F. Coetzee and G.P. Cunningham, *J. Am. Chem. Soc.*, 1965, **87**, 2529

(c) A.K.R. Unni, L. Elias, and H.I. Schill, *J. Phys. Chem.*, 1963, **67**, 1216

(d) M.A. Coplan and R.M. Fuoss, *J. Phys. Chem.*, 1964, **68**, 1181

331 J.-C. Bardin, *Analusis*, 1977, **1**, 140

332 T. Osa and T. Kuwana, *Electroanal. Chem., Interfacial Electrochem.*, 1969, **22**, 389

333 (a) A. Murray, and D.L. Williams, 'Organic Synthesis with Isotopes', Interscience Publishers Inc., New York, 1958, vol 1, p 129

(b) 'Synthesis with Stable Isotopes of Carbon, Nitrogen and Oxygen', D.G. Ott, John Wiley & Sons, New York, 1981, p 63–65

334 (a) A. Murray, and D.L. Williams, 'Organic Synthesis with Isotopes', Interscience Publishers Inc., New York, 1958, vol 1, p 813

(b) 'Synthesis with Stable Isotopes of Carbon, Nitrogen and Oxygen', D.G. Ott, John Wiley & Sons, New York, 1981, p 131–132

335 (a) V.J. Traynelis, W.L. Hergenrothen, H.T. Hanson, and J.A. Valicenti, J. Org. Chem., 1964, 29, 123

(b) U. Messow, R. Pfestorf, and W. Hauthal, Chem. Techn., 1981, 33, 372

336 D. M. Smith in 'Comprehensive Organic Chemistry', Ed. D.H.R. Barton and W.D. Ollis, Pergamon Press, Oxford, 1979, vol 4, chapter 16.1

337 A.H. Jackson in 'Comprehensive Organic Chemistry', Ed. D.H.R. Barton and W.D. Ollis, Pergamon Press, Oxford, 1979, vol 4, chapter 17.1

338 O. Meth-Cohn in 'Comprehensive Organic Chemistry', Ed. D.H.R. Barton and W.D. Ollis, Pergamon Press, Oxford, 1979, vol 4, chapter 19.1

339 C.D. Johnson in 'Comprehensive Heterocyclic Chemistry', Ed. A.R. Katritzky and C.W. Rees, Pergamon Press, Oxford, 1984, vol 2, chapter 2.04

340 F.S. Yates in 'Comprehensive Heterocyclic Chemistry', Ed. A.R. Katritzky and C.W. Rees, Pergamon Press, Oxford, 1984, vol 2, chapter 2.09

341 C.W. Bird and G.W.H. Cheeseman in 'Comprehensive Heterocyclic Chemistry', Ed. A.R. Katritzky and C.W. Rees, Pergamon Press, Oxford, 1984, vol 2, chapter 3.01

342 D.J. Chadwick in 'Comprehensive Heterocyclic Chemistry', Ed. A.R. Katritzky and C.W. Rees, Pergamon Press, Oxford, 1984, vol 2, chapter 3.04

343 R..M. Kellogg in 'Comprehensive Heterocyclic Chemistry', Ed. A.R. Katritzky and C.W. Rees, Pergamon Press, Oxford, 1984, vol 2, chapter 3.13

344 J. Reedijk in 'Comprehensive Co-ordination Chemistry', Ed. E.G. Wilkinson, Pergamon Press, Oxford, 1987, vol 2, chapter 13.2

345 T.B. Rauchfuss, *Prog. Inorg. Chem.*, 1991, **39**, 259

346 W.H. Myers, J.I. Koontz, and W.D. Harman, *J. Am. Chem. Soc.*, 1992, **114**, 5684, and references therein

347 M. Draganjac, T.B. Rauchfuss, and C.J. Ruffing, *Organometallics*, 1985, **4**, 1909

348 A.K. Skaugset, T.B. Rauchfuss, and S.R. Wilson, *Organometallics*, 1990, **9**, 2875

349 J.R. Dilworth, Y.Zheng, S. Lu, and Q. Wu, *Transition Met. Chem.*, 1992, **17**, 364 and references therein

350 D.P. Riley and R.E. Shumate, *J. Am. Chem. Soc.*, 1984, **106**, 3181

351 D.P. Riley and J.D. Oliver, *Inorg. Chem.*, 1986, **25**, 1815

352 D.P. Riley and J.D. Oliver, *Inorg. Chem.*, 1986, **25**, 1822

353 D.P. Riley and J.D. Oliver, *Inorg. Chem.*, 1986, **25**, 1825

354 R.S. Scivastava, B. Milani, E. Alessio, and G. Mestroni, *Inorg. Chim. Acta*, 1992, **191**, 15

355 B.W. Arbuckle, Parimal K. Bharadwaj, and W.K. Musker, *Inorg. Chem.*, 1991, **30**, 440

356 (a) D.T.T. Yapp, J. Jaswal, S.J. Rettig, B.R. James, and K.A. Skov, *Inorg. Chim. Acta*, 1989, **177**, 199

(b) E. Alessio, B. Milani, G. Mestroni, M. Calligaris, P. Faleschini, and W.M. Attia, *Inorg. Chim. Acta*, 1990, **177**, 255

357 K. Krogh-Jesperen, X. Zhang, J.D. Westbrook, R. Fikar, K. Nayak, W.-L. Kwik, J.A. Potenza, and H.J. Schugar, *J. Am. Chem., Soc.*, 1989, **111**, 4082

358 B.R. Manzana, F.A. Jalon, F.J. Lahez, B. Chaudret, and D. de Montauzon, *J. Chem. Soc., Dalton trans.*, 1992, 977

359 L.-S. Kau, E.W. Svastits, J.H. Dawson, and K.O. Hodgson, *Inorg. Chem.*, 1986, **25**, 4307

360 T. Moshiko, M.E. Kastner, K. Spartalian, W.R. Scheidt, and C.A. Reed, *J. Am. Chem. Soc.*, 1978, **100**, 6354

361 G.N. Glavee, L.M. Daniels, and R.J Angelici, *Organometallics*, 1989, **8**, 1856

362 (a) H.A. Brune, H. Roth, and G. Schmitberg, *J. Organometallic Chem.*, 1991, **412**, 237

(b) T. Debaerdemaeker, H. Roth, and H.-A. Brune, *J. Organometallic Chem.*, 1991, **412**, 243

363 B. Norén and Å Oskarsson, *Acta Chem. Scand. Section A*, 1985, **39**, 701

364 R. Uson, A. Laguna, A. Navarro, R.V. Parish, and L.S. Moore, *Inorg. Chim. Acta*, 1986, **112**, 205

365 R. El-Mehdawi, F.R. Fronczek, and D.M. Roundhill, *Inorg. Chem.*, 1986, **25**, 1155

366 T. Mahiko, C.A. Reed, K.J. Haller, M.E. Kastner, and W.R. Scheidt, *J. Am. Chem. Soc.*, 1981, **103**, 5758

367 K. Blechschmitt, E. Guggolz, and M.L. Ziegler, *Z. Naturforsch, Section B*, 1985, **40**, 85

368 T.-F. Lai and C.-K. Poon, *J. Chem. Soc., Dalton Trans.*, 1982, 1465

369 C.-K. Poon and C.-M. Che, *J. Chem. Soc., Dalton Trans.*, 1980, 756

370 C.-K. Poon and C.-M. Che, *J. Chem. Soc., Dalton Trans.*, 1981, 495

371 C.-K. Poon, S.-S. Kwong, C.-M. Che, and Y.-P. Kon, *J. Chem. Soc., Dalton Trans.*, 1981, 495

372 T. Ueda, H Yamanaka, T. Adachi, and T. Yoshida, *Chem. Lett.*, 1985, 525

373 T. Yoshida, T. Adachi, T. Ueda, T. Tanaka and F. Goto, *J. Chem. Soc., Chem. Commun.*, 1990, 343

374 A.J. Blake, G. Reid, and M. Schröder, *J. Chem. Soc., Dalton Trans.*, 1985, 1692

375 K. Travis and D.H. Busch, *Inorg. Chem.*, 1974, **13**, 2591

376 T. Yoshida, T. Ueda, T. Adachi, K. Yamamoto, and T. Higuchi, J. *Chem. Soc., Chem. Commun.*, 1985, 1137

377 C.A. Tollman, *Chem. Rev.*, 1977, **77**, 813

378 E.E. Mercer and R.R. Buckley, *Inorg. Chem.*, 1965, **4**, 1692

379 J.E. Fergusson and A.M. Greenaway, *Aust. J. Chem.*, 1978, **31**, 497

380 (a) K.W. Buck, A.B. Foster, W.D. Pardoe, M.H. Qadir, and J.M. Webber, *J.Chem.Soc., Chem Commun.*, 1966, 759

(b) R.R. Fraser, T Durst, M.R McClory, R. Viau, and Y.Y. Wigfield, *Internat. J. Sulfur Chem.(A)*, 1971, **1**, 133

(c) R. Lett, S. Bory, B. Moreau, and A Marquet, *Bull.Soc.Chim.France.*, 1973, 2851

(d) G.W. Buchanan and T. Durst, *Tetrahedron Lett.*, 1975, 1683

381 T. Durst in " Comprehensive Organic Chemistry", Ed D.H.R. Barton and W.D. Ollis, Pergammon Press, Oxford, 1979, Vol 3, Chapters 11.6, 11.7, 11.8, 11.9

382 (a) J.L. Bellamy in 'Organic Sulfur Compounds", Ed N. Kharash, Pergammon Press, Oxford, 1961, Vol 1, Chapter 6

(b) D. Bernard, L. Batemann, and J.I. Cuneen in 'Organic Sulfur Compounds", Ed N. Kharash, Pergammon Press, Oxford, 1961, Vol 2, Chapter 21

383 (a) J. Drabowicz, P. Kielbasinki, and M. Mikolajczyk in " The Chemistry of Sulphones and Sulphoxides", Ed S. Patai, Z. Rappoport, and C.J.M. Stirling, J. Wiley and Sons, Chichester, 1988, Chapter 8

(b) E. Block in " The Chemistry of Sulphones and Sulphoxides", Ed S. Patai, Z. Rappoport, and C.J.M. Stirling, J. Wiley and Sons, Chichester, 1988, Chapter 20

(c) U. Zoller in " The Chemistry of Sulphones and Sulphoxides", Ed S. Patai, Z. Rappoport, and C.J.M. Stirling, J. Wiley and Sons, Chichester, 1988, Chapter 9

(d) J. Hoyle in " The Chemistry of Sulphones and Sulphoxides", Ed S. Patai, Z. Rappoport, and C.J.M. Stirling, J. Wiley and Sons, Chichester, 1988, Chapter 21

(e) K. Schank in " The Chemistry of Sulphones and Sulphoxides", Ed S. Patai, Z. Rappoport, and C.J.M. Stirling, J. Wiley and Sons, Chichester, 1988, Chapter 7

(f) E. Block in " The Chemistry of Functional Groups, Supplement E : The Chemistry of Ethers, Crown Ethers, Hydroxyl Groups and their Sulphur Analogues", Ed S. Patai, J. Wiley and Sons, Chichester, 1980, Vol 1, Chapter 13

384 M. Madesclaire, *Tetrahedron*, 1986, **42**, 5459

385 (a) S Uemura in " Comprehensive Organic Synthesis", Ed B.H. Trost and I. Flemming, Pergammon Press, Oxford, 1991, Vol 7, Chapter 6.2

(b) I.W.J. Still in " Comprehensive Organic Synthesis", Ed B.H. Trost and I. Flemming, Pergammon Press, Oxford, 1991, Vol 8, Chapter 2.3

386 C. Sheu, C.S. Foote, and C.-L. Gu, *J.Am.Chem.Soc.*, 1992, **114**, 3015

387 P. Broughham, M.S. Cooper, D.A. Cummerson, M. Heaney, and N. Thompson, *Synthesis* , 1987, 1015

388 (a) R.S. Glass, A. Petsom, G.S. Wilson, R. Martinez, and E. Juaristi, *J.Org.Chem.*, 1986, 51, 4337
(b) Q. Porter, Utley, P. Machion, V. Bardini, P Scumacher, and . Viertler, *J.Chem.Soc., Perkin Trans. 1*, 1984, 973
389 M. Nonayama and K Nonayama, *Transition Metal Chem.*, 1985, **10**, 382
390 (a) A. Taylor, A.J. Blake, A.J. Holder, T.I. Hyde, and M. SchrÖder, *Nouv. J. Chem.*, 1991, **15**, 1511
(b) Dr A. Taylor, Ph.D. Thesis, Edinburgh, 1991
391 H.-J. Küppers, K. Wieghardt, B. Nuber, J. Weiss, E. Bill, and A.X. Trautwein, *Inorg. Chem*, 1987, **26**, 3762
392 H.C. Freeman and M.L. Golomb, *J.Chem.Soc., Chem.Commun..*, 1970, 1523
393 W.A. Freeman, *Acta Cystallogr. Section B*, 1977, **33**, 191
394 T. Kageyama, Y. Ueno, and M. Okaware, *Synthesis* , 1982, 815
395 C. Strinivista, A Chellamani, and P. Kuthalingen, *J.Org.Chem*, 1982, **47**, 428
396 D.N. Gupta, P.Hodge, and J.E. Davies, *J.Chem.Soc..,Perkin 1,*, 1981, 2970
397 D.J. Cavanaugh, *Science*, 1957, **125**, 1040
398 T. Takata, M. Yamazaki, K. Fujimori, Y.H. Kim, T. Iganagi, and S. Oae, *Bull.Chem.Soc.Jpn.*, 1983, **56**, 2300
399 Y. Naruta, F. Tani, and K. Maruyama, *Tetrahedron Assymetry*, 1991, 1189
400 (a) S. Oae, Y. Watanabe, and K. Fujimori, *Tetrahedron Lett*, 1982, 1189
(b) T. Takata and W. Ando, *Tetrahedron Lett.*, 1983, 3631
(c) A. Miller, *Tetrahedron Lett* , 1982, 753
401 H. Saltzman and J.G. Sharejkin , " Organic Synthesis" ,Vol 43, 60
402 C.K.Chang, R.K. Di Nello, and D. Dolphin, " Inorganic Synthesis", Vol 20, 147
403 W. Clegg, *Acta Crystallogr. Section A*, 1981, **37**, 22
404 SHELX-86, program for crystal structure solution, G.M. Sheldick, Univ. of Göttingen, Germany, 1986
405 H.-J. Küppers, A Neves, C. Pomp, D. Ventur, K. Wieghardt, B. Nuber, and J. Weiss, *Inorg.Chem.* , 1986, **25**, 2400
406 J.A. Davies, *Adv. Inorg. Chem. Radiochem.*, 1981, **24**, 115
407 K. Eriks, C.B.Shoemaker, and R. Thomas, *Acta Crystallogr.*, 1966, **21**, 12
408 (a) A.J. Blake, A.J. Holder, T.I. Hyde, H.-J. Küppers, M. Schröder, S. Stözel, and K. Wieghardt, *J.Chem.Soc., Chem.Commun.* , 1989, 1600
(b) S. Stözel, Diplomarbeit, Rühr Universität, Bochum Germany, 1989

409 M.A. Bennett, L.Y. Goh, and A.C. Willis, *J.Chem.Soc.., Chem. Commun.* 1992, 1180

410 (a) D. Sellman, I. Barth, F. Knoch, and M. Moll, *Inorg Chem.* , 1990, **29**, 1823

(b) I. Barth, Dissetation, Erlangen Universität, Erlangen, Germany, 1989

411 D. Sevdic and L. Fekete, *Polyhedron* , 1985, **4**, 1371

List of Abbrevisations

[9]aneN$_3$	1,4,7-triazacyclononane
[9]aneS$_3$	1,4,7-trithiacyclononane
[12]aneS$_4$	1,4,7,10-tetrathiacyclododecane
[14]aneS$_4$	1,4,8,11-tetrathiacyclotetradecane
[16]aneS$_4$	1,5,9,13-tetrathiacyclohexadecane
br	broad
COD	Cyclooctadiene
Cy	Cyclohexyl
DEPT	Distortionless Enhancement by Polarisation Transfer
DMF	Dimethylformamide
DMSO	Dimethylsulfoxide
E.I.	Electron Impact
e.s.d.	Estimated Standard Deviation
e.s.r	Electron Spin Resonance
Et	Ethyl
Et_2O	Diethylether
EtOH	Ethanol
F.A.B.	Fast Atom Bombardment
Fc	Ferrocene
Hz	Hertz
ir	Infrared
m	Medium
MCPBA	meta–Chloroperbenzoic Acid
Me	Methyl
MeOH	Methanol
MeCN	Acetonitrile
MMPP	Magnesium Monoperphthalate
N.M.R.	Nuclear Magnetic Resonance

3-NOBA	3-Nitrobenzylalcohol
OAc	Acetate
OEP	Octaethylporphyrin
p.p.m.	parts per million
Ph	Phenyl
s	Strong
sh	Shoulder
TBA	Tetrabutylammonium
THF	Tetrahydrofuran
THT	Tetrahydrothiophene
THT-S-Oxide	Tetrahydrothiophene–S–Oxide
TPP	Tetraphenylporphyrin
v/v	volume for volume
w	weak
w/w	weight for weight

Lecture Courses and Meetings Attended

1. Aspects and Applications of N.M.R. Spectroscopy, Drs I.H. Sadler and D. Reed
2. X-ray Crystallography - Structure Solution and Refinement, Drs Gould and Blake
3. Current Advancess in Inorganic Chemistry, Drs S. Chapman, M. Schröder and R.E.P. Winpenny
4. Inorganic Medicinal Chemistry, Drs Chapman and Welch
5. E. S. R. Spectroscopy, Dr Winpenny
6. Departmental Inorganic Colloquia and Friday Discussion Groups, 1989-1992
7. University of Strathclyde Inorganic Club, 1990, 1991, 1992
8. RSC Scottish Dalton Meeting, Glasgow, 1990
9. Butler Postgraduate Electrochemistry Symposium, 1990, 1991
10. RSC Annual Chemical Congress, Belfast, 1990
11. Platinum Metals Meeting, Cambridge, 1990
12. UK Macrocyclic Meeting, Warwick, 1990, Manchester. 1991
13 International Conference on Co-ordination Chemistry, Lausanne, Switzerland, 1992

PUBLICATIONS

Heteronuclear Cluster Formation: The Synthesis and Structure of the Chloro-bridged Tetranuclear Complex $[TlCl_2Ru(PPh_3)([9]aneS_3)]_2(PF_6)_2$ Incorporating a $[RuCl_2Tl_2Cl_2Ru]$ Ladder ([9]aneS$_3$ = 1,4,7-Trithiacyclononane)

Alexander J. Blake, Robert M. Christie, Yvonne V. Roberts, Martin J. Sullivan, Martin Schröder* and Lesley J. Yellowlees*

Department of Chemistry, The University of Edinburgh, West Mains Road, Edinburgh EH9 3JJ, Scotland

Treatment of $[RuCl_2(PPh_3)([9]aneS_3)]$, formed in high yield by reaction of $[RuCl_2(PPh_3)_3]$ with [9]aneS$_3$, with $TlPF_6$ in CH_2Cl_2 at 273 K affords the yellow hetero-cluster species $[TlCl_2Ru(PPh_3)([9]aneS_3)]_2(PF_6)_2$ incorporating a $[RuCl_2Tl_2Cl_2Ru]$ ladder; dissolution of $[TlCl_2Ru(PPh_3)([9]aneS_3)]_2(PF_6)_2$ in acetone leads to precipitation of TlCl and the formation of the orange chloro-bridged dimer $[RuCl(PPh_3)([9]aneS_3)]_2(PF_6)_2$.

The macrocycle [9]aneS$_3$ has been shown to be an effective six-electron capping ligand for a range of transition metal centres.[1–4] [9]aneS$_3$ is, therefore, the thioether S-donor analogue of cyclopentadienyl, aryl, tris(pyrazolyl)borate and triphos $[(Ph_2PCH_2)_3CMe]$, and might be expected to form a range of half-sandwich organometallic and coordination compounds. We have reported previously the synthesis and properties of the low-valent complexes $[M([9]aneS_3)(alkene)_2]^+$ (M = Rh, Ir),[5] and describe herein the first examples of half-sandwich complexes of [9]aneS$_3$ with Ru^{II}, and the formation of an unusual heteronuclear Ru_2Tl_2 cluster.

Treatment of $[RuX_3(PR_3)_3]$ (X = Cl, PR_3 = PMe_2Ph, PEt_2Ph, $PEtPh_2$; X = Br, PR_3 = $PEtPh_2$) with [9]aneS$_3$ in EtOH or CH_2Cl_2 affords $[RuCl(PR_3)_2([9]aneS_3)]^+$, while reaction of $[RuX_2(PPh_3)_3]$ (X = Cl, Br) with [9]aneS$_3$ gives $[RuX_2(PPh_3)([9]aneS_3)]$ in high yield.† The bright yellow complex $[RuCl_2(AsPh_3)([9]aneS_3)]$ can be prepared by reaction of $[RuCl_3(AsPh_3)_2(MeOH)]$ with [9]aneS$_3$ in refluxing EtOH. $[RuX_2(PPh_3)([9]aneS_3)]$ is a particularly useful starting material for the synthesis of chiral complexes of the type $[RuX(PPh_3)(L)([9]aneS_3)]^+$. Thus, reaction of $[RuX_2(PPh_3)([9]aneS_3)]$ with $TlPF_6$ in the presence of coordinating solvents or ligands gives $[RuX(PPh_3)(L)([9]aneS_3)]^+$ (X = Cl, L = NCMe, NCPh, PMe_2Ph, $P(OMe)_2Ph$, CO, CS, py; X =

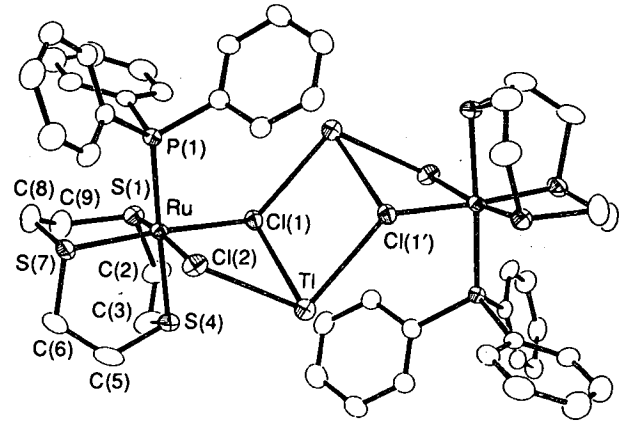

Fig. 1 The single crystal X-ray structure of $[TlCl_2Ru(PPh_3)([9]aneS_3)]_2^{2+}$ with numbering scheme adopted. H atoms are omitted for clarity. Tl–Cl(1) 3.0734(11), Tl–Cl(1′) 3.0014(11), Tl–Cl(2) 3.0026(12), Ru–Cl(1) 2.4416(12), Ru–Cl(2) 2.4526(12), Ru–S(1) 2.2804(13), Ru–S(4) 2.3501(13), Ru–S(7) 2.2821(13), Ru–P(1) 2.3539(12) Å. The primed atom is related to its unprimed equivalent by inversion through (0,1,1).

† All complexes reported herein have been fully characterised using elemental analysis, IR, NMR, electronic and FAB mass spectroscopy, and in the case of $[RuCl(PEtPh_2)_2([9]aneS_3)]^+$ and $[RuCl(PPh_3)(NCMe)([9]aneS_3)]^+$ by single crystal X-ray diffraction.[4]

Br, L = PMe_2Ph, py; py = pyridine).[4†] Interestingly, the complex $[RuCl(PPh_3)_2([9]aneS_3)]^+$ could not be prepared under these conditions, presumably owing to the steric hindrance of the relatively large phosphine ligands. We were interested in the reactions of $[RuX_2(PPh_3)([9]aneS_3)]$ with $TlPF_6$ in the absence of coordinating ligands, particularly with regard to the possibility of forming oligomers of the $[Ru([9]aneS_3)]^{2+}$ fragment.

Reaction of $[RuCl_2(PPh_3)([9]aneS_3)]$ with $TlPF_6$ in CH_2Cl_2 at 273 K leads to the formation of a yellow complex. Elemental analysis of the product indicated a stoichiometry $[RuCl_2(PPh_3)([9]aneS_3)]\cdot TlPF_6$, while FAB mass spectroscopy showed a molecular ion peak at $M^+ = 819$ assigned to $[^{102}Ru^{35}Cl_2(PPh_3)([9]aneS_3)^{205}Tl]^+$ with the correct isotopic distribution; IR and NMR spectroscopy confirmed the presence of $[9]aneS_3$, PPh_3 and PF_6^- counter-ion. Crystals of the complex were obtained from CD_3NO_2 and a single crystal X-ray structural determination was undertaken. The crystal structure‡ confirms the presence of Ru and Tl within a tetranuclear cluster (Fig. 1). Two octahedral $[RuCl_2(PPh_3)([9]aneS_3)]$ units are bridged *via* the coordinated Cl^- ligands to two Tl^+ ions to form a highly unusual $RuCl_2Tl_2Cl_2Ru$ ladder structure. The cluster incorporates two μ^2-Cl^- and two μ^3-Cl^- bridges with the two halves of the cation related by an inversion centre; ∠Cl(1)TlCl(2) 69.36(3), ∠Cl(1)TlCl(1′) 72.61(3), ∠Cl(2)TlCl(1′) 107.38(3)°. There are no apparent M–M interactions: Tl···Ru = 4.0596(4) Å. The $[9]aneS_3$ ligand is coordinated facially to Ru^{II} with the Ru–S bond *trans* to PPh_3 [2.3501(13) Å] being longer than those *trans* to Cl^- [2.2804(13), 2.2821(13) Å]; additionally, there is a potential long-range interaction between Tl and S(4) at 3.6481(13) Å. Although there are a number of documented heterometallic Tl-containing species in the literature,[6–8] most of them incorporate direct M–Tl bonding rather than the bridged M–halide–Tl units observed in our structure. Mingos and coworkers have reported the structure of $[Pt_3(CO)_3(PCy_3)_3Tl][Rh(C_8H_{12})Cl_2]$ (Cy = cyclohexyl) incorporating direct Pt–Tl bonding and an additional Rh···Cl···Tl interaction.[7] Schmidbauer and coworkers have reported $[(C_6H_3Me_3)_6Tl_4][GaBr_4]_4$, an adduct of $[GaBr_4]^-$ with $[Tl(C_6H_3Me_3)]^+$ and $[Tl(C_6H_3Me_3)_2]^+$. This species incorporates an array of Ga···Br···Tl bridges.[8] The use of $TlPF_6$ to remove coordinated Cl^- from metal complexes is well documented. The formation of $[TlCl_2Ru(PPh_3)([9]aneS_3)]_2(PF_6)_2$ suggests that the first step in the reaction involves interaction of Tl^+ with the Cl^- within the coordination sphere of the parent complex.

Dissolution of $[TlCl_2Ru(PPh_3)([9]aneS_3)]_2(PF_6)_2$ in acetone or $MeNO_2$ leads to precipitation of TlCl and the formation of the orange chloro-bridged dimer $[RuCl(PPh_3)([9]aneS_3)]_2(PF_6)_2$. The single crystal structure of the complex‡ shows (Fig. 2) two Cl^- ligands [Ru–Cl = 2.4654(10), 2.4945(10) Å], bridging $[Ru(PPh_3)([9]aneS_3)]^{2+}$ units, Ru–S(*trans* to Cl) = 2.2880(10), 2.2817(10), Ru–S(*trans* to P) = 2.3456(10) Å, Ru···Ru = 3.7768(6), Cl···Cl = 3.2151 Å. The two halves of the dimer are related by a crystallographic inversion centre. Dissolution of $[TlCl_2Ru(PPh_3)([9]aneS_3)]_2(PF_6)_2$ in more strongly coordinating solvents or in the presence of donor ligands (L) leads to the formation of the mononuclear species $[RuCl(PPh_3)(L)([9]aneS_3)]^+$.

The results described herein suggest that the first step in the thalliation of metal–halide bonds involves the interaction of Tl^+ with the M–Cl bond to form an M–Cl–Tl bridge, and that the synthesis of mixed main group–transition metal clusters might be readily achieved using this methodology. Current work is aimed at developing these electrophilic Ru^{II} complexes of $[9]aneS_3$ towards C–H bond activation and organic transformations.

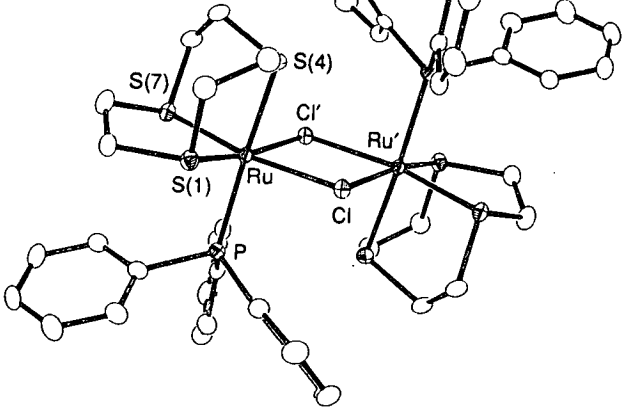

Fig. 2 The single crystal X-ray structure of $[RuCl(PPh_3)([9]aneS_3)]_2^{2+}$ with numbering scheme adopted. H atoms are omitted for clarity. Ru–S(1) 2.2880(10), Ru–S(4) 2.3456(10), Ru–S(7) 2.2817(10), Ru–Cl 2.4654(10), Ru–Cl′ 2.4945(10), Ru–P 2.3741(10) Å. The primed atom is related to its unprimed equivalent by inversion through (½,0,½).

‡ *Crystal data* for $C_{48}H_{54}Cl_4P_2Ru_2S_6Tl_2^{2+}2PF_6^-\cdot 4CD_3NO_2$. M = 2184.15, triclinic, space group $P\bar{1}$, a = 10.2202(23), b = 10.7668(18), c = 16.4498(24) Å, α = 96.206(15), β = 100.971(16), γ = 90.862(14)°, V = 1765.4 Å^3 [from 2θ values of 42 reflections measured at ±ω (2θ = 31–32°, λ = 0.71073 Å), T = 150 ± 0.1 K], Z = 1, D_c = 2.053 g cm^{-3}, μ(Mo-Kα) = 5.45 mm^{-1}. A yellow column (0.08 × 0.16 × 0.43 mm) was mounted on a Stoë STADI-4 four-circle diffractometer. Data collection at 150 K using Mo-Kα X-radiation (λ = 0.71073 Å), ω–2θ scans and the learnt-profile method[9] gave 4620 unique reflections ($2\theta_{max}$ 45°), of which 4193 with $F \geq 4\sigma(F)$ were used in all calculations. A correction for *ca.* 5% linear isotropic decay was incorporated in the data reduction. Following solution by heavy-atom methods, the structure was refined by full-matrix least-squares (on F),[10] with anisotropic thermal parameters for all non-H atoms except that F and O atoms with occupancies of 0.5 or less were treated isotropically. Phenyl rings were refined with idealised D_{6h} symmetry. H atoms were included in fixed, calculated positions except for those in the solvent CD_3 groups which were treated as part of rigid groups.[10] Disorder affects both the PF_6^- anions and the solvent; it was modelled by allowing split occupancies for the equatorial F atoms and the O atoms. At isotropic convergence, corrections for absorption were applied empirically using DIFABS.[11] At final convergence, R = 0.0251, R_w = 0.0321, S = 1.053 for 439 parameters and the final ΔF synthesis showed no Δρ beyond ±0.72 e Å^{-3}. A secondary extinction parameter refined to 1.4 × 10^{-8}.

Crystal Data for $C_{48}H_{54}Cl_2P_2Ru_2S_6^{2+}2PF_6^-\cdot 2CH_3NO_2$. M = 1570.18, monoclinic, space group $P2_1/n$, a = 14.5986(24), b = 13.1911(23), c = 15.6282(17) Å, β = 103.425(9)°, V = 2927.3 Å^3 [from 2θ values of 31 reflections measured at ±ω (2θ = 24–26°, λ = 0.71073 Å)], Z = 2, D_c = 1.781 g cm^{-3}, T = 150 ± 0.1 K, orange tablet, 0.085 × 0.23 × 0.23 mm, μ = 0.994 mm^{-1}, $F(000)$ = 1584. Data collection under the conditions described above yielded 4461 absorption-corrected reflections, 3631 unique (R_{int} 0.030), giving 3222 with $F \geq 4\sigma(F)$ for use in all calculations. No significant crystal decay or movement was observed. A Patterson synthesis located the Ru and iterative cycles of least-squares refinement and difference Fourier synthesis located all remaining non-H atoms. Four of the F atoms in the PF_6^- anion were found to be disordered over two orientations, the major component having occupancies of 0.84–0.95. The F atoms of the minor component were refined with a common U_{iso} of 0.08 Å^2 and occupancies ranging from 0.05 to 0.16; all other non-H atoms were refined (by least-squares on F)[10] with anisotropic thermal parameters. Phenyl rings were constrained to refine with idealised D_{6h} symmetry. H atoms were included at fixed, calculated positions, excepting those of the solvate methyl group which was refined as a rigid group: a common U_{iso} of 0.0408(22) Å^2 was refined for all H atoms. At final convergence R, R_w = 0.0293, 0.0434 respectively, S = 1.312 for 354 refined parameters and the final ΔF synthesis showed no Δρ above 0.47 or below −0.69 e Å^{-3}.

Atomic scattering factors were inlaid,[10] or taken from ref. 12. Molecular geometry calculations utilised CALC[13] and the Figures were produced by XP.[14] Atomic coordinates, bond lengths and angles, and thermal parameters have been deposited with the Cambridge Crystallographic Data Centre. See Notice to Authors, Issue No. 1.

We thank the Royal Society of Edinburgh for a Support Research Fellowship (to M. S.), Johnson Matthey Plc for generous loans of platinum metals and the SERC for support.

Received, 6th February 1992; Com. 2/00655C

References

1 A. J. Blake and M. Schröder, *Adv. Inorg. Chem.*, 1990, **35**, 1 and references therein; M. Schröder, *Pure Appl. Chem.*, 1988, **60**, 517.
2 S. R. Cooper and S. C. Rawle, *Struct. Bonding, (Berlin)*, 1990, **72**, 1.
3 R. M. Christie, PhD Thesis, University of Edinburgh, 1989.
4 M. N. Bell, A. J. Blake, H-J. Küppers, M. Schröder and K. Wieghardt, *Angew. Chem.*, 1987, **99**, 253; *Angew. Chem., Int. Ed. Engl.*, 1987, **26**, 250.
5 A. J. Blake, M. A. Halcrow and M. Schröder, *J. Chem. Soc., Chem. Commun.*, 1991, 253.
6 S. K. Searle and J. L. Atwood, *J. Organomet. Chem.*, 1974, **64**, 57; R. C. Burns and J. D. Corbett, *J. Am. Chem. Soc.*, 1981, **103**, 2627; 1982, **104**, 2804; M. Veith and R. Rosker, *Angew. Chem.*, 1982, **92**, 867; *Angew. Chem., Int. Ed. Engl.*, 1982, **21**, 858; G. B. Ansell, M. A. Modrick and J. S. Bradley, *Acta Crystallogr., Sect. C*, 1984, **40**, 1315; K. Strumpf, H. Pritzkow and W. Siebert, *Angew. Chem.*, 1985, **97**, 64; *Angew. Chem., Int. Ed. Engl.*, 1985, **24**, 71; K. H. Whitmire, R. R. Ryan, H. J. Wasserman, T. A. Albright and S. W. Kang, *J. Am. Chem. Soc.*, 1986, **108**, 6831; A. L. Balch, J. K. Nagle, M. M. Olmstead and P. E. Reedy Jr., *J. Am. Chem. Soc.*, 1987, **109**, 4123; K. H. Whitmire, J. M. Cassidy, A. L. Rheingold and R. R. Ryan, *Inorg. Chem.*, 1988, **27**, 1347; R. Guilard, A. Zrinch, M. Ferhat, A. Taberd, P. Mitain, C. Swistak, P. Richard, C. Lecomte and K. M. Kadish, *Inorg. Chem.*, 1988, **27**, 697; W. A. W. A. Bakar, J. L. Davidson, W. E. Lindsell, K. J. McCullough and K. W. Muir, *J. Organomet. Chem.*, 1987, **322**, C1; *J. Chem. Soc., Dalton Trans.*, 1989, 999.
7 O. J. Ezomo, D. M. P. Mingos and I. D. Williams, *J. Chem. Soc., Chem. Commun.*, 1987, 924.
8 H. Schmidbauer, W. Bublak, J. Riede and G. Muller, *Angew. Chem.*, 1985, **97**, 402; *Angew. Chem., Int. Ed. Engl.*, 1985, **24**, 414.
9 W. Clegg, *Acta Crystallogr., Sect. A.*, 1981, **37**, 22.
10 SHELX76, program for crystal structure refinement, G. M. Sheldrick, University of Cambridge, 1976.
11 DIFABS, program for empirical absorption correction, N. Walker and D. Stuart, *Acta Crystallogr., Sect. A*, 1983, **39**, 158.
12 D. T. Cromer and J. B. Mann, *Acta Crystallogr., Sect. A*, 1968, **24**, 321.
13 CALC, program for molecular geometry calculations. R. O. Gould and P. Taylor, University of Edinburgh, 1985.
14 SHELXTL PC Version 4.2, Siemens Analytical X-Ray Instrumentation Inc, Madison, Wisconsin, 1990.

Acta Cryst. (1991). C47, 2717–2718

Structure of O_6[9]aneS_3 (1,4,7-Trithiacyclononane 1,1,4,4,7,7-Hexaoxide)

BY ALEXANDER J. BLAKE,* MARTIN SCHRÖDER AND MARTIN J. SULLIVAN

Department of Chemistry, The University of Edinburgh, West Mains Road, Edinburgh EH9 3JJ, Scotland

(*Received* 31 *October* 1990; *accepted* 29 *April* 1991)

Abstract. $C_6H_{12}O_6S_3$, $M_r = 276.31$, monoclinic, $P2_1/n$, $a = 5.9978$ (5), $b = 12.9947$ (16), $c = 13.8201$ (12) Å, $\beta = 101.294$ (8)°, $V = 1056.3$ Å^3, $Z = 4$, $D_x = 1.737$ Mg m^{-3}, λ(Mo $K\alpha$) = 0.71073 Å, $\mu = 4.68$ mm^{-1}, $F(000) = 576$, $T = 298$ K, $R = 0.0246$ for 1672 unique observed reflections. Although O_6[9]aneS_3 lacks the crystallographically imposed C_3 symmetry of the parent [9]aneS_3, it also adopts a symmetrical [333] conformation in the crystal.

Experimental. Compound prepared by oxidation of [9]aneS_3 using H_2O_2/H_2O/glacial acetic acid (Küppers, Wieghardt, Nuber, Weiss, Bill & Trautwein, 1987) at 333 K, crystals obtained by diffusion of MeOH into DMSO solution. Colourless columnar crystal, 0.18 × 0.21 × 0.42 mm; Stoe-Stadi-4 four-circle diffractometer, graphite-monochromated Mo $K\alpha$ X-radiation; cell parameters from 2θ values of 18 reflections measured at $\pm\omega$ ($30 \le 2\theta \le 32°$). For data collection, ω–2θ scans employing the Learnt-profile method (Clegg, 1981), $2\theta_{max} = 50°$, h −6→6, k 0→15, l 0→16; no significant crystal movement or decay; 1937 unique reflections, giving 1672 with $F > 6\sigma(F)$ for structure solution [by automatic direct methods (Sheldrick, 1986)] and refinement [using full-matrix least squares on F (Sheldrick, 1976)]. Anisotropic thermal parameters for all non-H atoms, H atoms refined freely with a common U_{iso} of 0.0368 (16) Å^2. At final convergence $R = 0.0246$, $wR = 0.0370$, $S = 1.322$ for 173 parameters; $(\Delta/\sigma)_{max}$ in final cycle 0.07, maximum and minimum residues in final ΔF synthesis 0.35, −0.28 e Å^{-3} respectively. The weighting scheme $w^{-1} = \sigma^2(F) + 0.000225F^2$ gave satisfactory agreement analyses. Scattering factors were inlaid (Sheldrick, 1976). Atomic coordinates and equivalent isotropic thermal parameters are given in Table 1, while bond lengths, angles and torsion angles appear in Table 2.† Fig. 1 was generated using an interactive version of *ORTEP*II (*GX*; Mallinson & Muir, 1985) and shows (*a*) a projection onto the least-squares molecular plane with the atom-numbering scheme used and (*b*) an orthogonal view illustrating the conformation

Table 1. *Atomic coordinates and equivalent isotropic thermal parameters* (Å^2) *with e.s.d.'s in parentheses*

$U_{eq} = (1/3)\sum_i\sum_j U_{ij}a_i^*a_j^*\mathbf{a}_i.\mathbf{a}_j$.

	x	y	z	U_{eq}
S(1)	0.22286 (7)	0.81848 (3)	0.71777 (3)	0.0236 (3)
O(1A)	0.14158 (22)	0.92314 (10)	0.71563 (10)	0.0343 (7)
O(1B)	0.44842 (22)	0.79873 (11)	0.70156 (10)	0.0355 (8)
C(2)	0.2063 (3)	0.76402 (15)	0.83449 (12)	0.0266 (9)
C(3)	−0.0323 (3)	0.76380 (14)	0.85749 (13)	0.0263 (9)
S(4)	−0.09831 (8)	0.64568 (3)	0.91200 (3)	0.0268 (3)
O(4A)	−0.32594 (23)	0.65627 (11)	0.92914 (10)	0.0417 (9)
O(4B)	0.08376 (25)	0.62255 (12)	0.99258 (9)	0.0425 (8)
C(5)	−0.1009 (4)	0.54884 (14)	0.82013 (13)	0.0288 (10)
C(6)	−0.2696 (3)	0.57101 (15)	0.72422 (13)	0.0276 (10)
S(7)	−0.16383 (8)	0.55492 (3)	0.61309 (3)	0.0255 (3)
O(7A)	−0.33424 (25)	0.59498 (12)	0.53507 (10)	0.0422 (8)
O(7B)	−0.09129 (25)	0.45034 (10)	0.60703 (9)	0.0370 (8)
C(8)	0.0818 (3)	0.63461 (14)	0.62433 (14)	0.0285 (10)
C(9)	0.0265 (3)	0.74957 (14)	0.62732 (12)	0.0277 (10)

Table 2. *Bond lengths* (Å), *angles* (°) *and torsion angles* (°) *with e.s.d.'s in parentheses*

S(1)—O(1A)	1.4431 (14)	S(4)—C(5)	1.7855 (20)
S(1)—O(1B)	1.4370 (14)	C(5)—C(6)	1.529 (3)
S(1)—C(2)	1.7820 (19)	C(6)—S(7)	1.7852 (19)
S(1)—C(9)	1.7817 (19)	S(7)—O(7A)	1.4306 (15)
C(2)—C(3)	1.525 (3)	S(7)—O(7B)	1.4344 (14)
C(3)—S(4)	1.7881 (19)	S(7)—C(8)	1.7826 (19)
S(4)—O(4A)	1.4373 (15)	C(8)—C(9)	1.533 (3)
S(4)—O(4B)	1.4306 (15)		

O(1A)—S(1)—O(1B)	119.32 (8)	O(4A)—S(4)—C(5)	107.96 (9)
O(1A)—S(1)—C(2)	108.32 (8)	O(4B)—S(4)—C(5)	107.73 (9)
O(1A)—S1—C(9)	106.56 (8)	S(4)—C(5)—C(6)	113.31 (13)
O(1B)—S(1)—C(2)	106.93 (8)	C(5)—C(6)—S(7)	115.92 (13)
O(1B)—S(1)—C(9)	108.30 (8)	C(6)—S(7)—O(7A)	106.49 (9)
C(2)—S(1)—C(9)	106.81 (8)	C(6)—S(7)—O(7B)	108.92 (8)
S(1)—C(2)—C(3)	114.22 (13)	C(6)—S(7)—C(8)	106.50 (9)
C(2)—C(3)—S(4)	112.56 (13)	O(7A)—S(7)—O(7B)	118.74 (9)
C(3)—S(4)—O(4A)	106.45 (8)	O(7A)—S(7)—C(8)	108.10 (9)
C(3)—S(4)—O(4B)	108.06 (9)	O(7B)—S(7)—C(8)	107.49 (8)
C(3)—S(4)—C(5)	106.10 (9)	S(7)—C(8)—C(9)	112.89 (13)
O(4A)—S(4)—O(4B)	119.79 (9)	S(1)—C(9)—C(8)	113.08 (13)

O(1A)—S1—C(2)—C(3)	58.70 (15)	O(4A)—S(4)—C(5)—C(6)	56.20 (15)
O(1B)—S(1)—C(2)—C(3)	−171.51 (13)	O(4B)—S(4)—C(5)—C(6)	−173.12 (13)
C(9)—S(1)—C(2)—C(3)	−55.74 (15)	S(4)—C(5)—C(6)—S(7)	133.28 (12)
O(1A)—S(1)—C(9)—C(8)	−176.74 (13)	C(5)—C(6)—S(7)—O(7A)	−170.91 (14)
O(1B)—S(1)—C(9)—C(8)	53.73 (15)	C(5)—C(6)—S(7)—O(7B)	59.92 (16)
C(2)—S(1)—C(9)—C(8)	−61.12 (15)	C(5)—C(6)—S(7)—C(8)	−55.72 (16)
S(1)—C(2)—C(3)—S(4)	137.52 (11)	C(6)—S(7)—C(8)—C(9)	−65.72 (15)
C(2)—C(3)—S(4)—O(4A)	−179.80 (13)	O(7A)—S(7)—C(8)—C(9)	48.37 (15)
C(2)—C(3)—S(4)—O(4B)	50.33 (15)	O(7B)—S(7)—C(8)—C(9)	177.67 (13)
C(2)—C(3)—S(4)—C(5)	−64.98 (15)	S(7)—C(8)—C(9)—S(1)	137.22 (11)
C(3)—S(4)—C(5)—C(6)	−57.59 (15)		

* Author to whom correspondence should be addressed.

† Lists of structure factors, anisotropic thermal parameters and H-atom coordinates have been deposited with the British Library Document Supply Centre as Supplementary Publication No. SUP 54149 (13 pp.). Copies may be obtained through The Technical Editor, International Union of Crystallography, 5 Abbey Square, Chester CH1 2HU, England.

0108-2701/91/122717-02$03.00

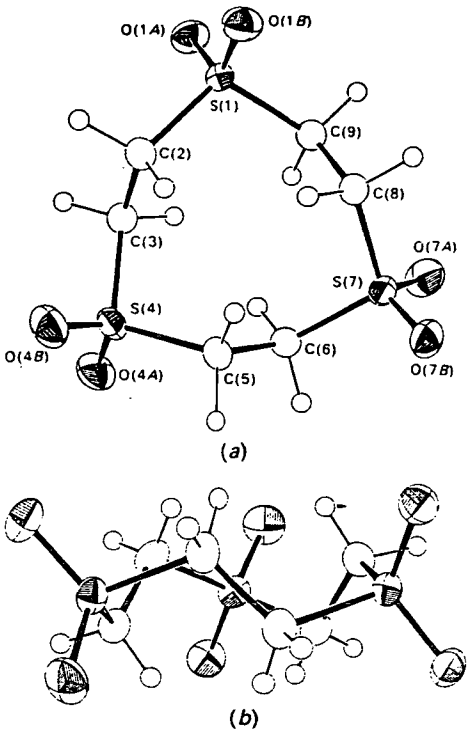

Fig. 1. (*a*) A general view of the O_6[9]aneS_3 molecule showing the atom-numbering scheme: thermal ellipsoids are drawn at the 30% probability level, except those of H which have artificial radii of 0.1 Å for clarity. (*b*) An orthogonal view showing the conformation of the nine-membered ring.

of the ring. Molecular geometry calculations were performed using *CALC* (Gould & Taylor, 1985).

Related literature. Structure determinations have been reported for [9]aneS_3 (Glass, Wilson & Setzer, 1980) and for other oxidation products such as the sulfoxide in $[Fe([9]aneS_3)\{[9]aneS_2(SO)\}]^{2+}$ (Küppers, Wieghardt, Nuber, Weiss, Bill & Trautwein, 1987) and the bicyclic sulfonium cation 4,7-dithia-1-thioniabicyclo[4.3.0]nonane (Blake, Holder, Hyde, Schröder & Taylor, 1991).

We thank the SERC for support.

References

BLAKE, A. J., HOLDER, A. J., HYDE, T. I., SCHRÖDER, M. & TAYLOR, A. (1991). *New J. Chem.* **15**, 511–514.

CLEGG, W. (1981). *Acta Cryst.* A**37**, 22–28.

GLASS, R. S., WILSON, G. S. & SETZER, W. N. (1980). *J. Am. Chem. Soc.* **102**, 5068–5069.

GOULD, R. O. & TAYLOR, P. (1985). *CALC*. Program for molecular geometry calculations. Univ. of Edinburgh, Scotland.

KÜPPERS, H.-J., WIEGHARDT, K., NUBER, B., WEISS, J., BILL, E. & TRAUTWEIN, A. X. (1987). *Inorg. Chem.* **26**, 3762–3769.

MALLINSON, P. D. & MUIR, K. W. (1985). *J. Appl. Cryst.* **18**, 51–53.

SHELDRICK, G. M. (1976). *SHELX76*. Program for crystal structure determination. Univ. of Cambridge, England.

SHELDRICK, G. M. (1986). *SHELXS86*. Program for the solution of crystal structures. Univ. of Göttingen, Germany.